

Synthesis and characterization of homo- and copolymers of α -olefins using metallocene catalysts

by

Nyambeni Luruli

Thesis

Presented in fulfillment of the requirements for the degree of

Master

of

Science

in the



Faculty of Science

at the

University of Stellenbosch

Supervisor: Prof H. G. Raubenheimer.

Co-supervisor: Prof. H. Pasch.

MARCH 2002

Declaration

I, the undersigned, hereby declare that the work contained in this thesis is my own original work and that I have not previously in its entirety or in part submitted it at any university for a degree.

Signature :

Date

Summary

This study comprises the synthesis and characterization of propene/lower α -olefin copolymers and α -olefin homopolymers using metallocene catalyst systems.

Incorporation of α -olefin comonomer into the polypropene backbone led to a change in properties such as microstructure and melting and crystallization temperatures. Synthesis of propene/ α -olefin (1-butene, 1-pentene, 1-hexene and 4-methyl-1-pentene) copolymers was carried out using the $\text{Me}_2\text{Si}(2\text{-Methylbenz[e]indenyl})_2\text{ZrCl}_2/\text{MAO}$ catalyst combination. Copolymers were characterized by NMR, GPC, DSC and CRYSTAF. Comonomer incorporation was generally kept below 6 % to ensure crystallizable copolymers. Comonomer content influences tacticity. It was especially pronounced for propene/1-butene copolymers and attributed to the formation of clusters.

Melting and crystallization temperatures, (T_m (DSC), T_c (DSC) and T_c (CRYSTAF)), of propene/lower α -olefin copolymers decreased linearly with an increase in comonomer incorporation and strongly depend on comonomer type displaying a different behaviour compared to that of propene/ higher α -olefins (1-octene, 1-decene, 1-tetradecene, and 1-octadecene) copolymers. The melting and crystallization temperatures of propene/4-methyl-1-pentene copolymers occur between those of propene/1-pentene and propene/1-hexene.

Poly- α -olefins (1-pentene, 1-hexene, 1-octene and 1-decene) were prepared using a series of $(\text{R}-\eta^5\text{-C}_9\text{H}_6)_2\text{ZrCl}_2/\text{MAO}$ [$\text{R} = \text{benzyl, phenyl and Si}(\text{CH}_3)_3$] and $\text{Me}_2\text{C}(\eta^5\text{-C}_5\text{H}_4-\eta^5\text{-C}_9\text{H}_6)\text{ZrCl}_2/\text{MAO}$ catalysts under different conditions. The resulting oligomers and polymers were characterized by GPC and NMR. Better conversions were obtained using catalysts with less bulky substituents and high MAO/catalyst ratios. Products ranged from dimeric oligomers to poly- α -olefins with molar masses between ca. $300 \text{ g}\cdot\text{mol}^{-1}$ and $6000 \text{ g}\cdot\text{mol}^{-1}$. Polydispersities, M_w/M_n , of poly- α -olefins synthesized at room temperatures were approximately 2, however, higher polydispersities were obtained at higher

temperatures. Various end groups such as vinylidene, 1,2 disubstituted and 1,1,2 trisubstituted double bonds were observed and attributed to different propagation and termination reactions. The most important vinylidene end group corresponds to a specific 1,2 monomer insertion and termination by β -elimination.

Opsomming

Hierdie studie behels die sintese en karakterisering van propeen/laer- α -olefien ko-polimere en α -olefien homo-polimere wat berei is deur van metalloseen-katalisatore gebruik te maak. Die insluiting van 'n α -olefien ko-monomeer in die ruggraat van propileen het 'n verandering in eienskappe soos mikrostruktuur, smelting en die temperatuur van kristallisatie tot gevolg gehad.

Die sintese van propeen/ α -olefien (1-buteen, 1-penteen, 1-hekseen en 4-metiel-1-penteen) ko-polimere is uitgevoer met die katalisatorkombinasie $\text{Me}_2\text{Si}(2\text{-Metielbenz[e]indieniel})_2\text{ZrCl}_2/\text{MAO}$. Daar is gepoog om die inkorporasie van die ko-monomeer tot <6% te beperk, om sodoende kristalliseerbare ko-polimere te verseker. Die ko-monomeerinhoud beïnvloed taktisiteit. Dit was veral opvallend in die propeen/1-buteen ko-polimere, en is toegeskryf aan die vorming van trosse (klusters). Die ko-polimere is gekarakteriseer deur van KMR, GPK, DSK en KRISTAF gebruik te maak.

Die smelt- en kristallisatie-temperature (T_m (DSC), T_c (DSC) en T_c (CRYSTAF)) van die propeen/laer- α -olefien ko-polimere het lineêr afgeneem met 'n toename in ko-monomeer inkorporasie en het sterk afgehang van van die tipe ko-monomeer. Die gedrag van laasgenoemde ko-polimere het verskil van dié van die propeen/hoër- α -olefien ko-polimere (1-okteen, 1-dekeen, 1-tetradekaan, en 1-oktadeekaan). Die smelt- en kristallisatie-temperature van die propeen/4-metiel-1-penteen ko-polimere lê tussen dié van propeen/1-penteen en propeen/1-hekseen.

Die poli- α -olefiene (1-penteen, 1-hekseen, 1-okteen en 1-dekeen) is onder verskillende reaksiekondisies berei deur van die katalisatore $(R-\eta^5-C_9H_6)_2ZrCl_2/MAO$ [R =bensiel, feniel en $Si(CH_3)_3$] en $Me_2C(\eta^5-C_5H_4-\eta^5-C_9H_6)ZrCl_2/MAO$ gebruik te maak. Die nuwe oligomere en polimere is met behulp van GPK en KMR gekarakteriseer. Katalisatore met kleiner substituenten en hoër MAO/katalisator-verhoudings lewer beter omskakelings. Produkte het gevarieer vanaf dimeriese oligomere tot poli- α -olefiene met molêre massas tussen 300 en 6000 $g \cdot mol^{-1}$. Die polidispersie van die poli- α -olefiene by kamertemperatuur gesintetiseer was ongeveer 2; hoër polidispersies is egter by hoër temperature verkry.

Vinilideen, 1,2-disgesubstitueerde- en 1,1,2-trigesubstitueerde dubbelbindings is as eindgroepe waargeneem. Dit is toegeskryf aan verskillende voortplantings- en termineringsreaksies. Die belangrikste vinilideen-eindgroep stem ooreen met 'n spesifieke 1,2 monomeerinvoeging en terminering deur β -eliminasië.

Acknowledgements

My promoters **Prof Raubenheimer** and **Prof Pasch** for their guidance and support

My mentor **Dr. Robert Brull** for all the help throughout this study

Dr Valerie Grumel and **Dr Udo Wahner** for their valuable inputs without which this study would be nothing

The commercial manager at Cape Wrappers PTY(LTD) **Mr Maarten Schurer** for allowing the opportunity to study further.

Dr A.J van Reenen for fruitful discussions we had on NMR

Prof. R.D. Sanderson all the help he gave me

Elisna for NMR measurements

Derreck McCauley, Sven Graef, Andre van Zyl for analytical work done on DSC, CRYSTAF and GPC.

NRF for financial support

My colleagues in the Olefins Lab, **Liesel Coetzee, Lufuno Siphuma, Charl Morkel, Siyabonga Mange, Marius Pretorius, Livingstone Vokwana, Marietjie Coetzee and Madri Smith.**

My friends **Mboneni Muofhe, Louis Makubele, Fulu Netswera, Mashudu Mudau, Mukwevho Israel, Netangaheni Pumudzo, Steven Kwindu, Wezile Chita.**

Ndivhuwo for being so special and unconditionally supportive. Your love and sacrifice will always be remembered.

Special thanks to my **family** for love and support.

This thesis is dedicated to my mom

Mrs Phophi Luruli (†)

1938/04/10 - 1998/11/04

“.....Never turn your back on molecular side of things.....”

J.R. Bull

List of abbreviations

| | |
|-----------------|---|
| 4M1P | 4-methyl-1-pentene |
| br | Branch |
| Bz | Benzyl |
| CCD | Chemical composition distribution |
| Cp | Cyclopentadienyl |
| CRYSTAF | Crystallization analysis fractionation |
| DSC | Differential scanning calorimetry |
| Flu | Fluorenyl |
| GPC | Gel permeation chromatography |
| HDPE | High density polyethylene |
| Ind | Indenyl |
| LDPE | Low density polyethylene |
| LLDPE | Linear low density polyethylene |
| MAO | Methylaluminoxane |
| M-C | Metal carbon |
| Me | Methyl |
| M_n | Number average molecular weight |
| M_w | Weight average molecular weight |
| n.a | Not available |
| n.d | not determined |
| NL | Sample code |
| NMR | Nuclear magnetic resonance |
| Ph | Phenyl |
| SCBD | Short chain branching distribution |
| T_C (CRYSTAF) | Crystallization temperature determined by CRYSTAF |
| T_c (DSC) | Crystallization temperature determined by DSC |
| T_m (DSC) | Melting temperature determined by DSC |
| δ | Chemical shift (ppm) |

LIST OF STRUCTURES, FIGURES AND SCHEMES

CHAPTER 2

| | |
|------------|---|
| Complex | $(\eta^5\text{-C}_5\text{H}_5)_2\text{Fe}$ or Cp_2Fe (2.1) |
| Complex | Cp_2MCl_2 (2.2) |
| Complex | $(\eta^5\text{-C}_5\text{R}_5)_2\text{MCl}_2$ (2.3) |
| Complex | $\text{Et}[\text{Ind}]_2\text{HfCl}_2$ (2.4) |
| Complex | $(\eta^5\text{-C}_5\text{R}_5)\text{TiMe}_3$ (2.5) |
| Complex | $(2\text{-Ph}-\eta^5\text{-C}_9\text{H}_6)_2\text{ZrCl}_2$ (2.6) |
| Complex | $\text{Et}(\text{Ind})_2\text{ZrCl}_2$ (2.7) |
| Scheme 2.1 | Formation of the first active cationic species during olefin polymerization |
| Scheme 2.2 | Mechanistic details of olefin polymerization with metallocenes |
| Scheme 2.3 | Possible insertion mechanism of olefin monomer |
| Complex | Cp_2ZrCl_2 (2.8) |
| Complex | $\text{Me}_2\text{Si}(2\text{-Methylbenz[e]indenyl})_2\text{ZrCl}_2$ (2.9) |
| Complex | $[\text{Me}_2\text{C}(\text{Flu})\text{Cp}]\text{ZrCl}_2$ (2.10) |
| Complex | $[\text{Me}_2\text{C}(\text{Flu})(3\text{-MeCp})]\text{ZrCl}_2$ (2.11) |
| Complex | $[\text{Me}_2\text{C}(\text{Flu})(3t\text{-MeCp})]\text{ZrCl}_2$ (2.12) |
| Scheme 2.4 | The effect of the substituent on propene stereoregularity |
| Scheme 2.5 | Typical stereoerrors during polymerization |
| Scheme 2.6 | Ten possible stereochemical pentads of a polyolefin |
| Scheme 2.7 | Metallocene oligomerization of α -olefins |
| Figure 2.1 | Molecules of polyethylene polymers |

CHAPTER 3

| | |
|----------------|--|
| Complex | $\text{Me}_2\text{Si}(2\text{-Methylbenz[e]indenyl})_2\text{ZrCl}_2$ (3.1) |
| Scheme 3.1: | General reaction scheme for the copolymerization of propene with linear α -olefins |
| Figure 3.1(a) | ^{13}C NMR spectrum of propene/1-butene copolymers |
| Figure 3.1(b) | ^{13}C NMR spectrum of propene/1-pentene copolymers |
| Figure 3.1(c) | ^{13}C NMR spectrum of propene/1hexene copolymers |
| Figure 3.2 | The backbone structure of propene/1-hexene copolymer |
| Figure 3.3(a) | Assigned ^{13}C NMR spectrum of propene/1-butene copolymer |
| Figure 3.3(b) | Assigned ^{13}C NMR spectrum of propene/1-pentene copolymer |
| Figure 3.3(c) | Fully assigned ^{13}C NMR spectrum of propene/1-hexene copolymer |
| Figure 3.4 | Expanded methyl region of propene/1-butene copolymer with pentad assignments |
| Figure 3.5 | Relative intensity (%) of the mmmm signal obtained by ^{13}C NMR spectroscopy |
| Figure 3.6 | The ^{13}C NMR spectral region between δ 33 - 44 for propene/1-butene copolymers |
| Figure 3.7 | Typical curves from CRYSTAF measurements |
| Figure 3.8 | Changing concentration of propene/1-butene copolymers in solution with temperature for different comonomer incorporation |
| Figure 3.9 | First derivative of the curves in Fig. 3.9 as a function of temperature for propene/1-butene copolymers |

CHAPTER 4

- Figure 4.1 ^{13}C NMR spectrum of propene/4-methyl-1-pentene copolymer with 1.6 [mol-%] of comonomer
- Figure 4.2 ^{13}C NMR spectrum of propene/4-methyl-1-pentene copolymer with 2.5 [mol-%] of comonomer
- Figure 4.3 DSC curves (2nd heating cycle) of propene/4-methyl-1-pentene copolymer (sample NL 2.1)
- Figure 4.4 DSC cooling curves of propene/4-methyl-1-pentene copolymer (sample NL 2.1)
- Figure 4.5 Melting temperature, T_m (DSC), and crystallization temperatures from the melt, T_c (DSC), as a function of comonomer content of propene/4-methyl-1-pentene copolymers
- Figure 4.6 Changing concentration of propene/4-methyl-1-pentene copolymers in solution with temperature
- Figure 4.7 First derivative of the curves in Fig. 4.6 as a function of temperature for propene/1-butene copolymers
- Figure 4.8 Crystallization temperatures from solution, T_c (CRYSTAF), as a function of comonomer content
- Figure 4.9 Melting peak temperatures, T_m (DSC), crystallization peak temperature, T_c (DSC), and crystallization peak temperature, T_c (CRYSTAF), of propene/4-methyl-1-pentene copolymers

CHAPTER 5

- Figure 5.1 Propene polymer structures available by use of metallocene catalysts
- Figure 5.2 DSC curves (2nd heating curves) of propene/1-hexene copolymer placed according to comonomer content

- Figure 5.3 Variations of melting temperatures, T_m (DSC), of propene/ linear olefin copolymers with changes in comonomer content
- Figure 5.4 DSC curves (cooling cycle) of propene/1-hexene placed according to comonomer content
- Figure 5.5 Crystallization temperature, T_c (DSC), of propene/ linear olefin copolymers determined by DSC
- Figure 5.6 First derivative of the concentration in solution determined by CRYSTAF
- Figure 5.7 Crystallization temperature, T_c (CRYSTAF), of propene/ linear olefin copolymers determined by CRYSTAF
- Figure 5.8 Melting temperature, T_m (DSC), of branched and linear propene/ α -olefin copolymers determined by DSC
- Figure 5.9 Crystallization temperature, T_c (DSC), of branched and linear propene/ α -olefin copolymers determined by DSC
- Figure 5.10 Crystallization temperature, T_c (CRYSTAF), of branched and linear propene/ α -olefin copolymers determined by CRYSTAF
- Figure 5.11 Melting temperature, T_m (DSC), crystallization temperature from melt, T_c (DSC), and crystallization temperature from solution, T_c (CRYSTAF), of propene/higher α -olefin copolymers determined by DSC and CRYSTAF

CHAPTER 6

- Scheme 6.1
- Figure 6.1 The structure of poly-1-decene
- Figure 6.2 (a) ^{13}C NMR spectrum of poly-1-pentene
- Figure 6.2 (b & c) ^{13}C NMR spectrum of poly-1-hexene and poly-1-octene respectively

- Figure 6.2 (d) ^{13}C NMR spectrum of poly-1-decene
- Scheme 6.2 -Possible mechanisms for the chain termination reaction leading to different end groups
- Figure 6.3 ^1H NMR spectrum of poly-1-hexene
- Figure 6.4 Expanded region (4.2-5.6ppm) of ^1H NMR spectrum for poly-1-hexene
- Figure 6.5 Expanded region (4.2-5.6ppm) of the ^1H NMR spectrum for poly-1-hexene synthesized at two different temperatures
- Figure 6.6 Yields of poly-1-hexene as a function of temperature
- Figure 6.7 Yields of poly-1-hexene as a function of MAO/catalysts ratio
- Figure 6.8 Yields of poly-1-hexene as a function of monomer/catalysts ratio
- Figure 6.9 Molecular weight distribution of poly-1-hexene prepared at different temperatures using catalyst 6.2 as determined by GPC
- Figure 6.10 Molecular weight distribution of poly-1-hexene prepared at room temperature using catalyst 6.2 as determined by GPC

LIST OF TABLES

CHAPTER 2

- Table 2.1 Historical events of metallocene developments for olefin polymerization
- Table 2.2 The relationship between catalyst symmetry and polymer tacticity

CHAPTER 3

- Table 3.1 Experimental parameters and results for propene/ α -olefin copolymers.
- Table 3.2 Chemical shift constants determined by Grant and Paul.
- Table 3.3 Chemical shifts for propene/ α -olefin copolymers
- Table 3.4 Comonomer concentration of propene/ α -olefin copolymers
- Table 3.5 ^{13}C NMR signals and polymer sequence assignment

CHAPTER 4

- Table 4.1 The calculated and observed chemical shifts of propene/4-methyl-1-pentene copolymers
- Table 4.2 Summary of results (comonomer content, T_m (DSC), T_c (DSC), T_c (CRYSTAF), M_n and M_n/M_w) for propene/4-methyl-1-pentene copolymers

CHAPTER 6

| | |
|-----------|--|
| Table 6.1 | Polymerization results obtained using complex $(\text{Ind})_2\text{ZrCl}_2$ (6.7) |
| Table 6.2 | Chemical shifts (ppm) in the ^{13}C NMR spectra of poly- α -olefins |
| Table 6.3 | Polymerization results obtained using $\text{Me}_2\text{C}(\eta^5\text{-C}_5\text{H}_4\text{-}\eta^5\text{-C}_9\text{H}_6)\text{ZrCl}_2$ (6.1) as catalysts |

LIST OF CONTENTS

| | |
|------------------------------|-----|
| List of Abbreviations | I |
| List of Figures | II |
| List of Tables | VII |
| List of Contents | IX |

CHAPTER 1

Introduction and objectives

| | |
|------------------|---|
| 1.1 Introduction | 1 |
| 1.2 Objectives | 2 |

CHAPTER 2

Historical and theoretical background

| | |
|---|----|
| 2.1 Introduction | 3 |
| 2.2 Historical development of metallocenes | 4 |
| 2.3 Theoretical background | 8 |
| 2.3.1 Mechanisms for the α -olefins polymerization with metallocene catalyst systems | 8 |
| 2.3.1.1 The homopolymerization of α -olefins with metallocene catalysts | 8 |
| 2.3.1.2 The role of MAO as co-catalyst | 9 |
| 2.3.1.3 Mechanistic details of the formation of the cationic species during the polymerization reaction | 10 |
| 2.3.1.4 Copolymerization kinetics | 12 |
| 2.3.2 Stereospecific polymerization of α -olefins with metallocene catalysts | 13 |

| | |
|--|----|
| 2.3.2.1 Regioselectivity | 13 |
| 2.3.2.2 The effect of metallocene structure on tacticity | 14 |
| 2.3.2.3 The effect of the substituent on catalyst symmetry and tacticity | 16 |
| 2.3.2.4 Tacticity and stereoerrors | 17 |
| 2.4 Advantages of metallocene catalyzed polymers | 19 |
| 2.5. Polymer characterization | 20 |
| 2.5.1 Molecular weight distributions | 21 |
| 2.5.2 Chemical structure and microstructures | 21 |
| 2.5.3 Chemical composition distribution | 21 |
| 2.5.4 Thermal and mechanical properties | 22 |
| 2.6 Conclusions | 22 |
| 2.7 References | 23 |

CHAPTER 3

Synthesis and characterization of metallocene-catalyzed random propene/linear α -olefin copolymers

| | |
|--|----|
| Abstract | 29 |
| 3.1 Introduction | 30 |
| 3.2 Reaction scheme | 31 |
| 3.3 Experimental | 32 |
| 3.3.1 Materials and methods | 32 |
| 3.3.1.1 Purification of reagents | 32 |
| 3.3.1.2 Copolymerization procedures | 32 |
| 3.3.2 Analytical techniques for the characterization of the propene/ α -olefin copolymers | 33 |
| 3.3.2.1 NMR measurements | 33 |
| 3.3.2.2 DSC measurements | 34 |

| | |
|---|----|
| 3.3.2.3 CRYSTAF measurements | 34 |
| 3.3.2.4 GPC measurements | 34 |
| 3.4 Results and discussion | 35 |
| 3.4.1 The assignment of ^{13}C NMR data | 37 |
| 3.4.2. Microstructure of propene/ α -olefin copolymers | 44 |
| 3.4.3 Melting and crystallization behaviour of propylene/ α -olefin copolymers | 47 |
| 3.4.3.1. DSC analysis | 48 |
| 3.4.3.2 CRYSTAF analysis | 48 |
| 3.4 Conclusions | 51 |
| 3.5 Recommendations | 51 |
| 3.6 References | 52 |

CHAPTER 4

Synthesis and characterization of metallocene-catalyzed propene/ 4-methyl-1-pentene copolymers

| | |
|---|----|
| Abstract | 54 |
| 4.1 Introduction | 55 |
| 4.2 Experimental | 56 |
| 4.2.1 Materials purification | 56 |
| 4.2.2 Polymerization procedures | 56 |
| 4.2.3 Analytical procedures | 56 |
| 4.3 Results and discussion | 57 |
| 4.4 Thermal properties of propene/4-methyl-1-pentene copolymers | 59 |
| 4.4.1 Melting and crystallization from the melt | 59 |
| 4.4.2 Crystallization from solution | 61 |
| 4.5 Conclusions | 64 |
| 4.6 Recommendations | 64 |
| 4.6 References | 65 |

CHAPTER 5

Investigation of melting and crystallization behavior of propene/ α -olefin copolymers by DSC and CRYSTAF

| | |
|---|----|
| Abstract | 66 |
| 5.1. Introduction | 67 |
| 5.2 Melting and crystallization behaviour of propene/linear α -olefin copolymers | 69 |
| 5.2.1 Melting and crystallization analysis investigated by DSC | 70 |
| 5.2.2 Crystallization analysis investigated by CRYSTAF | 73 |
| 5.3 Comparison of melting and crystallization behaviour of branched and linear propene/ α -olefin copolymers | 75 |
| 5.4 Conclusions | 78 |
| 5.5 References | 79 |

CHAPTER 6

The influence of reaction conditions and catalyst systems on polymerization behaviour of α -olefins

| | |
|--|----|
| Abstract | 80 |
| 6.1 Introduction | 81 |
| 6.2 Experimental | 82 |
| 6.2.1 Reaction Scheme | 82 |
| 6.2.2 Material and methods of purification | 83 |
| 6.2.3 General synthetic procedure | 83 |
| 6.2.3 Purification of the polymer | 83 |
| 6.3 Results and discussion | 84 |
| 6.3.1 Poly- α -olefins | 84 |
| 6.3.2 ^{13}C NMR analysis | 85 |

| | |
|---|-----|
| 6.3.3 Analysis of end groups | 89 |
| 6.4 The influence of reaction conditions and substituent effects of (R- η^5 -C ₉ H ₆) ₂ ZrCl ₂ on poly-1-hexene polymerization behaviour | 93 |
| 6.4.1 The effects of steric factors, temperature, MAO/catalyst and monomer/catalysts ratios on poly-1-hexene yields (conversions) | 94 |
| 6.4.2 The effects of steric factors, temperature, MAO/catalyst and monomer/catalysts ratios on poly-1-hexene molecular weight | 96 |
| 6.5 Conclusions | 99 |
| 6.6 References | 101 |
| Appendix A: NMR DATA | 103 |
| Appendix B: GPC DATA | 122 |
| Appendix C: CRYSTAF CURVES | 133 |
| Appendix D: DSC CURVES | 142 |

CHAPTER 1

INTRODUCTION AND OBJECTIVES

1.1 Introduction

Metallocenes are special members of a class of compounds known as organometallic compounds. Metallocenes activated with Methylaluminoxane (MAO) form single-site catalyst systems effective in α -olefins polymerization to produce polymers with uniform controlled properties.

Metallocenes do not only allow the direct control of properties but also enable the synthesis of polymers and copolymers that could not have been produced with heterogeneous Ziegler-Natta catalysts. In addition, new monomers (oligomers) with new application possibilities can be obtained using metallocene catalysts.

Metallocene-catalyzed processes for large scale industrial polymer synthesis are used by companies such as Exxon Chemical, Dow, BP Chemicals, Du Pont and Sumitomo. Industrial applications of metallocene-catalyzed polymers include biaxially oriented polypropene (BOPP) films, adhesives, fragrances, lubricants, cosmetics and fuel additives¹.

¹ Hungenberg, K. D.; Kerth, J.; Langhauser, F.; Mueller, H. J.; Mueller, P. J.; *Angew. Makromol. Chem.* **1995**, *227*, 159.

1.2 Objectives

The main purpose of this study was to synthesize and characterize metallocene-catalyzed homo-polymers of long chain α -olefins and copolymers of α -olefins with propene.

Specific goals were to:

1.2.1 Synthesize propene copolymers with:

- 1-butene
- 1-pentene
- 1-hexene
- 4-methyl-1-pentene

1.2.2 Characterize propene copolymers (in 1.2.1) and investigate the following:

- Microstructure and compositional analysis
- Melting behavior
- Crystallization behaviour
- Mechanical properties of selected propene copolymers

1.2.3 Synthesize homopolymers of the following α -olefins:

- 1-pentene
- 1-hexene
- 1-octene
- 1-decene

1.2.4 Characterize α -olefins homopolymers with regard to their structures

1.2.5 Investigate the effect of various metallocene structures and different reaction conditions on polyolefin formation.

CHAPTER 2

HISTORICAL AND THEORETICAL BACKGROUND

2.1 Introduction

The development of co-ordination chemistry of transition metal complexes and more specifically organometallic compounds has stimulated research in the field of polymer chemistry and material science in general. Polymerization of α -olefins and other vinyl monomers using coordination metal complexes has been studied extensively and is still continuing¹⁻⁵.

Three types of transition metal based catalysts that have been widely used for ethylene and propene polymerization are Ziegler-Natta mixtures, metallocenes and chromium oxide-based catalysts. These catalysts have led to the discovery and improvement of commercial material such as high density polyethylene (HDPE), linear low density polyethylene (LLDPE), ethylene-propylene rubber (EPR), ethylene/propene/diene/rubber (EPDR) and ethylene-butene (EB) copolymers.

Ziegler-Natta catalysts are multiple active sites catalysts and are formed from reactions involving certain transition metal compounds of Group IV-VIII (commonly halides) combined with alkyls, aryls or hydrides of Group I-IV metals in the presence of inert solvent or diluent⁶.

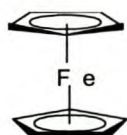
Metallocene catalysts generally contain a transition metal (usually a group IV metal such as Ti, Zr or Hf) sandwiched between cyclopentadienyl ring structures⁷. Variations of metallocene structures include ring functionalization with various alkyl or aromatic groups, ring bridging (*ansa*-types) with silyl or carbon atoms and metal coordination to either alkyl or halogen groups.

Metallocene catalysts are also known as “single-site catalysts” because of their ability to confine polymerization to a single active site. Their single site nature allows precise control over product polymer structure.

This chapter focuses largely on the development of metallocenes and the advancement of olefin polymerization. Other theoretical background studies related to the objectives of this study will also be highlighted.

2.2 Historical development of metallocenes

Metallocene catalysts were discovered in the 1950's following the discovery of the sandwich compound known as ferrocene (2.1) which is based on Fe (II) coordinated to two cyclopentadienyl ligands⁸⁻¹⁰. The stability, structure, and bonding of ferrocene defied the classical Lewis description of bonding and therefore captured the imagination of chemists. This puzzle in turn generated an interest in synthesizing, characterizing and theorizing that led to rapid development of d-block organometallic chemistry.



2.1

In 1953 Karl Ziegler and his co-workers discovered catalyst systems based on transition metal compounds (zirconium and titanium halides), which were used to study the polymerization of α -olefins¹¹. In the presence of aluminium alkyls activators these catalyst systems were able to polymerize ethylene to yield HDPE at low pressure, but could not polymerize propylene.

In 1954 Natta reported the successful polymerization of propene using the same catalyst system¹². After characterizing the resulting polymer, he was able to define the three stereo conformations of polypropylene: isotactic, syndiotactic and atactic polypropylene. This was the first stereospecific polymerization of propylene to be reported.

The catalyst systems used by Ziegler and Natta are now generally known as Ziegler-Natta catalysts. Ziegler-Natta catalysis and Phillips-type catalysts led to the discovery of polyolefin materials exhibiting a broad range of properties from thermoplastic to rubber materials. Ziegler and Natta both received the Nobel Prize in chemistry in 1963 for their important ground breaking contribution.

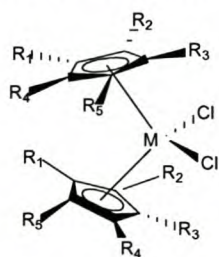
Metallocene catalysts (e.g **2.2**) used for ethylene polymerization, were reported in 1958 by Breslow and Newburg¹³. These catalysts were based on *bis*(cyclopentadienyl) titanium dichloride. Activation was achieved with aluminium alkyls (specifically AlEt₃).



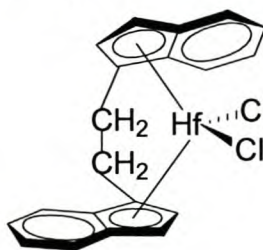
2.2

Early metallocene catalysts, Cp₂TiCl₂/AlR₃, showed poor activity towards ethylene polymerization and could not polymerize propylene. Reichert and Meyer discovered that addition of traces of water, originally thought to be poisonous, improves the activity of metallocene/aluminiumalkyl systems¹⁴. Shortly after this discovery, unexpected increase in reactivity was obtained by substantial water addition.¹⁵ These developments led to the separate synthesis of methylaluminoxane (MAO)¹⁶. MAO has since been used as a cocatalyst in conjunction with metallocenes for olefin polymerization.

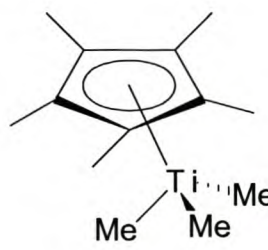
The structure of metallocenes has also received a lot of attention in order to optimize it for the polymerization of α -olefins. Metallocenes can be unsubstituted, substituted (**2.3**) bridged (stereorigid) (**2.4**), unbridged, or of the halfsandwich type (**2.5**). Structures shown below illustrate some of these examples.



2.3



2.4



2.5

Ligands such as indenyl (Ind) and fluorenyl (Flu) (shown below) have been used instead of cyclopentadienyl (Cp).



indenyl (Ind)



fluorenyl (Flu)

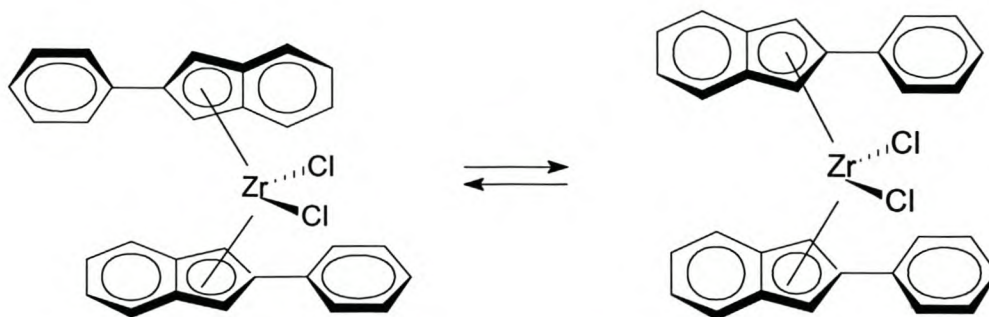
The synthesis of bridged metallocenes by Brintzinger et al. in 1982 led to the stereospecific polymerization of propylene¹⁷. Two years later Ewen correlated catalyst symmetry with the polymer structure and reaction mechanisms¹⁸.

The major events of metallocene developments for olefin polymerization are listed in Table 2.1.

Table 2.1 Historical events of metallocene developments for olefin polymerization

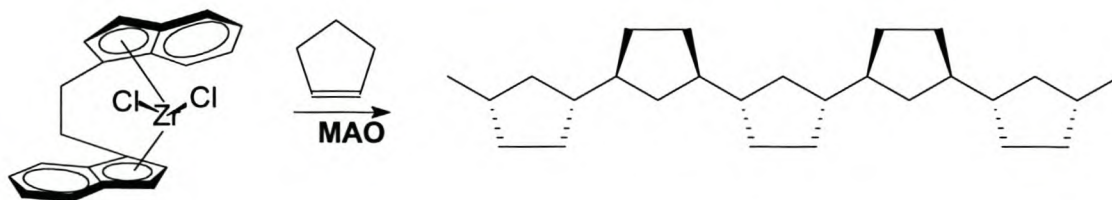
| Year | Developments | Reference |
|------|--|-----------|
| 1952 | Synthesis of Ferrocene by Fischer as a model compound for metallocenes. | 8 |
| 1955 | Metallocene activated with AlEt ₃ , showed low activity toward ethylene polymerization. | 12,13 |
| 1973 | Addition of small amount of water (Al:H ₂ O=1:0.5) increased the activity. | 14 |
| 1975 | High activity upon addition of substantial amount of water (Al:H ₂ O=1:2). | 15 |
| 1977 | Methylaluminoxane (MAO) was separately prepared as a cocatalyst for olefin polymerization. | 16 |
| 1982 | Synthesis of ansa-metallocene with C ₂ symmetry. | 17 |
| 1984 | Polymerization of propylene using a rac/meso mixture of ansa-titanocenes led to partially isotactic propylene. | 18 |
| 1984 | Chiral ansa-zirconocenes produce highly isotactic polypropylene. | 22 |

Waymouth and co-workers recently reported an unbridged metallocene catalyst, (2-phenylindenyl)₂ZrCl₂/MAO (**2.6**), which appears to isomerize by restricted rotation of its indenyl ligand between chiral and achiral coordination geometries during chain growth. This catalyst yields a highly stretchable atactic-isotactic stereoblock polypropylene with elastomeric properties¹⁹⁻²¹.

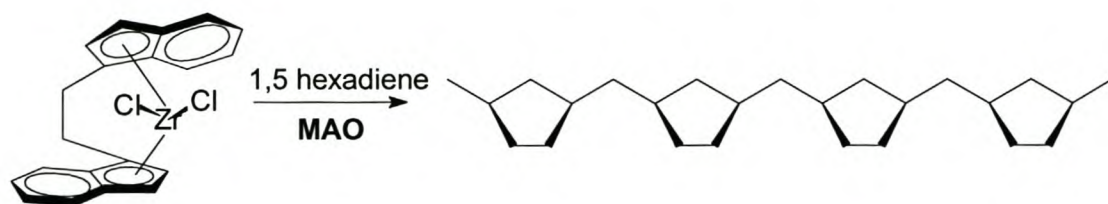
**2.6**

The investigation of this catalysts family for higher α -olefins polymerization is described in Chapter 6.

Kaminsky et al. reported the use of metallocene catalysts to synthesize cyclic homopolymers without ring opening²²⁻²⁴. Cyclopentene was the first cyclic monomer to be polymerized by *rac*-[Et(Ind)₂]ZrCl₂ (**2.7**)/MAO at room temperature. The resulting polymer was semicrystalline and was insoluble in common organic solvents.

**2.7**

The use of metallocene catalyst systems to polymerize non-conjugated and conjugated diene monomers furnished new types of cyclic polymers with ring structures interspaced by CH₂-groups²⁵⁻²⁷.



Other cyclic polymers of cyclic monomers such as norbornene have been synthesized using metallocene catalyst systems^{28,29}.

2.3 Theoretical background

2.3.1 Mechanisms for α -olefins polymerization using metallocene catalyst systems

2.3.1.1 The homopolymerization of α -olefins with metallocene catalysts

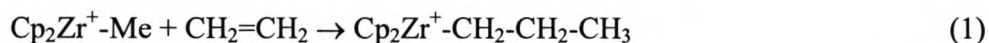
The polymerization reaction of α -olefins with metallocenes is initiated by active centers of metallocene catalysts. Active species (chain initiators) are ionic pairs containing cationic species like $\text{Cp}_2\text{M}^+-\text{R}$. These species are either synthesized or are formed in the reaction between metallocene complexes, such as Cp_2ZrMe_2 or Cp_2ZrCl_2 and MAO. Cationic metallocene complexes can also be formed by other counterion initiators such as $\text{Ph}_3\text{C}^+\text{B}(\text{C}_6\text{F}_5)_4^-$ or $\text{B}(\text{C}_6\text{F}_5)_3$ ³⁰⁻³².

The structure of MAO is not known, however, it is generally believed to be an oligomer with molecular weight between 1000 and 1500 g/mol³³⁻³⁷. The mechanism surrounding the generation of the cationic species and chain propagation will be discussed in the following sections.

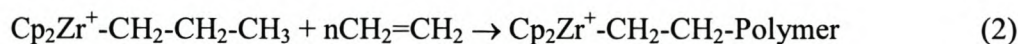
The mechanism of olefin polymerization with metallocenes can be summarized by a number of $\text{M}-\text{R}^+$ reaction steps:

(i) Initiation

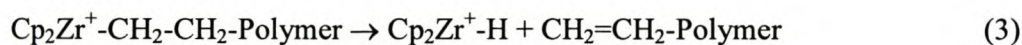
The polymerization reaction starts when an α -olefin coordinates to the transitional metal atom bearing a positive charge, and subsequently inserts into the Zr-Me bond (probably by Me-migration):

(ii) Chain propagation

Another molecule of alkene coordinates and inserts:

(iii) Termination

The chain propagation is usually terminated by β -hydride elimination:



A Zr-C bond is regenerated by the first ethylene monomer inserted into the Zr-H bond:



The methyl group present in the first cycle is now, and in all following cycles, absent.

2.3.1.2 The role of MAO as co-catalyst

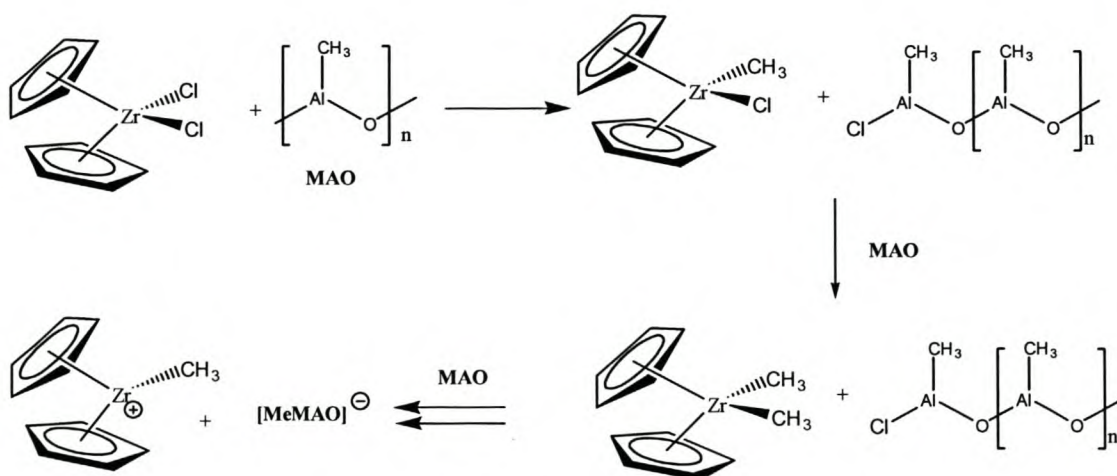
The primary role of the co-catalyst is the methylation of the halogenated metallocene precursor and abstraction of Me^5 which leads to the formation of the active complex (Scheme 2.1) ³⁸⁻⁴¹. Methylaluminoxane (MAO) is widely used as a cocatalyst. Other

functions of the MAO are to scavenge impurities and moisture and to reactivate the inactive complexes formed. High ratio of MAO:Zr ($\approx 5000:1$) is needed for catalyst activation.

As mentioned before, other cocatalysts such as tetraphenylborate ($(C_6H_5)_4B^-$), carborane ($C_2H_9H_{12}^+$) or fluorinated borate can also be used for the formation of $M-CH_3^+$ (cationic species)⁴²⁻⁴⁵. The main advantage of borate cocatalysts is that they are more economical with a ratio of 1:1 of borate to metallocene. The disadvantage of using borate cocatalysts is that they are very sensitive to poisons, decompose easily and must be stabilized by addition of aluminiumalkyls such as tri-isobutylaluminium⁴⁶⁻⁴⁸.

2.3.1.3 Mechanistic details of the formation of the cationic species during the polymerization reaction

The formation of cationic species described above results from the reaction between the catalyst and MAO⁴⁹. The addition of MAO to the metallocene leads to the abstraction of chloride and substitution by a methyl group. The abstraction of chloride is a fast reaction. Excess MAO is needed for the abstraction of a second chlorine and the subsequent formation of a catalytically active cationic species (Scheme 2.1)⁵⁰⁻⁵².

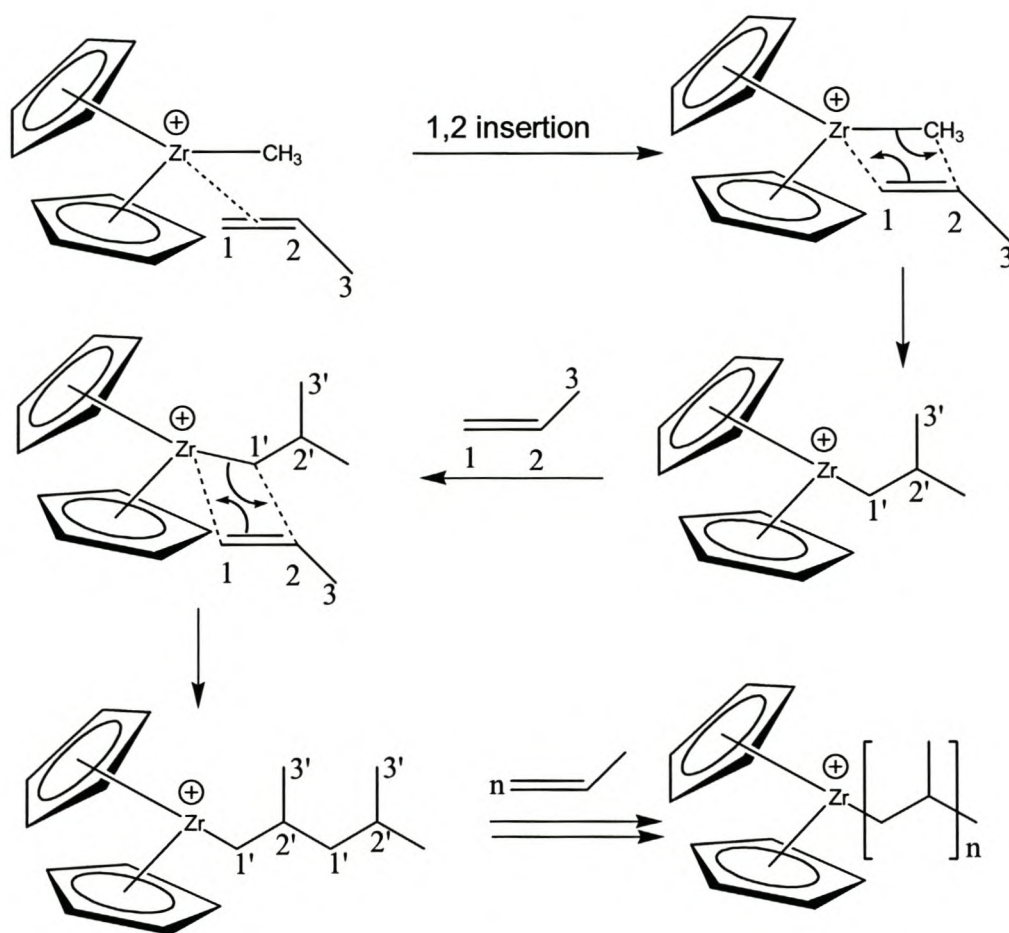


Scheme 2.1 Formation of the first active cationic species during olefin polymerization⁵³

This stepwise process leading to a weakly-bonded ion pair, is supported by spectroscopic evidence^{54,55}.

Several reports have been published that cover the mechanism of monomer insertion into the M-C (and later M-H) bond⁵⁶.

The mechanistic details are shown in Scheme 2.2. Propylene polymerization with cyclopentadienylzirconium dichloride is used as an example, effecting a 1,2-insertion of the monomer in the Zr-CH₃ bond, which is mainly observed with metallocene catalysts.

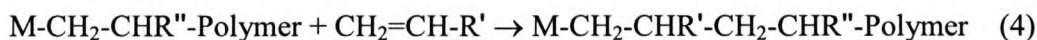
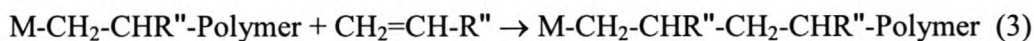
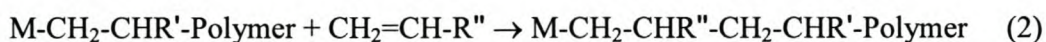
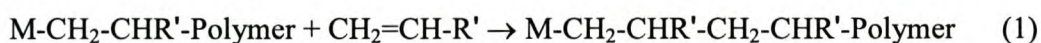


Scheme 2.2 Mechanistic details of olefin polymerization with metallocenes

2.3.1.4 Copolymerization kinetics

In copolymerization reactions, two or more different α -olefin monomers are competitively inserted into the transition metal carbon bonds at the active center. The simplest case is when two α -olefins, e.g. $\text{CH}_2=\text{CH-R}'$ and $\text{CH}_2=\text{CH-R}''$, are copolymerized.

Now four chain growth reactions must be considered instead of a single chain propagation reaction.



Reactions (1) and (3) represent homopolymerization reactions of $\text{CH}_2=\text{CH-R}'$ and $\text{CH}_2\text{-CH-R}''$ with rate constants k_{11} and k_{22} respectively. The reactions, (2) and (4) represent cross-growth reactions with rate constants k_{12} and k_{21} respectively.

The values for all four rate constants k_{11} , k_{12} , k_{21} and k_{22} are different since the rate of insertion of a particular α -olefin into an M-C bond depends on the structure of the α -olefin and also on the structure of the last inserted monomer unit.

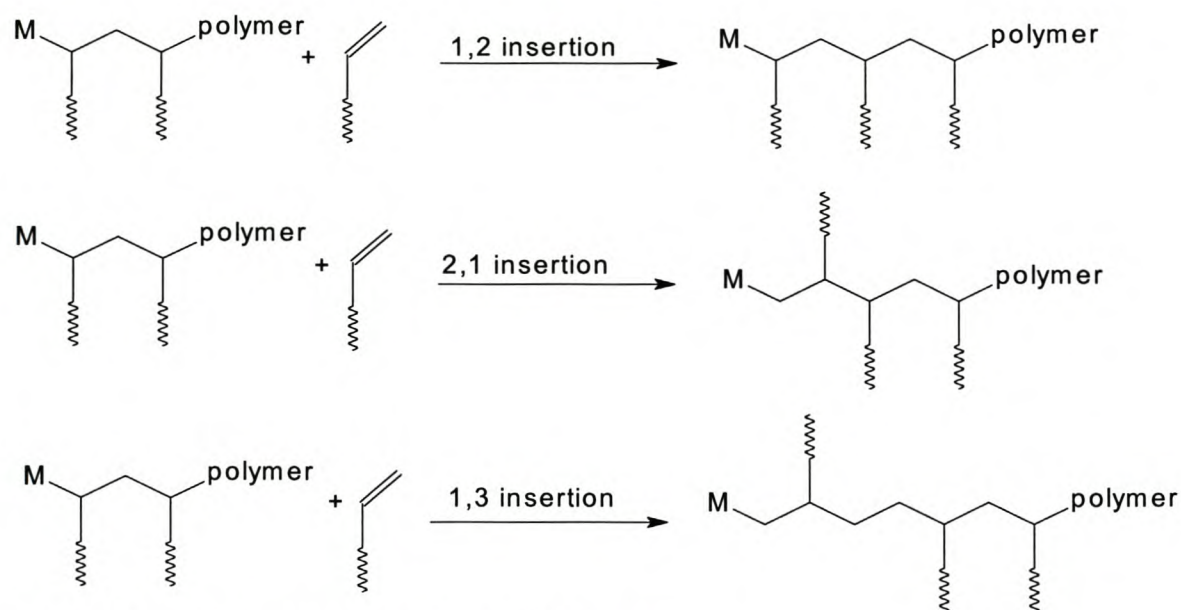
The four rate constants are normally reported as reactivity parameters $r_1=k_{11}/k_{12}$ and $r_2=k_{22}/k_{21}$ ⁵⁷⁻⁵⁹. Reactivity ratio constants r_1 and r_2 , differ for the same pair of monomers with the catalyst system and solvent.

2.3.2 Stereospecific polymerization of α -olefins with metallocene catalysts

Metallocenes have been used for many years for polymerization of monomers ranging from ethylene to tetradecene including cyclic monomers such as cyclopentene, norbornene, etc. Copolymerization of these monomers was reported and detailed studies have shown that the catalyst type has an influence on the regio- and stereoregularity⁶⁰⁻⁷⁵.

2.3.2.1 Regioselectivity

The microstructure is also determined by the regioselectivity of the incoming monomer incorporation into the growing polymer chain. Regioselective polymerization of the monomers gives an insight into the mechanism of insertion into the growing polymer. Several possibilities are shown in Scheme 2.3. The first is 1,2 (head to tail) insertion which lead to 1,3 branching. Other possibilities are 2,1 (head to head) or 1,3 (tail to tail) which lead to 1,2 and 1,4 branching respectively³.



Scheme 2.3 Possible insertion mechanism of olefin monomer

With metallocene catalysts monomer insertion generally occurs in the 1,2-mode⁷⁶⁻⁸⁹. The 2,1 misinsertions are also observed but are slow and cause chain termination. The choice of reaction conditions such as temperature and metallocene type also influences a particular insertion mode. The 1,3 insertion results from isomerization of the Zr-Polymer bond prior to insertion of the next monomer^{97,98}.

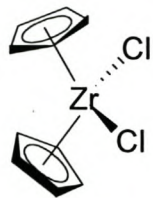
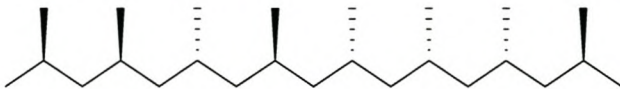
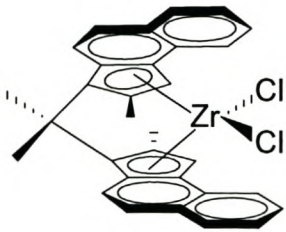

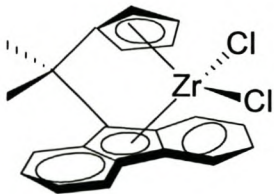
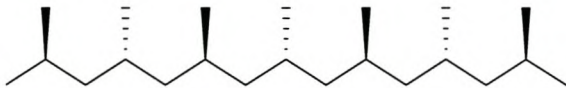
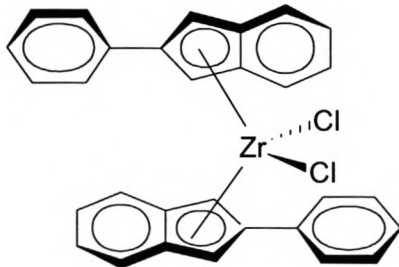
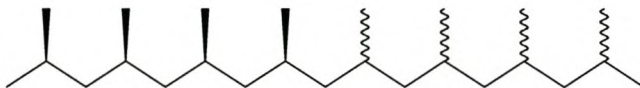
2.3.2.2 The effect of metallocene structure on tacticity

Monomer units are enchainned with each other in a particular regular manner, which depends on the catalyst structure and on the polymerization conditions. This type of regularity is known as tacticity.

One of the advantages of metallocenes or “single-site” catalysts over heterogeneous Ziegler-Natta catalysts is that their structure or symmetry can be designed to produce a particular tacticity.

Table 2.2 shows the relationship between catalyst symmetry and the resulting polymer tacticity (structure).

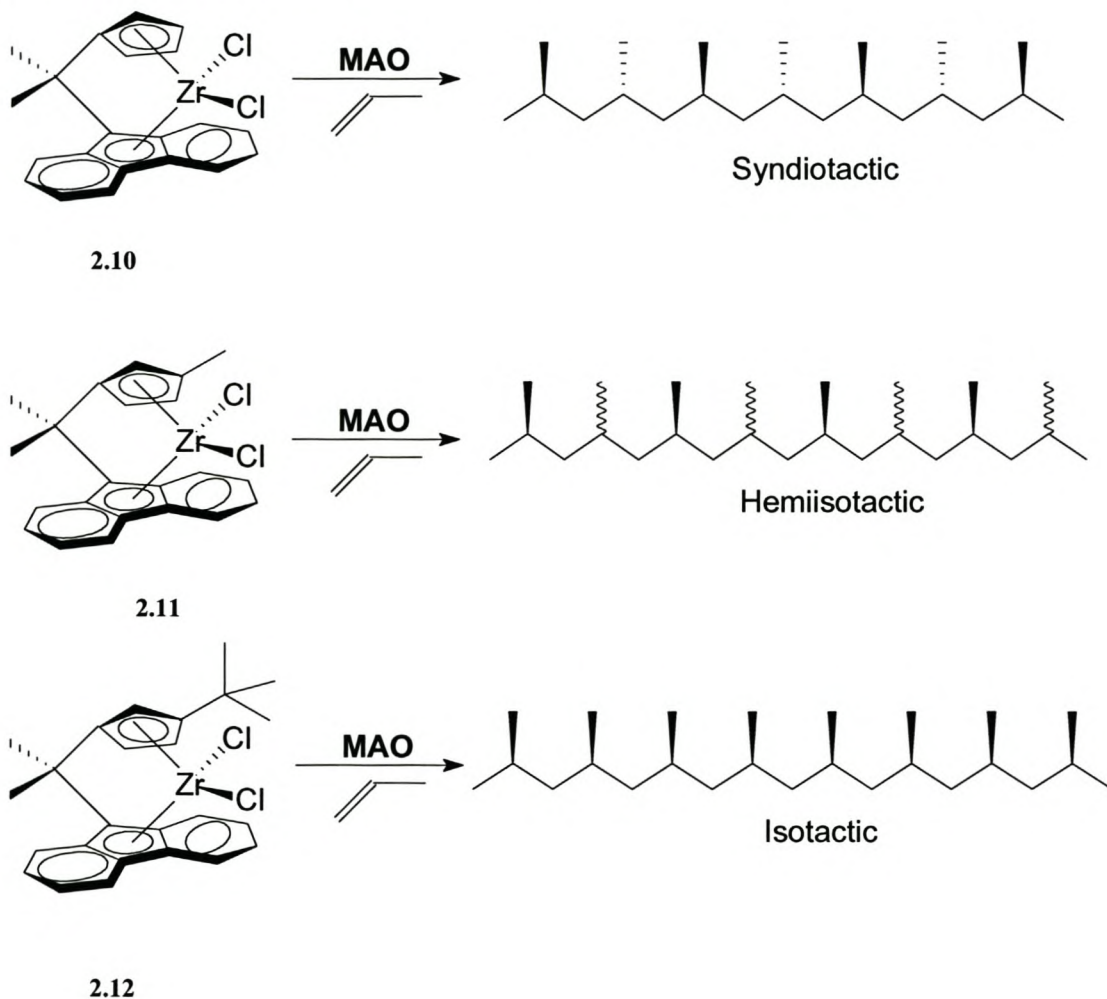
Table 2.2 The relationship between catalyst symmetry and polymer tacticity

| Catalyst Structure | Catalyst Symmetry | Polymer Structure (Sawhorse model) |
|--|---|--|
|  <p>2.8</p> | C_{2v} |  <p>Atactic</p> |
|  <p>2.9</p> | C_2 |  <p>Isotactic</p> |
|  <p>2.10</p> | C_s |  <p>Syndiotactic</p> |
|  <p>2.6</p> | Oscillating between rac- and meso phase |  <p>Isotactic-atactic stereo block</p> |

2.3.2.3 The effect of the substituent on catalyst symmetry and tacticity

The degree of stereoregularity of the polymer can be tailored by introduction of a substituent on the Cp ring (Scheme 2.4). Ewen and co-workers used complexes **2.10-2.12** to demonstrate the influence of the substituent on catalyst symmetry and tacticity^{90,91}.

The introduction of methyl and isobutyl groups on the Cp ring changed the syndiospecific catalyst $iPr(CpFlu)ZrCl_2$ (**2.10**) to hemiispecific (**2.11**) and isospecific (**2.12**), catalysts respectively.



Scheme 2.4 The effect of the substituent on propene stereoregularity

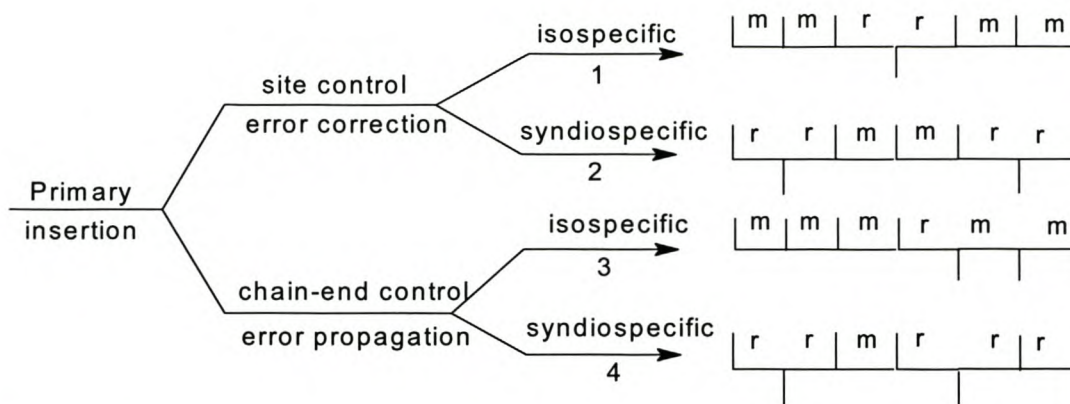
The size of the substituent can also improve the percentage of tacticity. The effect of a bulky substituent on the cyclopentadienyl (Cp) ring on tacticity was investigated by Erker et al.⁷¹⁻⁷⁵. The tacticity of the obtained polypropylene was found to increase with the bulkiness of the substituent.

2.3.2.4 Tacticity and stereoerrors

Stereoregularity of propene and higher α -olefins can be controlled by suitably designed metallocene catalysts as shown in Table 2.2. Characterization of these polymers, polypropylene in particular, by ¹³C NMR give rise to signals which can readily be related to the microstructure of the polymer. Bovey developed a nomenclature system which is widely used to designate neighbouring units as *m* (meso) for equally and *r* (racemo) for unequally positioned substituents⁹².

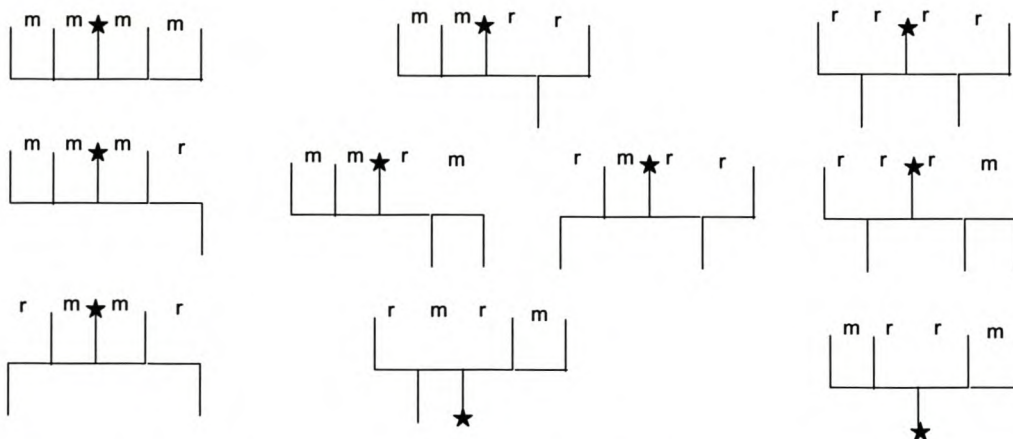
It is almost impossible to produce a polymer which has 100% stereoregularity, due to occasional errors which occur during polymerization⁹³⁻¹⁰¹. During isotactic polymerization, monomers are inserted into the metal-carbon bond in a particular regular manner facing one direction. If one monomer is inserted in a syndiotactic position it causes an error on the growing polymer chain. Catalysts that produce highly isotactic polymers usually correct this error during the next insertion step of the olefin monomer.

There are two types of errors that can occur (Scheme 2.5)¹⁰². The first is the so-called catalytic site control error (also known as enantiomorphic site control). Metallocenes are known for catalytic site controlled error. The second is chain-end controlled error and is caused by the last monomer inserted.



Scheme 2.5 Typical stereoerrors during polymerization

In polypropylene, the signal of the CH₃ group from ¹³C NMR measurements is usually used to determine the polymer microstructure. The ¹³C NMR chemical shift for CH₃ is determined by neighbouring repeat units on both sides. Each CH₃ signal is assignable to a particular “pentad” pattern, represented by the four consecutive *m* or *r* designators framing the CH₃ (★) under consideration. The possible pentads are listed below (Scheme 2.1)¹⁰³⁻¹⁰⁸.



Scheme 2.6 Ten possible stereochemical pentads of a polyolefin

All ten possible pentad signals (*mmmm*, *mmmr*, *rmmr*, *mmrm*, *mmrr*, *rmrr*, *rmr**m*, *rrrr*, *rrrm*, and *mrrm*) are observed in atactic polypropylene. Isotactic polypropylene is characterized by a single ¹³C NMR signal for the *mmmm* pentad. The degree of

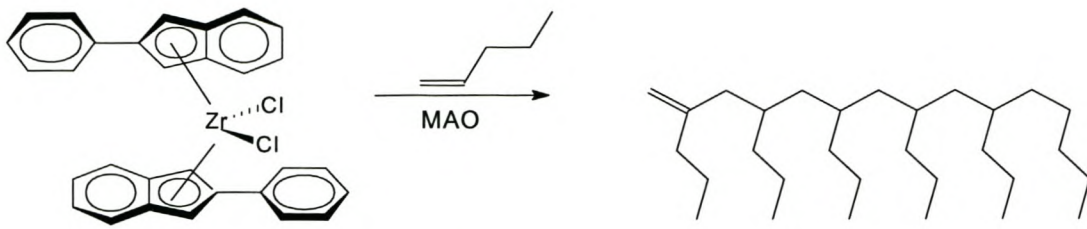
isotacticity is expressed as the ratio of the *mmmm* pentad integral to the sum of all pentad integrals observed and is designated as [*mmmm*]. Syndiotactic polypropylene contains only *rrrr* pentads and is also characterized by a single ^{13}C NMR signal. The syndiotacticity is expressed as the ratio of the *rrrr* pentad integral to the sum of all pentad integrals and designated as [*rrrr*].

Polypropylene produced by Ziegler-Natta catalysts is highly isotactic with [*mmmm*] > 0.95¹⁰⁹⁻¹¹². Bridged metallocene/MAO catalysts on the other hand, produce isotactic polypropylene with stereoregularity of [*mmmm*] $\approx 0.8 - 0.9$ ^{113,114}.

2.4 Advantages of polymers produced with metallocenes

The advantage of metallocenes compared to traditional Ziegler-Natta catalysts is that their structures are designable to produce polymers with desired properties. The single site nature of the metallocene's active sites, allows the production of polymers with uniform properties (narrow molecular weight distribution, regioregularity, stereoselectivity and chemical composition distribution).

Another advantage of metallocenes is their ability to produce oligomers. Oligomers are polymers with very low molecular weights (number of monomer units less than 100) with unsaturated reactive end groups. Scheme 2.7 shows an example of a 1-pentene oligomer. The fact that the product oligomer contains no methyl group on the chain means that the catalyst was a hydride (formed after the first cycle by β -elimination). These end groups can further be functionalized to produce molecules that can have new applications. Detailed analysis of poly α -olefins unsaturated end groups is described in Chapter 6. Oligomers can also be used as comonomers.



Scheme 2.7 Metallocene oligomerization of 1-pentene

2.5 Polymer characterization

Polymers are highly complex multicomponent macromolecules. Polymers with the same identical repeating units may not necessarily have the same structural, thermal or mechanical properties (Figure 2.1). The differences in these properties may result from different techniques or reaction conditions used during polymerization (e.g. LDPE and HDPE).

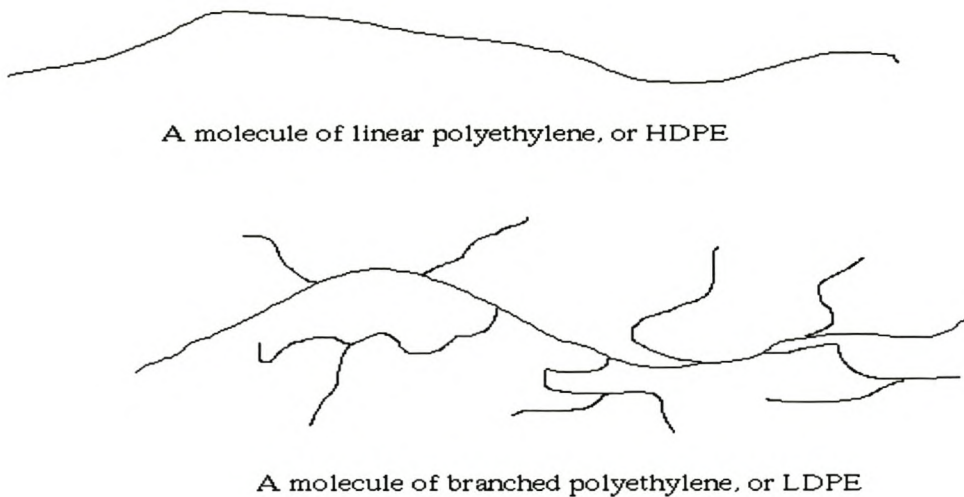


Figure 2.1 Molecules of polyethylene polymers

HDPE is linear and highly crystalline while LDPE is highly branched and amorphous. There are various analytical techniques available for characterization of the chemical, thermal and physical properties of the polymers.

2.5.1 Molecular weight distributions

The chains inside a material resulting from the polymerization process are not identical either by the size of polymer chain or by composition in a case of a copolymer. The molecular weight of a given polymer is represented by mean values such as number-average molecular weight (M_n) and weight-average molecular weight (M_w). Analytical techniques for the determination of these values are light scattering, intrinsic viscometry, osmometry, gel permeation chromatography (GPC). The most recent technique is matrix-assisted laser desorption ionization (MALDI) mass spectroscopy. GPC is the most widely used due to the relative short analysis time. It is a relative method and, therefore, calibration is required. A polystyrene standard is most commonly used.

2.5.2 Chemical structure and microstructures

Chemical structure and different functional groups within the polymer chain can be accurately characterized by nuclear magnetic resonance (NMR) and infrared (IR) studies. Of these, NMR yields more information than IR. ^{13}C and ^1H NMR provide information such as regularity, comonomer amount and sequence and endgroups. Information about the mechanism of polymerization can also sometimes be deduced from such NMR data.

2.5.3 Chemical composition distribution

Copolymers also possess chemical composition distribution (CCD) (also known as short chain branching distribution (SCBD)). Temperature rising elution fractionation (TREF) has been used to study the CCD of polymers. The drawback of TREF is long analysis time (one sample per day). Recently a technique known as crystallization analysis fractionation (CRYSTAF), which provides similar information as TREF has been

developed¹¹⁵. CRYSTAF has short analysis time (five samples in ca. 6h). The principles surrounding CRYSTAF will be explained in Chapter 3.

2.5.4 Thermal and mechanical properties

Thermal transitions such as glass transition (T_g), crystallization and melting temperatures can be studied using differential scanning calorimetry (DSC), thermogravimetric analysis (TGA), dynamic mechanical analysis (DMA), dielectric analysis (DEA) and thermomechanical analysis (TMA). The most common thermal analysis techniques are DSC and TGA.

Generally a combination of two or more of these analytical techniques is used. Analytical techniques employed in this study include NMR, GPC, DSC and CRYSTAF.

2.6 Conclusions

Metallocene/MAO catalyst systems afford new opportunities for materials which were not accessible with traditional Ziegler-Natta catalyst systems. These single-site catalyst systems are able to produce polymers with a wide variety of properties. Metallocene structures can, to a certain extent, be tailored to produce polymers with desired properties.

2.7 References

1. Resconi, L.; Cavallo, L.; Fait, A.; Piemontesi, F.; *Chem. Rev.* **2000**, 100, 1253.
2. Coates, G. W.; *Chem. Rev.* **2000**, 100, 1223.
3. Kaminsky, W.; Arndt, M.; Ringshof, H, (Eds), *Advances in polymer science*, **1997**, 127, 144.
4. Pino, P.; Mulhaupt, R.; *Angew. Chem. Int. Ed. Engl.* **1980**, 19, 857.
5. Brintzinger, H. H.; Fischer, D.; Mülhaupt, R.; Rieger, B.; Waymouth, R. M.; *Angew. Chem. Int. Ed. Engl.* **1995**, 34, 1143.
6. Krentsel, B. A.; Kissin, Y. V.; Kleiner, V. I.; Stotskaya, L. L.; *Polymers and copolymers of higher α -olefins*, Hanser/Gardner publishers, Munich, **1997**, p.2.
7. Scheirs, J.; Kaminsky, W.; *Metallocene-based polyolefins*, John Wiley & Sons, **1999**, vol, 2, p. xvii.
8. Wilkinson G; Birmingham I.M.; *J. Am. Chem. Soc.* **1954**, 76, 4281.
9. Shriver, D. F.; Atkins, P. W.; Langford, C. H.; *Inorganic chemistry (2nd Edn)*, Oxford University Press, **1992**, p 660.
10. Wilkinson.; *J. Organometallics. Chem.* **1975**, 100, 273.
11. Ziegler, K.; Holzkamp, E.; Breil, H.; *Angew Chem.* **1955**, 67, 541.
12. Natta, G.; *Angew Chem.* **1956**, 68, 393.
13. Breslow, D.S.; Newburg, N.R.; *J. Am. Chem. Soc.* **1957**, 79, 5072.
14. Reichert, K.H.; Meyer, K.R.; *Makromol. Chem.* **1973**, 169, 163.
15. Andersen, A.; Cordes, H.G.; Herwig, J.; Kaminsky, K.; Merck, A.; Mottweiler, R.; Pein, J.; Sinn, H.; Vollmer, H.J.; *Angew. Chem. Int. Ed. Engl.* **1976**, 15, 630.
16. Sinn, H.; Kaminsky, W.; *Adv. Organomet. Chem.* **1980**, 18, 99.
17. Wild, F. R. W. P.; Zsolnai.; L.; Huttner, G.; Brintzinger, H. H.; *J. Organomet. Chem.* **1982**, 232, 233.
18. Ewen, J. A.; Jones, R. L.; Razavi, A.; Ferrara, J. P.; *J. Am. Chem. Soc.* **1988**, 4, 417.
19. Murray, M. C.; Baird, M. C.; *J. Mol. Catal. A: Chem.* **1998**, 128, 1.
20. Tagge, C. D.; Kravchenko, R. L.; Lal, T. K.; Waymouth, R. M.; *Organometallics* **1999**, 18, 380.
21. Bruce, M. D.; Waymouth, R. M.; *Macromolecules* **1998**, 18, 2707.

-
22. Kaminsky, W.; Bark, A.; Spiehl, R.; Moller-Lindenhof, N.; Niedoba, S.; in Sinn, H.; and Kaminsky, W. (Eds), *Transition metals and organometallics as catalysts for olefin polymerisation*, Springer, Berlin, **1988**, p. 291.
 23. Kaminsky, W.; and Steiger, R.; *Polyhedron* **1988**, 7, 2375.
 24. Kaminsky, W.; Spiehl, R.; *Makromol. Chem.* **1989**, 190, 515.
 25. Resconi, L.; Waymouth, R. M.; *J. Am. Chem. Soc.* **1990**, 112, 5953.
 26. Resconi, L.; Coates, G. W.; Mogstad, A.; Waymouth, R. M.; *J. Macromol. Sci. Chem. Ed.* **1991**, A28.1255.
 27. Kesti, M. R.; Waymouth, R. M.; *J. Am. Chem. Soc.* **1991**, 114, 3565.
 28. Arndt, M.; Engehausen, R.; Kaminsky, W.; Zoumis, K.; *J. Mol. Catal. A: Chem.* **1995**, 101, 171.
 29. Arndt, M.; Kaminsky, W.; *Makromol. Symp.* **1995**, 97, 225.
 30. Hlatky, G. G.; Upton, D. J.; Tuner, H. W.; *Chem Abstr*, **1991**, 115, 256897v.
 31. Yang, X.; Stern, C. L.; Marks, T. J.; *Organometallics*, **1991**, 10, 840
 32. Zambelli, A.; Grassi, A.; Luongo, P.; *Macromolecules*, **1989**, 22, 2186.
 33. Sinn, H.; Bliemeister, J.; Clausnitzer, D.; Tikwe, L.; Winter, H.; Zarncke, O; In: Kaminsky, W; Sinn, H. (Eds), *Transition metals and organometallics as catalysts for olefin polymerization*. Springer, Berlin, **1988**, p 257.
 34. Piccolrovazzi, N.; Pino, P.; Consiglio, G.; Sironi, A.; Moret, M.; *Organometallics* **1989**, 9, 3098.
 35. Resconi, L.; Bossi, S.; Abis, L.; *Macromolecules* **1990**, 23, 4489.
 36. Cam, D.; Giannini, U.; *Makromol Chem* **1992**, 193, 1049.
 37. Siedle, A.R.; Newmark, R. A.; Lamanna, W. M.; Schroepfer, J. N; *Polyhedron* **1990**, 9, 301.
 38. Tritto, I., Li, S.; Sacchi, M.C.; Zannoni, G.; *Macromolecules* **1993**, 26, 7111.
 39. Eisch, J. J.; Pombick, S. I.; Zheng, G. X.; *Organometallics* **1993**, 12, 3856.
 40. Gassmann, G. P.; Callstrom, M. R.; *J. Am. Chem. Soc.* **1987**, 109, 7875.
 41. Shista, C.; Harton, R.M.; Marks, T. J.; *J. Am. Chem. Soc.* **1992**, 114, 1112
 42. Hlatky, G. G.; Upton, D. J.; Tuner, H. W.; *Chem Abstr.* **1991**, 115, 256897v.
 43. Yang, X.; Stern, C. L.; Marks, T. J.; *Organometallics* **1991**, 10, 840.

-
44. Zambelli, A.; Grassi, A.; Luongo, P.; *Macromolecules* **1989**, 22, 2186.
 45. Kaminsky, W.; Arndt, M.; In *Advances in polymer science* **1997**, 127, p 148.
 46. Chien, J. C. W.; Tsai, W. M.; Rausch, M. D.; *J. Am. Chem. Soc.* **1991**, 113, 8570.
 47. Bochmann M.; Lancaster, S. J.; *Organometallics* **1993**, 12, 633.
 48. Bochmann M.; Lancaster, S. J.; *Angew. Chem* **1994**, 106, 1715 ; *Angew. Chem Int. Ed. Engl.*, 33, 1634.
 49. Kaminsky, W.; Bark, A.; Steiger, R.; *J. Mol. Catal.* **1992**, 74, 109.
 50. Tritto, I., Li, S.; Sacchi, M.C.; Zannoni, G.; *Macromolecules* **1993**, 26, 7111.
 51. Jordaan, R.F.; Bajgur, C. S.; Willet, R.; Scott, B.; *J. Am. Chem. Soc.* **1986**, 108, 7410.
 52. Jordaan, R.F.; *Adv. Organomet. Chem.* **1991**, 32, 325.
 53. More, E.P, Jnr.; *Polypropylene Handbook*, **1996**, p 49.
 54. Siedle, A. R.; Lammana, W.N., Newmark, R. A.; *Makromol. Chem. Macromol. Symp.* **1993**, 66, 215.
 55. Shista, C.; Harton, R.M.; Marks, T. J.; *J. Am. Chem. Soc.* **1992**, 114, 1112.
 56. Michelotti, M.; Altomare, A.; Ciardelli, F.; *Polymer* **1996**, 22, 5011.
 57. Boor, J; *Ziegler-Natta Catalysts and Polymerisation*. Academic Press, New York, **1979**, p. 21.
 58. Kissin, Y.V. *Isospecific polymerization of olefins with heterogeneous Ziegler-Natta catalysts*. Springer-Verlag, New York, **1985**, p. 597.
 59. Kissin, Y. V. *Adv. Polym. Sci.* **1974**, 15, 91.
 60. Paukkeri, R.; Lehtinen, A.; *Polymer* **1993**, 34(16), 4083.
 61. Martuscelli, E.; Pracella, M.; Crispino, L.; *Polymer* **1983**, 24, 693.
 62. Martuscelli, E.; Avella, M.; Segre, A.; Rossi, E.; Drusco, G.; Galli, P.; Simonazzi, T.; *Polymer* **1985**, 26, 259.
 63. Burfield, D.; Loi, P.; *J. Appl. Polym. Sci.* **1990**, 41, 1095.
 64. Janimak, J.; Cheng, S.; Zhang, A.; Hsieh, E.; *Polymer* **1992**, 33, 729.
 65. Luongo J, *J. Appl. Polym. Sci.* **1960**, 3, 302.
 66. Inoue, Y.; Itabashi, Y.; Chujo, R.; Doi, Y.; *Polymer* **1984**, 25, 1640.
 67. Busico, V.; Corradini, P.; De Martino, L.; Graziano, F.; Iadicicco, A.; *Makromol. Chem.* **1991**, 192, 49.

-
68. Kakugo, M.; Miyatake, T.; Naito, Y.; Mizunuma, K.; *Macromolecules* **1998**, 30, 314,
69. Hayashi, Y.; Inoue, Y.; Chujo, R.; Doi, Y.; *Polymer* **1989**, 30, 1640.
70. Dharmarajan, N. R.; Yu, T. C.; *Metallocenes catalysed polymers, Published by Plastics Design Library Inc.* **1998**, p. 127.
71. Erker, G.; *Chem. Ber.* **1991**, 124, 1301.
72. Erker, G.; Nolte, R.; Aul, R.; Wiker, S.; Kruger, C.; Noe, R.; *J. Am. Chem. Soc.* **1991**, 113, 7594.
73. Erker, G.; Aulbach, M.; Knickmeier, M.; Wingbermuehle, D.; Kruger, C.; Nolte, R.; Werner, S.; *J. Am. Chem. Soc.* **1993**, 115, 4590.
74. Erker, G.; Temme, B.; *J. Am. Chem. Soc.* **1992**, 114, 4004.
75. Erker, G.; *Pure and Applied Chem.* **1992**, 64, 393.
76. Natta, G.; Farina, M.; Peraldo, M.; *Chim. Ind. (Paris)* **1960**, 42, 255.
77. Miyazawa, T.; Ideguchi, Y.; *J. Polym. Sci. Part B.* **1963**, 1, 389.
78. Zambelli, A.; Giongo, M. G.; Natta, G.; *Makromol. Chem.* **1968**, 112, 183.
79. Zambelli, A.; Gatta, G.; Sacchi, C.; Crain, Jr, W. O.; Roberts, J. D.; *Macromolecules* **1971**, 4, 475
80. Crain, Jr, W. O.; Zambelli, A.; *Macromolecules* **1971**, 4, 330.
81. Zambelli, A.; Tosi.; *Adv. Polym. Sci.* **1974**, 15, 31.
82. Zambelli, A.; Tosi.; *Adv. Polym. Sci.* **1974**, 25, 32.
83. Corradini, P.; Barone, V.; Fusco, R.; Guerra, G.; *Eur. Polym. J.* **1979**, 15, 1133.
84. Corradini, P.; Guerra, G.; Fusco, R.; Barone, V.; *Eur. Polym. J.* **1980**, 16, 835.
85. Corradini, P.; Barone, V.; Fusco, R.; Guerra, G.; *J. Catal* **1982**, 77, 32.
86. Corradini, P.; Barone, V.; Guerra, G.; *Macromolecules* **1982**, 15, 1242.
87. Zambelli, A.; Sacchi, C.; Locatelli, P.; Zannoni, G.; *Macromolecules* **1982**, 15, 211.
88. Zambelli, A.; Locatelli, P.; Sacchi, C.; Tritto, I.; *Macromolecules* **1982**, 15, 831.
89. Zambelli, A.; Ammendola, P.; Sacchi, C.; Locatelli, P.; *NMR and macromolecules*, J. C. Randall (ed), ACS. Symp, Ser. **1984**, 274, p 223.
90. Ewen, J. Aelder, M. J.; *Eur. Pat. Appl.* **1993**, Ep-A 0537 130
91. Ewen, J. A.; Jones, R. L.; Razavi, A.; Ferrara, J. D.; *J. Am. Chem. Soc.* **1988**, 110, 6255.

-
92. Frisch, H. L.; Mallows, C. L.; Bovey, F. A.; *J. Chem. Phys.* **1966**, 45, 1565.
93. Reiger, B.; Chien, J. C. W.; *Polym. Bull.* **1989**, 21, 159.
94. Reiger, B.; Mu, X.; Mallin, D. T.; Rausch, M. D.; Chien, J. C. W.; *Macromolecules* **1990**, 23, 3559.
95. Toyota, A.; Tsutsui, T.; Kashiwa, N.; *J. Mol. Cat.* **1989**, 56, 237.
96. Kioka, M.; Tsutsui, T.; Ueda, T.; Toyota, A.; Kashiwa, N.; *Stud. Surf. Sci. Catal.* **1990**, 56, 483.
97. Soga, K.; Shiono, T.; Takemura, S.; Kaminsky, W.; *Makromol. Chem. Rapid. Commun* **1987**, 8, 305.
98. Grassi, A.; Zambelli, A.; Resconi, L.; Albizzati, E.; Mazzocchi, R.; *Macromolecules* **1988**, 21, 617.
99. Grassi, A.; Ammendola, P.; Longo, E.; Albizzati, E.; Resconi, L.; Mazzocchi, R.; *Gazz. Chim. Ital.* **1988**, 118, 539.
100. Tsutsui, T.; Mizuno, A.; Kashiwa, N.; *Makromol. Chem.* **1989**, 190, 1177.
101. Asakura, T.; Nakayama, N.; Demura, M.; Asano, A.; *Macromolecules* **1992**, 25, 4876.
102. Moore, E. P., Jr.; *Propylene handboock*, **1996**, p 60.
103. Bovey, F. A.; *High resolution NMR of macromolecules*, Academic Press, New York, **1972**, p. 123.
104. Zambelli, A.; Locatelli, P.; Bajo, B.; Bovey, F. A.; *Macromolecules* **1975**, 8, 687.
105. Randall, J. C.; Woodward, A. E.; Bovey, A. E. (Eds); *Polymer characterization by NMR and ESR.*; Press, New York, **1987**; (ACS Symp. Ser. **1980**, p.142).
106. Farina, M.; *Top. Stereochem.* **1987**, 17, 1.
107. Tonelli, A. E.; *NMR spectroscopy and polymer microstructure*, VCH, Weinheim, **1989**, p. 73.
108. Koenig, J. L.; *Spectroscopy of polymers*, American Chemical Society, Washington, **1991**, p. 48.
109. Kashiwa, N.; *Polymer* **1980**, 12, 603.
110. Kashiwa, N.; Yoshitake, J.; *Makromol. Chem.* **1984**, 185, 1133.
111. Galli, P.; Haylock, J. C.; *Prog. Polym. Sci.* **1991**, 16, 303.

-
112. Galli, P.; Haylock, J. C.; *Makromol. Chem.* **1992**, 63, 19.
113. Kaminsky, W.; Kulper, K.; Brintzinger, H. H.; Wild, F. R. W. P.; *Angew. Chem.* **1985**, 97, 507.
114. Kaminsky, W.; Kulper, K.; Brintzinger, H. H.; Wild, F. R. W. P.; *Angew. Chem. Int. Ed. Engl.* **1985**, 25, 507.
115. Monrabal, B.; *J. Appl. Polym. Sci.* **1994**, 52, 491.

CHAPTER 3

SYNTHESIS AND CHARACTERISATION OF METALLOCENE-CATALYZED RANDOM PROPENE/LINEAR α -OLEFIN COPOLYMERS

Abstract

The synthesis of random propene copolymers with 1-butene, 1-pentene, 1-hexene was carried out using the isospecific $\text{Me}_2\text{Si}(2\text{-Methylbenz[e]indenyl})_2\text{ZrCl}_2/\text{MAO}$ catalyst system. The resulting copolymers were characterized by NMR, GPC, CRYSTAF and DSC. All copolymers possessed high molecular weights (ranging from 300,000 to 700,000 $\text{g}\cdot\text{mol}^{-1}$) and narrow molecular weight distributions ($M_w/M_n \approx 2$). Comonomer incorporation was generally kept below 6 %. The influence of comonomer content and type on stereoregularity was investigated. The [mmmm] ratio decreased with increasing comonomer content for each comonomer used. Melting and crystallization temperatures decreased with increasing comonomer content.

3.1 Introduction

The copolymerization of propene with α -olefins via metallocene catalysts allows the synthesis of random propene copolymers with a great variety of properties. The use of metallocene catalyst systems allows control of molecular weight, molecular weight distribution, stereo regularity and comonomer incorporation.

A disadvantage of using typical Ziegler-Natta catalyst systems for the copolymerization of propene with α -olefins is poor reactivity of the α -olefins towards these catalyst systems¹. The discovery of metallocene/MAO catalysts led to the successful copolymerization of propene with bulky comonomers of up to 18 carbons as well as cyclic comonomers²⁻⁷. It has been shown that *ansa*-metallocenes, particularly substituted ones, are most effective in the copolymerization of propene and α -olefins⁸⁻¹¹.

Melting point and crystallinity of highly isotactic polypropene are lowered by incorporation of comonomer units. Small amounts of comonomer incorporated in the copolymer can influence the thermal properties significantly as was reported for propene/ethylene copolymers¹².

Copolymerization of propene with higher α -olefins (C₆-C₁₈) produces copolymers with properties ranging from thermoplastic polymers to properties of typical rubbers^{13,14}. Our research group investigated melting and crystallization behaviour of random propene/higher α -olefins (1-octene, 1-decene, 1-tetradecene and 1-octadecene) copolymers synthesized by both isospecific and syndiospecific catalyst systems¹⁵⁻¹⁸.

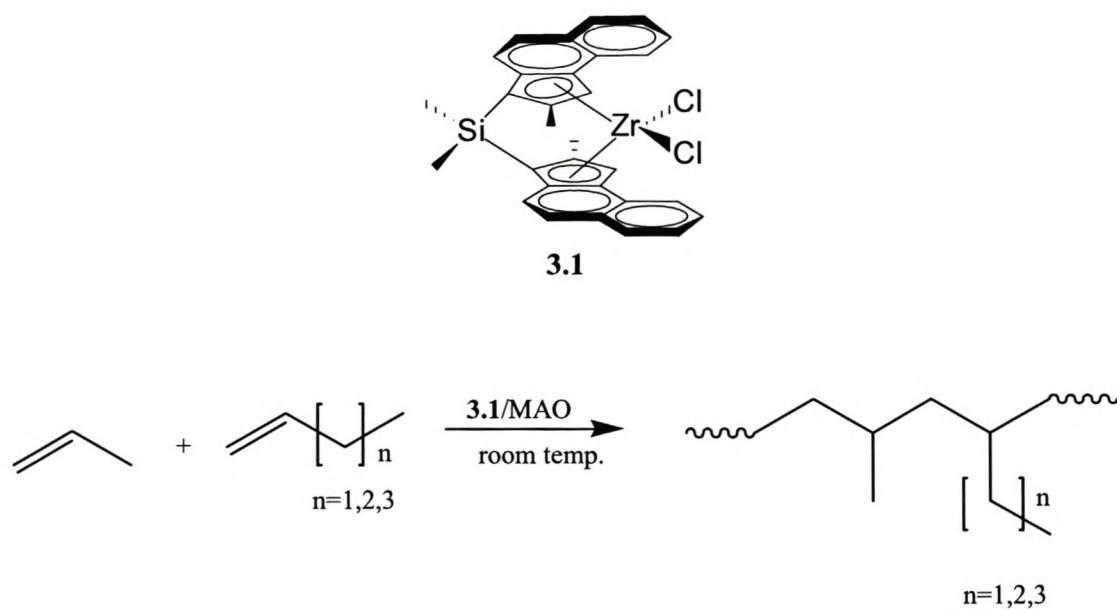
These investigations indicated a linear dependence of both melting and crystallization temperature on comonomer content of the copolymer. Melting and crystallization temperature decreased linearly with increase of the comonomer content, but were independent of the comonomer type.

As part of an ongoing investigation, random copolymers of propene/linear α -olefins (1-butene, 1-pentene and 1-hexene) were synthesized utilizing $\text{Me}_2\text{Si}(2\text{-Methylbenz[e]indenyl})_2\text{ZrCl}_2/\text{MAO}$.

Properties such as structure, microstructure, comonomer content, molecular weight, melting and crystallization behaviour of the synthesized propene/ α -olefin copolymers were characterized by NMR, GPC, DSC and CRYSTAF.

3.2 Reaction scheme

The copolymerization of propene with 1-butene, 1-pentene, 1-hexene was carried out using the constrained geometry catalyst, $(\text{CH}_3)_2\text{Si}(2\text{-methylbenz[e]indenyl})_2\text{ZrCl}_2$ (**3.1**) (Scheme 3.1).



Scheme 3.1: General reaction scheme for the copolymerisation of propene with linear α -olefins

3.3 Experimental

3.3.1 Materials and methods

3.3.1.1 Purification of reagents

Propene, polymerization grade, was obtained from Fedgas and purified by passing through a column containing BASF catalyst R 3-12. Toluene was dried by refluxing over sodium/benzophenone and then distilled under inert gas. Methylaluminoxane was purchased from Sigma-Aldrich and used without further purification (10 % solution in toluene). 1-Butene was purchased from Sigma-Aldrich and used without further purification. 1-Pentene and 1-hexene, received from SASOL, were dried over CaCl_2 prior to distillation. They were then refluxed and distilled over CaCl_2 and LiAlH respectively for 5 hours. The catalyst used, $(\text{CH}_3)_2\text{Si}(2\text{-methylbenz[e]indenyl})_2\text{ZrCl}_2$, was obtained from Boulder Scientific.

3.3.1.2 Copolymerization procedures

All reactions were carried out under inert gas atmosphere using standard Schlenk techniques. The polymerization reactions were carried out in a 350 mL stainless steel Parr autoclave with inlet and pressure gauge. A glass liner was used. Typically the reactor was charged in an inert atmosphere with catalyst ($8\mu\text{ mol}$ in 10 mL of toluene), MAO (10 % solution in toluene) and 50 mL toluene. The catalyst solution was stirred for 5 min. and the comonomer was added. Subsequently, the reactor was pressurized with propene and stirred for 3 hours at room temperature. The catalyst/MAO ratio was kept at 1: 6000 for all reactions.

After 3h the reaction was quenched with 10 % HCl/MeOH . The resulting polymer was filtered off, washed several times with methanol and subsequently dried in a vacuum oven at $80\text{ }^\circ\text{C}$ for 15h.

Experimental parameters for the copolymerization reactions performed under the above conditions are summarized in Table 3.1.

Table 3.1 Experimental parameters^{a,b} and results for propene/ α -olefin copolymers.

| Entry No. | Comonomer | Sample No | Comonomer [mol-%] in feed | Comonomer [mol-%] in copolymer. | Yield (g) | Molecular Weight (M_w) | M_w/M_n |
|-----------|-----------|-----------|---------------------------|---------------------------------|-----------|----------------------------|-----------|
| 1 | None | - | - | - | 15.30 | 460700 | 2.8 |
| 2 | 1-butene | 4.8 | n.a | 5.66 | 1.03 | 540400 | 2.1 |
| 3 | | 4.1 | n.a | 4.43 | 1.90 | 582500 | 2.1 |
| 4 | | 4.3 | n.a | 2.63 | 11.06 | 343200 | 2.4 |
| 5 | | 4.11 | n.a | 2.57 | 3.03 | 394500 | 2.1 |
| 6 | | 4.9 | n.a | 1.43 | 26.85 | 320600 | 3.3 |
| 7 | | 4.10 | n.a | 0.56 | 2.77 | 673700 | 2.4 |
| 8 | | 4.2 | n.a | 0.45 | 7.41 | 222800 | 2.5 |
| 9 | | 1-pentene | 5.32 | 9.84 | 4.16 | 0.92 | 509600 |
| 10 | 5.38 | | 9.17 | 4.13 | 0.49 | 519200 | 2.3 |
| 11 | 5.37 | | 6.67 | 3.10 | 0.93 | 622200 | 2.4 |
| 12 | 5.33 | | 5.83 | 2.58 | 1.56 | 694300 | 2.5 |
| 13 | 5.27 | | 4.80 | 2.10 | 2.95 | 486400 | 2.5 |
| 14 | 5.26 | | 2.92 | 1.49 | 1.29 | 390500 | 2.6 |
| 15 | 5.34 | | 2.04 | 1.16 | 1.22 | 750200 | 2.0 |
| 16 | 5.24 | | 1.57 | 0.41 | 2.89 | 460400 | 2.5 |
| 17 | 1-hexene | 6.7 | 5.36 | 2.53 | 5.10 | 574400 | 2.2 |
| 18 | | 6.8 | 5.78 | 2.28 | 5.80 | 572800 | 2.3 |
| 19 | | 6.9 | 4.19 | 1.71 | 2.10 | 395100 | 2.2 |
| 20 | | 6.6 | 3.52 | 1.36 | 5.50 | 520100 | 2.2 |
| 21 | | 6.5 | 2.72 | 1.17 | 7.40 | 331600 | 2.0 |
| 22 | | 6.4 | 2.17 | 1.01 | 4.90 | 343000 | 2.2 |
| 23 | | 6.2 | 1.16 | 0.58 | 4.30 | 339900 | 2.1 |
| 24 | | 6.1 | 0.70 | 0.35 | 3.30 | 422100 | 2.1 |

^a MAO/catalyst:ratio = 6000

^b room temperature

3.3.2 Analytical techniques for the characterization of the propene/ α -olefin copolymers

3.3.2.1 NMR measurements

NMR spectra (^{13}C NMR) were recorded at 100 $^{\circ}\text{C}$ on a Varian VXR 300 in a 9:1 mixture of 1,2,4-trichlorobenzene/ C_6D_6 , using C_6D_6 at $\delta 127.9$ as internal secondary reference. The pulse angle was 45 degrees and the repetition time 0.82 seconds. Calibration

spectrum: In order to calculate the degree of error involved, a gated proton decoupling experiment (decoupler gated experiments off for 4.2 seconds) with a long repetition time of 5.02 seconds was conducted.

3.3.2.2 DSC measurements

DSC measurements were carried out on a Pyris 1 from Perkin Elmer. Three cycles were performed for each sample. Firstly the samples (about 10mg) were heated in cramped aluminium pans from $-50\text{ }^{\circ}\text{C}$ to $180\text{ }^{\circ}\text{C}$ at a rate of $10\text{ }^{\circ}\text{C}/\text{min}$. Secondly, they were cooled from $180\text{ }^{\circ}\text{C}$ to $-50\text{ }^{\circ}\text{C}$. The crystallization temperature, T_c (DSC), from the maximum of the endotherm, was determined from the cooling cycle. Lastly, the copolymers were heated for the second time at $10\text{ }^{\circ}\text{C}/\text{min}$ to $180\text{ }^{\circ}\text{C}$. This was done to determine the melting temperature T_m from the maximum of the second heating cycle.

3.3.2.3 CRYSTAF measurements

Crystallization analysis fractionation was carried out using a CRYSTAF commercial apparatus model 200 manufactured by Polymer Char S.A. (Valencia, Spain). The crystallization was carried out in stirred stainless steel reactors of 60 mL volume where dissolution and filtration takes place automatically. About 20 mg of a sample were dissolved in 30 mL 1,2,4-trichlorobenzene. The temperature was decreased at a rate of $0.10\text{ }^{\circ}\text{C}/\text{min}$ from $100\text{ }^{\circ}\text{C}$ to $30\text{ }^{\circ}\text{C}$. Fractions were taken automatically and the polymer concentration from solution was determined by an infrared detector using 3.5μ as the chosen wavelength.

3.3.2.4 GPC measurements

Molecular weights were determined using gel permeation chromatography. The measurements were performed at a flow rate of $1.06\text{ mL}/\text{min}$ in 1,2,4-trichlorobenzene at $140\text{ }^{\circ}\text{C}$ using a Waters 150 C high temperature GPC system. A polystyrene calibration curve was used for all molecular weights determinations.

3.4 Results and discussion

All copolymers (Table 3.1) have high molecular weights (M_w) and narrow molecular weight distributions as expected for metallocene catalysts. The molecular weights (M_w) ranged between 300,000 and 700,000 $\text{g}\cdot\text{mol}^{-1}$. The ^{13}C NMR spectra of propene/ α -olefin copolymers with low comonomer content are shown in Figure 3.1 (a, b, c).

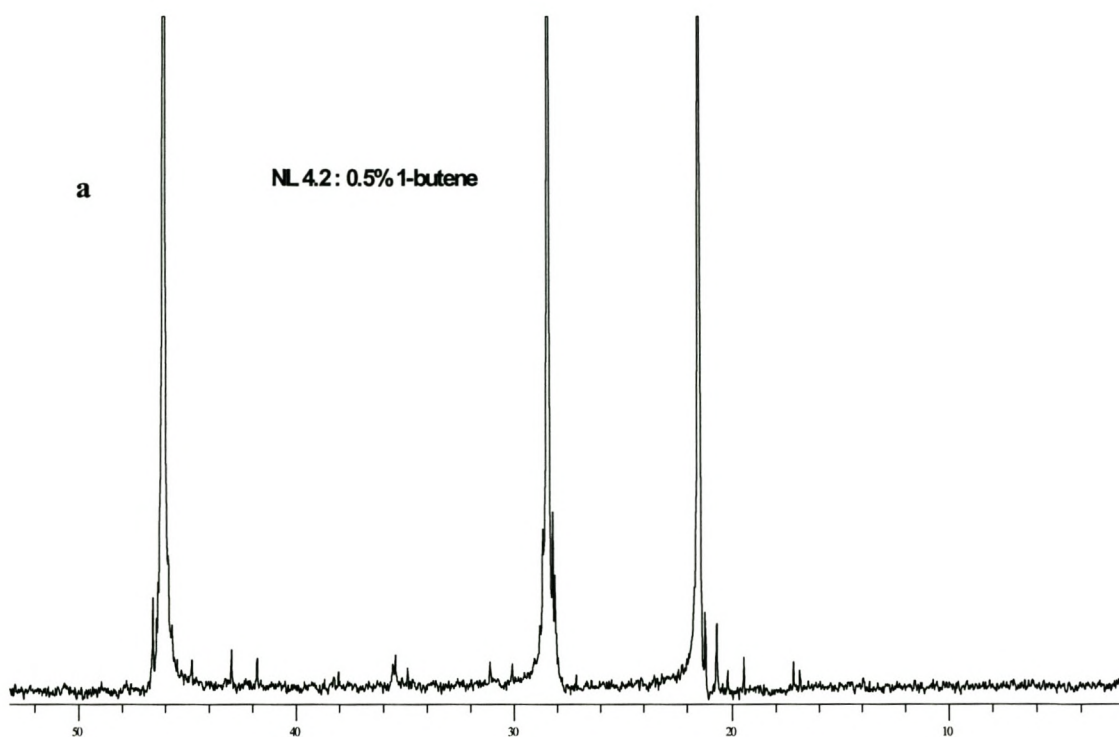


Figure 3.1(a) ^{13}C NMR spectrum of propene/1-butene copolymers

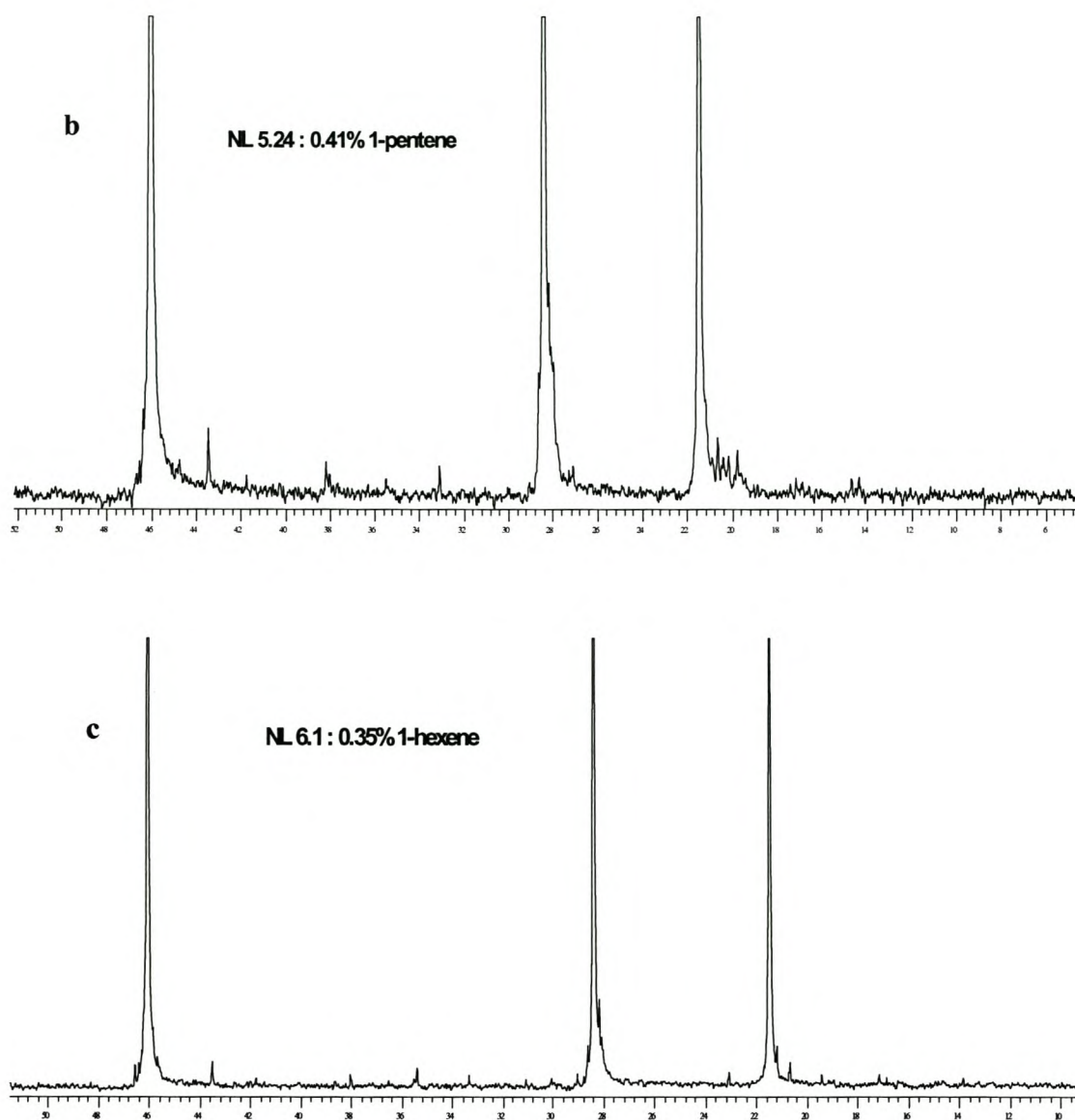


Figure 3.1(b and c) ¹³C NMR spectrum of propene/1-pentene(b) and 1-hexene(c) copolymers

Three prominent peaks that appear at approximately δ 21, δ 28, δ 46 correspond to the methyl, methylene and methine carbons respectively. The small peaks correspond to the carbons from the respective comonomer. Details on the full assignment of these peaks will be the subject of the following section.

The spectra shown in Figure 3.1 (a, b, c) are of copolymers of propene with higher comonomer content. Spectra of copolymers with lower comonomer content, have very

small peaks that are difficult to assign and also to integrate because they interfere with instrumental noise.

3.4.1 The assignment of ^{13}C NMR data

There are very few publications dealing with full ^{13}C NMR spectral assignment of propene/lower α -olefin copolymers. A number of publications discuss ethylene/ α -olefin and propene/ α -olefin copolymers, with the latter components ranging from 1-octene to tetradecene¹⁹⁻²³.

To carry out full ^{13}C NMR characterization, the copolymer backbone was constantly numbered as shown in Figure 3.2^{15,21-29}. For the sake of simplicity, propene/1-hexene will be used as example in all explanations.

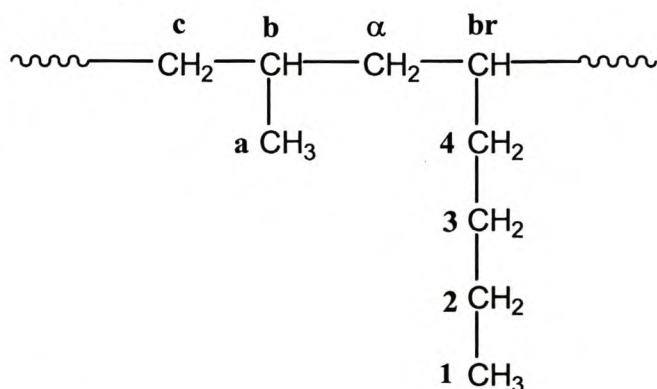


Figure 3.2 The backbone structure of propene/1-hexene copolymer

Several empirical rules were developed to assign the chemical shifts of all the propene/ α -olefins. The most commonly used are the rules developed by Grant and Paul³⁰. Grant and Paul rules allow the calculation of the chemical shift for carbon atoms in different environments. The chemical shift of a particular carbon is given by the sum of the α , β , γ , δ and ϵ constants. These constants are listed in Table 3.2. A correction factor arises from the branches $\{3^\circ(2^\circ), 2^\circ(3^\circ), 1^\circ(3^\circ)\}$ and a constant is also added.

Table 3.2 Chemical shift constants determined by Grant and Paul

| Carbon Position | Chem.Shifts ppm |
|----------------------|-----------------|
| α | 8.61 |
| β | 9.78 |
| γ | -2.88 |
| δ | 0.37 |
| ϵ | 0.06 |
| Const | -1.87 |
| $3^\circ(2^\circ)^a$ | -2.65 |
| $2^\circ(3^\circ)^b$ | -2.45 |
| $1^\circ(3^\circ)^c$ | -1.4 |

In order to calculate or predict the chemical shift of a given carbon atom with the aid of the Grant and Paul rules, the structure of a propene/1-hexene copolymer (Figure 3.2) is considered.

^a $3^\circ(2^\circ)$ = tertiary carbon attached to secondary carbon

^b $2^\circ(3^\circ)$ = secondary carbon attached to tertiary carbon

^c $1^\circ(3^\circ)$ = primary carbon attached to tertiary carbon

The chemical shift of the **a** CH₃ carbon in propene/1-hexene copolymer, for example, is calculated as follows:

$$\begin{aligned} \delta_{(\mathbf{a} \text{ CH}_3)} &= 1*\alpha + 2*\beta + 2*\delta + 2*\gamma + 4*\epsilon + 3^\circ(2^\circ) + 2^\circ(3^\circ) + 1^\circ(3^\circ) + \text{Const.} \\ &= (1*8.61) + (2*9.78) + (2*0.37) + (2*-2.88) + (4*0.06) + (-1.4) + (-1.87) \\ &= 20.8\text{ppm} \end{aligned}$$

The chemical shifts for all propene/ α -olefin copolymers calculated from these empirical rules are listed in Table 3.3.

For some carbons with complicated environments some chemical shifts are only approximate and may further complicate assignment of the peaks.

To avoid ambiguity, rules such as those of Bovey et al. and other available on ChemDraw software, were also used^{31,32}. The values of the chemical shifts obtained from these rules were compared with experimental values and are listed in Table 3.3.

Table 3.3 Chemical shifts for propene/ α -olefin copolymers

Propene/1-Butene

| Carbon | α | β | γ | δ | ϵ | Const | $3^\circ(2^\circ)$ | $2^\circ(3^\circ)$ | $1^\circ(3^\circ)$ | Calculated ^a | BV ^b | Chem Draw ^c | EXP ^d |
|----------|----------|---------|----------|----------|------------|-------|--------------------|--------------------|--------------------|-------------------------|-----------------|------------------------|------------------|
| | 8.61 | 9.78 | -2.88 | 0.37 | 0.06 | -1.87 | -2.65 | -2.45 | -1.4 | ppm | ppm | ppm | ppm |
| a | 1 | 2 | 2 | 4 | 3 | 1 | 0 | 0 | 1 | 20.8 | 21.00 | 20.70 | 21.45 |
| b | 3 | 2 | 4 | 3 | 5 | 1 | 2 | 0 | 0 | 28.11 | 27.90 | 27.30 | 28.40 |
| c | 2 | 4 | 2 | 4 | 3 | 1 | 0 | 2 | 0 | 45.47 | 45.00 | 44.70 | 46.07 |
| α | 2 | 4 | 3 | 4 | 2 | 1 | 0 | 2 | 0 | 42.53 | 42.40 | 42.20 | 42.93 |
| br | 3 | 3 | 4 | 2 | 4 | 1 | 3 | 0 | 0 | 34.81 | 33.25 | 32.70 | 34.84 |
| 1 | 1 | 1 | 2 | 2 | 4 | 1 | 0 | 0 | 0 | 11.74 | 12.20 | 11.80 | 10.69 |
| 2 | 2 | 2 | 2 | 4 | 2 | 1 | 0 | 1 | 0 | 28.3 | 28.60 | 28.40 | 27.92 |

Propene/1-Pentene

| Carbon | α | β | γ | δ | ϵ | Const | $3^\circ(2^\circ)$ | $2^\circ(3^\circ)$ | $1^\circ(3^\circ)$ | Calculated | BV | ChemDraw | EXP |
|----------|----------|---------|----------|----------|------------|-------|--------------------|--------------------|--------------------|------------|-------|----------|-------|
| | 8.61 | 9.78 | -2.88 | 0.37 | 0.06 | -1.87 | -2.65 | -2.45 | -1.4 | ppm | ppm | ppm | ppm |
| a | 1 | 2 | 2 | 4 | 3 | 1 | 0 | 0 | 1 | 20.8 | 21.00 | 21.70 | 21.47 |
| b | 3 | 3 | 4 | 4 | 4 | 1 | 3 | 0 | 0 | 35.55 | 27.90 | 27.30 | 28.39 |
| c | 2 | 4 | 2 | 4 | 3 | 1 | 0 | 0 | 0 | 50.37 | 45.00 | 44.70 | 46.06 |
| α | 2 | 4 | 3 | 5 | 3 | 1 | 0 | 0 | 0 | 47.86 | 42.70 | 42.50 | 43.44 |
| br | 3 | 3 | 5 | 2 | 4 | 1 | 3 | 0 | 0 | 31.93 | 30.75 | 30.20 | 33.08 |
| 1 | 1 | 1 | 1 | 2 | 2 | 1 | 0 | 0 | 0 | 14.5 | 14.50 | 14.30 | 14.31 |
| 2 | 2 | 1 | 2 | 2 | 4 | 1 | 0 | 0 | 0 | 20.35 | 21.30 | 20.90 | 19.76 |
| 3 | 2 | 3 | 2 | 4 | 2 | 1 | 0 | 1 | 0 | 38.08 | 38.00 | 37.80 | 38.15 |

Propene/1-Hexene

| Carbon | α | β | γ | δ | ϵ | Const | $3^\circ(2^\circ)$ | $2^\circ(3^\circ)$ | $1^\circ(3^\circ)$ | Calculated | BV | ChemDraw | EXP |
|----------|----------|---------|----------|----------|------------|-------|--------------------|--------------------|--------------------|------------|-------|----------|-------|
| | 8.61 | 9.78 | -2.88 | 0.37 | 0.06 | -1.87 | -2.65 | -2.45 | -1.4 | ppm | ppm | ppm | ppm |
| a | 1 | 2 | 2 | 4 | 3 | 1 | 0 | 0 | 1 | 20.8 | 21.00 | 20.70 | 21.44 |
| b | 3 | 2 | 4 | 3 | 5 | 1 | 2 | 0 | 0 | 28.11 | 27.90 | 27.30 | 28.40 |
| c | 2 | 4 | 2 | 4 | 3 | 1 | 0 | 2 | 0 | 45.47 | 45.00 | 44.70 | 46.07 |
| α | 2 | 4 | 3 | 5 | 4 | 1 | 0 | 0 | 0 | 47.92 | 42.80 | 42.50 | 43.51 |
| br | 3 | 3 | 5 | 3 | 4 | 1 | 3 | 0 | 0 | 32.3 | 31.05 | 30.50 | 33.36 |
| 1 | 1 | 1 | 1 | 1 | 2 | 1 | 0 | 0 | 0 | 14.13 | 14.20 | 14.00 | 13.80 |
| 2 | 2 | 1 | 1 | 2 | 2 | 1 | 0 | 0 | 0 | 23.11 | 23.60 | 23.40 | 23.05 |
| 3 | 2 | 2 | 2 | 2 | 4 | 1 | 0 | 0 | 0 | 30.13 | 30.70 | 30.30 | 31.39 |
| 4 | 2 | 3 | 3 | 4 | 2 | 1 | 0 | 1 | 0 | 35.2 | 35.50 | 35.30 | 35.39 |

^a Calculated chemical shifts (ref. 30)^b Calculated chemical shifts according Bovey (BV) (ref. 31)^{c, d} Chemical shifts according to ref. 32 and experimental observation respectively.

The spectral peaks of all propene/1-butene, 1-pentene, 1-hexene copolymers were assigned according to the above calculations. As shown in Table 3.3, the values obtained from all empirical rules are in agreement with experimental values within 5 % error. Fully assigned spectra of all the copolymers are shown in Figure 3.3 (a, b, c).

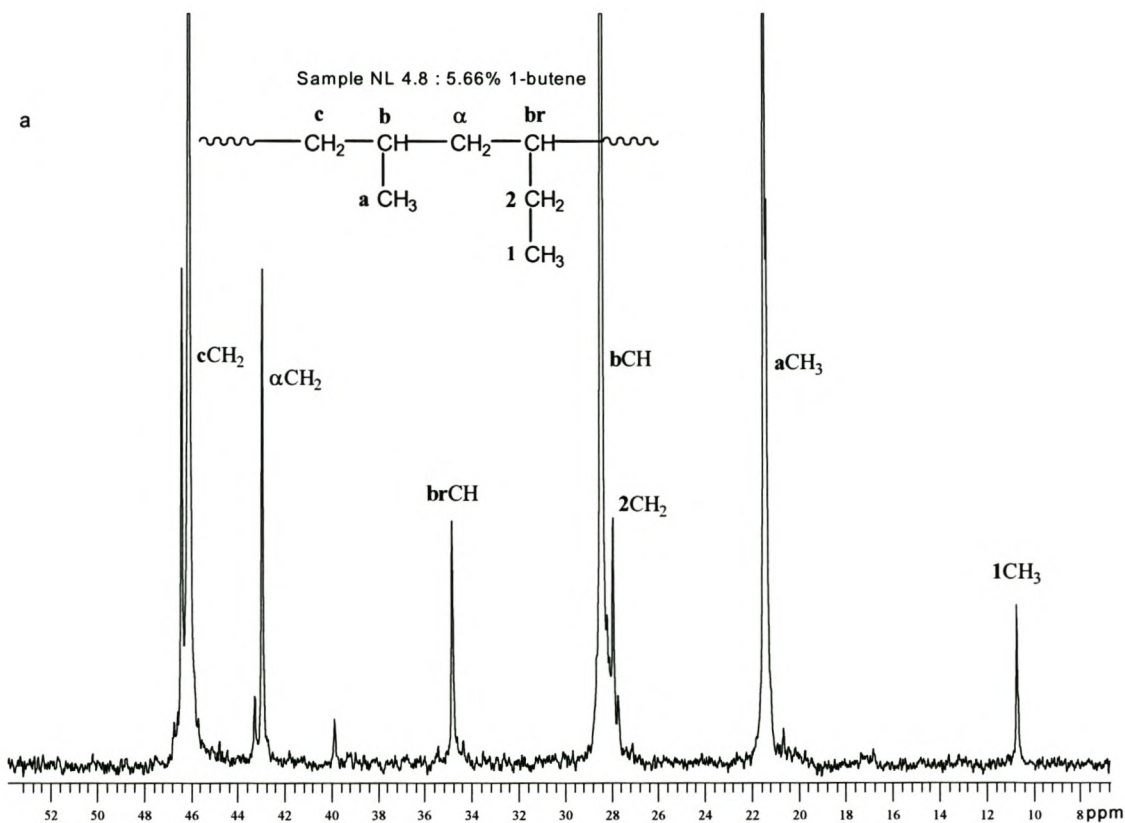


Figure 3.3(a) Assigned ^{13}C NMR spectrum of propene/1-butene copolymers

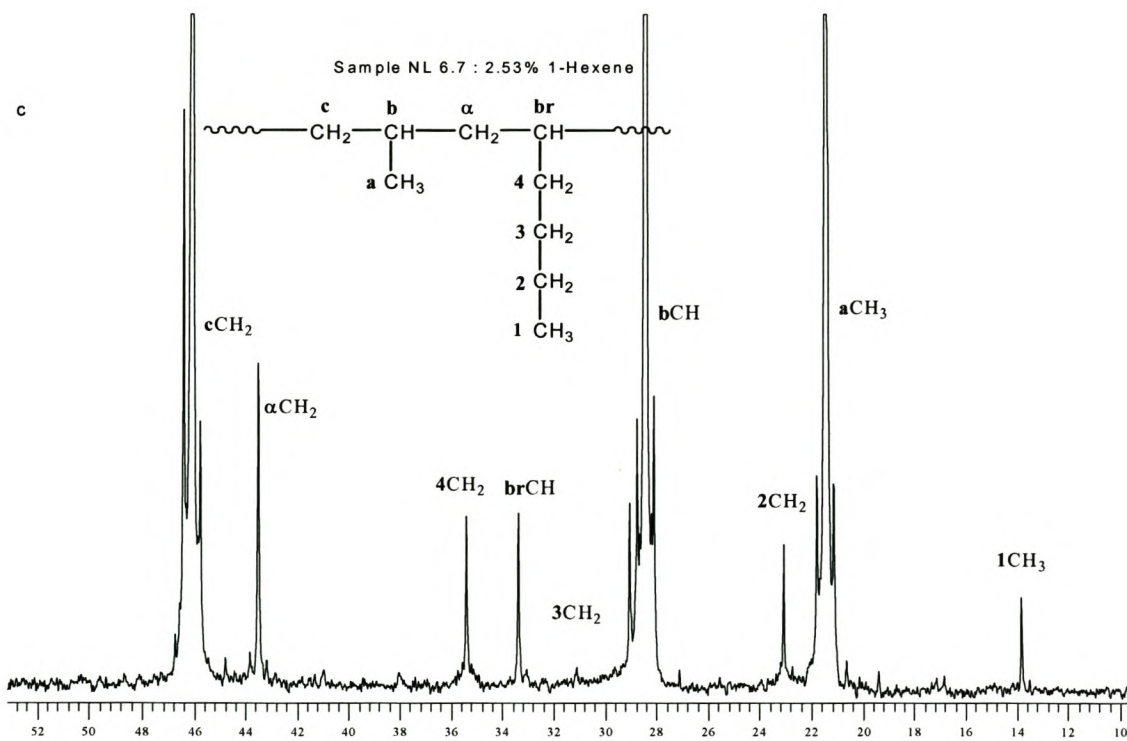
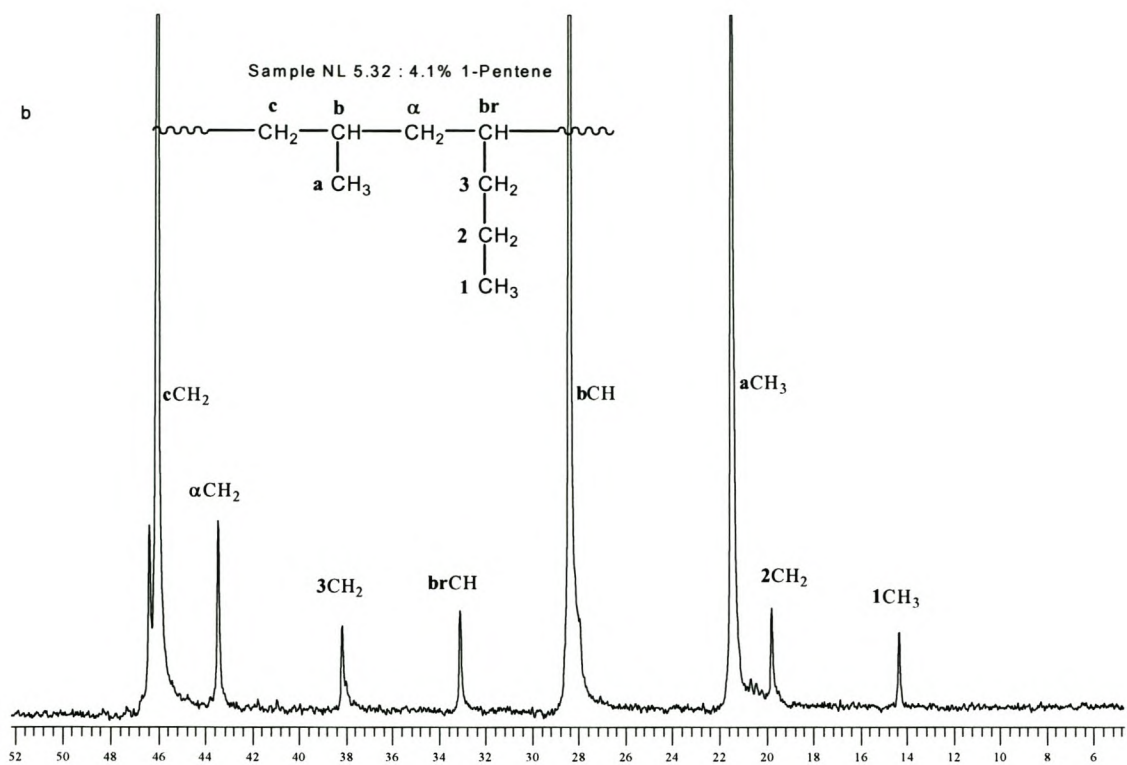


Figure 3.3(b,c) Assigned ^{13}C NMR spectrum of propene/1-pentene (b) and 1-hexene (c) copolymers

The amount of comonomer in the copolymer was determined once all the spectra were fully assigned. Several mathematical formulae exist to calculate comonomer content for ethylene or propylene/ α -olefin copolymers from ^{13}C NMR spectral data^{26-28,33,34}.

Equation 3.1²⁶ was used to calculate the comonomer content of all propylene copolymers.

$$\text{Percentage of comonomer [mol-\%]} = [0.5(I_{\alpha}+I_{br})]/I_T \dots\dots\dots(3.1)$$

Where I_T is the total intensity of the signals of the backbone carbons (**c**, **b**, α and **br**), I_{α} and I_{br} are the intensity of the signals of C_{α} and C_{br} respectively (see Figure 3a, b, c). The results are summarized in Table 3.4.

Table 3.4 Comonomer concentration of propene/ α -olefin copolymers

| Entry No. | Comonomer | Sample No | Comonomer [mol-%] in feed | Comonomer [mol-%] in copolymer. | [mmmm] |
|-----------|-----------|-----------|---------------------------|---------------------------------|--------|
| 1 | None | - | - | - | 0.96 |
| 2 | 1-butene | 4.8 | n.a | 5.66 | 0.69 |
| 3 | | 4.1 | n.a | 4.43 | 0.75 |
| 4 | | 4.3 | n.a | 2.63 | 0.82 |
| 5 | | 4.11 | n.a | 2.57 | 0.83 |
| 6 | | 4.9 | n.a | 1.43 | 0.87 |
| 7 | | 4.10 | n.a | 0.56 | 0.91 |
| 8 | | 4.2 | n.a | 0.45 | 0.94 |
| 9 | 1-pentene | 5.32 | 9.84 | 4.16 | 0.81 |
| 10 | | 5.38 | 9.17 | 4.13 | 0.86 |
| 11 | | 5.37 | 6.67 | 3.10 | 0.88 |
| 12 | | 5.33 | 5.83 | 2.58 | 0.88 |
| 13 | | 5.27 | 4.80 | 2.10 | 0.90 |
| 14 | | 5.26 | 2.92 | 1.49 | 0.93 |
| 15 | | 5.34 | 2.04 | 1.16 | 0.94 |
| 16 | | 5.24 | 1.57 | 0.41 | 0.95 |
| 17 | 1-hexene | 6.7 | 5.36 | 2.53 | 0.80 |
| 18 | | 6.8 | 5.78 | 2.28 | 0.92 |
| 19 | | 6.9 | 4.19 | 1.71 | 0.93 |
| 20 | | 6.6 | 3.52 | 1.36 | 0.93 |
| 21 | | 6.5 | 2.72 | 1.17 | 0.93 |
| 22 | | 6.4 | 2.17 | 1.01 | 0.93 |
| 23 | | 6.2 | 1.16 | 0.58 | 0.90 |
| 24 | | 6.1 | 0.70 | 0.35 | 0.95 |

n.a = not available (could not be quantified).

The comonomer incorporation decreased with increasing comonomer chain length. Up to 5 % 1-butene incorporation in the copolymer was achieved compared to about 4 and 2.5 % for 1-pentene and 1-hexene respectively. This could be attributed to poor reactivity of the comonomer due to steric effects resulting from the increased size of the comonomer chain. A similar trend was observed elsewhere^{15,25,35}.

3.4.2 Microstructure of propene/ α -olefin copolymers

The methyl ^{13}C NMR signals were used to determine the microstructure of propene copolymers.

The expanded region of the methyl signal is shown below (Figure 3.4).

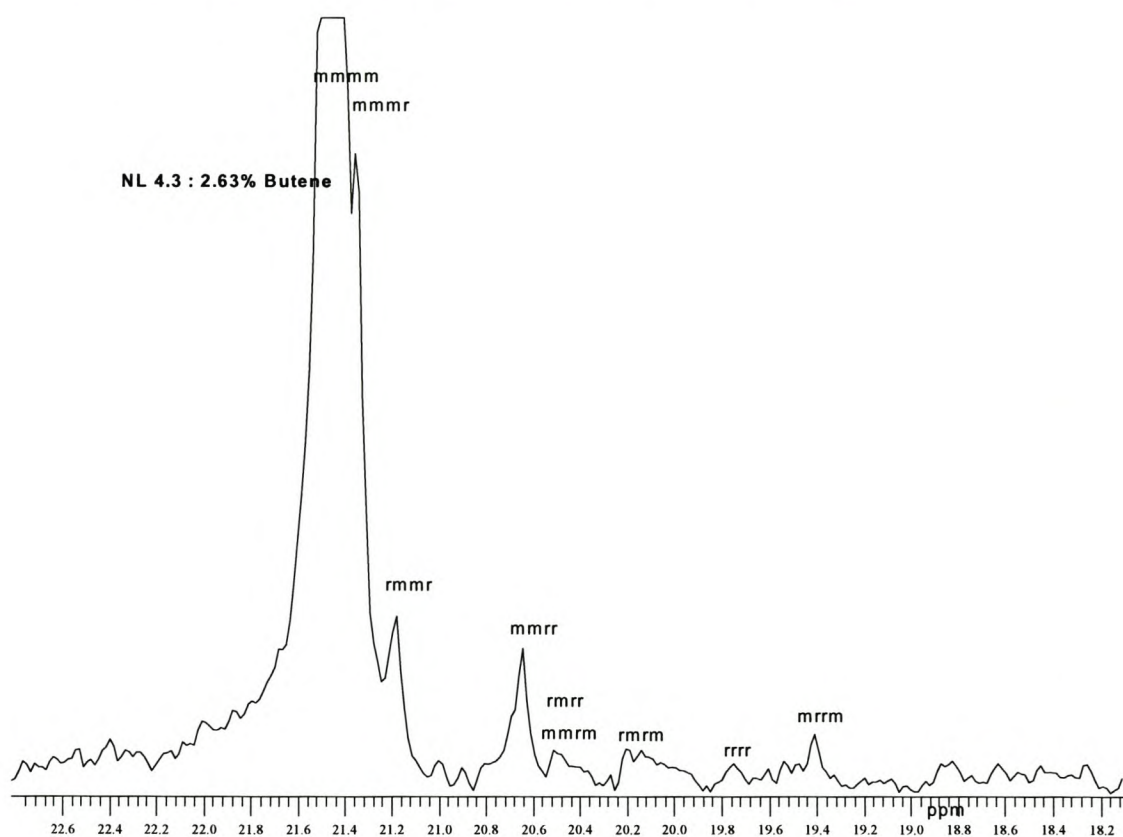


Figure 3.4 Expanded methyl region of propene/1-butene copolymer with pentad assignments

Since the catalyst system 3.1/MAO (Scheme 3.1) used to synthesize all the copolymers produces isotactic polymers, the ratio of the *mmmm* integral to the integral sum of all the other pentad signals in the CH₃ region, was used to determine the degree of isotacticity expressed as [*mmmm*].

The abundance of *mmmm* pentad signals was plotted against comonomer content [mol-%] in the copolymer (Figure 3.5).

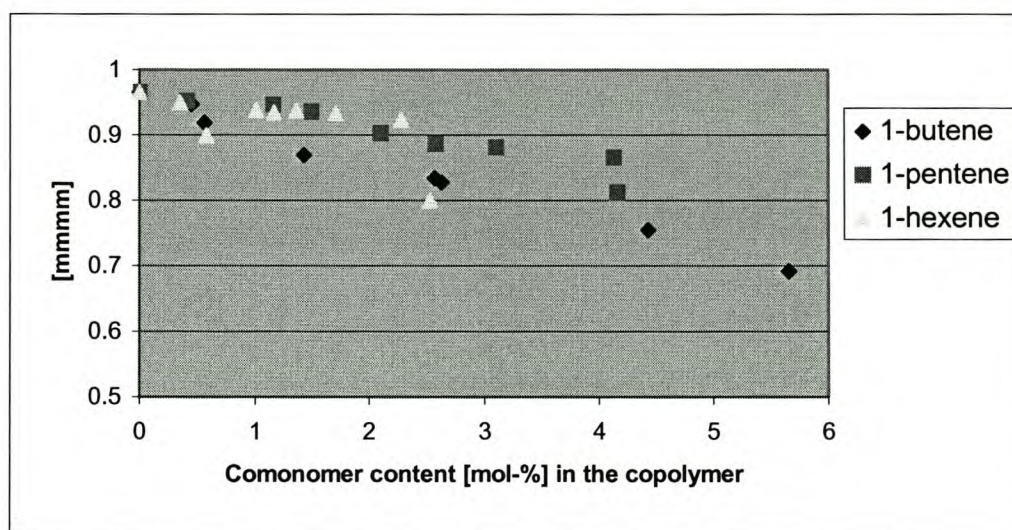


Figure 3.5 Relative intensity (%) of the *mmmm* signal obtained by ¹³C NMR spectroscopy

It is clear that the relative abundance of the *mmmm* signal of all propene copolymers decreased with increase in comonomer content. The effect of the amount of comonomer on stereoregularity is more pronounced for propene/1-butene copolymers than for 1-pentene and hexene. The concentration of the *mmmm* pentad of propene/1-butene series decreased linearly with increase in comonomer content. This could be attributed to the fact that the chain length of 1-butene comonomer is relatively short and as a result could be included in the crystal lattice forming copolymers with clusters³⁶. These observations are confirmed by the presence of an unpredicted resonance at δ 39.85 (Figure 3.6) which was assigned to an isolated CH₂ (BBBB sequence) unit resulting from clustering of 1-butene comonomers.

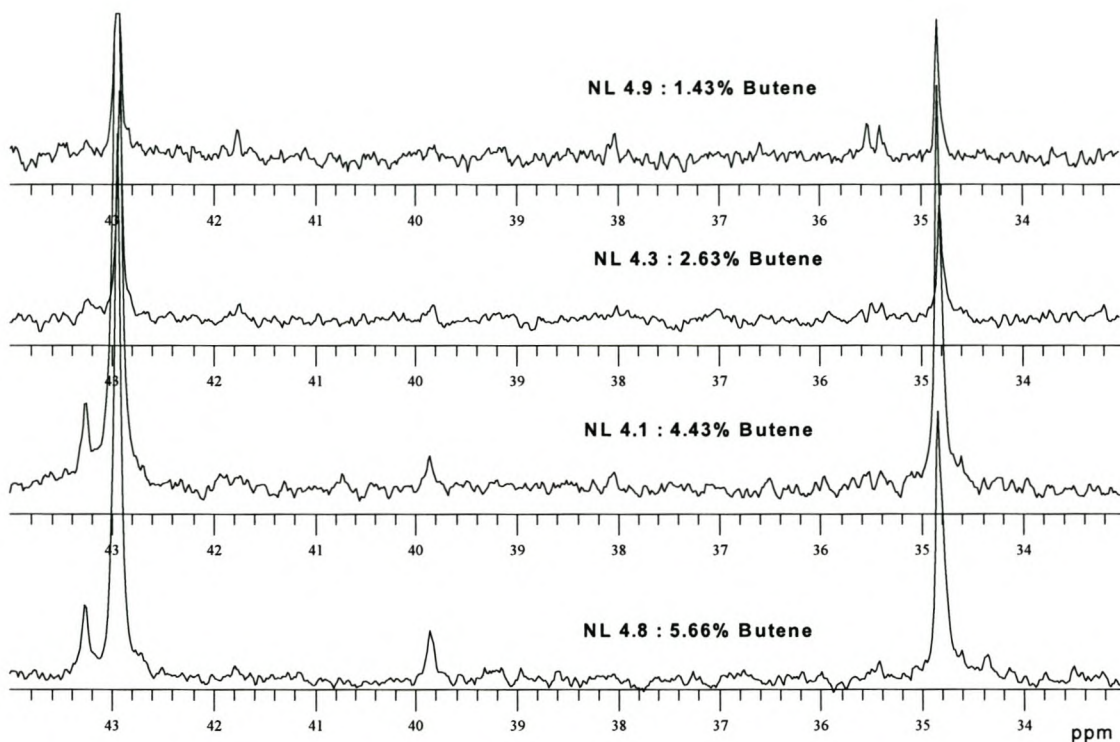


Figure 3.6 The ^{13}C NMR spectral region between $\delta 33 - 44$ for propene/1-butene copolymers

The appearance of a CH_2 signal at $\approx \delta 40$ was observed elsewhere³⁷⁻³⁹. Detailed spectral assignments and comonomer sequences are shown in (Table 3.5). As the chain length of the comonomer increases, the effect of the amount of comonomer on stereoregularity does not play a major role as observed for 1-pentene and 1-hexene (Figure 3.5).

Table 3.5 ^{13}C NMR signals and polymer sequence assignment

| Chemical shift | Assignment (marked with ★) | Polymer sequence |
|----------------|--|------------------|
| 10.60 | ★ $\text{CH}_3\text{—CH}_2\text{—CH}$ | BBB, BBP, PBP |
| 20.67 | ★ $\text{CH}_3\text{—CH}$ | BPB |
| 21.37 | ★ $\text{CH}_3\text{—CH}$ | PPP |
| 27.95 | $\text{CH}_3\text{—}\overset{\star}{\text{C}}\text{H}_2\text{—CH}$ | PBP |
| 28.42 | $\text{CH}_3\text{—}\overset{\star}{\text{C}}\text{H}$ | PPP, PPB, BPB |
| 34.75 | $\text{CH}_3\text{—CH}_2\text{—}\overset{\star}{\text{C}}\text{H}$ | BBB, BBP, PBP |
| 39.85 | $\begin{array}{c} \text{—CH—}\overset{\star}{\text{C}}\text{H}_2\text{—CH} \\ \qquad \qquad \\ \text{Et} \qquad \qquad \text{Et} \end{array}$ | BBBB, BBBP, PBBP |
| 42.99 | $\text{—CH}_2\text{—CH—}\overset{\star}{\text{C}}\text{H}_2\text{—CH} \\ \qquad \qquad \\ \text{Et} \qquad \qquad \text{Et}$ | PBPP |
| 43.34 | $\text{—CH}_2\text{—CH—}\overset{\star}{\text{C}}\text{H—CH} \\ \qquad \qquad \\ \text{Et} \qquad \qquad \text{Et}$ | BBPB, BBPP, PBPB |
| 46.07 | $\begin{array}{c} \text{—CH—}\overset{\star}{\text{C}}\text{H}_2\text{—CH—} \\ \qquad \qquad \\ \text{Me} \qquad \qquad \text{Me} \end{array}$ | PPPB |
| 46.37 | $\begin{array}{c} \text{—CH—}\overset{\star}{\text{C}}\text{H}_2\text{—CH—} \\ \qquad \qquad \\ \text{Me} \qquad \qquad \text{Me} \end{array}$ | BPPB |

3.4.3 Melting and crystallization behaviour of propylene/ α -olefin copolymers

Melting and crystallization behaviour of propene/ α -olefin copolymers were investigated by DSC and CRYSTAF. The analytical procedures followed for the two techniques have been explained in Sections 3.2.2.2 and 3.2.2.3.

3.4.3.1 DSC analysis

As mentioned before, the melting temperature, T_m (DSC), and crystallization temperature from the melt, T_c (DSC), were determined from the second heating cycle. Both T_m (DSC) and T_c (DSC) decreased with increasing comonomer content in the copolymer. Melting and crystallization temperatures of propene/1-butene were higher than these of propene/1-hexene. Propene/1-pentene exhibited intermediate behaviour. Melting and crystallization behaviour of propene/ α -olefin copolymers are discussed in detail in Chapter 5.

3.4.3.2 CRYSTAF analysis

The crystallization analysis fractionation (CRYSTAF) technique was recently developed to analyze composition of semicrystalline polymers⁴⁰. CRYSTAF is based on the analysis of the concentration of the polymer in the liquid phase during crystallization. Typical results from CRYSTAF consist of two curves (Figure 3.7) accompanied by sample data. The sample under investigation is dissolved at a temperature above its crystallization temperature. After complete dissolution the temperature of the solution is lowered while the concentration of the polymer is monitored by a detector. At this stage the sample has a constant concentration equal to the initial polymer solution concentration (Section A). Upon cooling, the crystalline fractions with few or no branches will crystallize first, followed by fractions with increased branch content (Section B). Section C represents a fraction that has not crystallized. Curve 1 corresponds to cumulative SCBD and curve 2 corresponds to the first derivative of curve 1.

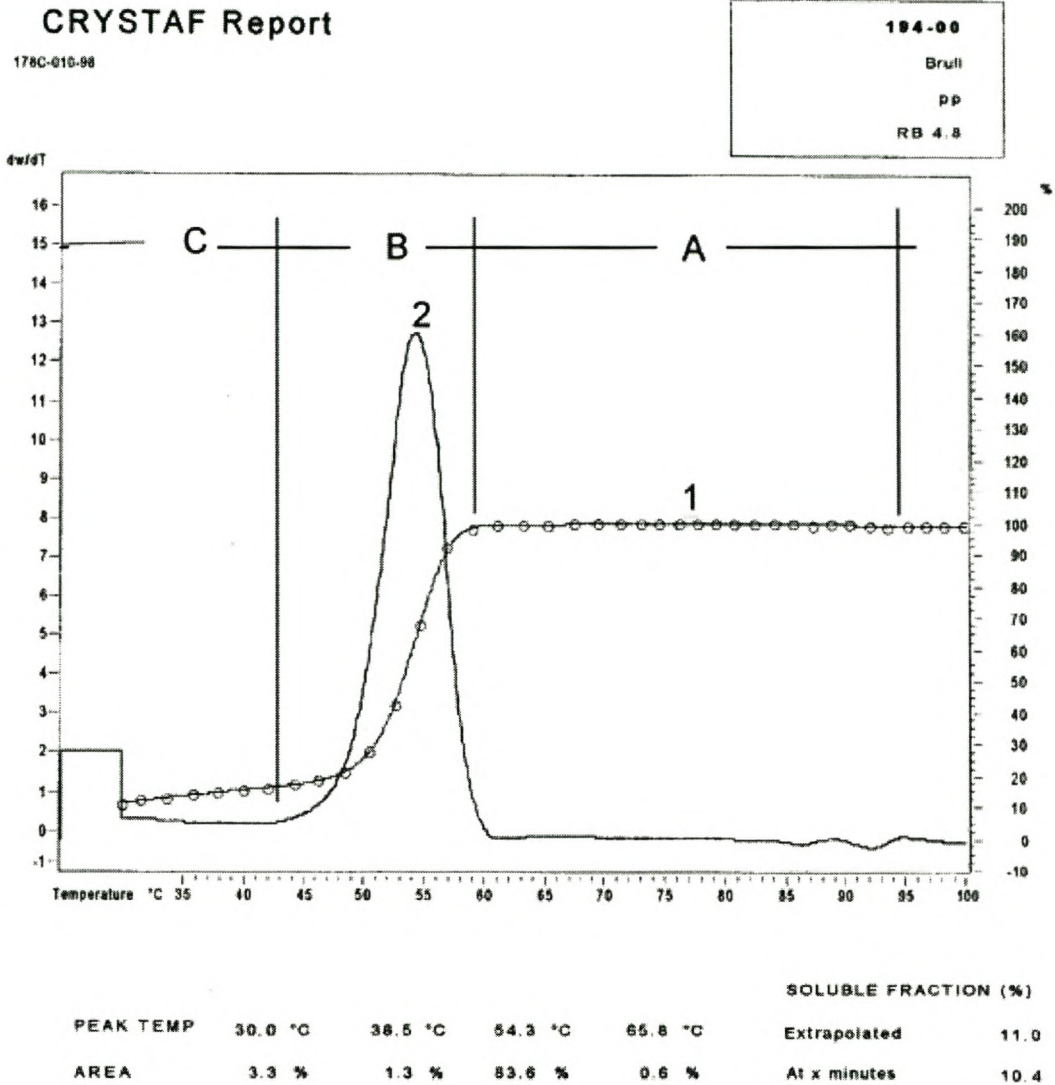


Figure 3.7 Typical curves from CRYSTAF measurements

To observe the effect of comonomer incorporation on crystallization temperature from solution, the two curves were arranged according to comonomer content. The resulting relationships for propene/1-butene copolymers are shown in Figures 3.8 and 3.9.

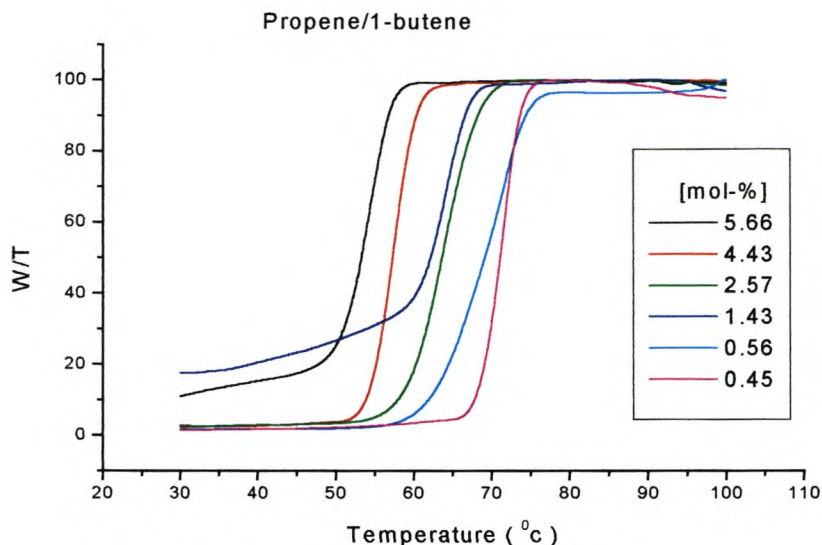


Figure 3.8 Changing concentration of propene/1-butene copolymers in solution with temperature for different comonomer incorporation

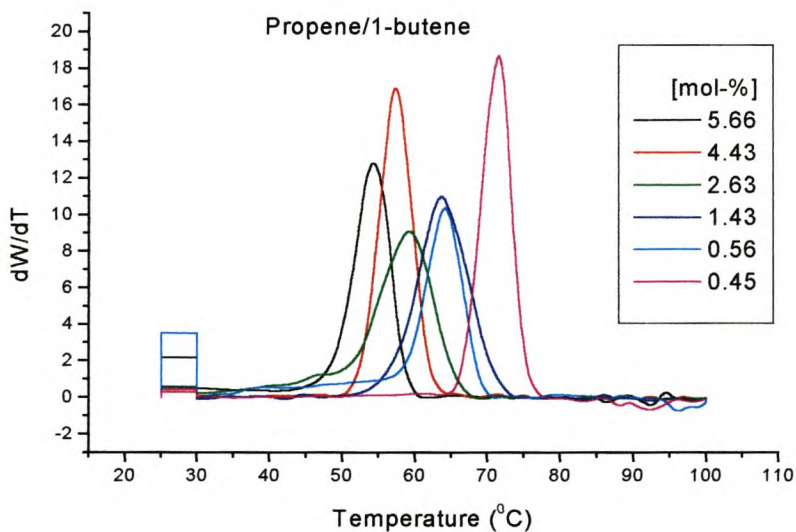


Figure 3.9 First derivative of the curves in Fig. 3.8 as a function of temperature for propene/1-butene copolymers

The maximum of the second derivative of the crystallization curve shown in Figure 3.9 was taken as crystallization temperature from solution, T_C (CRYSTAF). Crystallization

temperatures from solution also decreased with increasing comonomer content. This is also discussed in detail in Chapter 5.

3.5 Conclusions

The copolymers of propene/ α -olefin were successfully synthesized with $\text{Me}_2\text{Si}(2\text{-Methylbenz[e]indenyl})_2\text{ZrCl}_2/\text{MAO}$. Comonomer incorporation was confirmed by ^{13}C NMR spectroscopy and was below 6 % for all the copolymers. End group analysis was not done due the fact that all copolymers possessed high molecular weight. The stereoregularity of propene/linear α -olefin (1-butene, 1-pentene, 1-hexene) copolymers is influenced by comonomer incorporation. This influence is more pronounced for propene/1-butene than for the other copolymers.

Stereoregularity, melting and crystallization temperatures of propene/ α -olefin copolymers decrease with increasing comonomer content.

3.6 Recommendations

A detailed ^{13}C NMR study of all propene/ α -olefin (1-butene, 1-pentene, 1-hexene) copolymers would be needed to explain the influence of microstructures and comonomer content on melting and crystallization temperatures.

3.7 References

1. Yang, S. L.; Xu, Z. K.; Feng, X. L.; *Makromol. Chem., Makromol. Symp.* **1992**, 63, 233.
2. Herfert, N.; Montag, P.; Fink, G.; *Makromol. Chem.* **1993**, 194, 3167.
3. Muhlenbrock, P. H.; Fink, G. Z.; *Naturforsch* **1995**, 50b, 423.
4. Koivumaki, J.; Seppala, J. V.; *Macromolecules* **1993**, 26, 5535.
5. Koivumaki, J.; Fink, G.; Seppala, J. V.; *Macromolecules* **1994**, 27, 6254
6. Koivumaki, J.; Seppala, J. V.; *Polymer* **1993**, 34, 1958.
7. Batistini, A.; *Macromol. Symp.* **1995**, 100, 137.
8. Schneider, M. J.; Suhm, J.; Mülhaupt, R.; Prosenc, M. H.; Brintzinger, H. H.; *Macromolecules* **1997**, 30, 3164.
9. Schneider, M. J.; Huttenloch, M. E.; Stehling, U.; Kirsten, R.; Schaper, F.; Brintzinger, H. H.; *Organometallics* **1997**, 16, 3413.
10. Suhm, J.; Schneider, M. J.; Mülhaupt, R.; *J. Molecular Catalysis A: Chemical* **1998**, 128, 215.
11. Suhm, J.; Schneider, M. J.; Mülhaupt, R.; *J. Molecular.; J. Polym. Sci. A.* **1997**, 35, 735.
12. Ficker, H. K.; Walker, D. A.; *Plast. Rubber Process. Appl.* **1990**, 14(2), 103.
13. Shih, C. K.; Su, A. C. L.; Legge, N. R., Holden, G.; Chroeder, H. E., Eds.; *Thermoplastic Elastomers*, Hanser, New York **1987**, p. 92
14. Shih, C. K.; *Polym. Eng. Sci.* **1987**, 27(6), 458.
15. Van Reenen, A. J.; Brüll, R.; Wahner, U.; Raubenheimer, H.G.; Sanderson, R.D.; Pasch, H.; *J. Polym. Sci. Part A: Polym Chem.* **2000**, 38, 4110.
16. Brüll, R.; Pasch, H.; Raubenheimer, H.G.; Sanderson, R.G., Wahner, U.; *Macromol. Chem. Phys.* **2001**, 202, 2001.
17. Wahner, U.; Brüll, R.; Luruli, N; Pasch, H.; Raubenheimer, H.G.; Sanderson, R.D.; Van Reenen, A. J.; *Macromol. Chem. Phys.* **2001**, Submitted for publication.
18. Graef, S.; Wahner, U.; Van Reenen, A. J.; Brüll, R.; Sanderson, R.D.; Pasch, H.; *J. Polym. Sci. Part A: Polym Chem.* **2002**, 40, 128.

-
19. Quijada, R.; Rojas, R.; Guevara, J.; Narvaez, A.; Delfin, D.; De Galland, G. B.; *Polimery*, **2000**, 45(2), 339-343.
 20. Babu, G. N.; Newmark, R. A.; Chien, J. C. W.; *Macromolecules*, 1994, **27**, 3383.
 21. Randall, J. C.; Rucker, S.P.; *Macromolecules*, 1994, **27**, 2120.
 22. Cheng, H. N.; Smith, D. A.; *Macromolecules*, 1986, **19**, 2065.
 23. Fan, Z.; Yasin, T.; Feng, L.; *J. Polym. Sci. Part A: Polym Chem.* **2000**, 38, 4299.
 24. Kim, I.; Zhou, J.; Chung, H.; *J. Polym. Sci. Part A: Polym Chem.*, **2000**, 38, 1687.
 25. Zhao, X.; Odian, G.; Rossi, A.; *J. Polym. Sci. Part A: Polym Chem.*, **2000**, 38, 3802.
 26. Geldenhuys, M.; *MSc Thesis*, University of Stellenbosch, Stellenbosch, South Africa, **1998**.
 27. Cheng, H. N.; *Macromolecules* **1991**, 24, 4813.
 28. Joubert, D.; *PhD Thesis*, University of Stellenbosch, Stellenbosch, South Africa, **2000**,
 29. Zhu, F.; Haung, Y.; Yang, Y.; Lin, S.; *J. Polym. Sci. Part A: Polym Chem.* **2000**, 38, 4258.
 30. Paul, E. G.; Grant, D. M.; *J. Am. Chem. Soc.* **1964**, 86, 15, 2984.
 31. Bovey, F. A.; Mirau, P. A.; *NMR of polymers*; **1996**; AT&T Bell Laboratories Murray Hill. New Jersey. Academic press.
 32. ChemDraw soft ware, www.upstream.ch
 33. Cheng, H. N.; Smith, D. A.; *Macromolecules* **1986**, 19, 2065.
 34. Hsieh, E. T.; Randall, J. C.; *Macromolecules* **1982**, 15; 353.
 35. Lehtinen, C.; Stark, P.; Lofgren, B.; *J. Polym. Sci. Part A: Polym Chem.* **1997**, 35, 307.
 36. Alamo, R. G.; Mandelkern, L.; *Thermochim. Acta*, **1994**, 238, 155.
 37. Bunn, A.; Cudby, E. A.; *Polymer*, **1976**, 17, 548.
 38. Randall, J. C.; *Macromolecules*, **1978**, 11(3), 592.
 39. Randall, J. C.; Cudby, E. A.; Bunn, A.; *Polymer*, **1980**, 21, 117.
 40. Monrabal, B.; *J. Appl. Polym. Sci.* **1994**, 52, 491.

CHAPTER 4

SYNTHESIS AND CHARACTERISATION OF METALLOCENE-CATALYSED PROPENE/ 4-METHYL-1-PENTENE COPOLYMERS

Abstract

Copolymers of propene/4-methyl-1-pentene with low comonomer content were prepared with $\text{Me}_2\text{Si}(2\text{-Methylbenz[e]indenyl})_2\text{ZrCl}_2/\text{MAO}$ and the resulting copolymers were characterized by NMR, GPC, DSC and CRYSTAF measurements. Thermal properties of propene/4-methyl-1-pentene copolymers were investigated. Melting and crystallization temperatures decreased linearly with an increase in comonomer content.

4.1 Introduction

Metallocenes of group 4 are able to incorporate linear and branched α -olefins into propene copolymers forming copolymers with a great variety of properties.

The reactivity of these monomers depends on the structure of the alkyl groups attached to the double bond¹⁻³. Analysis shows that the reactivity of α -olefin monomers with linear alkyl groups from ethylene to 1-octadecene decreases with an increase in chain length. Monomers with branched alkyl groups, especially with branches next to a double bond, exhibit reduced reactivity.

Recently copolymers of ethylene with branched α -olefins prepared by metallocene catalysts have been reported⁴⁻⁶. Thermal properties of propene copolymers with branched α -olefins have also been determined⁷⁻¹⁰. Arnold et al. investigated melting and glass transition temperatures of propene/4-methyl-1-pentene copolymers prepared with an isospecific catalyst^{8,9}. Naga et al investigated melting and crystallization behaviour of syndiotactic propene/ α -olefin copolymers including 4-methyl-1-pentene⁷.

The investigation of melting and crystallization behaviour of propene copolymers with branched comonomers, is the aim of this chapter. The question is whether the same linear relationships previously established for propene/linear α -olefins exist for such copolymers. Copolymers of propene/4-methyl-1-pentene were prepared using $\text{Me}_2\text{Si}(2\text{-Methylbenz[e]indenyl})_2\text{ZrCl}_2/\text{MAO}$. The resulting copolymers were characterized by NMR, GPC, DSC and CRYSTAF measurements.

4.2 Experimental

4.2.1 Materials purification

The 4-methyl-1-pentene comonomer, received from Merck, was dried on lithium aluminium hydride and stored on 3Å molecular sieves before use. Toluene was refluxed and distilled under a sodium metal/benzophenone mixture for 18 h. The same propene described in Chapter 3 was used.

4.2.2 Polymerization procedures

The polymerization reactions were carried out under inert gas atmosphere in a 350 mL stainless steel Parr autoclave with inlet and pressure gauge. All the manipulations and reactions conditions were similar as described before.

The 4-methyl-1-pentene comonomer was chilled with ice during manipulation to prevent it from evaporating.

After 3 h the reaction was quenched with 10 % HCl/MeOH. The resulting polymer was filtered off, washed several times with methanol and subsequently dried in a vacuum oven at 80 °C for 15 h.

4.2.3 Analytical procedures

The analytical procedures for with NMR, GPC, DSC and CRYSTAF characterized analytical procedures are explained in Section 3.3.2.

4.3 Results and discussion

The ^{13}C NMR spectra of propene/4-methyl-1-pentene copolymers are shown in Figures 4.1. and 4.2.

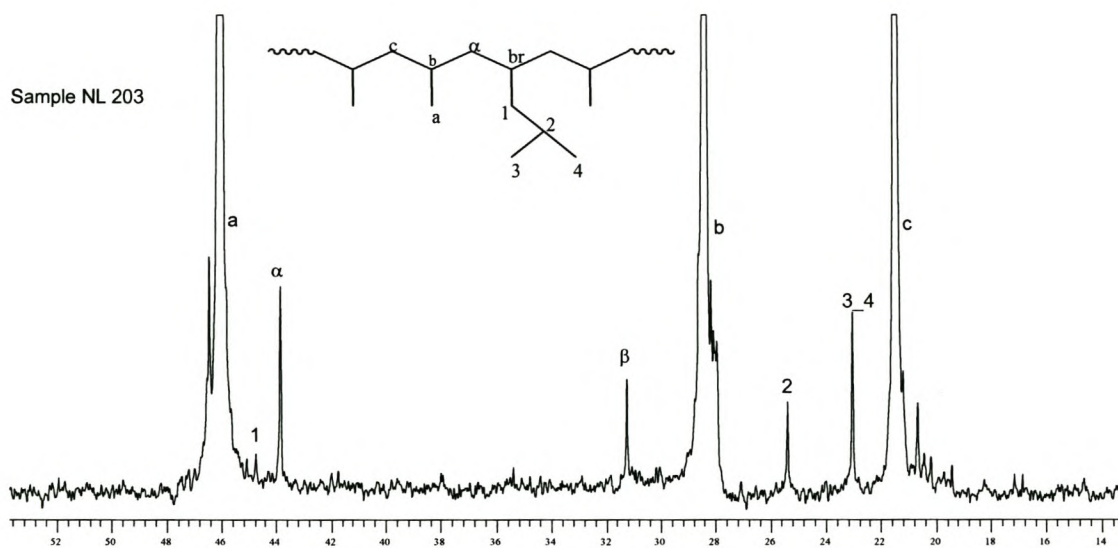


Figure 4.1 ^{13}C NMR spectrum of propene/4-methyl-1-pentene copolymer with 1.6 [mol-%] of comonomer

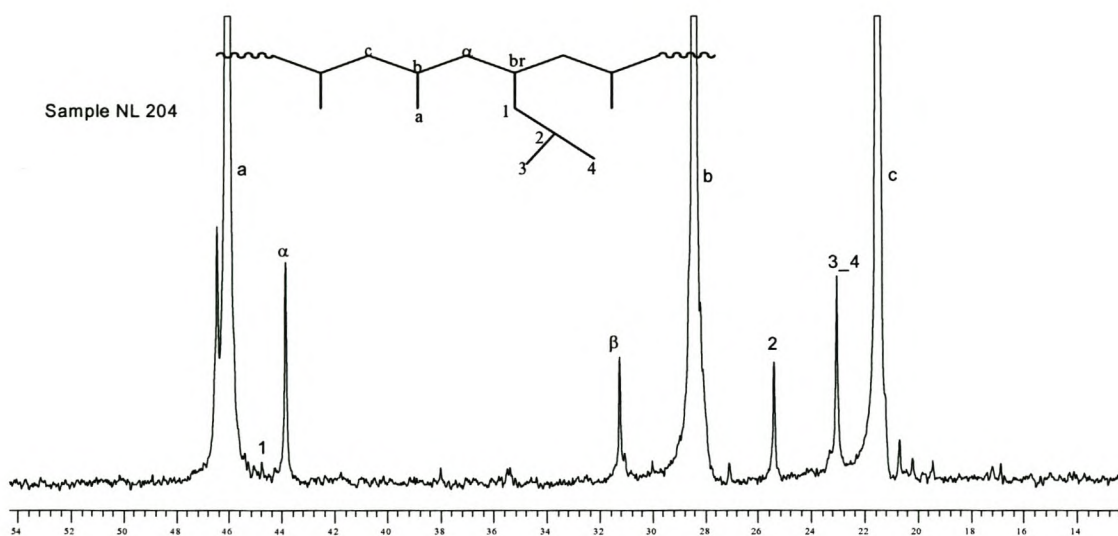


Figure 4.2 ^{13}C NMR spectrum of propene/4-methyl-1-pentene copolymer with 2.5 [mol-%] of comonomer

The incorporation of 4-methyl-1-pentene is confirmed by the ^{13}C NMR spectrum shown in Figure 4.1. The three large signals at δ 21.70, 28.37 and 46.04 arise from a, b, c, carbon atoms in the polypropene chain. The assignments have been done with the help of calculated chemical shifts according to the rules explained in Section 3.4 of the preceding chapter, and are given in Table 4.1.

Table 4.1 The calculated and observed chemical shifts of propene/4-methyl-1-pentene copolymers

| Carbon | α | β | γ | | | Const | $3^\circ(2^\circ)$ | $2^\circ(3^\circ)$ | $1^\circ(3^\circ)$ | δ (ppm) | Chem BV | Draw | EXP |
|----------|----------|---------|----------|----------|------------|-------|--------------------|--------------------|--------------------|-------------------|------------|-------|-------|
| | 8.61 | 9.78 | - | δ | ϵ | | 2.88 | 0.37 | 0.06 | | | | |
| a | 1 | 2 | 2 | 4 | 3 | 1 | 0 | 0 | 1 | 20.8 | 21.00 | 21.70 | 21.53 |
| b | 3 | 2 | 4 | 3 | 5 | 1 | 2 | 0 | 0 | 28.11 | 27.90 | 27.30 | 28.37 |
| c | 2 | 4 | 2 | 4 | 3 | 1 | 0 | 2 | 0 | 45.47 | 45.00 | 44.70 | 46.04 |
| α | 2 | 4 | 3 | 6 | 2 | 1 | 0 | 2 | 0 | 43.27 | 43.00 | 42.50 | 43.93 |
| br | 3 | 3 | 6 | 2 | 4 | 1 | 3 | 0 | 0 | 29.05 | 28.25 | 30.20 | 31.25 |
| 1 | 2 | 4 | 2 | 4 | 2 | 1 | 2 | 0 | 0 | 45.01 | 42.60 | 44.40 | 44.70 |
| 2 | 3 | 1 | 2 | 2 | 4 | 1 | 0 | 0 | 0 | 28.96 | 30.40 | 26.30 | 25.50 |
| 3 | 1 | 2 | 1 | 2 | 2 | 1 | 0 | 0 | 0 | 24.28 | 23.90 | 22.60 | 23.06 |
| 4 | 1 | 2 | 1 | 2 | 2 | 1 | 0 | 0 | 0 | 24.28 | 38.00 | 22.60 | 23.06 |

The calculation of chemical shifts and subsequent assignments allow also the determination of comonomer content in the copolymer. Values for the comonomer content were determined using Equation 3.1 in Section 3.4.1, and are listed in Table 4.2.

Table 4.2 Summary of results (comonomer content, T_m (DSC), T_c (DSC), T_c (CRYSTAF), M_n and M_n/M_w) for propene/4-methyl-1-pentene copolymers

| Sample | Yield (g) | [Mol-%] | T_m (DSC) | T_c (DSC) | T_c (CRYSTAF) | M_w | M_n/M_w |
|--------|-----------|---------|-------------|-------------|-----------------|-------|-----------|
| NL2.1 | 21.46 | 2.06 | 128.6 | 86.7 | 58.5 | n/a | n/a |
| NL2.2 | 24.86 | 2.22 | 124.6 | 81.9 | 50.2 | n/a | n/a |
| NL2.3 | 2.84 | 1.59 | 127.6 | 91.2 | 54.1 | n/a | n/a |
| NL2.4 | 1.25 | 2.49 | 117.6 | 77.0 | 44.4 | n/a | n/a |
| NL2.5 | 0.89 | 2.11 | 122.4 | 85.2 | 46.9 | n/a | n/a |
| NL2.6 | 1.27 | 1.88 | 124.9 | 90.2 | 50.7 | n/a | n/a |
| NL2.7 | 1.72 | 1.95 | 124.2 | 87.7 | 49.4 | n/a | n/a |
| NL2.8 | 7.6 | 0.90 | 137.9 | 96.67 | 59.6 | n/a | n/a |
| NL2.10 | 1.10 | 1.26 | 132.6 | 97.2 | 57.2 | n/a | n/a |
| NL2.11 | 0.6 | 0.50 | 143.3 | 106.4 | 67.5 | n/a | n/a |

n/a = not available

4.4 Thermal properties of propene/4-methyl-1-pentene copolymers

Thermal properties were investigated using DSC and CRYSTAF. The general analytical procedures for the measurement of melting and crystallization temperatures using these two techniques have been outlined in Section 3.3.2

4.4.1 Melting and crystallization from the melt

The typical melting and crystallization curves of propene/4-methyl-1-pentene copolymers from DSC are shown in Figure 4.3 & 4.4. The minimum of the curve (Figure 4.3) indicates melting temperature, T_m (DSC), while the maximum of the curve in Figure 4.4 gives the melt crystallization temperature, T_c (DSC).

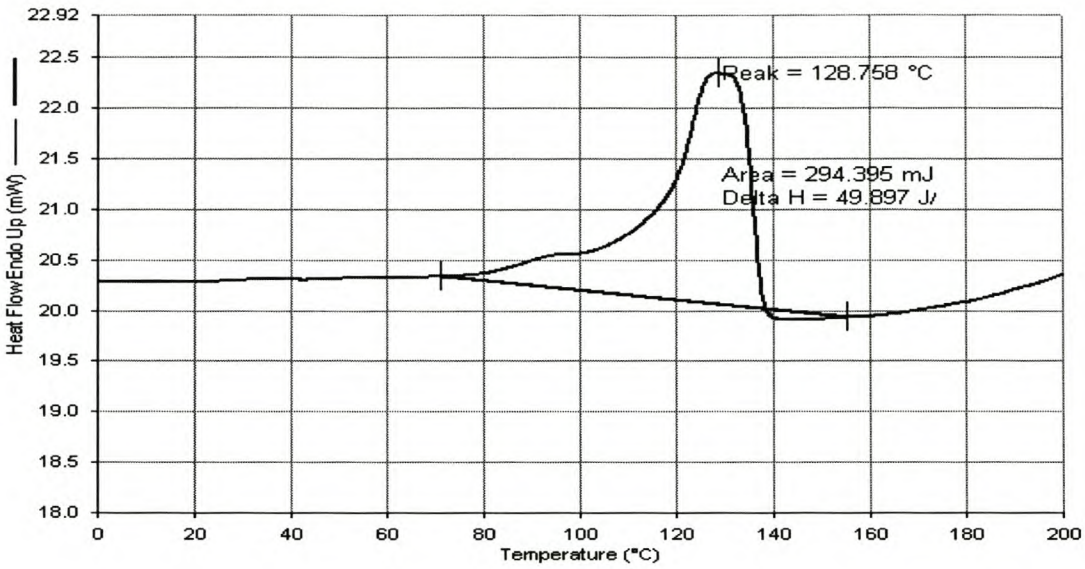


Figure 4.3 DSC curves (2nd heating cycle) of propene/4-methyl-1-pentene copolymer (sample NL 2.1)

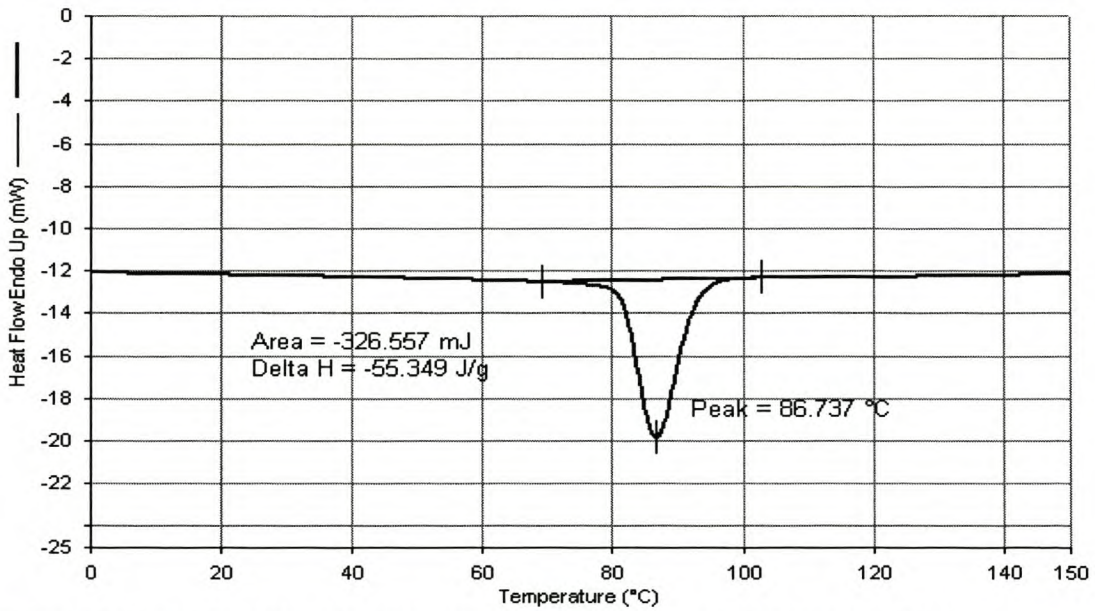


Figure 4.4 DSC cooling curves of propene/4-methyl-1-pentene copolymer (sample NL 2.1)

The melting ($T_m(DSC)$) and crystallization temperatures ($T_m(DSC)$) were determined in relation to comonomer content and the results are shown in Figure 4.5.

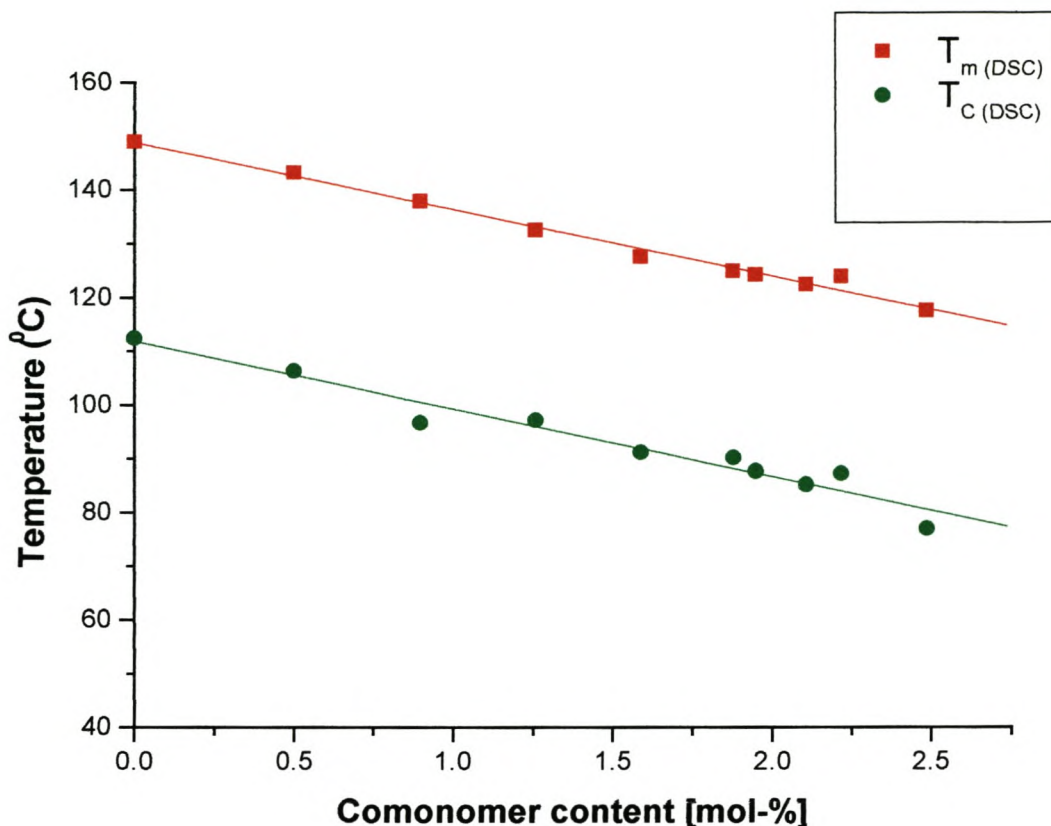


Figure 4.5 Melting temperature, $T_{m(DSC)}$, and crystallization temperatures from the melt, $T_{c(DSC)}$, as a function of comonomer content of propene/4-methyl-1-pentene copolymers

As shown in Figure 4.5 the melting and crystallization temperatures decrease linearly with increasing comonomer content and the two curves are parallel.

4.4.2 Crystallization from solution

Crystallization of propene/4-methyl-1-pentene copolymers from the solution was investigated by CRYSTAF and the results are shown in Figures 4.6 and 4.7. The maxima of the peaks in Figure 4.7 were read as crystallization temperatures from solution, T_c (CYRTAF).

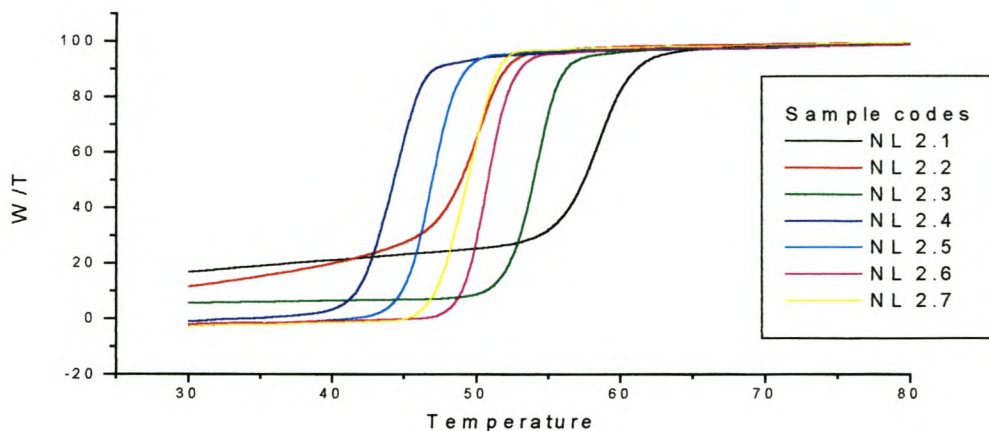


Figure 4.6 Changing concentration of propene/4-methyl-1-pentene copolymers in solution with temperature

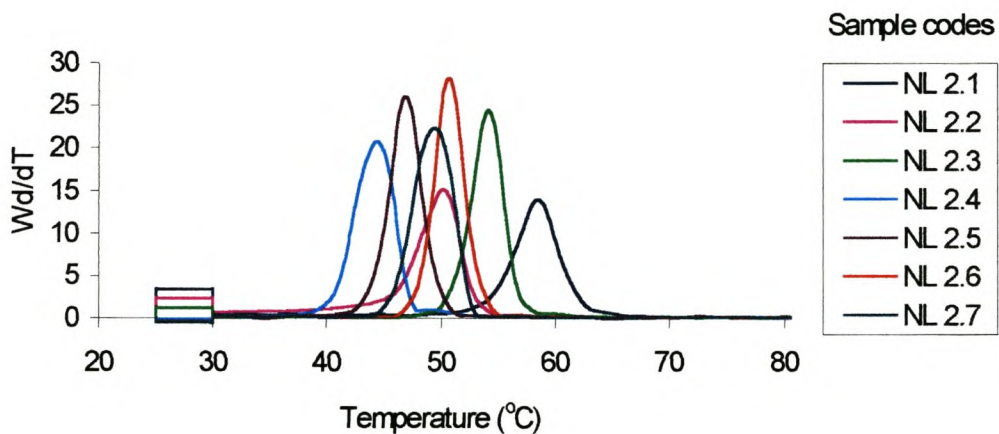


Figure 4.7 First derivative of the curves in Fig 4. 6 as a function of temperature for propene/1-butene copolymers

The crystallization temperatures from solution, $T_{c(CRYSTAF)}$, were plotted as a function of the comonomer content and the results are displayed in Figure 4.8.

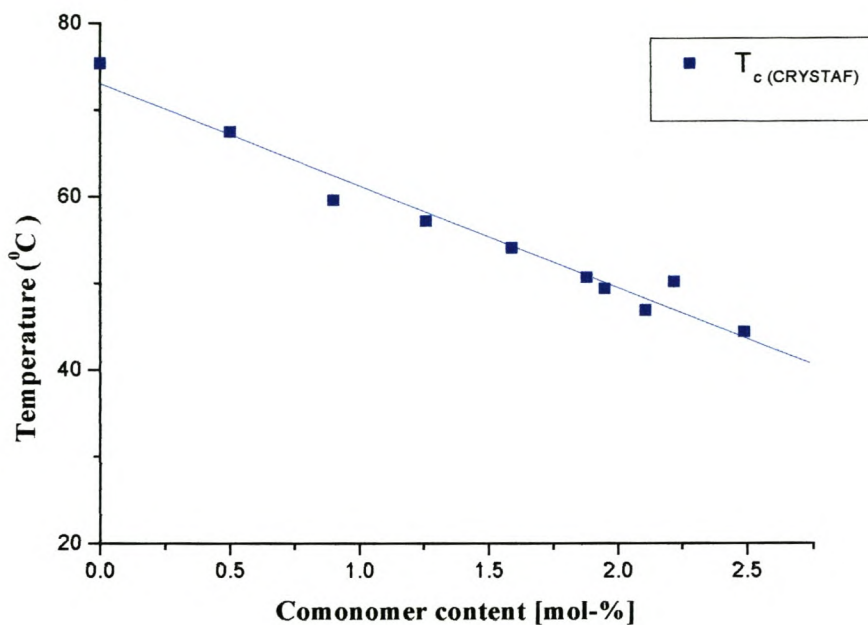


Figure 4.8 Crystallization temperatures from solution, $T_c(\text{CRYSTAF})$, as a function of comonomer content

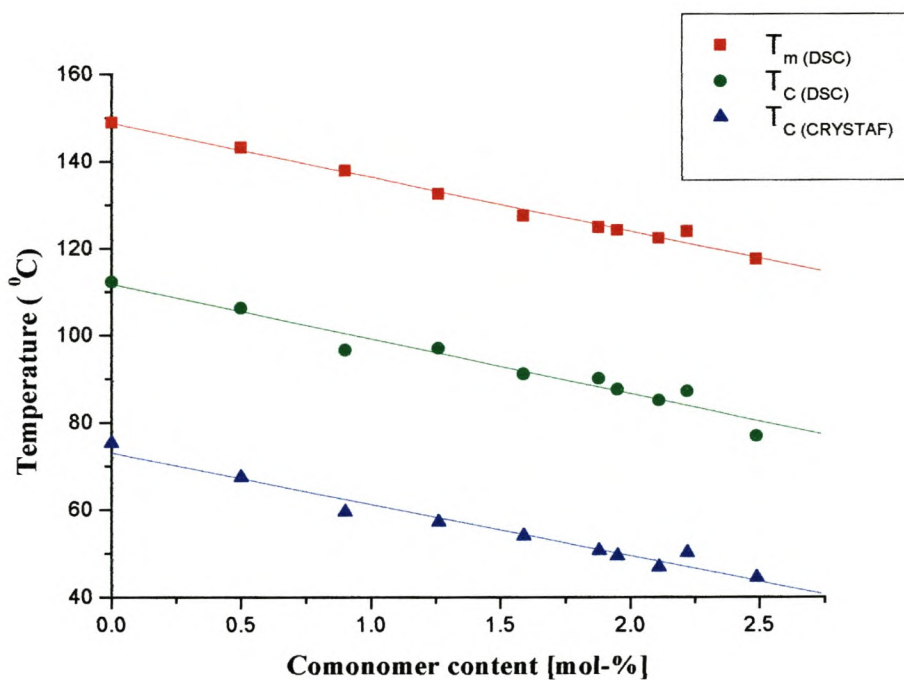


Figure 4.9 Melting peak temperatures, $T_m(\text{DSC})$, crystallization peak temperature, $T_c(\text{DSC})$, and crystallization peak temperature, $T_c(\text{CRYSTAF})$, of propene/4-methyl-1-pentene copolymers

Crystallization temperatures from solution also show a linear decrease with increasing comonomer content. The DSC and CRYSTAF results were compared and the results are shown in Figure 4.9. The $T_{c(\text{CRYSTAF})}$ values were found to be lower than $T_{c(\text{DSC})}$ which could be due to different sample matrixes employed by two analytical techniques.

4.5 Conclusions

Copolymers of propene/4-methyl-1-pentene were successfully synthesized with $\text{Me}_2\text{Si}(2\text{-Methylbenz[e]indenyl})_2\text{ZrCl}_2/\text{MAO}$ and characterized by NMR, GPC, DSC and CRYSTAF. The melting temperatures of propene/4-methyl-1-pentene copolymers decrease linearly with increasing comonomer content. Crystallization temperatures both from the melt, $T_{c(\text{DSC})}$, and from solution, $T_{c(\text{CRYSTAF})}$, decreased similarly with increasing comonomer content as was observed previously for propene/linear α -olefin copolymers (Chapter 3).

4.6 Recommendations

A detailed study of melting and crystallization behaviour of propene/4-methyl-1-pentene copolymers with high comonomer content (above 20 %) should be carried out. Arnold et al.⁸ reported that higher 4-methyl-1-pentene incorporation (above 60 %) into polypropene leads to an increase in melting temperatures. This suggests different behaviour of propene/4-methyl-1-pentene copolymers with high comonomer content than propene/4-methyl-1-pentene copolymers with low comonomer content.

4.7 References

1. Krentsel, B. A.; Kissin, Y. V.; Kleiner, V. I.; Stotskaya, L. L.; *Polymers and copolymers of higher α -olefins*, Hanser/Gardner publishers, Munich, **1997**, p.121.
2. Kissin, Y. V.; Quirk, R. P.; (Eds) *Transition metal catalyzed polymerization: Alkenes and dienes*, Harwood Academic Publishers, New York, **1985**, Part B. p. 597.
3. Belov, G. P.; Belova, V. N.; Raspopov, L. N.; Kissin, Y. V.; Brikenshtein, K. A.; Chirkov, N. M.; *Polym. J.* **1972**, 3, 681.
4. Simanke, A. G.; Galland, G. B.; Freitas, L. L.; Da Jornada, J. A. H.; Quijada, R.; Mauler, R. S.; *Macromol. Chem. Phys.* **2001**, 202(1), 172.
5. Simanke, A. G.; Galland, G. B.; Neto, R. B.; Quijada, R.; Mauler, R. S; *J. Appl. Polym. Sci.* **1999**, 74(5), 1194.
6. Mauler, R. S.; Galland, G. B.; Scipioni, R.B.; Quijada, R.; *Polym. Bull. (Berlin)*, **1996**, 37,(4), 469.
7. Naga, N.; Mizunuma, K.; Sadatoshi, H.; Kakugo, M.; *Polymer*, **2000**, 41, 203.
8. Arnold, M.; Knorr, J.; Koller, F.; Bornemann, S.; *J. M. S. Rev. Pure Appl. Chem.*, **1999**, A36(11), 1655.
9. Arnold, M.; Bornemann, S.; Koller, F.; Menke, T. J.; Kressler, J.; *Macromol. Chem. Phys.* **1998**, 199, 2647.
10. Naga, N.; Mizunuma, K.; Sadatoshi, H.; Kakugo, M.; *Macromolecules*, **1997**, 30, 2197.

CHAPTER 5

INVESTIGATION OF MELTING AND CRYSTALLIZATION BEHAVIOUR OF PROPENE/ α -OLEFIN COPOLYMERS BY DSC AND CRYSTAF

Abstract

The melting and crystallization temperatures of propene/ α -olefin (1-butene, 1-pentene, 1-hexene and 4-methyl-1-pentene) copolymers previously synthesized in Chapter 3 and 4 were investigated by DSC and CRYSTAF and compared. The influence of the incorporation of the branched monomer on melting and crystallization behaviour was also investigated. The results revealed a linear decrease in melting and crystallization temperatures of all the copolymers investigated with increasing comonomer incorporation. The melting and crystallization temperatures strongly depended on comonomer type. Melting and crystallization temperatures of propene/4-methyl-1-pentene copolymers were lower than those of propene/1-pentene but higher than those of propene/1-hexene.

5.1. Introduction

The physical and thermal properties of ethylene and propene copolymers depend on variables such as, among others, molecular weight, molecular structure, comonomer type and comonomer content. Copolymerization of ethylene and propene with α -olefins is an effective way of controlling the properties of these two semicrystalline polymers¹.

The manipulation of molecular structure by introducing branches in polyethylene has led to the discovery of commercial polymers such as low density polyethylene (LDPE) and linear low density polyethylene (LLDPE). LLDPE can be produced by metallocene catalyzed copolymerization of ethylene with higher α -olefins^{2,3}. Unlike LLDPE, propene/ α -olefins copolymers have gained less technical relevance.

Metallocene (single site) catalysts in conjunction with MAO offer a new methodology of synthesizing copolymers with controlled comonomer incorporation, uniform chain structure and chemical composition distribution (CCD) as well as improved physical and mechanical properties⁴. Another advantage in using metallocenes is ability of some of these catalysts to incorporate bulky monomers^{5,6}. These properties could not be realized with traditional Ziegler-Natta (multiple site) catalysts.

The use of metallocene/MAO catalyst systems for copolymerization of propene with α -olefins give rise to a variety of structures^{1,3} (Figure 5.1). The successful synthesis of some of these compounds was reported in the preceding chapters.

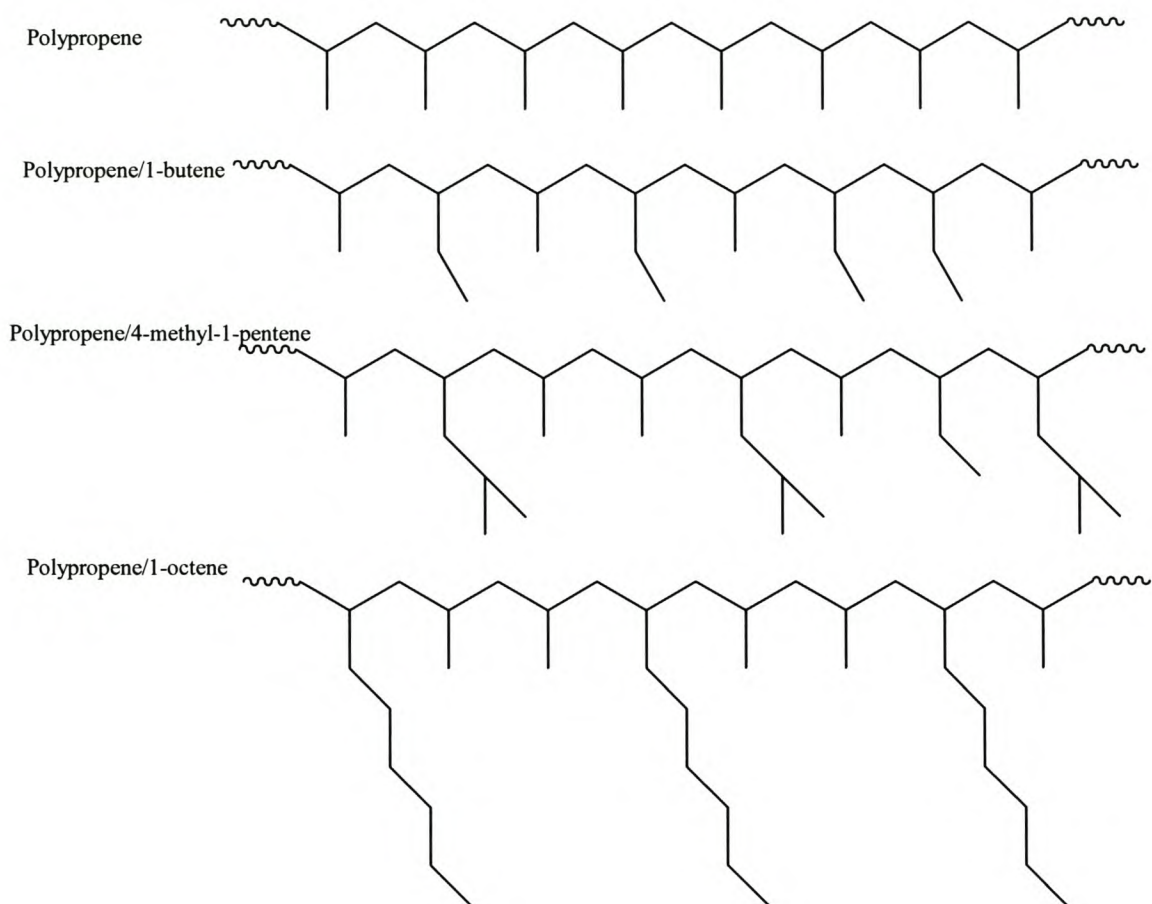


Figure 5.1 Propene polymer structures available by use of metallocene catalysts

The most common and widely used analytical technique for studying melting and crystallization behaviour of ethylene/ α -olefin and propene/ α -olefin copolymers has been DSC. A single technique is not sufficient to characterize copolymers with such complex structures. Multiple techniques are necessary.

Several techniques have been used to characterize the molecular architecture of polypropylene. These techniques include infrared (IR) carbon-13 nuclear magnetic resonance (^{13}C NMR) and various fractionation methods⁷⁻¹⁶. IR and ^{13}C NMR can be used to estimate the average stereoregularity of a polymer, with ^{13}C NMR considered the definitive method for tacticity determination¹⁶.

The fractionation methods are used for analytically separating the various tactic chains by crystallization. The highly isotactic chains will crystallize as the solvent is cooled, allowing for a separation based on branching, with the more branched and low molecular weight products remaining in solution.^{2,5,6,16}

Temperature rising elution fractionation (TREF) and crystallization analysis fractionation (CRYSTAF) are methods for the analysis of chemical composition distribution and crystallization. Due to long analysis time (typically more than one day per sample) associated with TREF, CRYSTAF is now preferred for short chain branching distribution (SCBD) and chemical composition distribution (CCD) analysis¹⁷.

In this chapter melting and crystallization behaviour of random propene/ α -olefin (1-butene, 1-pentene, 1-hexene and 4-methyl-1-pentene) copolymers investigated by DSC and CRYSTAF are described. The propene/ α -olefin copolymers were synthesized and characterized by NMR and GPC as described in Chapter 3 and 4. The comparison between melting and crystallization behaviour of branched and linear α -olefins is also described. Finally, melting and crystallization behaviour of random propene/ α -olefin copolymers is compared with the thermal properties of propene/ higher α -olefin (1-octene, 1-decene, 1-tetradecene and 1-octadecene) copolymers as studied previously in our group³.

5.2 Melting and crystallization behaviour of propene/linear α -olefin copolymers

The polymerizations and necessary analytical procedures are explained in Chapter 3. The NMR and GPC analysis have been fully outlined. The melting and crystallization behaviour was carried out using DSC and CRYSTAF and the results are discussed in the following sections.

5.2.1 Melting and Crystallization analysis investigated by DSC

In order to investigate the effect of comonomer content on melting and crystallization temperatures, the DSC curves of propene/linear α -olefin (1-butene, 1-pentene and 1-hexene) copolymers were arranged according to comonomer content. The comonomer content of the copolymers was determined as described in Chapter 3 and the sample designation is shown in Table 3.1. Second heating curves of propene/1-hexene samples are shown (as examples) in Figure 5.2.

The maximum of the second heating curves (Figure 5.2) and the minimum of the cooling curves (Figure 5.4) were recorded as melting temperatures, T_m (DSC), and crystallization temperatures from the melt, T_c (DSC), respectively. The T_m (DSC) and T_c (DSC) of all propene/linear α -olefin copolymers are plotted against comonomer contents and the results are shown in Figure 5.3 and 5.5 respectively.

Figures 5.3 and 5.5 depict a linear decrease in both T_m (DSC) and T_c (DSC) with increase in comonomer content. This is attributed to an increase in partially crystallizable or non-crystallizable materials in the crystal lattice, hence T_m (DSC) and T_c (DSC) decreased as comonomer content increases. Also shown is the effect of the comonomer type on T_m (DSC) and T_c (DSC) temperatures. This will be explained in the following sections.

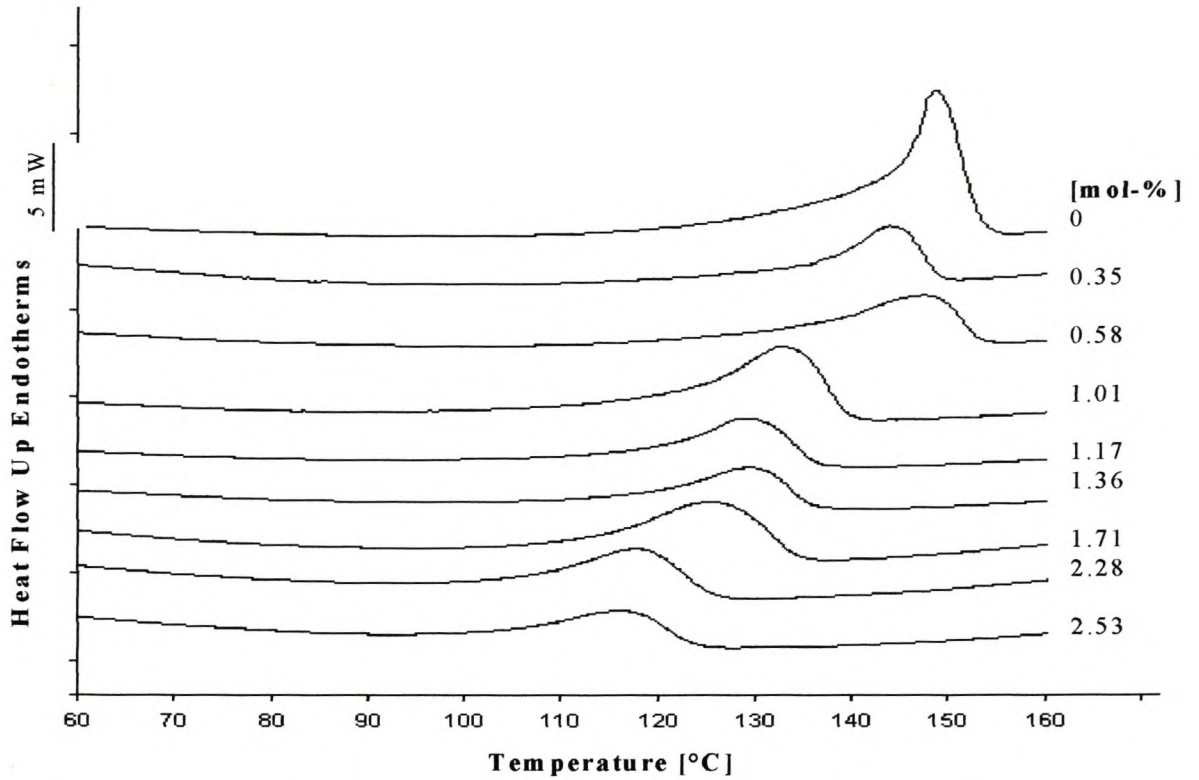


Figure 5.2 DSC curves (2nd heating curves) of propene/1-hexene copolymers placed according to comonomer content

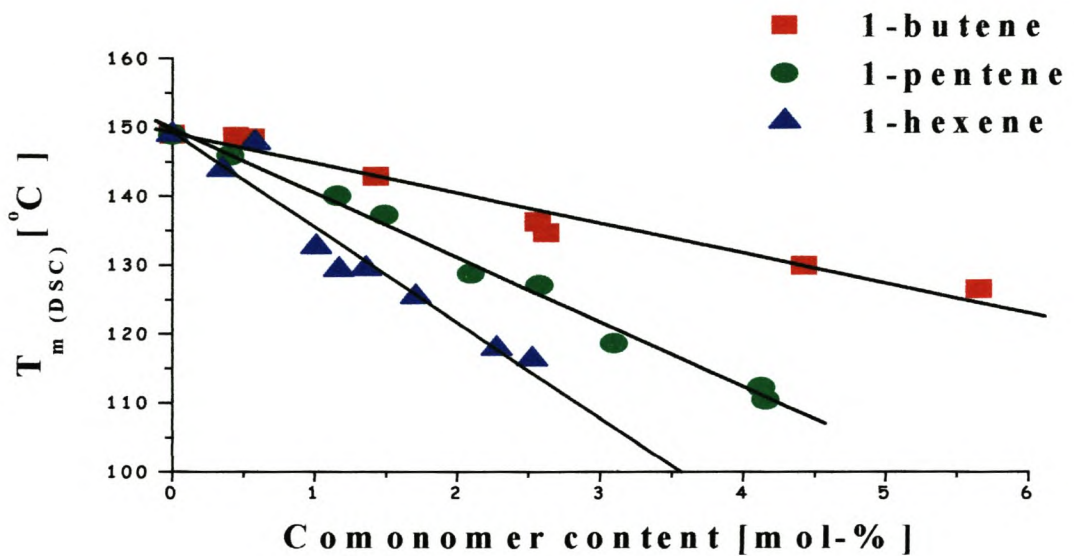


Figure 5.3 Variations of melting temperatures, T_m (DSC), of propene/ linear olefin copolymers with changes in comonomer content

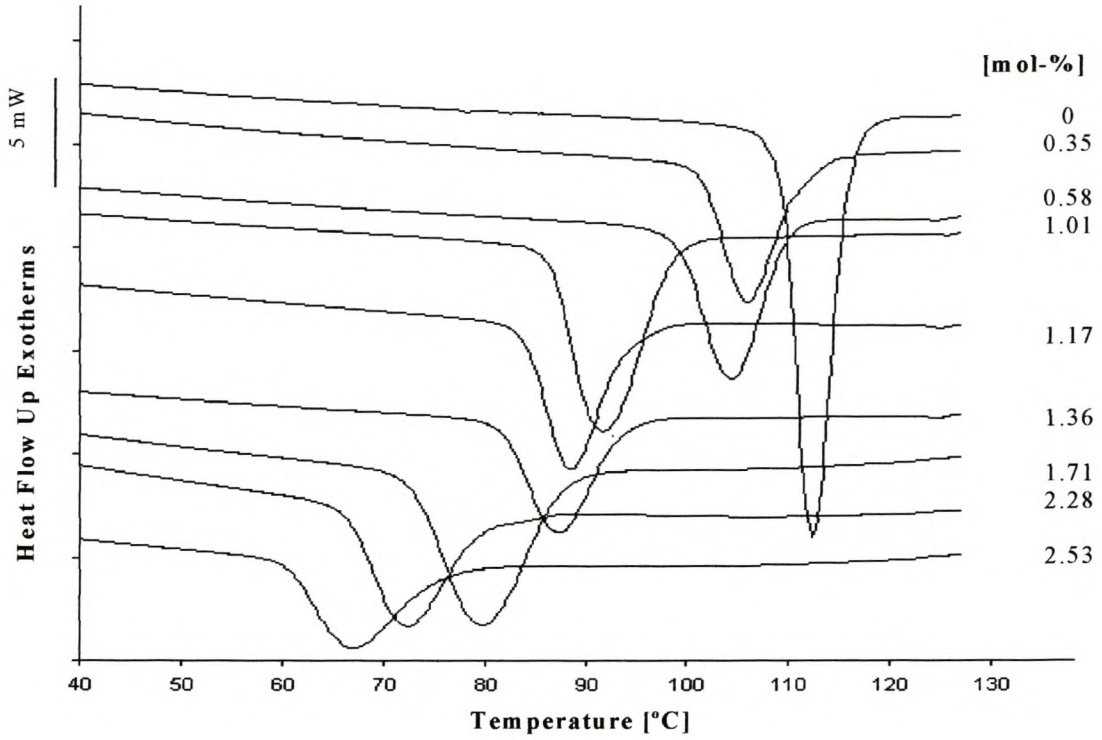


Figure 5.4 DSC curves (cooling cycle) of propene/1-hexene copolymer placed according to comonomer content

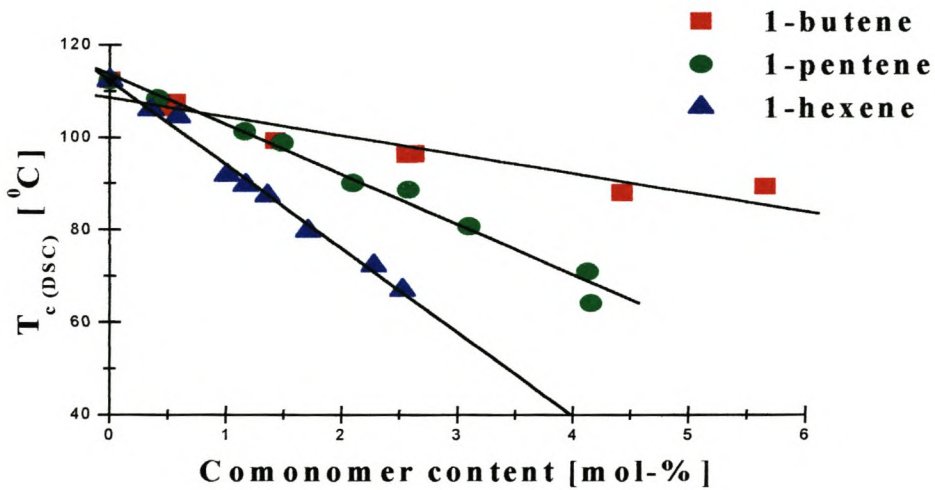


Figure 5.5 Crystallization temperature, $T_{c(DSC)}$, of propene/ linear olefin copolymers determined by DSC

5.2.2 Crystallization analysis investigated by CRYSTAF

The crystallization behaviour of the propene/linear α -olefin copolymers was also studied using CRYSTAF. The concentration of the polymer in solution was monitored as a function of temperature resulting in a changing concentration versus temperature curve. The first derivative of such a curve is then plotted against temperature. Typical results obtained for the propene/linear α -olefins are shown in Figure 5.6.

The maximum of the first derivative curves were recorded as crystallization temperature from solution, $T_{c \text{ (CRYSTAF)}}$. $T_{c \text{ (CRYSTAF)}}$ values of all propene/linear α -olefin copolymers investigated were then plotted against the percentage of comonomer incorporated (Figure 5.7).

Narrow first derivative curves indicate that the propene/linear α -olefins copolymers are highly homogeneous materials and that the short chain branches are randomly distributed¹⁷.

As shown in Figure 5.7, the crystallization temperatures from solution, $T_{c \text{ (CRYSTAF)}}$ values, of all propene/linear α -olefin copolymers decrease linearly with increasing comonomer incorporation as also the values for crystallization temperature from the melt, $T_{c \text{ (DSC)}}$. Copolymers with shorter comonomer chains have the highest $T_{c \text{ (DSC)}}$ values.

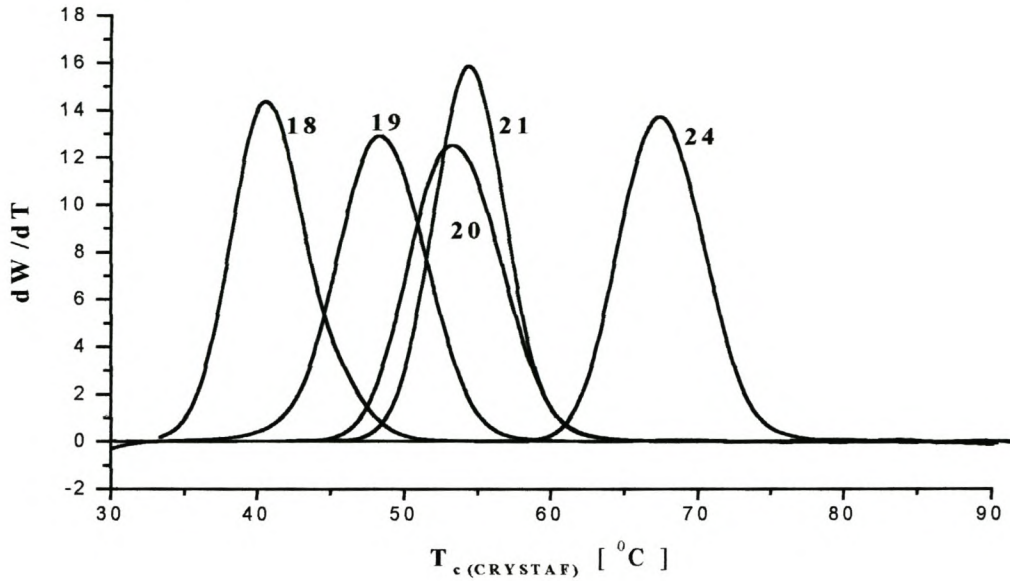


Figure 5.6 First derivative of the concentration in solution determined by CRYSTAF

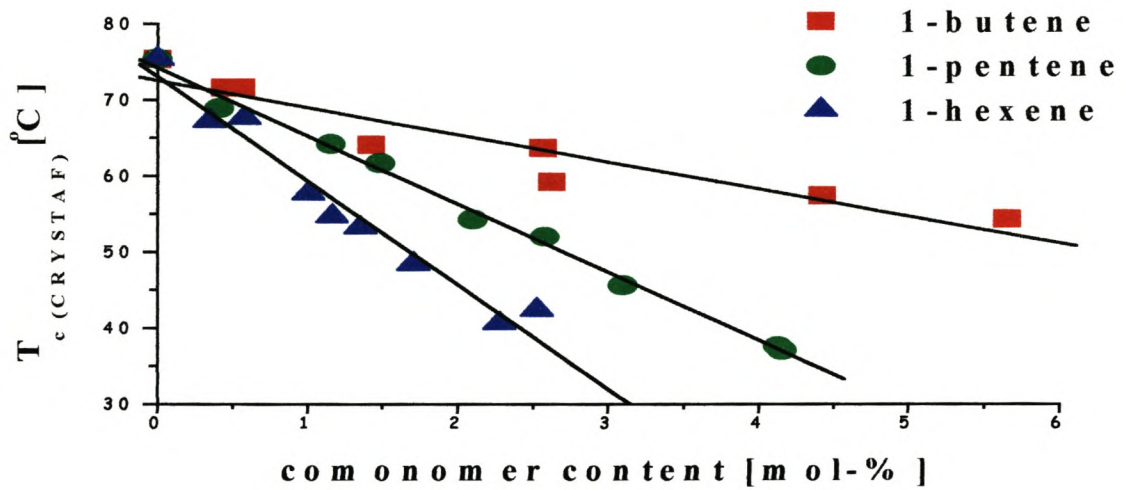


Figure 5.7 Crystallization temperature, $T_{c(CRYSTAF)}$, of propene/ linear olefin copolymers determined by CRYSTAF

5.3 Comparison of melting and crystallization behaviour of branched and linear propene/ α -olefin copolymers

The effect of incorporated branched comonomer on melting and crystallization behaviour, was investigated by comparing melting and crystallization temperatures (T_m (DSC), T_c (DSC) and T_c (CRYSTAF)) of propene/1-pentene, propene/1-hexene and propene/4-methyl-1-pentene copolymers. The results are displayed in Figures 5.8, 5.9 and 5.10.

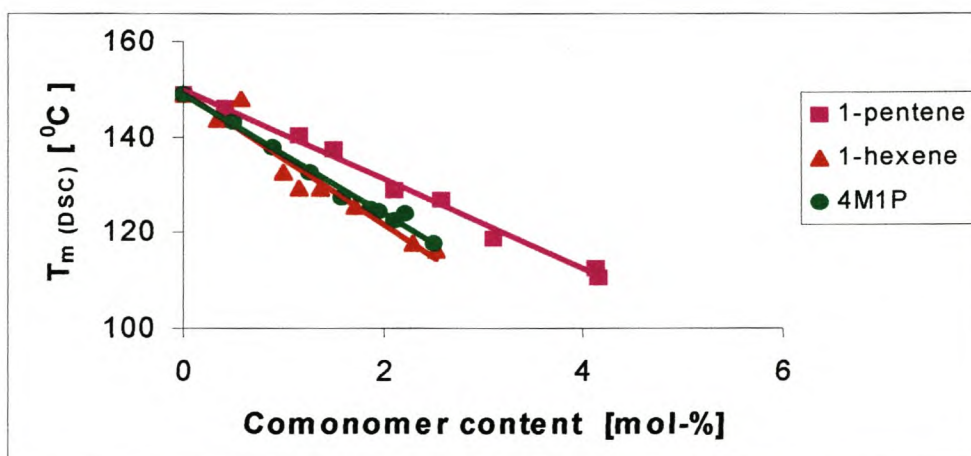


Figure 5.8 Melting temperature, $T_{m(DSC)}$, of branched and linear propene/ α -olefin copolymers determined by DSC

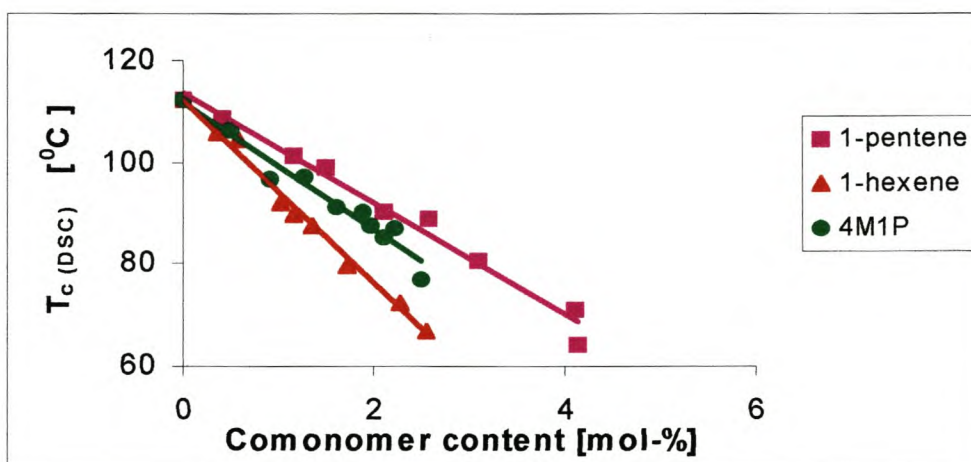


Figure 5.9 Crystallization temperature, $T_{c(DSC)}$, of branched and linear propene/ α -olefin copolymers determined by DSC

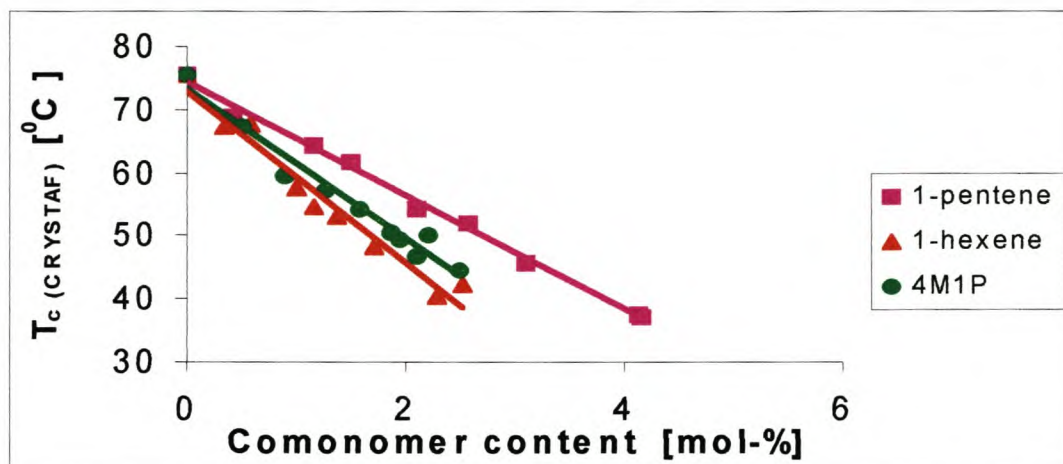


Figure 5.10 Crystallization temperature, $T_{c(\text{CRYSTAF})}$, of branched and linear propene/ α -olefin copolymers determined by CRYSTAF

As shown in Figure 5.8 the melting temperatures ($T_{m(\text{DSC})}$) of propene/4-methyl-1-pentene copolymers are lower than those of propene/1-pentene copolymers. Melting temperatures of propene/4-methyl-1-pentene copolymers are more or less similar to those of propene/1-hexene copolymers wherein the comonomer contains the same number of carbon atoms.

There is a significant difference in crystallization temperatures ($T_{c(\text{DSC})}$ and $T_{c(\text{CRYSTAF})}$) of propene/4-methyl-1-pentene copolymers and those of propene/linear α -olefin (1-pentene and 1-hexene) copolymers (Figures 5.9 and 5.10), with the line for the branched comonomer lying between the other two.

The present results show different melting and crystallization behaviour to that of propene/higher α -olefins (1-octene, 1-decene, 1-tetradecene, and 1-octadecene) copolymers previously obtained in our group. Earlier results (Figure 5.11) indicated that the melting and crystallization temperatures of propene/higher α -olefin copolymers were independent of comonomer type, but, as also now found, dependent on comonomer content³.

The dependency on comonomer content leads to the conclusion that comonomers with shorter side chains are partially crystallizable and can more readily be incorporated into a crystalline structure than higher α -olefins comonomers¹⁸. The degree of incorporation decreases with increase in chain length. Branches introduced by higher α -olefins are probably too large to be incorporated into crystal lattices and, therefore, only disrupts the sequence of crystallizable polymer, leading to lower melting points¹⁹.

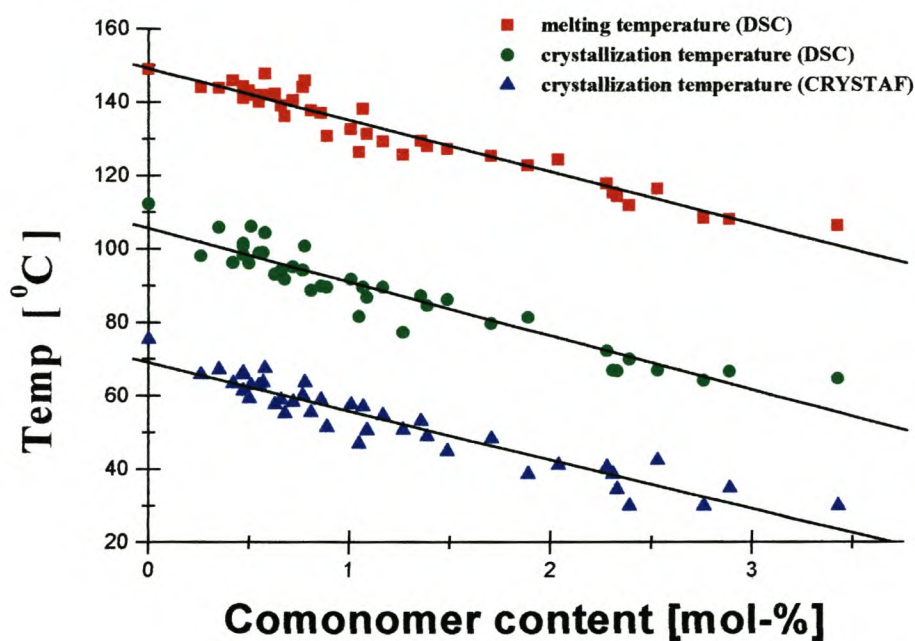


Figure 5.11 Melting temperature, $T_{m(DSC)}$, crystallization temperature from melt, $T_c (DSC)$, and crystallization temperature from solution, $T_c (CRYSTAF)$, of propene/higher α -olefin copolymers determined by DSC and CRYSTAF³

5.4 Conclusions

Melting and crystallization behaviour of propene/ α -olefin copolymers with shorter comonomer chains strongly depend on both comonomer type and content. Melting and crystallization temperatures from DSC and CRYSTAF measurements of propene/ α -olefin copolymers, decrease linearly with increasing comonomer content. Copolymers with shorter comonomer chains show higher melting and crystallization temperatures than copolymers with longer comonomer chains. Based on these observations it can be concluded that comonomers with shorter α -olefin chains are partially crystallizable unlike α -olefins comonomers with larger chains. The degree of incorporation decreases with increasing chain length.

The incorporation of the branched comonomer, 4-methyl-1-pentene, lowers T_m (DSC), T_c (DSC) and T_c (CRYSTAF) further. Melting and crystallization temperatures of propene/4-methyl-1-pentene copolymers are lower than those of propene/1-pentene copolymers but higher than propene/1-hexene (with the same number of carbon atoms in the comonomer) copolymers.

5.5 References

1. Arnold, M.; Knorr, J.; Bornemann, S.; *J. M. S. Pure Appl. Chem.* **1999**, A36(11), 1655.
2. Stevens, J. C.; *Stud. Surf. Sci. Catal.* **1996**, 101, 11.
3. Brüll, R.; Pasch, H.; Raubenheimer, H. G.; Sanderson, R.; van Reenen, A. J.; Wahner, U. M.; *Macromol. Chem. Phys.* **2001**, 202, 1281.
4. Arnold, M.; Bornemann, S.; Koller, F.; Menker, T. J.; Kressler, J.; *Macromol. Chem. Phys.* **1998**, 199, 2647.
5. Koivumaki, J.; Seppala, J. V.; *Polymer*, **1993**, 34, 1958.
6. Koivumaki, J.; Fink, G.; Seppala, J. V.; *Macromolecules*, **1994**, 34, 1958.
7. Paukkeri, R.; Lehtinen, A.; *Polymer* **1993**, 34(16), 4083.
8. Martuscelli, E.; Pracella, M.; Crispino, L.; *Polymer* **1983**, 24, 693.
9. Martuscelli, E.; Avella, M.; Segre, A.; Rossi, E.; Drusco, G.; Galli, P.; Simonazzi, T.; *Polymer* **1985**, 26, 259.
10. Burfield, D.; Loi, P.; *J. Appl. Polym. Sci.* **1990**, 41, 1095.
11. Janimak, J.; Cheng, S.; Zhang, A.; Hsieh, E.; *Polymer* **1992**, 33, 729.
12. Luongo J, *J. Appl. Polym. Sci.* **1960**, 3, 302.
13. Inoue, Y.; Itabashi, Y.; Chujo, R.; Doi, Y.; *Polymer* **1984**, 25, 1640.
14. Busico, V.; Corradini, P.; De Martino, L.; Graziano, F.; Iadicicco, A.; *Makromol. Chem.* **1991**, 192, 49.
15. Kakugo, M.; Miyatake, T.; Naito, Y.; Mizunuma, K.; *Macromolecules* **1998**, 30, 314.
16. Hayashi, Y.; Inoue, Y.; Chujo, R.; Doi, Y.; *Polymer* **1989**, 30, 1640.
17. B. Monrabal, *J. Appl. Polym. Sci.* **1994**, 52, 91.
18. Wahner, U.; Brüll, R.; Luruli, N, Pasch, H.; Raubenheimer, H.G.; Sanderson, R.D.; Van Reenen, A. J.; *Macromol. Chem. Phys.* **2001**, Submitted for publication.
- 19 Van Reenen, A. J.; Brüll, R.; Wahner, U.; Raubenheimer, H.G.; Sanderson, R.D.; Pasch, H.; *J. Polym. Sci. Part A: Polym Chem.* **2000**, 38, 4110.

CHAPTER 6

THE INFLUENCE OF REACTION CONDITIONS AND CATALYST SYSTEMS ON POLYMERISATION BEHAVIOUR OF α -OLEFINS

Abstract

Poly- α -olefins (1-pentene, 1-hexene, 1-octene and 1-decene) were polymerized using $(R-\eta^5-C_9H_6)_2ZrCl_2/MAO$ and $Me_2C(\eta^5-C_5H_4-\eta^5-C_9H_6)ZrCl_2/MAO$ catalyst systems under different conditions. The influence of the size and position of substituent R on the conversion, molecular weight and the end groups formed was investigated. Oligomers with number average molecular mass $M_n \approx 300 \text{ g.mol}^{-1}$ to poly olefins with $M_n \approx 6000 \text{ g.mol}^{-1}$ were obtained. The use of catalysts with bulkier substituents gave low conversions. The 1H NMR spectra were analyzed and end groups were attributed to different propagation and termination reactions.

6.1 Introduction

As mentioned previously, metallocene catalysts when activated by MAO are well known to polymerize ethene and propene, and lead to polymers with well defined properties and narrow molecular weight distribution¹⁻³. Polymerization of higher α -olefins received attention more recently, and a few excellent reviews have appeared²⁻⁸.

Polymers of higher α -olefins have not found major commercial application⁹. It has been proposed that poly- α -olefins with low molecular weight could later be converted into adhesives, fuel additives, lubricants, copolymers and fragrances¹⁰.

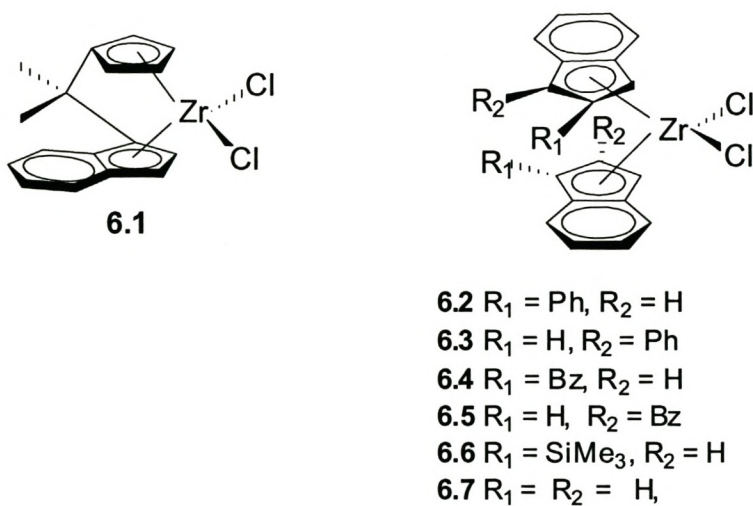
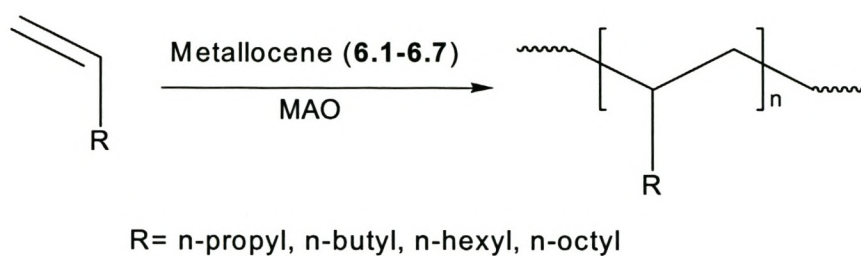
The steric and electronic factors of a particular substitution on metallocene catalysts can be correlated with the properties of the synthesized polymer. Coville et al. investigated the influence of substituent effects in $(\text{CpR})_2\text{ZrCl}_2$ catalysts on ethene polymerization¹¹. The influence of structure parameters on catalyst properties for ethene and propene polymerization was also studied by Helmut and Köppl⁷.

In this chapter the polymerization of a number of α -olefins (1-pentene, 1-hexene, 1-octene and 1-decene) using a series of $(\text{R}-\eta^5\text{-C}_9\text{H}_6)_2\text{ZrCl}_2$ catalysts is described. The influence of the size and position of substituent R on the conversion, molecular weight and resulting end groups was investigated. A further investigation probing the influence of reaction conditions such as temperature, MAO/catalyst ratio, and monomer/catalyst ratio on the conversion, molecular weight and end groups was carried out using only 1-hexene as reactant. The resulting polymers were characterized by NMR and GPC. These results were then compared with results of homopolymer synthesis using the *ansa*-catalyst $\text{Me}_2\text{C}(\eta^5\text{-C}_5\text{H}_4\text{-}\eta^5\text{-C}_9\text{H}_6)\text{ZrCl}_2$.

6.2 Experimental

6.2.1 Reaction Scheme

Homopolymers of 1-pentene, 1-hexene, 1-octene and 1-decene were prepared using metallocene/MAO catalyst systems (Scheme 6.1).



Scheme 6.1

6.2.2 Material and methods of purification

1-Pentene and 1-hexene (SASOL), 1-octene and 1-decene (Sigma-Aldrich) were dried and distilled over LiAlH_4 prior to use. Toluene was dried by refluxing over sodium/benzophenone and distillation under inert gas. MAO was purchased from Sigma-Aldrich and used without further purification (10 % solution in toluene).

6.2.3 General synthetic procedure

The mixture of MAO and catalyst (2.5 μmol dissolved in 1 mL of toluene) was prepared in a Schlenk tube and stirred for 5 min. The mixture was diluted with 10 mL of toluene. An appropriate amount of the monomer was subsequently added. All the reagents were handled and stored under nitrogen.

Homopolymers of 1-pentene, 1-hexene, 1-octene and 1-decene were prepared at room temperature according to a monomer/MAO/catalyst ratio of 30 000:10 000:1. Additional reaction conditions were employed for the synthesis of poly-1-hexene. The different reaction conditions were:

- Temperature : room temperature (RT), 50⁰C, 100⁰C and 140⁰C
- MAO/catalyst ratios : 500, 1 000, 2 500, 10 000
- Monomer/catalyst ratios : 5 000, 10 000, 30 000

6.2.3 Purification of the polymer

All the experiments were run for 20 h. Then each reaction was quenched with 9 mL methanol containing 1 mL of conc. HCl. The reaction mixture was diluted with toluene and washed three times with water. The organic phase was dried over CaCl_2 and the solvent subsequently removed under vacuum.

6.3 Results and discussion

6.3.1 Poly α -olefins

The results of the poly- α -olefins (1-pentene, 1-hexene, 1-octene and 1-decene) preparation with $(\text{Ind})_2\text{ZrCl}_2$ (**6.7**) are summarized in Table 6.1. The use of unsubstituted catalyst **6.7** under different polymerization conditions yielded oligomers with low molecular weights (M_n) ranging from 300 to about 9 000 $\text{g}\cdot\text{mol}^{-1}$. The molecular weight distribution was ≈ 2 as expected for metallocenes. The yields ranged from 1 to about 40 % (2 to 900 mg). The dependence of molecular weight and yield on reaction conditions is described in Section 6.4.2.

Table 6.1 Polymerization results obtained using complex $(\text{Ind})_2\text{ZrCl}_2$ (**6.7**)

| Sample | Monomer | Zr | Temp($^{\circ}\text{C}$) | MAO/Zr Ratio | Mon/Zr ratio | Yield (mg) | Conversion (%) | M_n ($\text{g}\cdot\text{mol}^{-1}$) | M_w ($\text{g}\cdot\text{mol}^{-1}$) | M_w/M_n |
|--------|---------|-----|----------------------------|--------------|--------------|------------|----------------|--|--|-----------|
| NL7.1 | C6 | 6.7 | RT | 500 | 30 000 | 2.6 | 0.11 | nd | nd | nd |
| NL7.2 | C6 | 6.7 | RT | 1 000 | 30 000 | 6.7 | 0.3 | nd | nd | nd |
| NL7.3 | C6 | 6.7 | RT | 2 500 | 30 000 | 136.7 | 6.28 | 3 530 | 8 780 | 2.48 |
| NL7.4 | C6 | 6.7 | RT | 10 000 | 30 000 | 570.6 | 26.24 | 2360 | 6 200 | 2.62 |
| NL7.5 | C6 | 6.7 | RT | 10 000 | 5 000 | 29.5 | 1.53 | nd | nd | nd |
| NL7.6 | C6 | 6.7 | RT | 10 000 | 10 000 | 163.7 | 8.51 | 2 340 | 5 930 | 2.53 |
| NL7.7 | C5 | 6.7 | RT | 10 000 | 30 000 | 97.9 | 7.24 | 2 680 | 6 670 | 2.48 |
| NL.8 | C8 | 6.7 | RT | 10 000 | 30 000 | 276.9 | 12.73 | 3 320 | 8 240 | 2.47 |
| NL7.9 | C10 | 6.7 | RT | 10 000 | 30 000 | 166.5 | 6.49 | 3 240 | 8 890 | 2.74 |
| NL7.10 | C6 | 6.7 | 50 | 10 000 | 30 000 | 950.3 | 43.71 | 770 | 1 380 | 1.79 |
| NL7.11 | C6 | 6.7 | 100 | 10 000 | 30 000 | 645.3 | 29.68 | 300 | 380 | 1.27 |
| NL7.12 | C6 | 6.7 | 140 | 10 000 | 30 000 | 59.5 | 2.74 | nd | nd | nd |

nd = not determined

RT = room temperature

6.3.2 ^{13}C NMR analysis

The very sharp, intensive ^{13}C NMR signals were assigned to the various carbons as shown in Figure 6.1. The observed and the expected chemical shifts according to Asakura et al.¹² are given in Table 6.2.

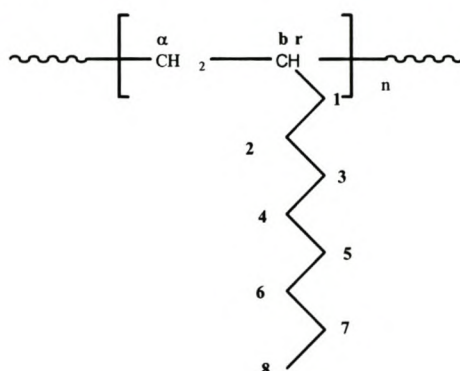


Figure 6.1 The structure of poly-1-decene

Table 6.2 Chemical shifts (ppm) for the ^{13}C NMR spectra of poly α -olefins

| Carbon | Poly-1-pentene | | Poly-1-hexene | | Poly-1-octene | | Poly-1-decene | |
|----------------|--------------------|-----------------------|---------------|----------|---------------|----------|---------------|----------|
| | Exptl ^a | Expected ^b | Exptl | Expected | Exptl | Expected | Exptl | Expected |
| α | 40.48 | 41.22 | 40.50 | 40.66 | 40.27 | 41.20 | 40.20 | 41.21 |
| br | 32.50 | 33.26 | 32.52 | 32.81 | 32.23 | 33.41 | 32.23 | 33.41 |
| C ₁ | 37.50 | 38.01 | 34.66 | 34.96 | 34.18 | 35.67 | 34.06 | 35.68 |
| C ₂ | 19.66 | 19.98 | 28.9 | 29.02 | 26.02 | 26.98 | 26.03 | 27.08 |
| C ₃ | 14.71 | 14.78 | 23.36 | 23.56 | 29.78 | 30.32 | 30.20 | 30.75 |
| C ₄ | | | 14.29 | 14.41 | 31.77 | 32.33 | 29.65 | 30.14 |
| C ₅ | | | | | 22.53 | 23.00 | 29.35 | 29.77 |
| C ₆ | | | | | 13.89 | 14.18 | 31.83 | 32.29 |
| C ₇ | | | | | | | 22.57 | 22.96 |
| C ₈ | | | | | | | 14.00 | 14.17 |

^a experimental

^b expected according to reference 12

A good agreement between the observed and the calculated values was found. The ^{13}C NMR spectra of poly-1-pentene, poly-1-hexene, poly-1-octene and poly-1-decene are shown in Figure 6.2 (a-d).

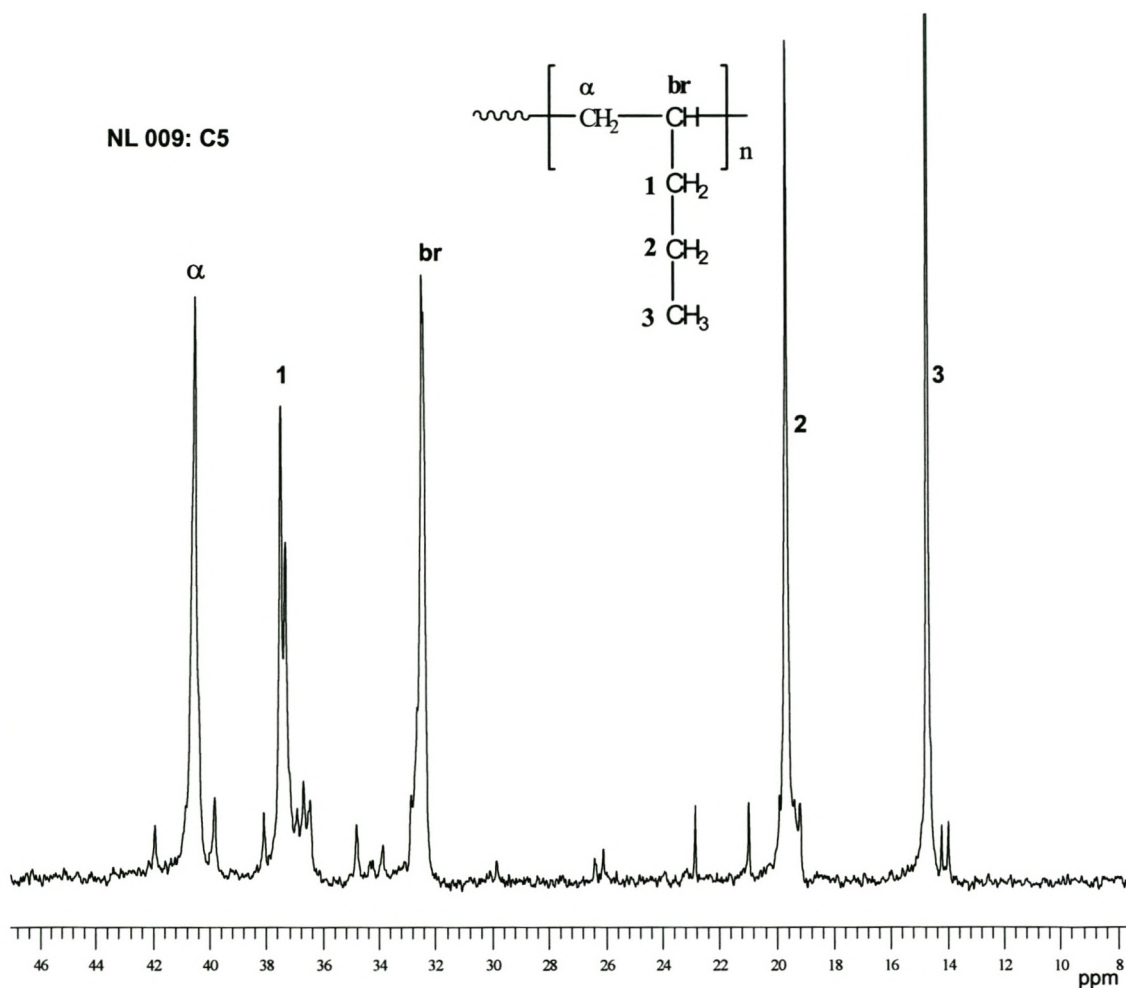
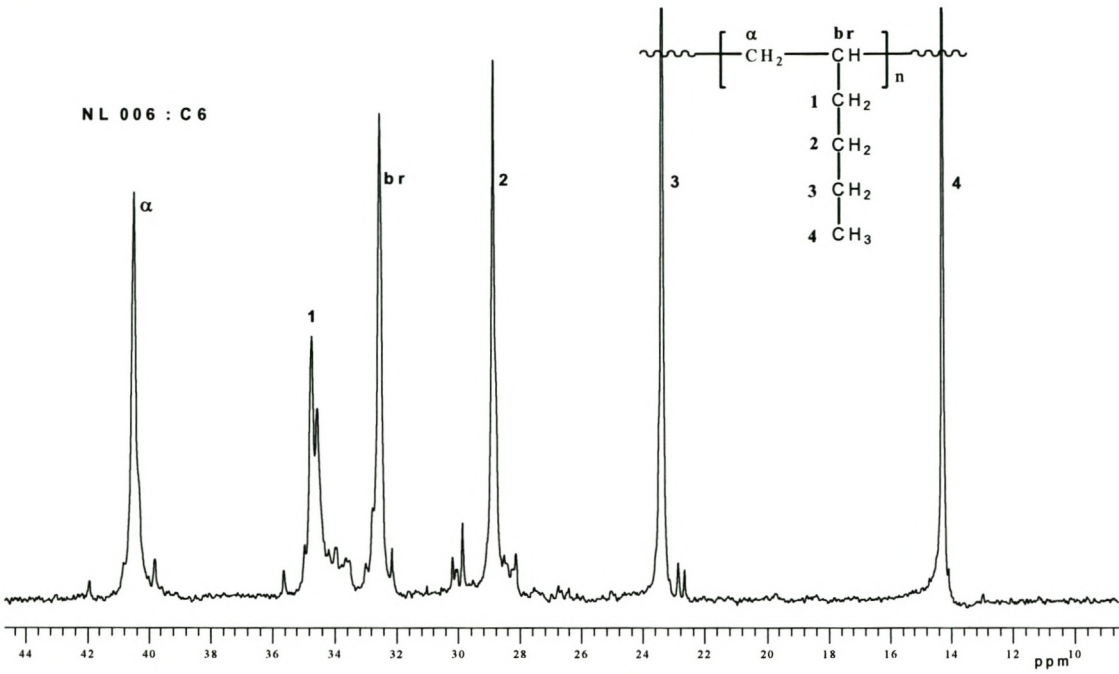


Figure 6.2 (a) ^{13}C NMR spectrum of poly-1-pentene

(b)



(c)

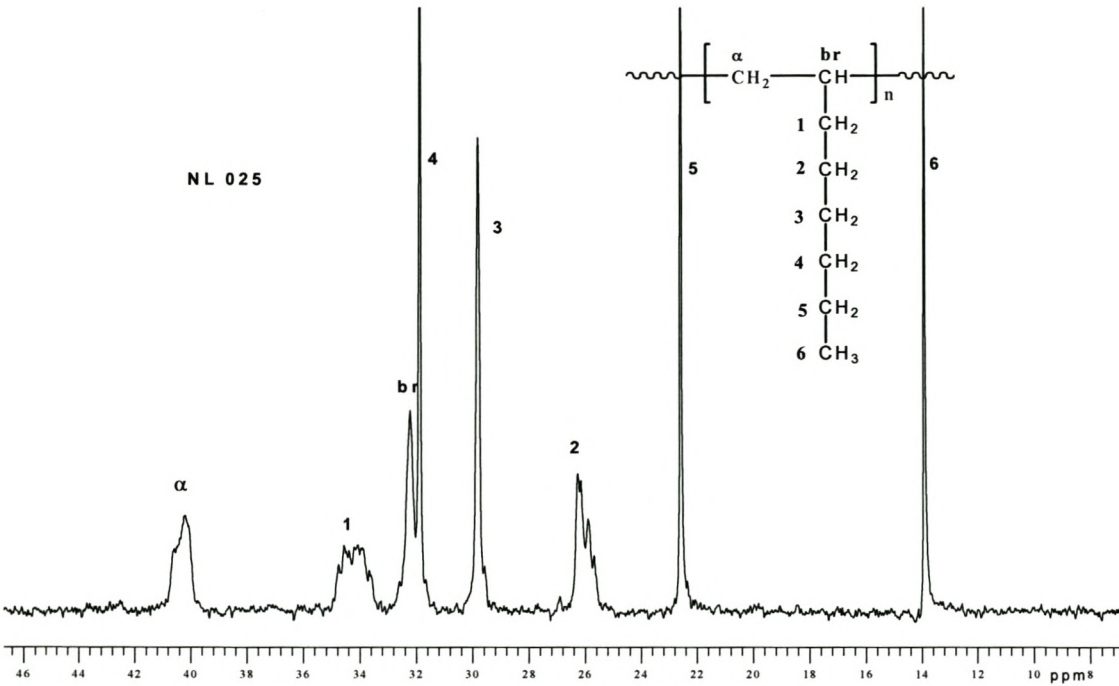


Figure 6.2 (b & c) ^{13}C NMR spectra of poly-1-hexene and poly-1-octene

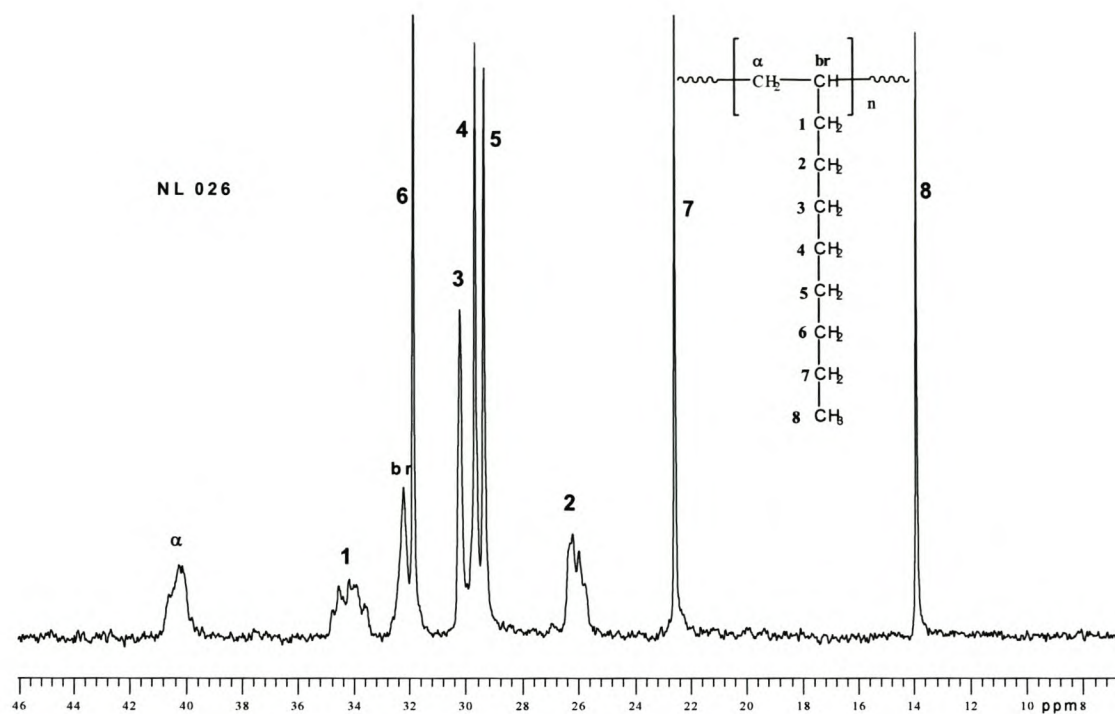
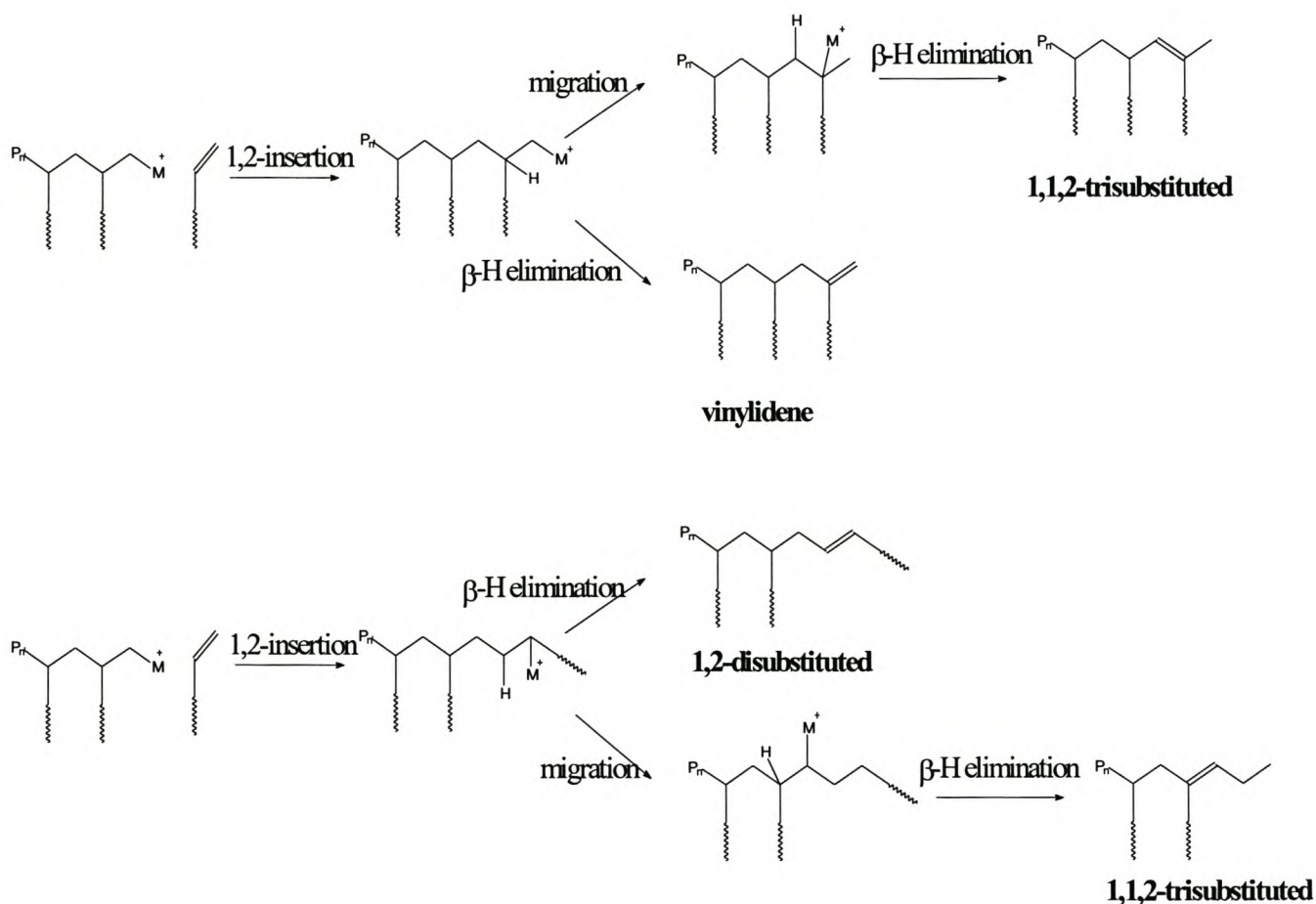


Figure 6.2 (d) ^{13}C NMR spectrum of poly-1-decene

Additional weak signals were observed in poly-1-pentene and poly-1-hexene ^{13}C NMR spectra. The weak signals might be mainly due to carbons arising from misinsertion reactions such as 2,1 misinsertions during polymerization, or even to the formation of saturated end groups. It has been pointed out by Kim et al.⁹ that saturated end groups are common for poly α -olefins synthesized with metallocene/MAO catalyst systems. These weak signals have also been observed before, but were not clearly identified^{9,13}. The chemical shifts of the main signals in the ^{13}C NMR spectra of all the poly α -olefins revealed that the chain propagation mechanism follows mainly 1,2 insertion.

6.3.3 Analysis of end groups

The end groups and internal double bonds were analyzed using ^1H NMR. Only the saturated end groups were considered, since the possible unsaturated end groups could not be easily – if at all – distinguished from the poly- α -olefin side chain signals. Several types of double bonds exist (Scheme 6.2)^{14,15}. Vinylidene end groups are a result of β -hydride elimination that terminates chain propagation occurring by 1,2 monomer insertion.



Scheme 6.2 Possible mechanisms for the chain termination reaction leading to different end groups

The 1,2-disubstituted double bonds may result from a chain termination process caused by 2,1-misinsertion followed by β -hydride elimination. The 1,1,2-trisubstituted double bonds could result from a migration of the metal moiety along the carbon backbone following either 1,2-insertion or 2,1-misinsertion and subsequent termination reaction by β -hydride elimination. The ^1H NMR of poly- α -olefins are very similar to each other and therefore ^1H NMR for poly-1-hexene will be used for illustrating these types of end groups.

The resonances were assigned following Kim et al⁹. The ^1H NMR spectrum in Figure 6.3 shows end groups of poly- α -olefins. The spectrum is expanded in Figure 6.4.

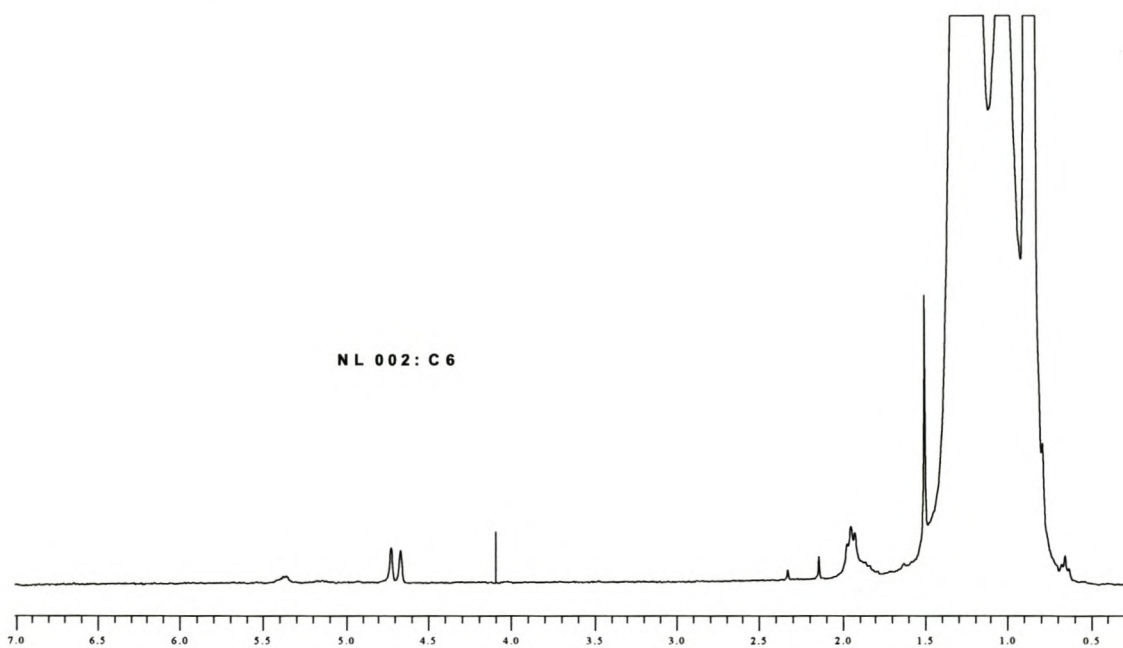


Figure 6.3 ^1H NMR spectrum of poly-1-hexene

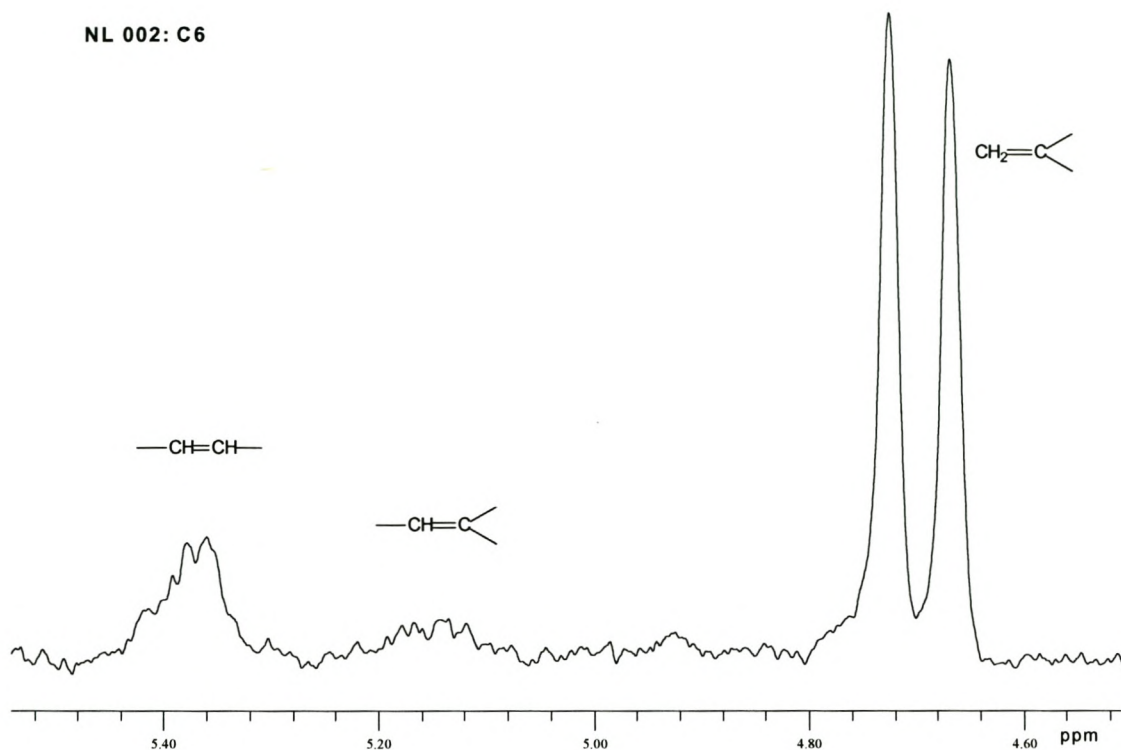


Figure 6.4 Expanded region (4.2-5.6ppm) of ^1H NMR spectrum for poly-1-hexene

The intense signals at δ 4.67-4.72, δ 5.09-5.2 and δ 5.32-5.44 are attributable to vinylidene, 1,1,2-trisubstituted, 1,2-disubstituted double bonds respectively.

The amount of 1,1,2-trisubstituted increases while 1,2-disubstituted double bonds decreases with increasing temperatures as shown in Figure 6.5. The relative abundance of olefinic end groups, is listed in Table A1 (Appendix A).

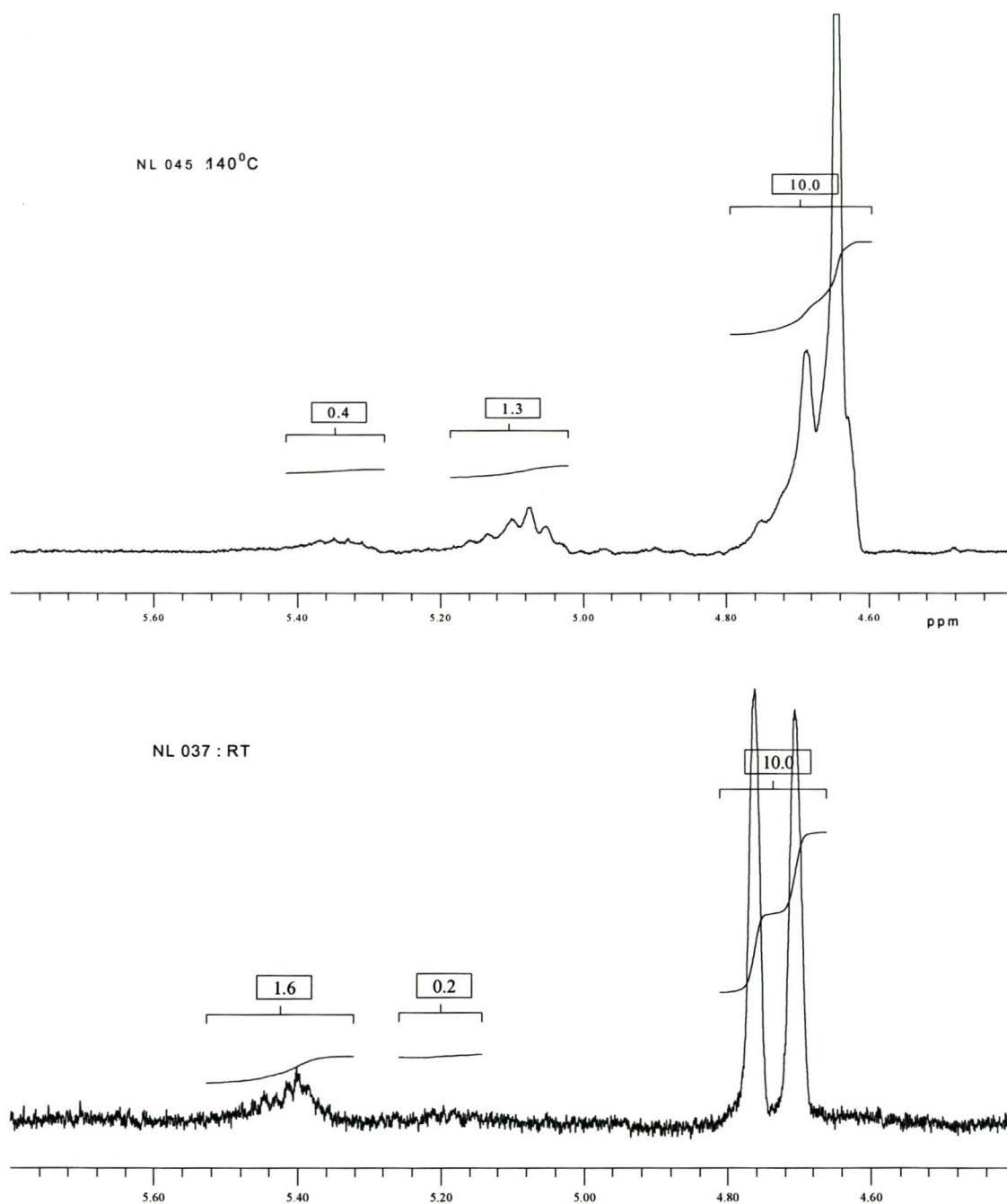


Figure 6.5 Expanded region (4.2-5.6ppm) of the ¹H NMR spectrum for poly-1-hexene synthesized at two different temperatures

6.4 The influence of reaction conditions and substituent effects of (R- η^5 -C₉H₆)₂ZrCl₂ on 1-hexene polymerization behaviour

The polymerization of poly-1-hexene was carried out as explained in Section 6.2.3. The results obtained using (Ind)₂ZrCl₂ are shown in Table 6.2. Results from various polymerizations of poly-1-hexene carried out using (R- η^5 -C₉H₆)₂ZrCl₂ catalysts are listed in Table (B1 –B5) (Appendix B). Table 6.3 shows results obtained using the bridged catalyst, Me₂C(η^5 -C₅H₄- η^5 -C₉H₆)ZrCl₂ (6.1).

Table 6.3 Polymerization results obtained using complex Me₂C(η^5 -C₅H₄- η^5 -C₉H₆)ZrCl₂

| Sample | Monomer | Zr | Temp(°C) | MAO/Zr ratio | Mon/Zr ratio | Yield (mg) | Conversion (%) | M _n (g.mol ⁻¹) | M _w (g.mol ⁻¹) | M _w /M _n |
|--------|---------|-----|----------|--------------|--------------|------------|----------------|---------------------------------------|---------------------------------------|--------------------------------|
| NL1.1 | C5 | 6.1 | RT | 2500 | 30 000 | 199.9 | 14.79 | 2 030 | 4 030 | 1.97 |
| NL1.2 | C6 | 6.1 | RT | 2500 | 30 000 | 174.9 | 15.92 | 2 210 | 4 280 | 2.01 |
| NL1.3 | C8 | 6.1 | RT | 2 500 | 30 000 | 106 | 4.88 | 2 540 | 4 700 | 1.84 |
| NL1.4 | C6 | 6.1 | 0 | 2 500 | 30 000 | 12.9 | 0.59 | nd | nd | nd |
| NL1.5 | C6 | 6.1 | 100 | 2 500 | 30 000 | 59.3 | 2.72 | 864 | 2 010 | 2.32 |
| NL1.6 | C6 | 6.1 | 140 | 2 500 | 30 000 | 28.7 | 1.32 | 692 | 1 040 | 1.5 |
| NL1.7 | C6 | 6.1 | 50 | 2 500 | 30 000 | 572.3 | 26.32 | 1 930 | 3 430 | 1.77 |
| NL1.8 | C6 | 6.1 | RT | 10 000 | 30 000 | 247 | 11.32 | 2 640 | 6 010 | 2.27 |
| NL1.9 | C6 | 6.1 | RT | 500 | 30 000 | 17.7 | 0.81 | 2 390 | 7 080 | 1.7 |
| NL1.10 | C6 | 6.1 | RT | 1 000 | 30 000 | 172.4 | 7.93 | 3 810 | 8 240 | 2.15 |
| NL1.12 | C6 | 6.1 | RT | 2 500 | 5 000 | 333.2 | 61.80 | 230 | 3 150 | 1.37 |

nd = not determined

6.4.1 The effects of steric factors, temperature, MAO/catalyst and monomer/catalysts ratio on poly-1-hexene yields (conversions)

The polymerization behaviour of different catalysts under various reaction conditions was investigated. The yields of poly-1-hexene obtained using different catalysts were plotted as a function of temperature, the MAO/catalyst ratio and monomer/catalyst ratio (Figures 6.6-6.8). The influence of steric factors is also shown.

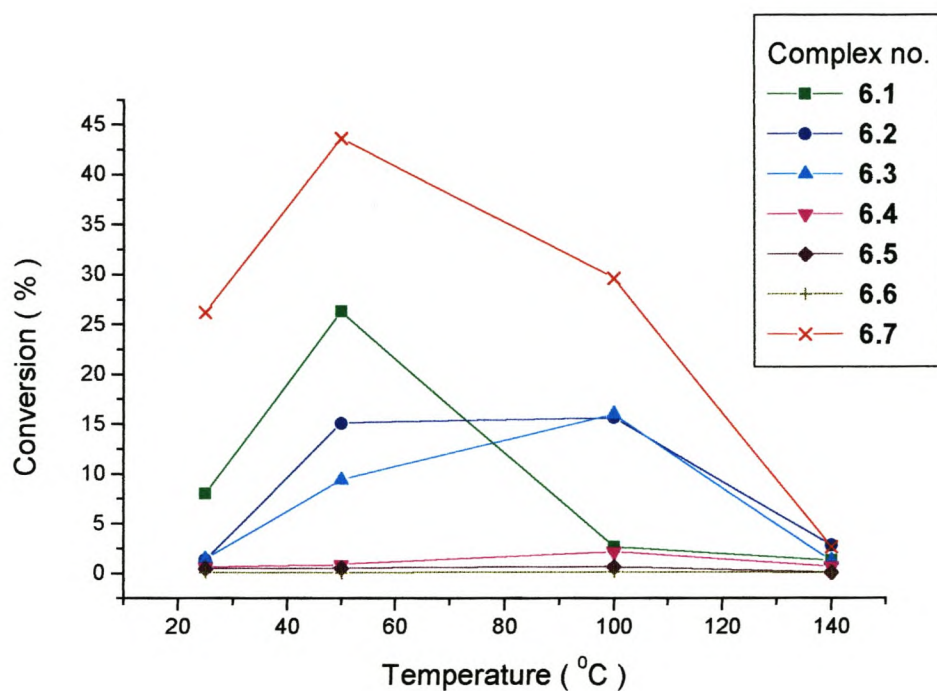


Figure 6.6 Yields of poly-1-hexene as a function of temperature

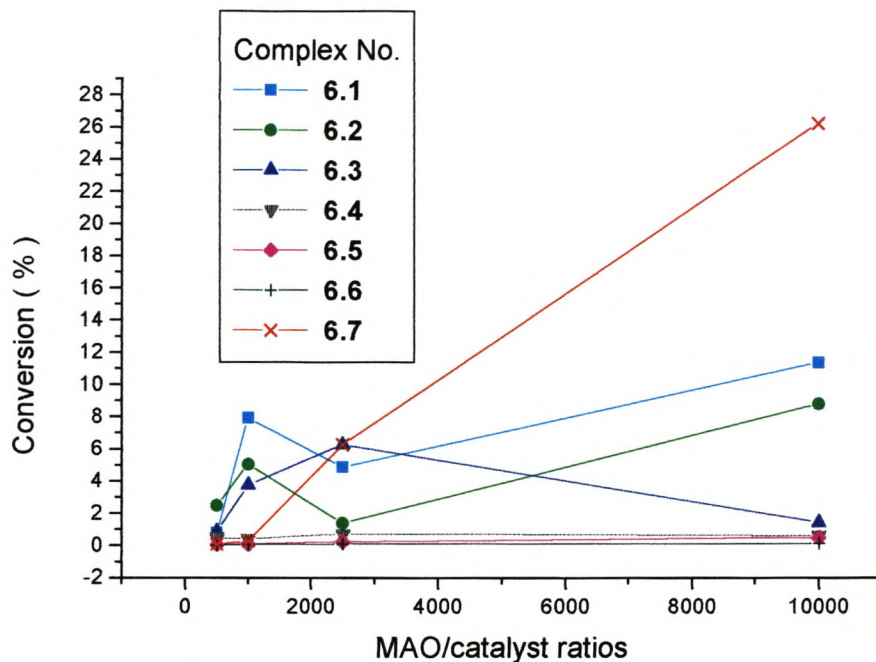


Figure 6.7 Yields of poly-1-hexene as a function of MAO/catalysts ratio

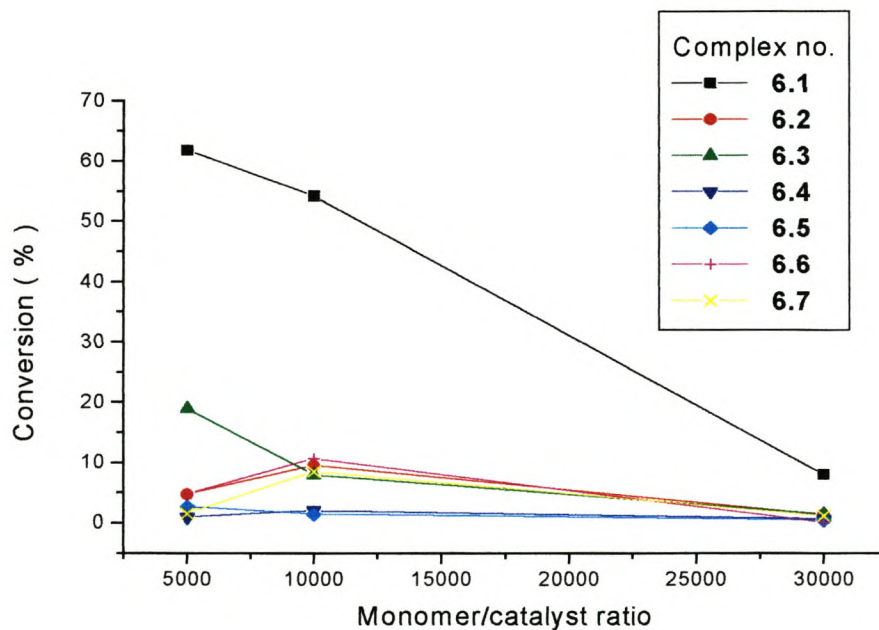


Figure 6.8 Yields of poly-1-hexene as a function of monomer/catalysts ratio

As shown in Figures 6.6-6.8 catalysts with less bulky substituents ($(1\text{-Ph-}\eta^5\text{-C}_9\text{H}_6)_2\text{ZrCl}_2$ (**6.2**) and $(2\text{-Ph-}\eta^5\text{-C}_9\text{H}_6)_2\text{ZrCl}_2$ (**6.3**) effected higher conversion or yields at any given temperature. Using the unsubstituted catalyst $(\text{Ind})_2\text{ZrCl}_2$ (**6.7**) the overall highest yields (close to 1g) were obtained. Catalysts with bulkier substituents, $(1\text{-Bz-}\eta^5\text{-C}_9\text{H}_6)_2\text{ZrCl}_2$ (**6.4**), $(2\text{-Bz-}\eta^5\text{-C}_9\text{H}_6)_2\text{ZrCl}_2$ (**6.5**), and $(1\text{-SiMe}_3\text{-}\eta^5\text{-C}_9\text{H}_6)_2\text{ZrCl}_2$ (**6.6**), produced lower yields (10-15mg) which are insufficient for further analysis.

Better conversions under the given conditions were obtained with catalyst containing substituents in the 1-position of the indenyl ligand than in the 2- position.

The influence of temperature on yields is depicted in Figure 6.6. Conversions increase with temperature reaching a maximum at ca. 50°C and then decrease again.

The yields increased with an increase in MAO/catalyst ratio as shown in Figure 6.7, but the effect of the monomer/catalyst ratios (Figure 6.8) is not conclusive.

6.4.2 The effects of steric factors, temperature, MAO/catalyst and monomer/catalysts ratios on poly-1-hexene molecular weight

The polymerization of 1-hexene with substituted catalyst, $(\text{R-}\eta^5\text{-C}_9\text{H}_6)_2\text{ZrCl}_2$ (**6.2-6.6**), generally yielded polymers with molecular weight (M_n) ranging from 300 to 3800 $\text{g}\cdot\text{mol}^{-1}$ (Table 6.1 and 6.3) with few exceptions. It is interesting to note that complex $(2\text{-Ph-}\eta^5\text{-C}_9\text{H}_6)_2\text{ZrCl}_2$ (**6.3**) with MAO ratios of 500 and 1000 produced poly-1-hexene with $M_n = 25\ 000$ and $12\ 500$ (Table B3, Appendix B) $\text{g}\cdot\text{mol}^{-1}$ respectively. Molecular weight obtained for polymers synthesized using complexes containing bulkier groups, such as $(2\text{-Bz-}\eta^5\text{-C}_9\text{H}_6)_2\text{ZrCl}_2$ (**6.5**) and $(1\text{-SiMe}_3\text{-}\eta^5\text{-C}_9\text{H}_6)_2\text{ZrCl}_2$ (**6.6**), were not analyzed due to insufficient yields as mentioned before (Section 6.4.1). The bridged complex, (**6.1**), produced polymers with molecular weights comparable to the ones obtained with $(\text{R-}\eta^5\text{-C}_9\text{H}_6)_2\text{ZrCl}_2$.

Low molecular weight (300-800 g.mol⁻¹) oligomers were obtained at higher temperatures, i.e. molecular weight decreased with increasing temperature. Brüll et al.¹⁶ reported that the molecular weight of poly- α -olefins (1-pentene to 1-octadecene) synthesized with the Me₂Si(2-Methylbenz[e]indenyl)₂ZrCl₂/MAO catalyst system, showed exponential decrease with increasing temperature. The dependence of molecular weight on reaction temperature suggests that chain propagation is favoured at low temperatures, whereas chain termination, via β -hydride elimination, is facilitated at high temperatures. Other unknown chain termination processes could also occur. The complexity of ¹³C NMR spectra of polymers synthesized at higher temperatures, supports this argument.

There seems to be no correlation between molecular weight or polydispersity on the one hand and MAO/catalyst and monomer/catalyst ratios on the other.

Polymers synthesized at room temperature had polydispersities (M_w/M_n) \approx 2 which is expected for metallocene polymers, however, multimodal distribution and high polydispersities (M_w/M_n) \approx 3.8-10 were recorded for oligomers synthesized at higher temperatures.

GPC curves of polymers synthesized at different temperatures and different MAO/catalysts ratios were compared and are displayed in Figures 6.9 and 6.10. Polymers synthesized at room temperature have monomodal but broad distributions whereas curves for polymers synthesized at high temperature have shoulders or multimodal distributions. Polymers synthesized at 50 °C gave sharp curves and even sharper at 100 °C. Oligomers of $M_n \approx$ 300-800 g.mol⁻¹ that were characterized by very narrow molecular weight distribution were obtained at 100 °C. These observations were consistent for all complexes used.

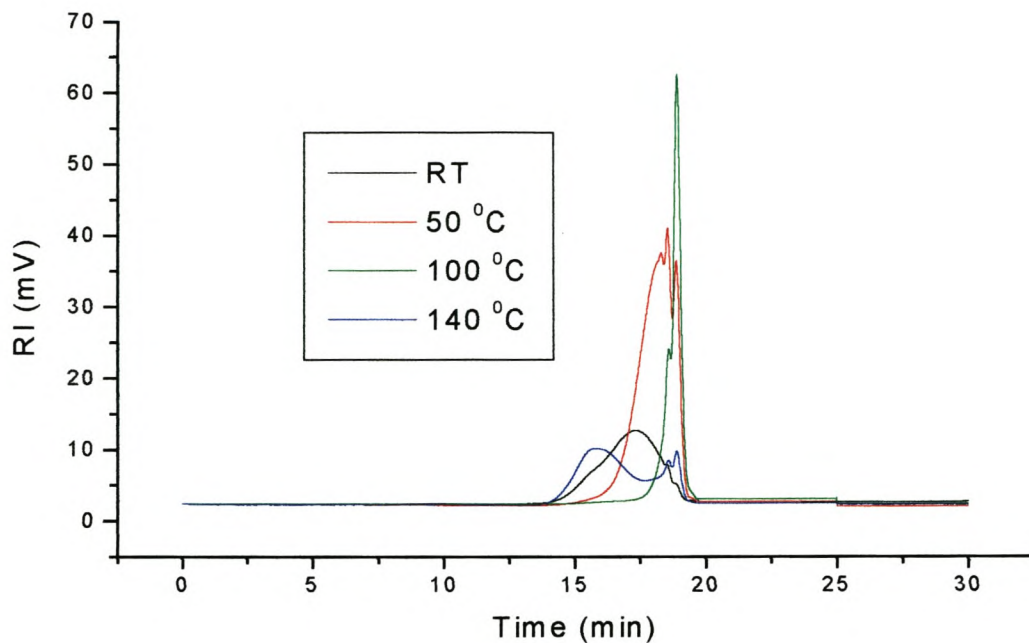


Figure 6.9 Molecular weight distribution of poly-1-hexene prepared at different temperatures using catalyst 6.2 as determined by GPC

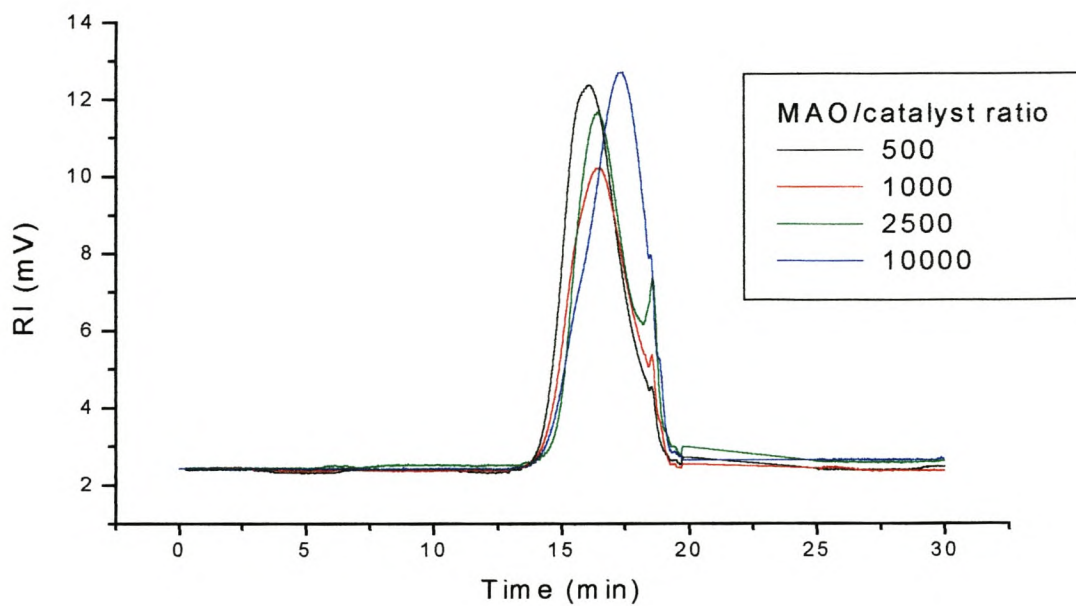


Figure 6.10 Molecular weight distribution of poly-1-hexene prepared at room temperature using catalyst 6.2 as determined by GPC

Multimodal distribution and high polydispersities for poly-1-pentene and 1-hexene synthesized with *rac*-[Et(Ind)₂ZrCl₂], [(CH₃)₂Si(Ind)₂ZrCl₂], Cp₂HfCl₂, Cp₂ZrCl₂ and (CpR₅)₂ZrCl₂ were also reported by Wahner et al.¹⁷ and Murray et al.¹⁸ respectively. This could be due to temperature fluctuations arising from instrumental fault. Another reason could be due to conversions taking place before the set temperature was reached.

6.5 Conclusions

The of α -olefins (1-pentene, 1-hexene, 1-octene and 1-decene) are readily polymerized with (R- η^5 -C₉H₆)₂ZrCl₂ and Me₂C(η^5 -C₅H₄- η^5 -C₉H₆)ZrCl₂ catalyst systems under different conditions producing polymers with number average molecular mass from Mn \approx 300 g.mol⁻¹ to Mn \approx 6000 g.mol⁻¹. The polydispersity of polymers synthesized at room temperatures are M_w/M_n \approx 2, which is typical for metallocene-catalysed poly- α -olefins. Multimodal distributions are observed for poly α -olefins synthesized at high temperatures.

The yields obtained are strongly dependent on the size of the substituent and on reaction conditions. Yields decrease with increasing size of the substituent. The unsubstituted complex (Ind)₂ZrCl₂ (6.7) gives higher yields than the bulky compounds (2-Bz- η^5 -C₉H₆)₂ZrCl₂ (6.5) and (1-SiMe₃- η^5 -C₉H₆)₂ZrCl₂ (6.6).

For poly-1-pentene and 1-hexene additional misinsertion mechanisms such as 2,1 misinsertions are indicated by the presence of additional small ¹³C NMR resonances. The chain propagation mechanism for all poly- α -olefins and 1-decene follow mainly a 1,2 insertion.

Various end groups such as vinylidene, 1,2 disubstituted and 1,1,2 trisubstituted double bonds are formed. A vinylidene double bond is the major end group for all polymers and oligomers indicating a 1,2 insertion propagation followed by eventual β -hydride elimination. The amount of 1,1,2 trisubstituted double bonds increase with an increase in temperature.

The stereoregularity of the materials is currently being investigated. Most of the catalysts used are expected to exhibit iso-aspecificity and hemiisospecificity¹⁹⁻²¹. Detailed ¹³C NMR analysis has to be done.

6.6 References

1. Kaminsky, W.; *Angew. Chem. Int. Ed. Engl* **1994**, 223, 101.
2. Pino, P.; Mulhaupt, R.; *Angew. Chem. Int. Ed. Engl.* **1980**, 19, 857.
3. Brintzinger, H. H.; Fischer, D.; Mulhaupt, R.; Rieger, B.; Waymouth, R. M.; *Angew. Chem. Int. Ed. Engl.* **1995**, 34, 1143.
4. Coates, G. W.; *Chem. Rev.* **2000**, 100, 1223.
5. Resconi, L.; Cavallo, L.; Fait, A.; Piemontesi, F.; *Chem. Rev.* **2000**, 100, 1253.
6. Arnold, M.; Knorr, J.; Bornemann.; *J. M. S. Pure Appl. Chem.* **1999**, A36(11), 1655.
7. Helmut, G. A.; Köppl, A.; *Chem. Rev.* **2000**, 100, 1205.
8. Kaminsky, W.; Arndt, M.; *Metallocenes for polymer catalysis*, In *Advances in Polymer Science*, Editor: Ringshof, H., **1997**, 27, 144.
9. Kim, I.; Zhou, J.; Chung, H.; *J. Polym. Sci. Part A* **2000**, 38, 1687.
10. Hungenberg, K. D.; Kerth, J.; Langhauser, F.; Mueller, H. J.; Mueller, P. J.; *Angew. Makromol. Chem.* **1995**, 227, 159.
11. Grimmer, N. E.; Coville, N. J.; de Koning, C. B.; *J. Organometal. Chem.* **1994**, 479,1-29.
12. Asakura, T.; Demura, M.; Nishiyama, Y.; *Macromolecules*, **1991**, 24, 2334.
13. Zhao, X.; Odian, G.; Rossi, A.; *J. Polym. Sci. Part A* **2000**, 38, 3802.
14. Grumel, V.; Brüll, R.; Pasch, H.; Raubenheimer, H. G.; Sanderson, R.; Wahner, U. M.; *Macromol. Mat. Eng.* **2001**, 286(8), 480.
15. Babu, N.; Newmark, Chien, J.C.W.; *Macromolecules*, **1994**, 27, 3383.
16. Brull, R.; Pasch. H.; Raubenheimer, H.; Sanderson, R.; Wahner, U.M.; *J. Polym. Sci. Part A* **2000**, 38, 2333.
17. Wahner, U.M.; Brull, R.; Pasch. H.; Raubenheimer, H.; Sanderson, R.; *Angew. Makromol. Chem.* **1999**, 270, 49.
18. Murray, M. C.; Baird, M. C.; *J. Mol. Catal. A: Chem.* **1998**, 128, 1.
- 19 Tagge, C. D.; Kravchenko, R. L.; Lal, T. K.; Waymouth, R. M.; *Organometallics* **1999**, 18, 380.
- 20 Bruce, M. D.; Waymouth, R. M.; *Macromolecules* **1998**, 18, 2707.

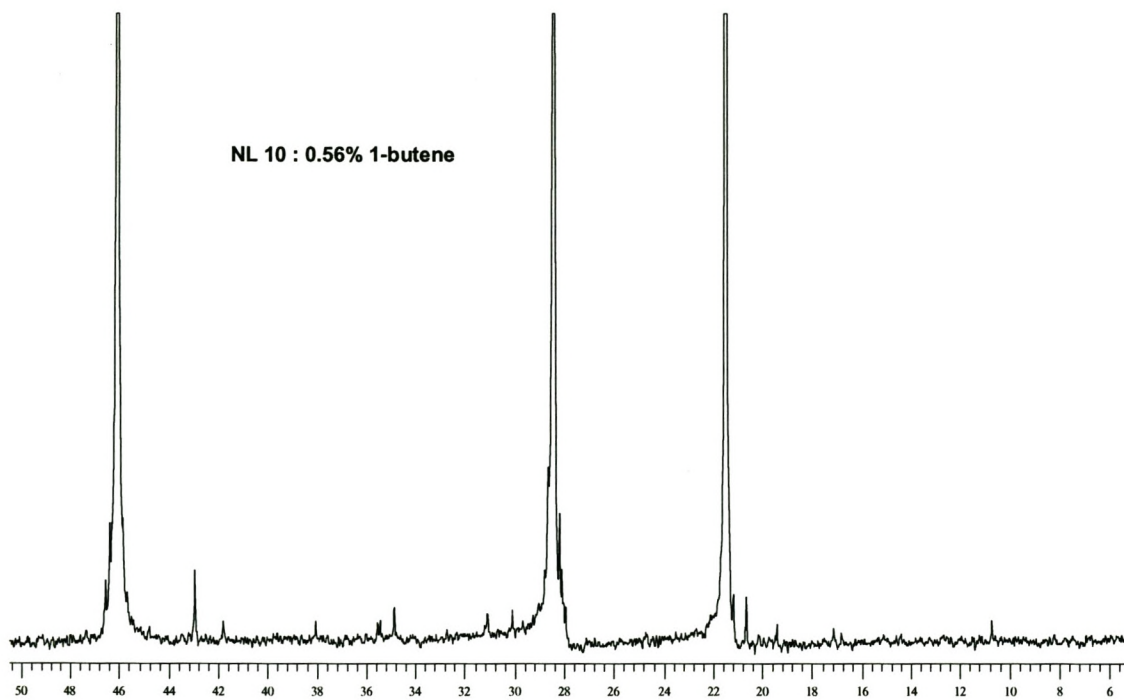
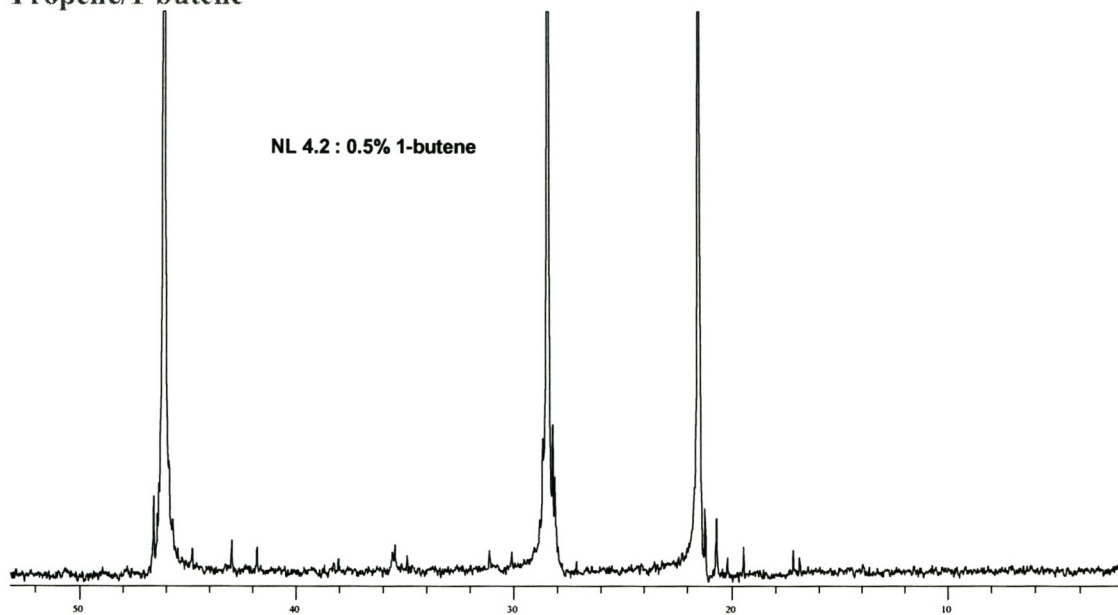
21 Fierro, R.; Chien, J. W. C.; Rausch, M, *J. Polym. Sci. Part A* **1994**, 32, 2817.

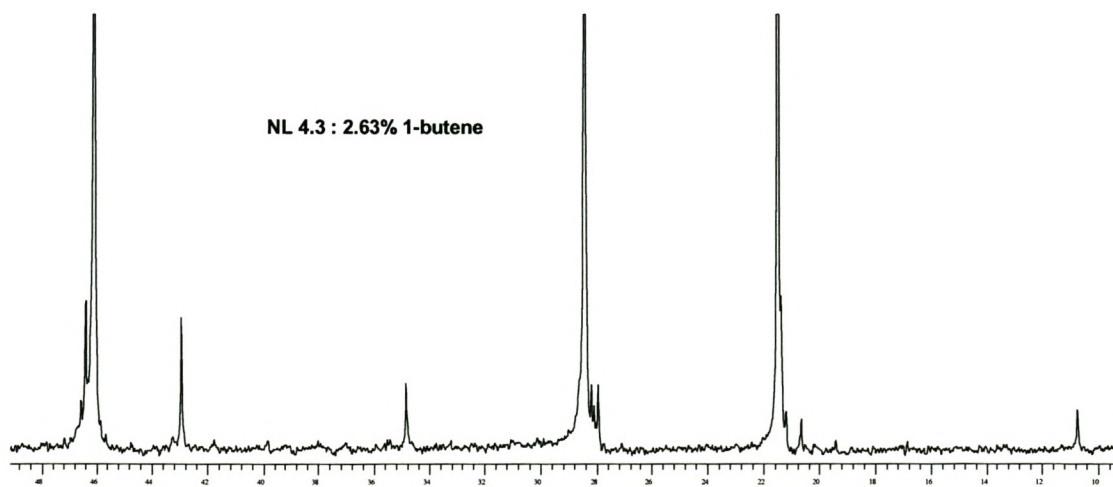
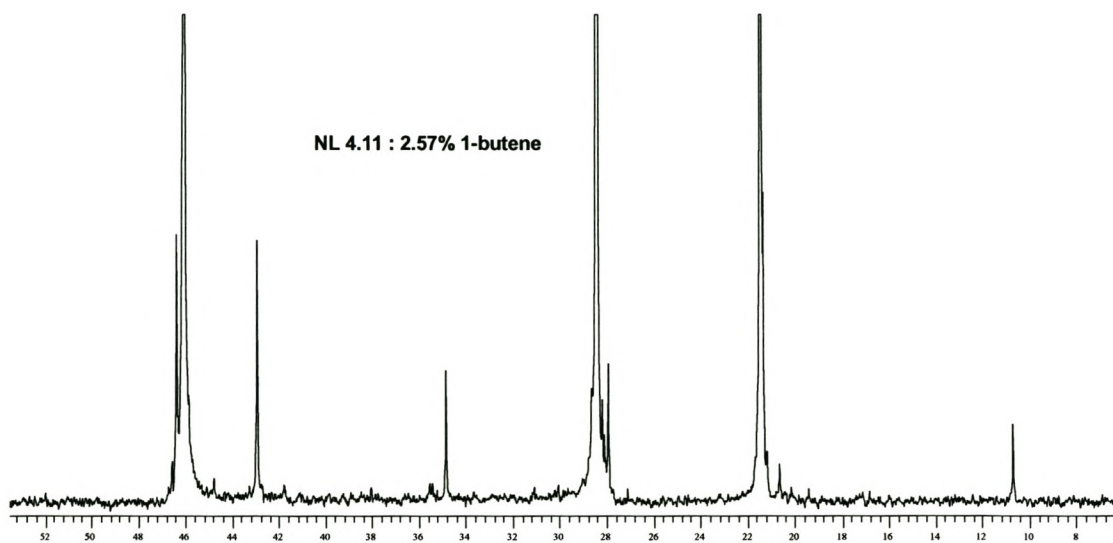
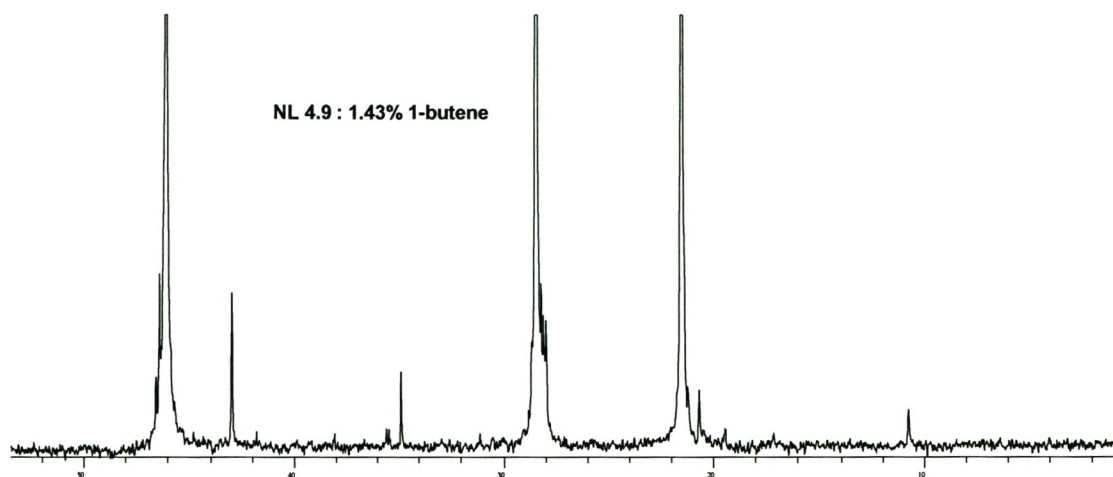
Appendix A

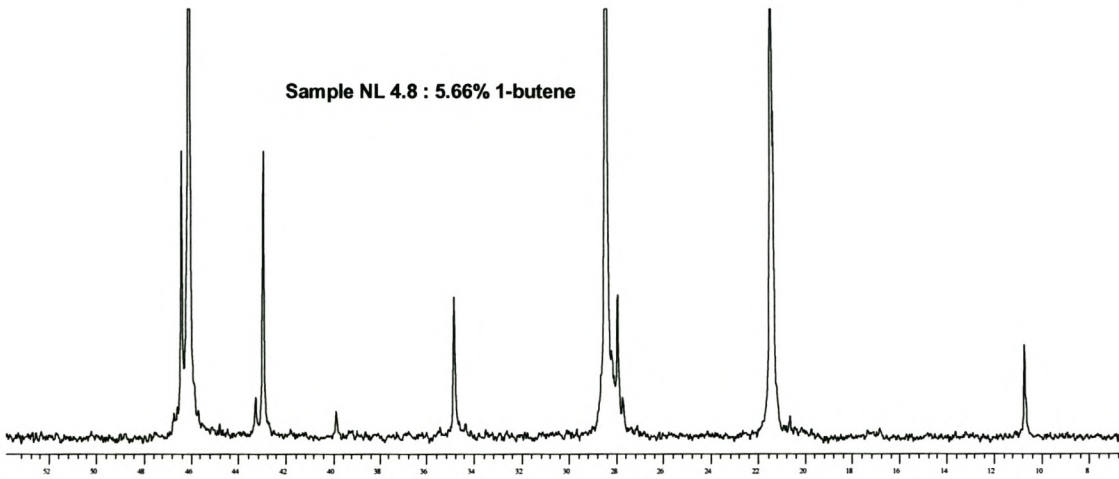
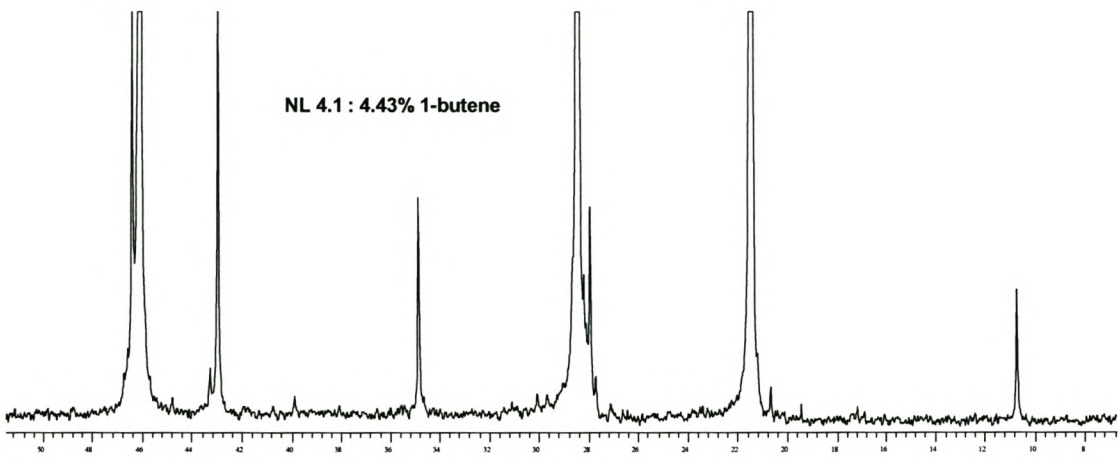
NMR DATA

Propene/ α -olefin copolymers

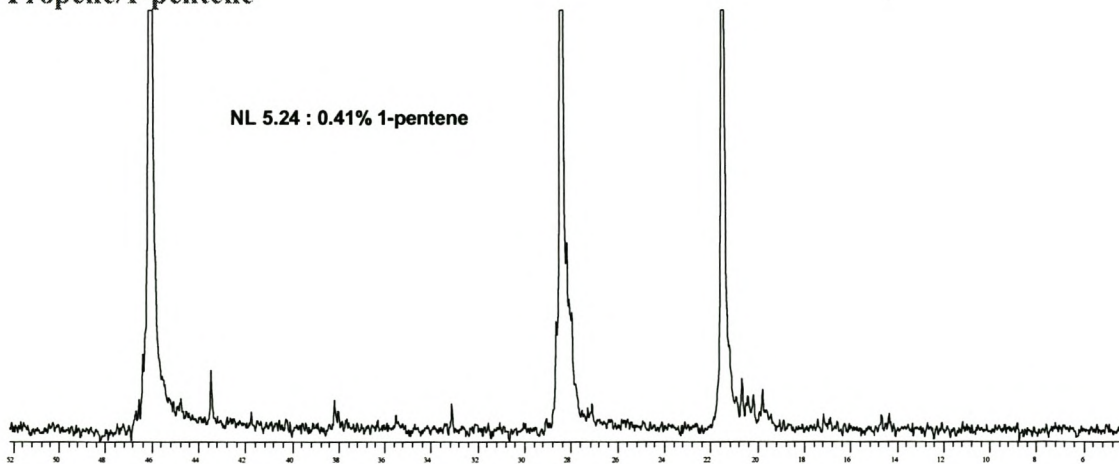
Propene/1-butene

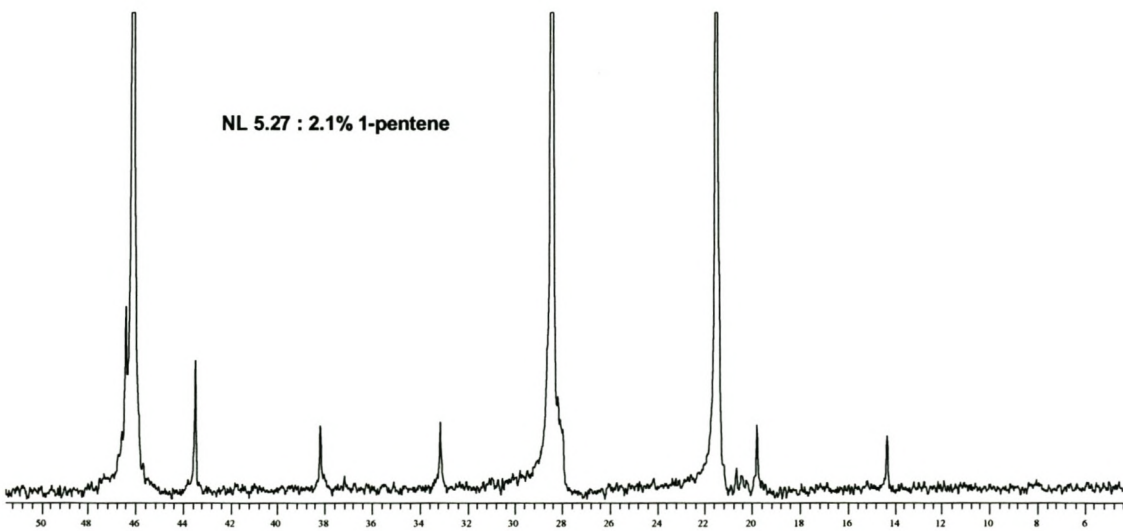
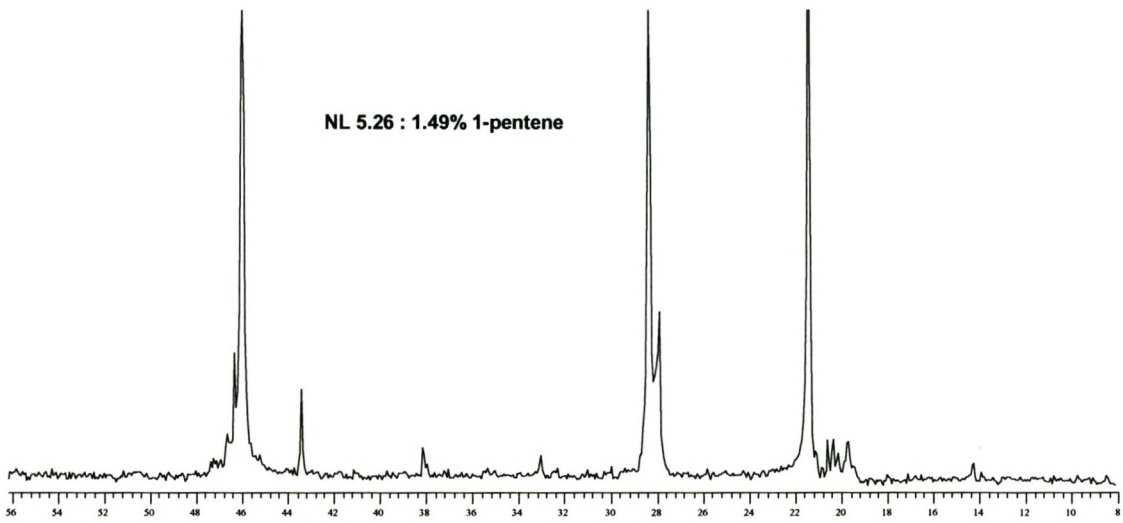
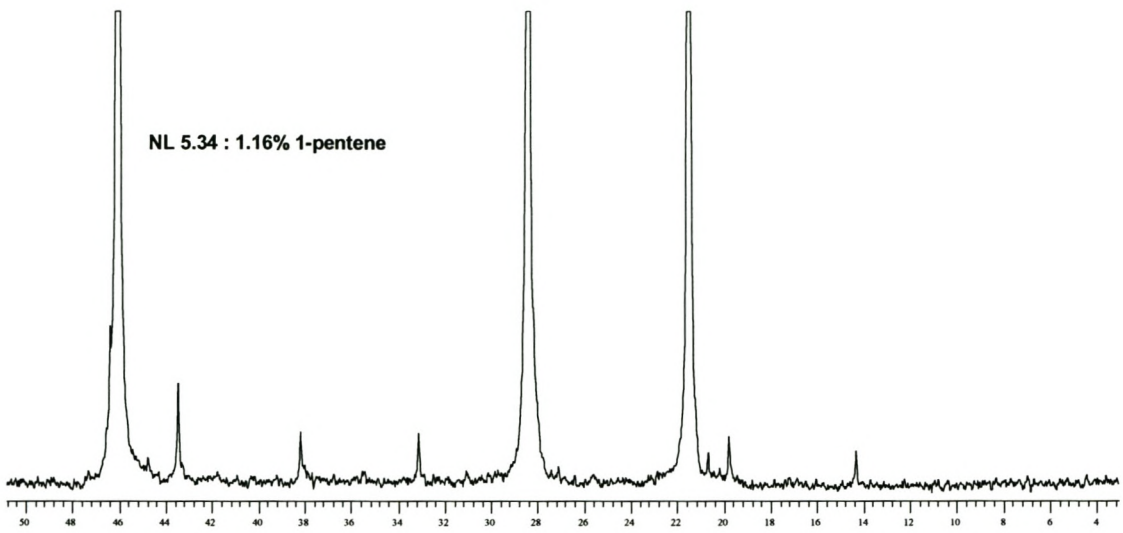


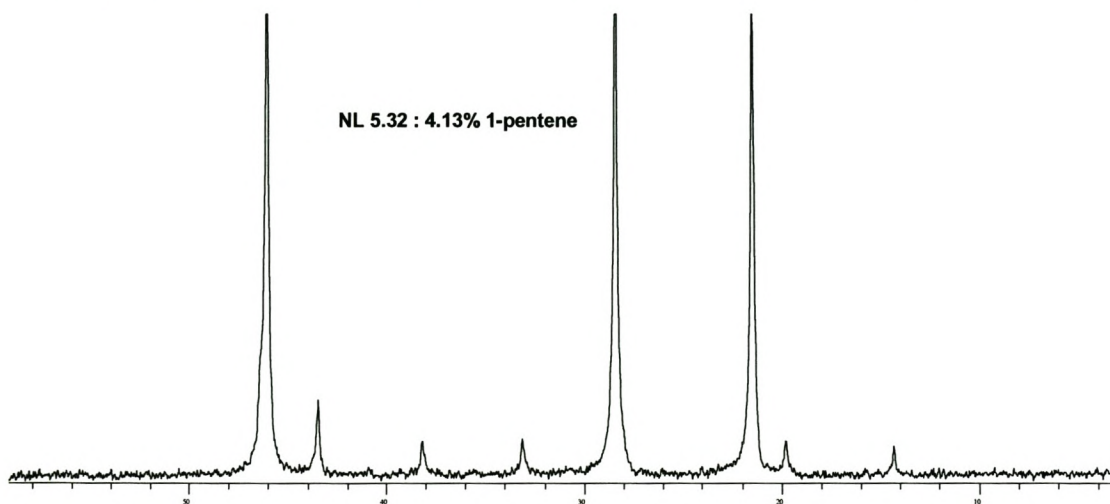
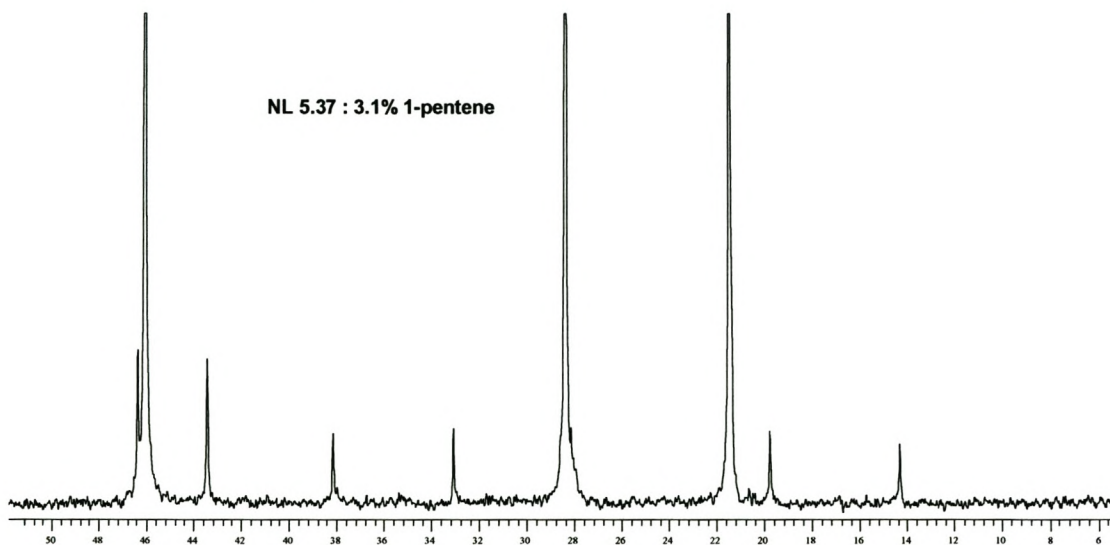
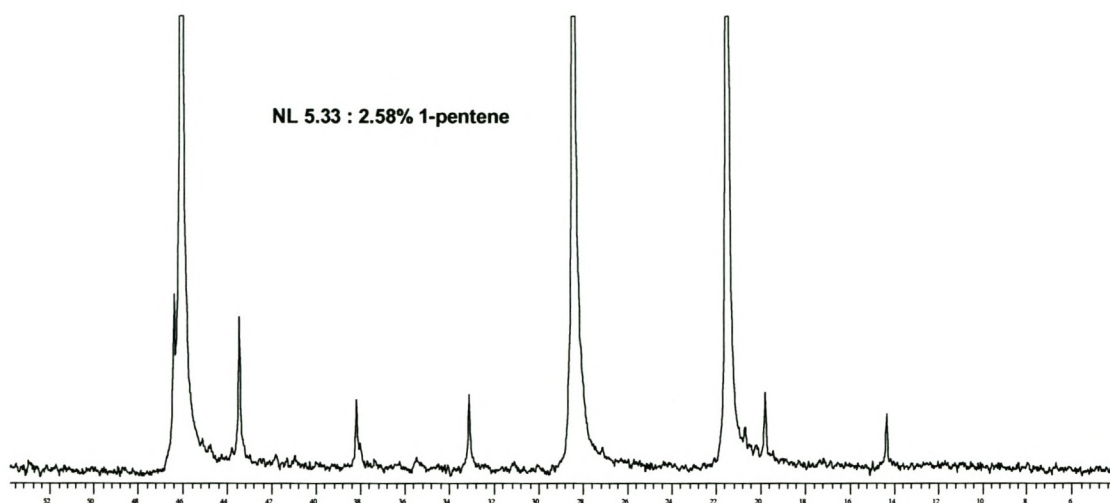


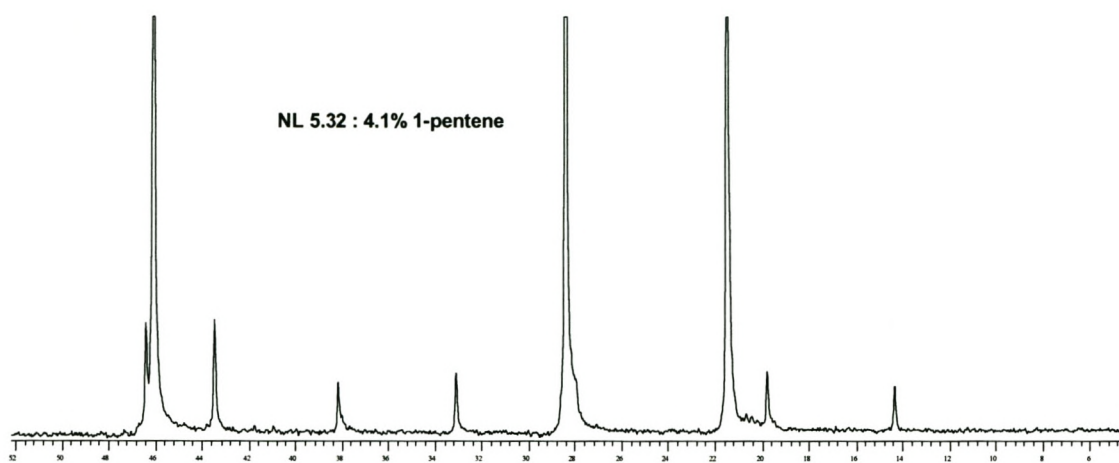


Propene/1-pentene

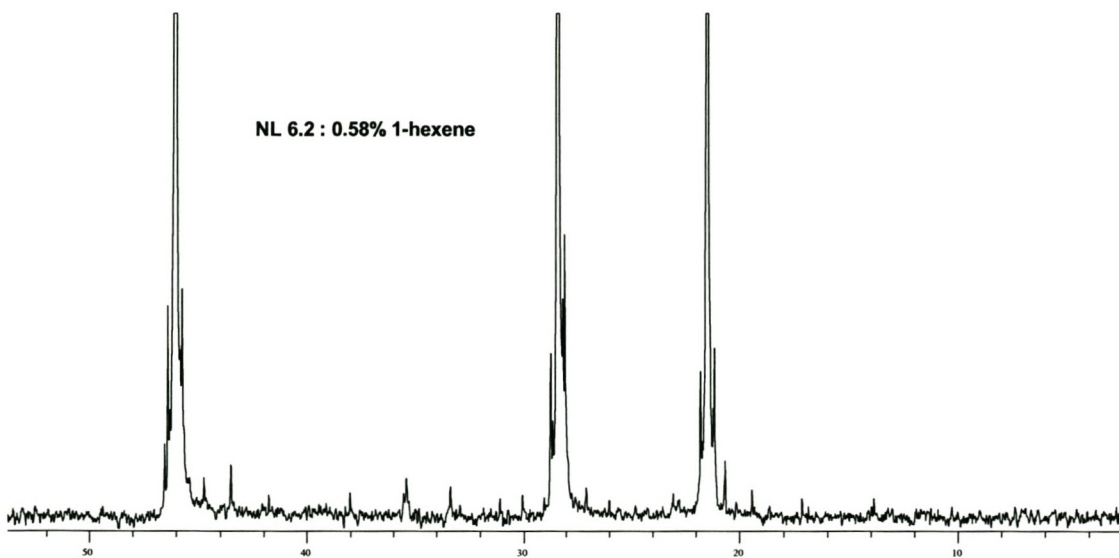
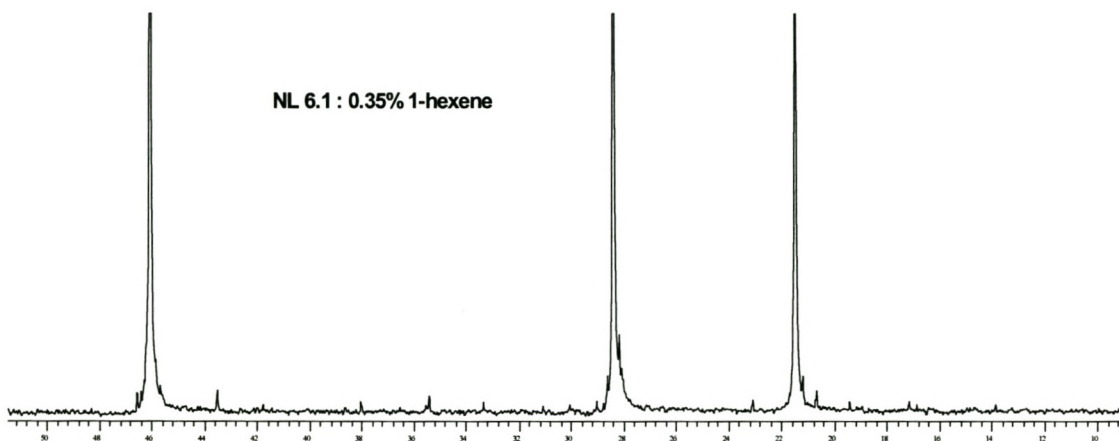


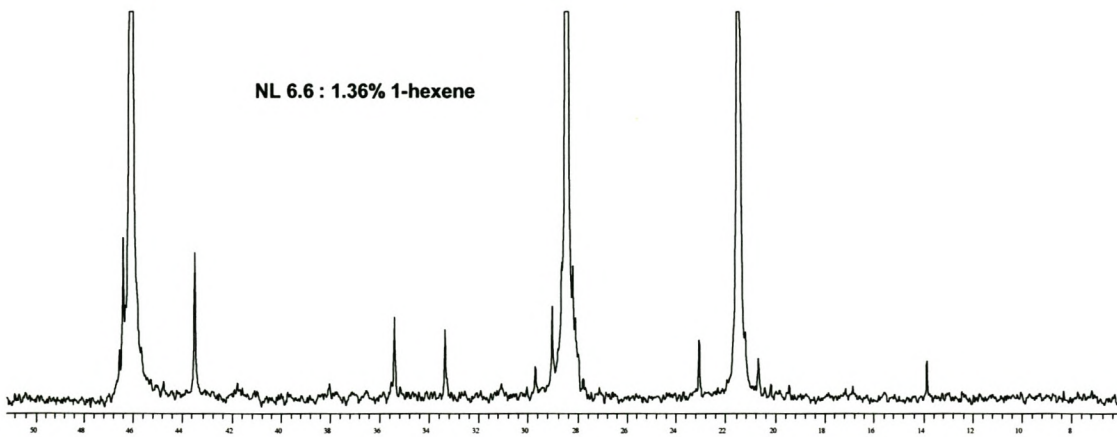
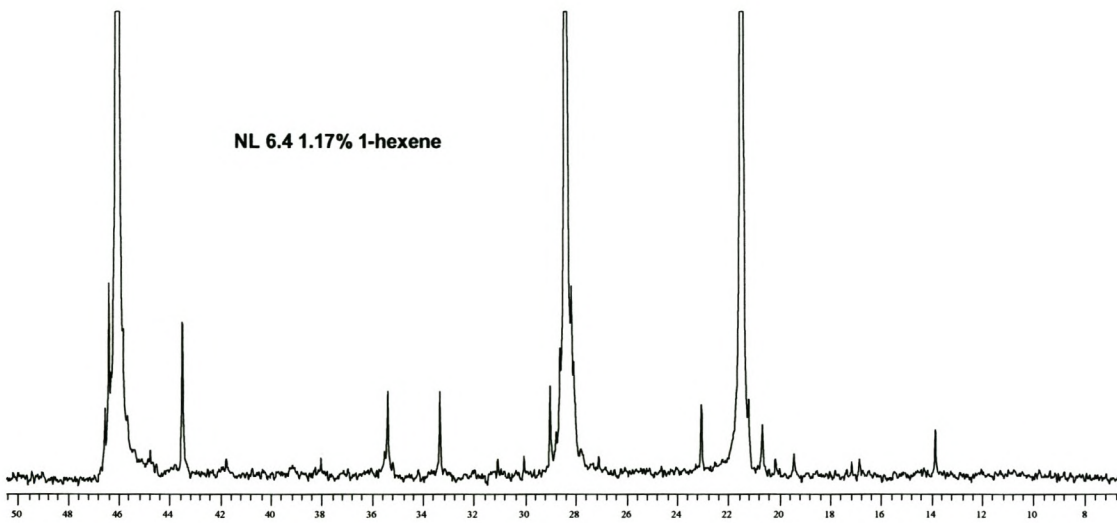
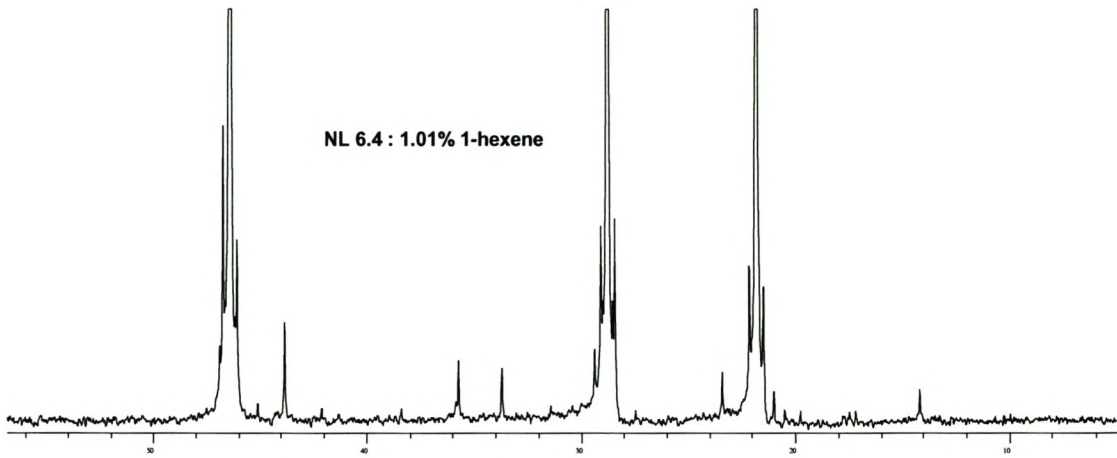


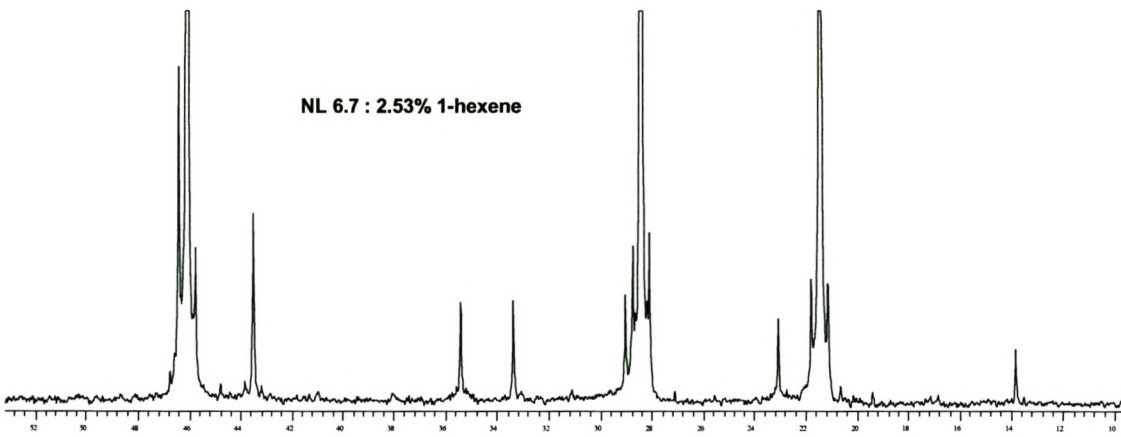
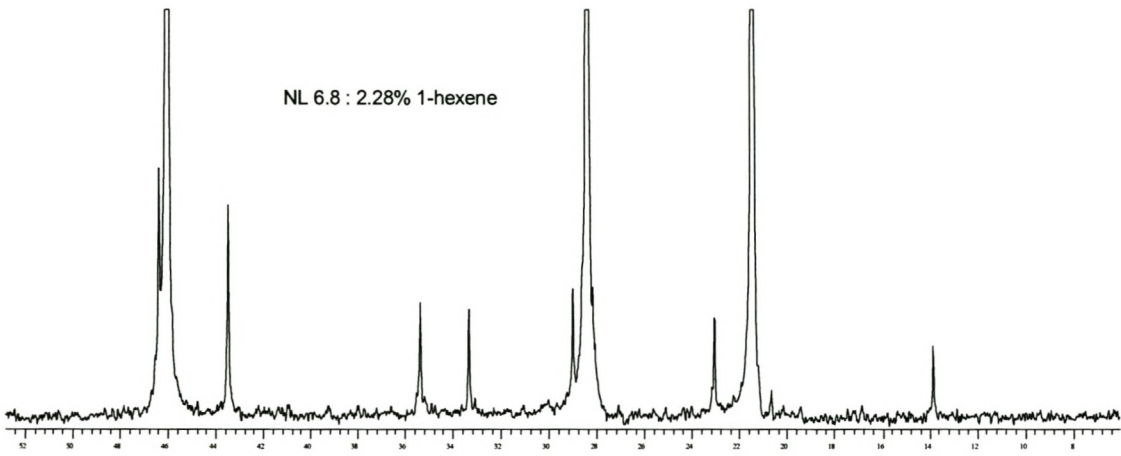
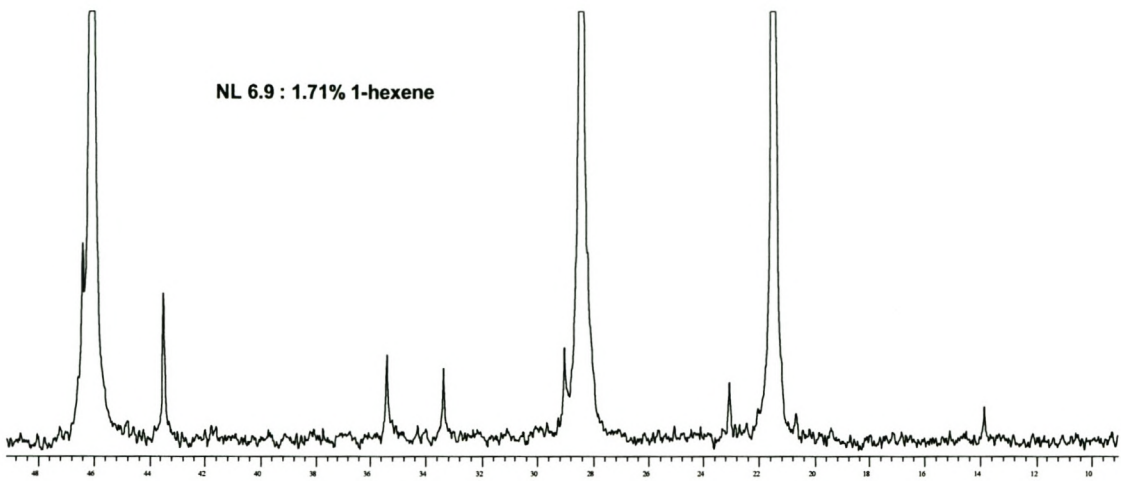




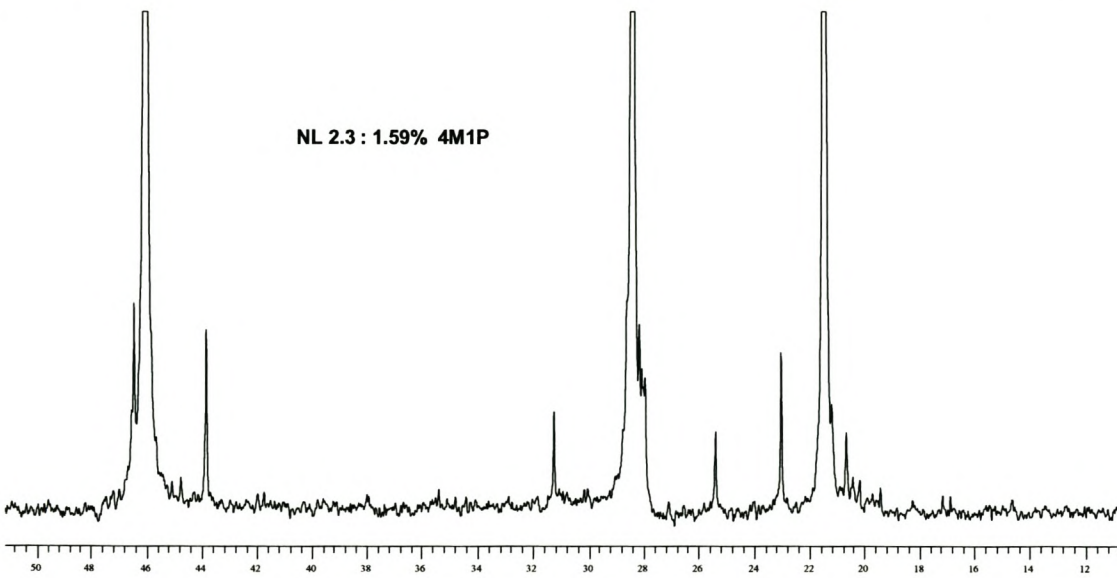
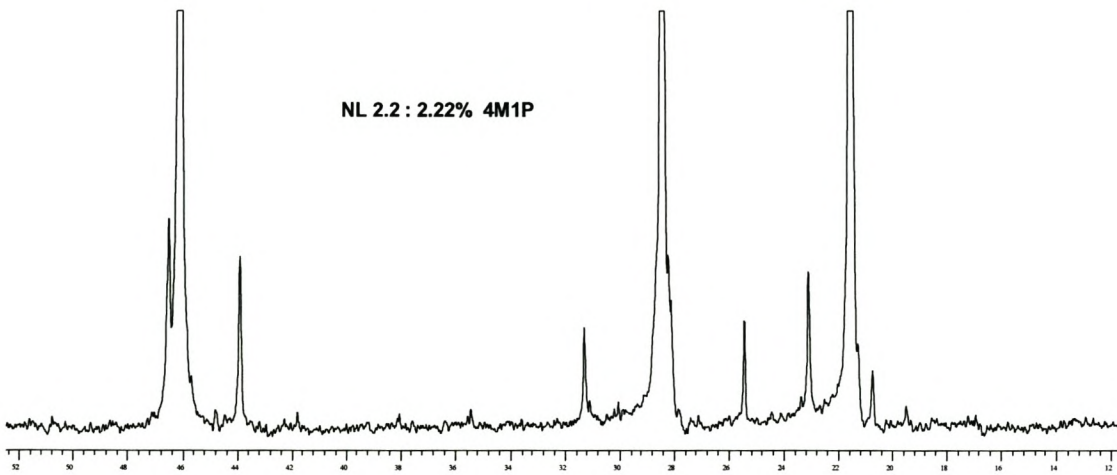
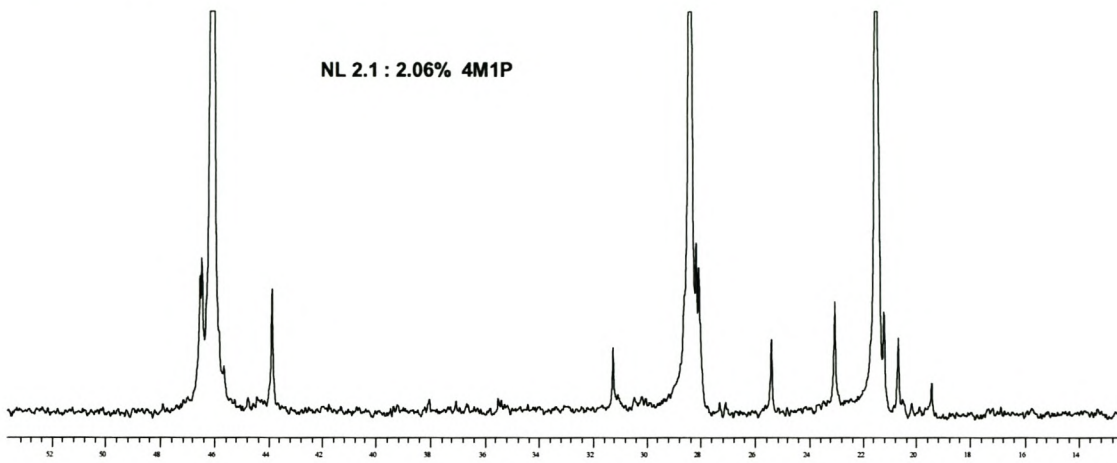
Propene/1-hexene

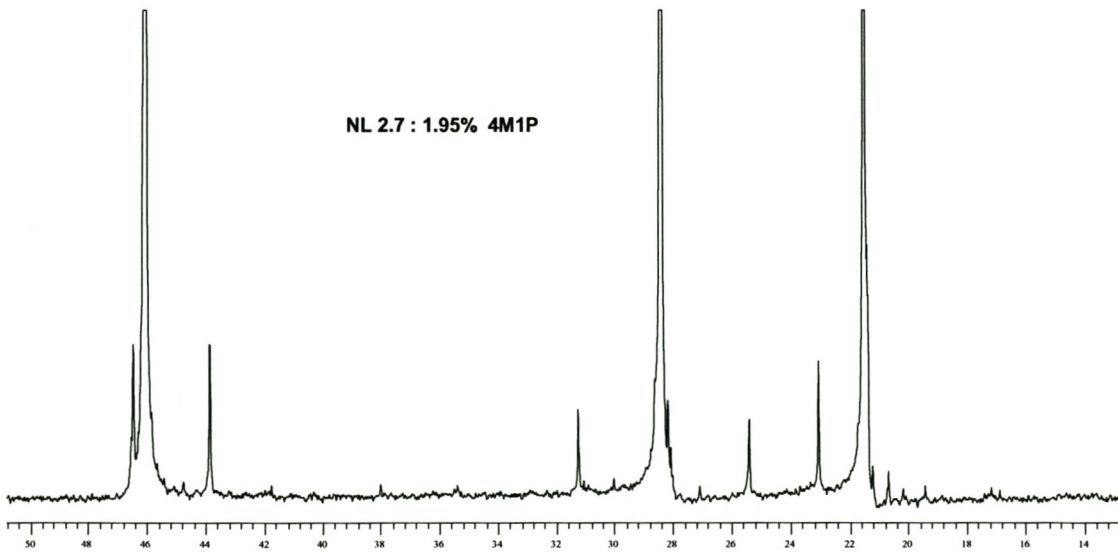
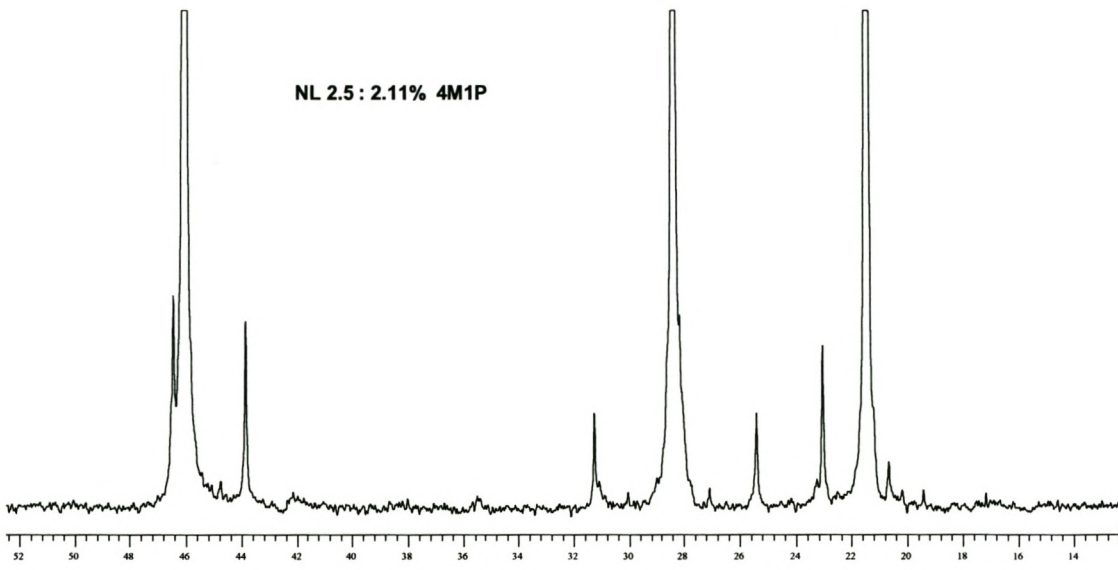
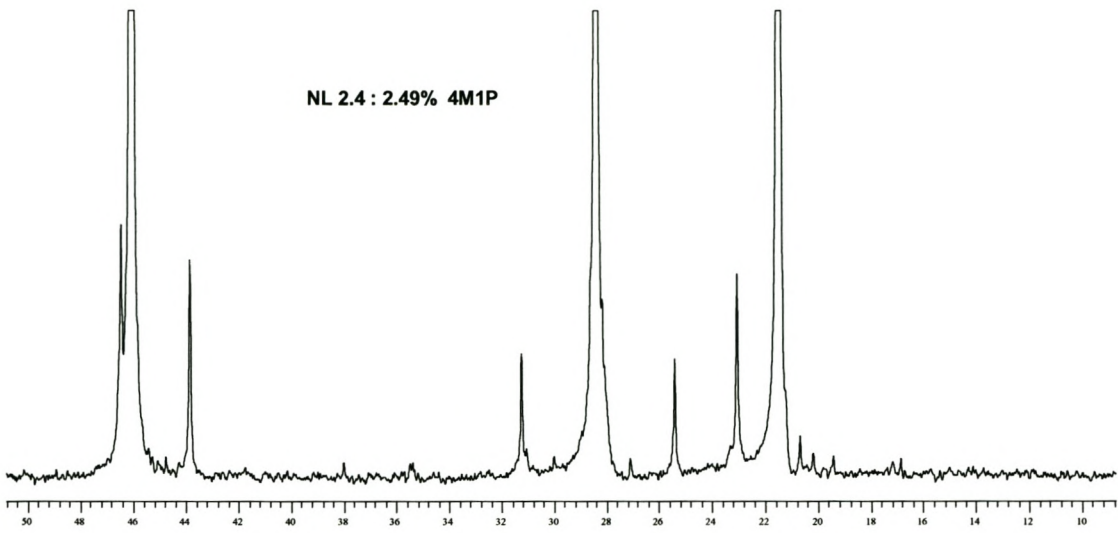


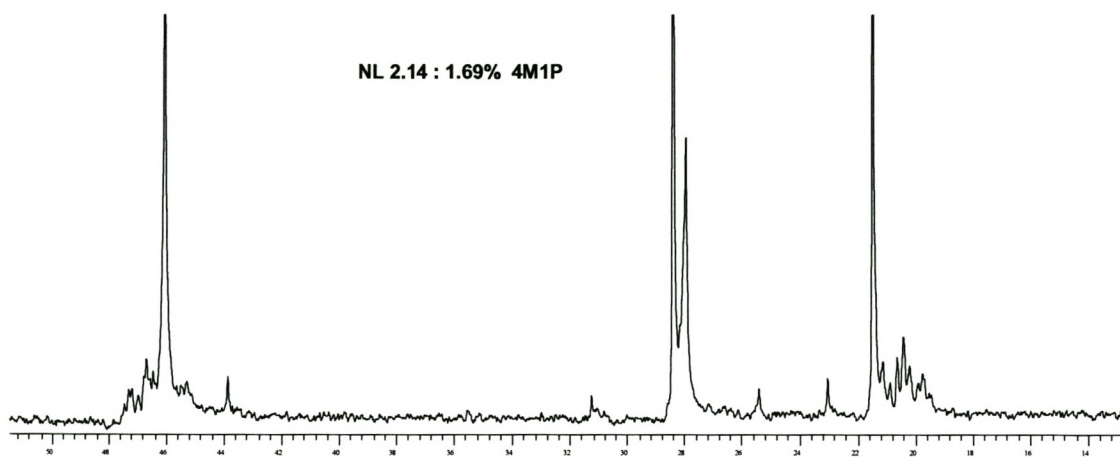
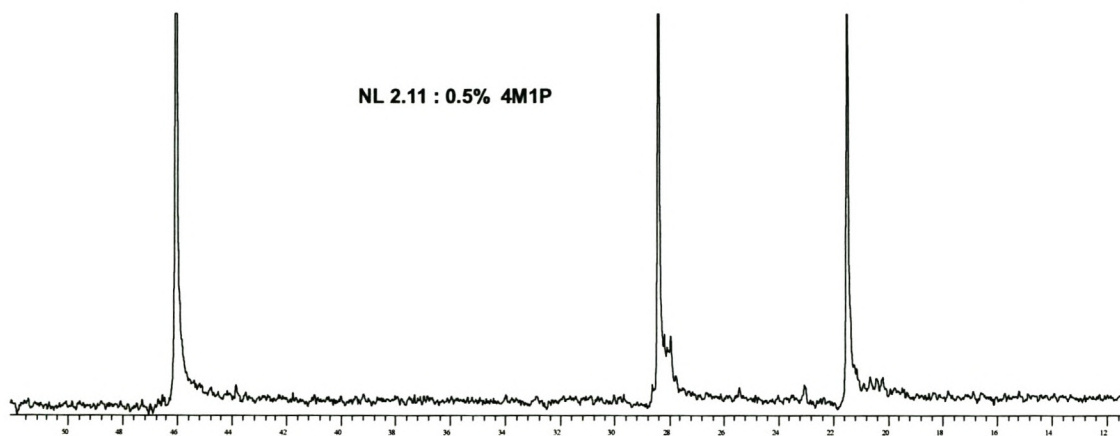
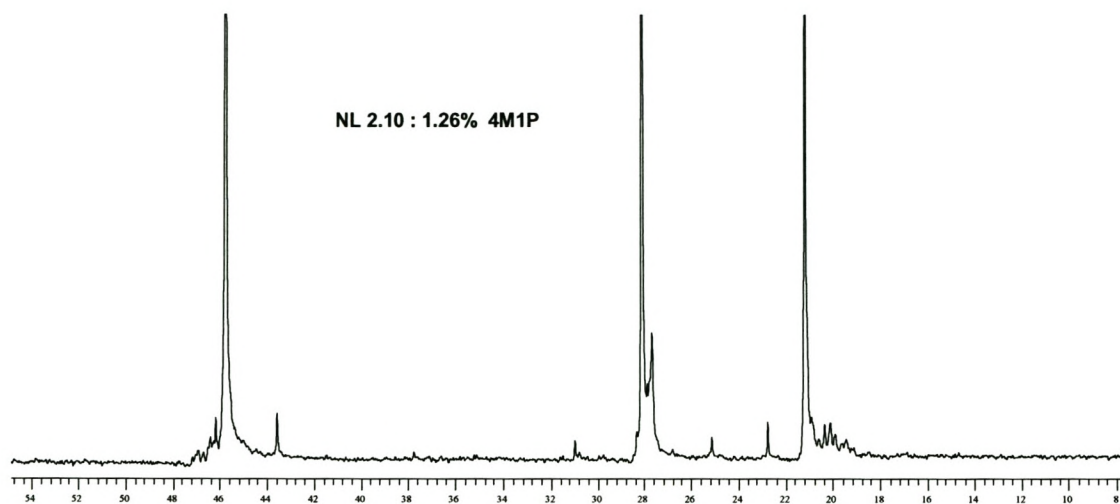


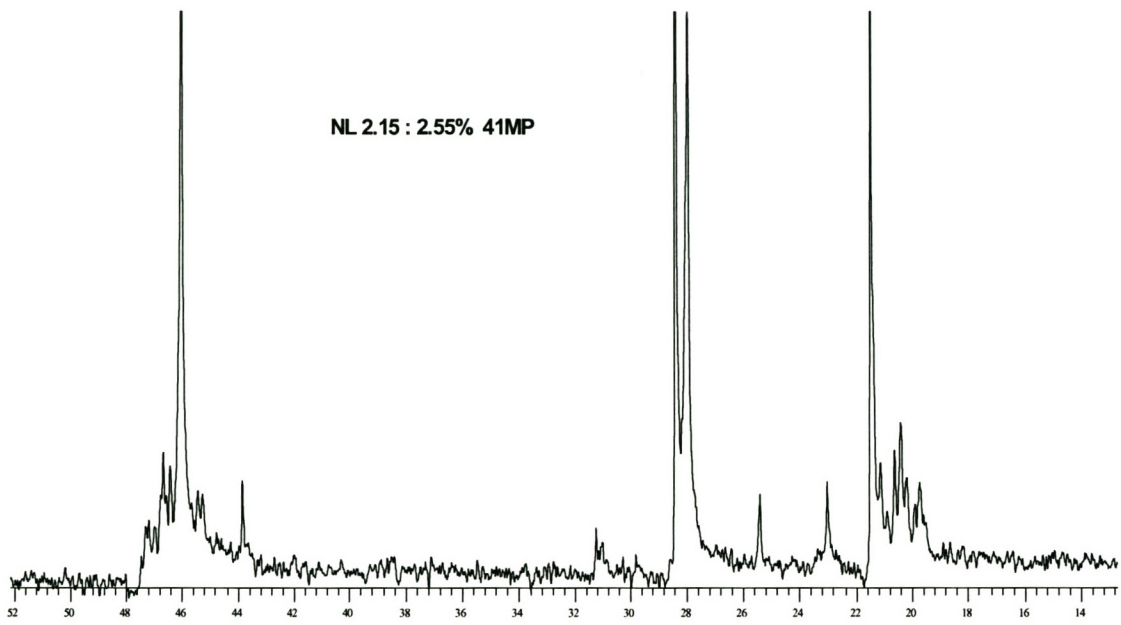


Propene/4-methyl-1-pentene

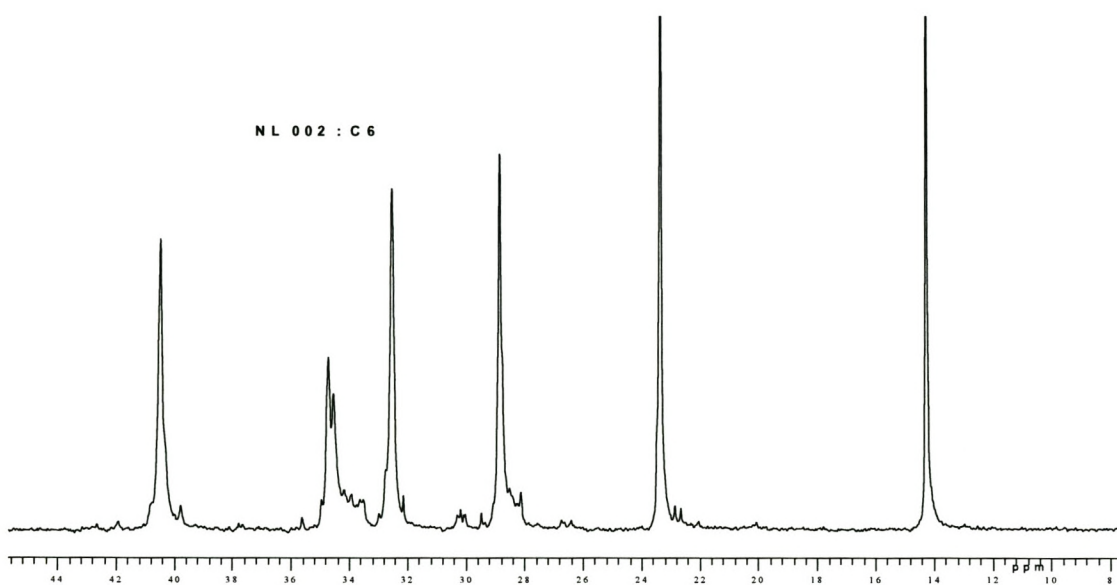
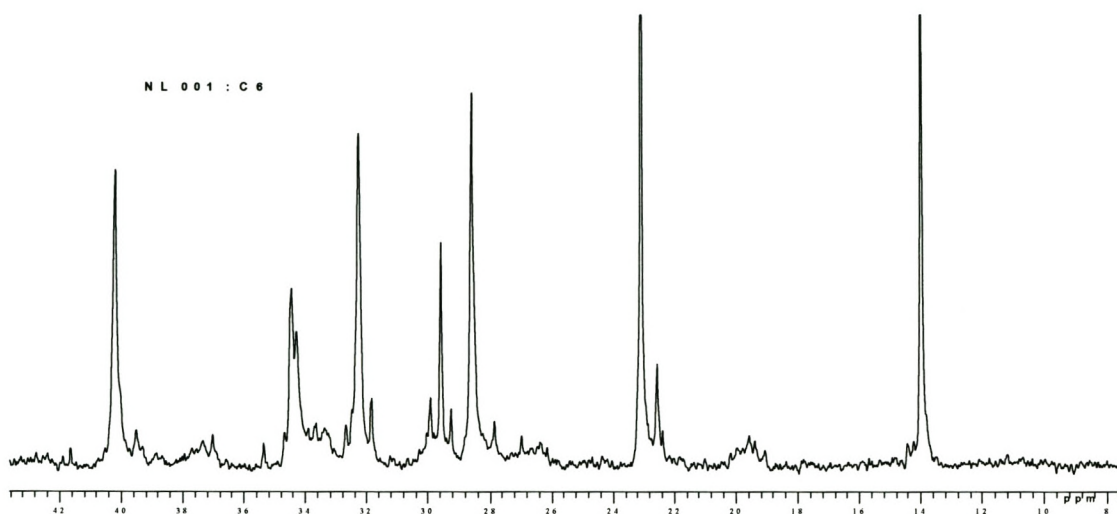


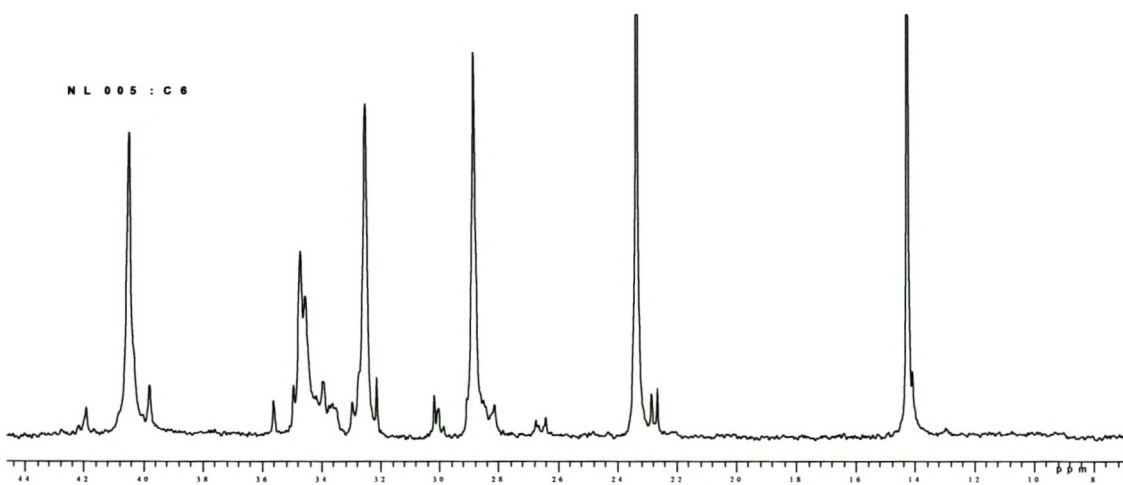
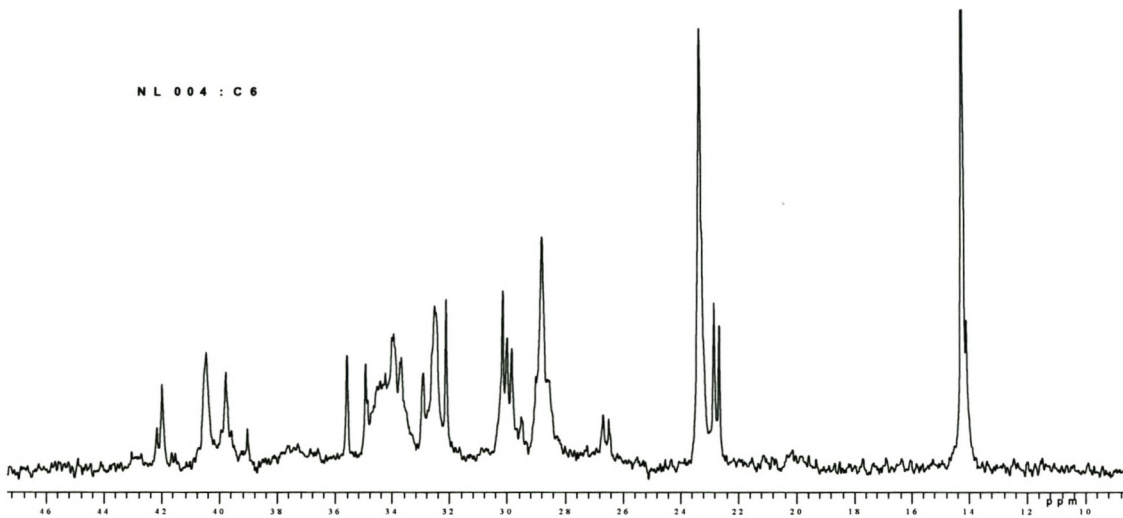
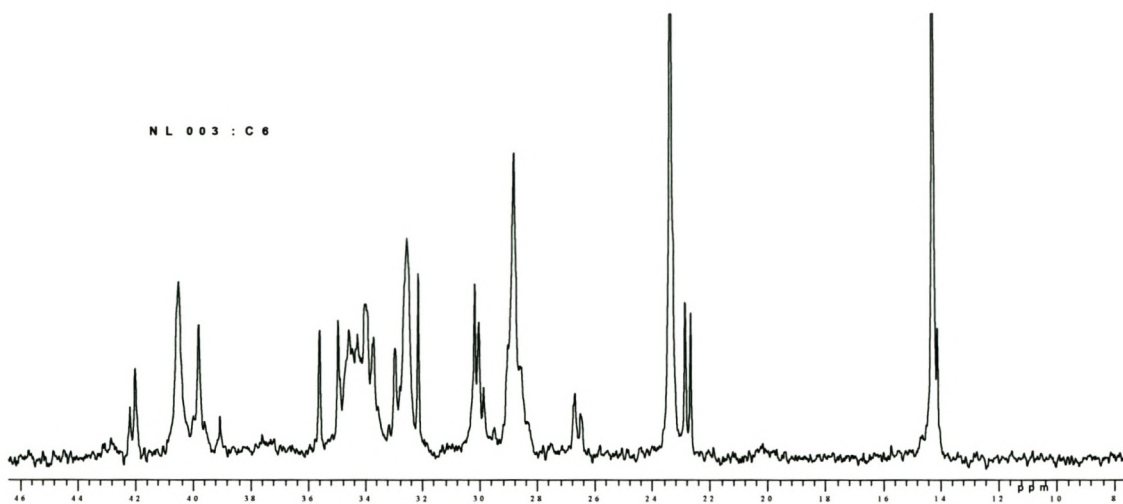


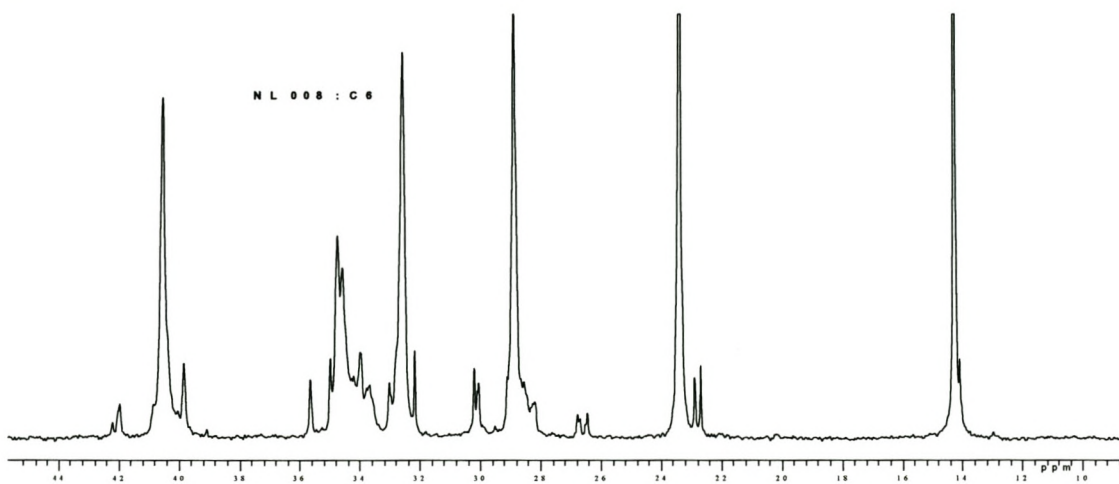
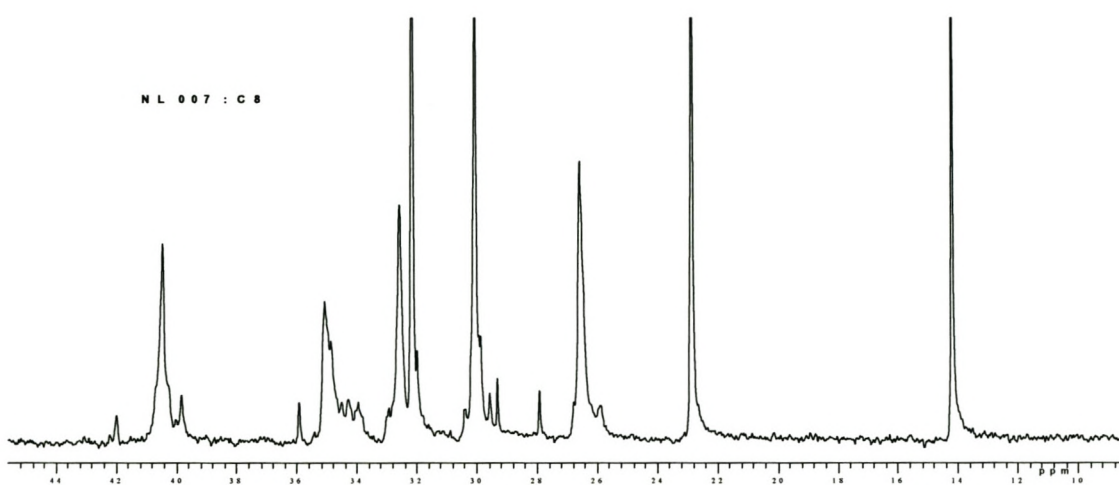
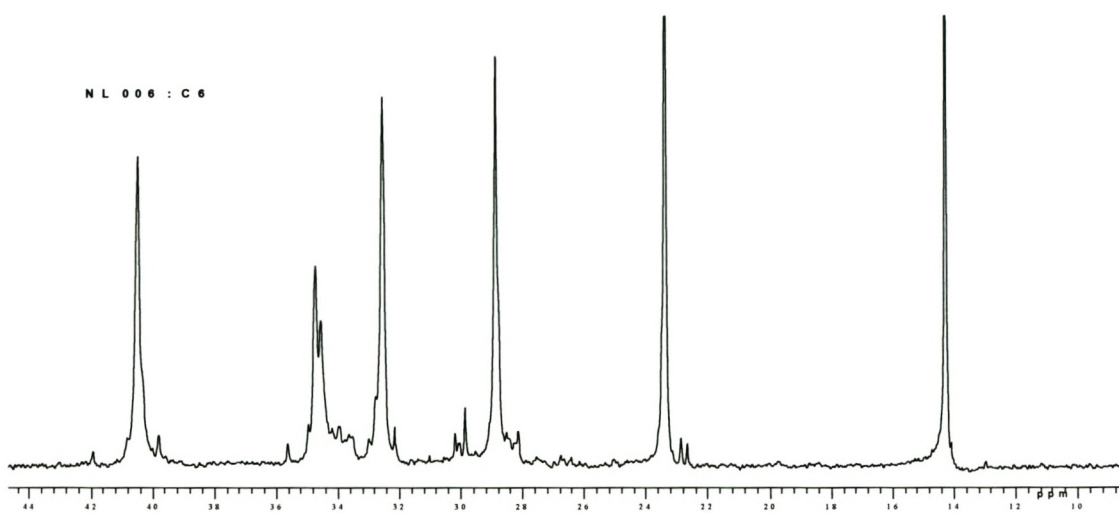


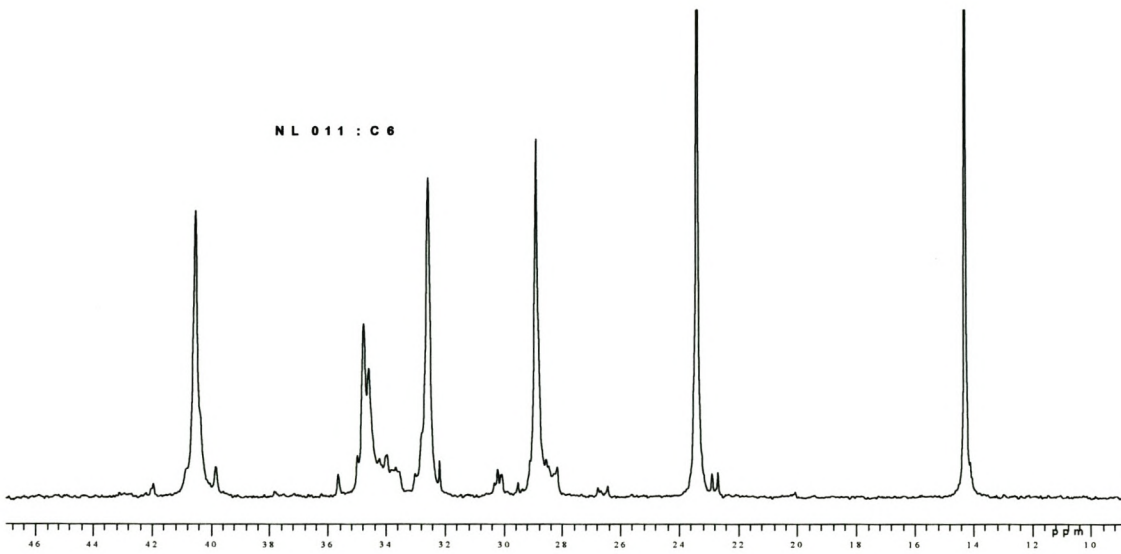
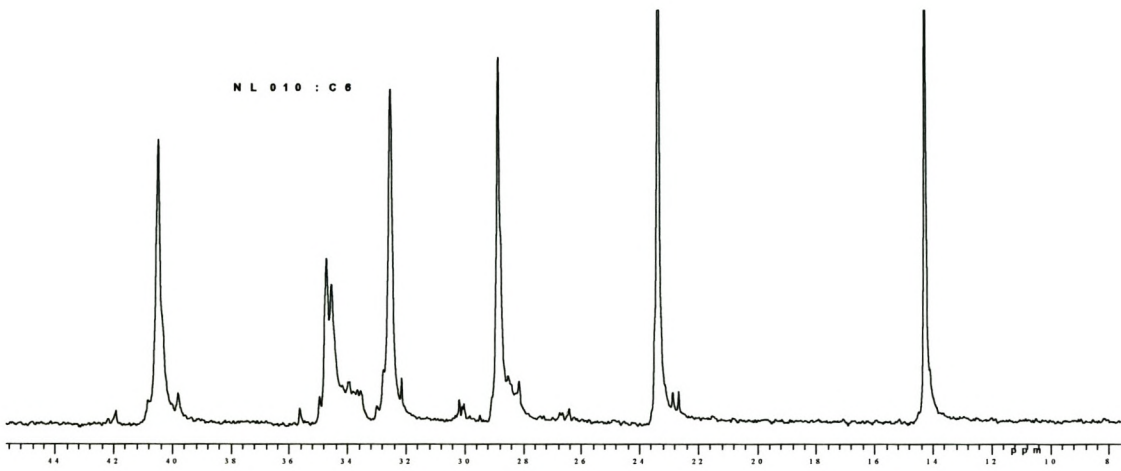
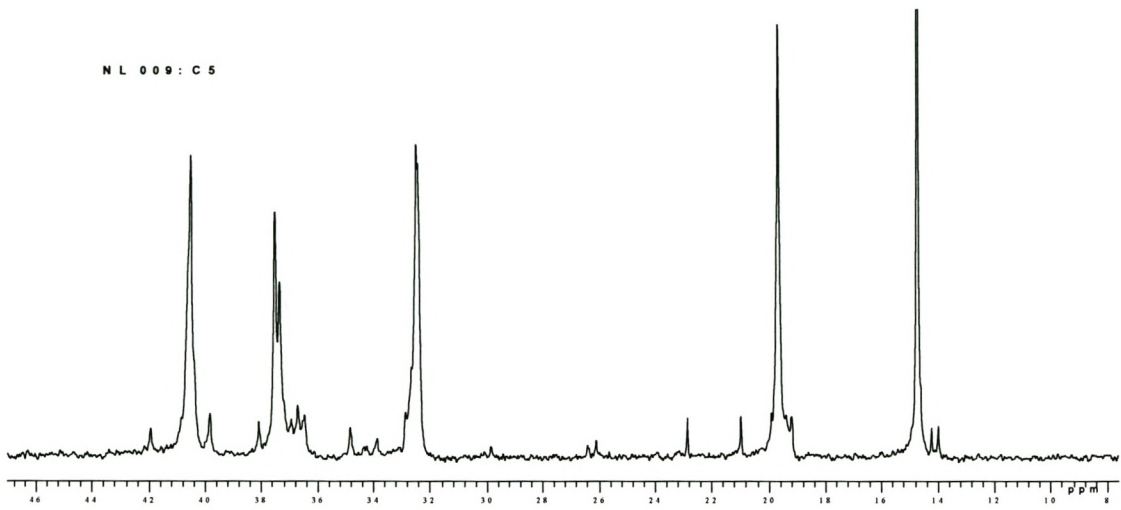


The NMR of poly α -olefins









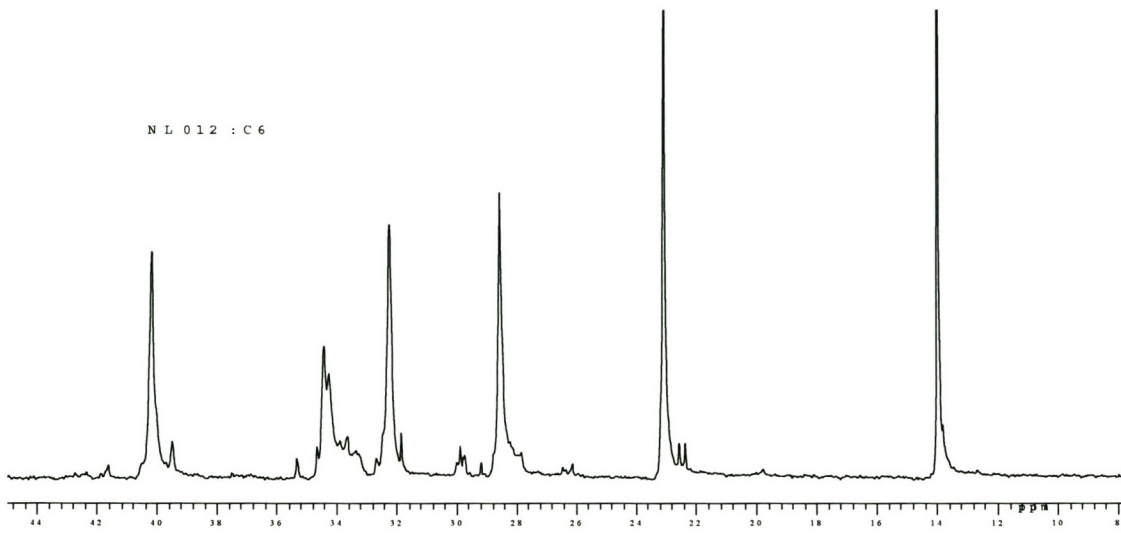


Table A1 : Percentage compositions of endgroups of poly α -olefins at various temperatures.

| Catalyst | Temperature(⁰ C) | 1,2 disubstituted(%) | 1,1,2- trisubstituted(%) | Vinylidene(%) |
|----------|------------------------------|-------------------------|-----------------------------|---------------|
| 1 | RT | 5.7 | 0.0 | 94.3 |
| 1 | 50 | 6.5 | 0.0 | 93.5 |
| 1 | 100 | 18.9 | 27.0 | 54.1 |
| 1 | 140 | nd | nd | nd |
| 2 | RT | 14.0 | 3.3 | 82.6 |
| 2 | 50 | 6.0 | 19.4 | 74.6 |
| 2 | 100 | 4.5 | 20.9 | 74.6 |
| 2 | 140 | 8.7 | 18.8 | 72.5 |
| 3 | RT | 0.0 | 0.0 | 100.0 |
| 3 | 50 | 0.0 | 44.4 | 55.6 |
| 3 | 100 | 0.0 | 35.1 | 64.9 |
| 3 | 140 | 0.0 | 27.5 | 72.5 |
| 7 | RT | 13.3 | 3.3 | 83.3 |
| 7 | 50 | 3.7 | 3.7 | 92.6 |
| 7 | 100 | 1.6 | 19.0 | 79.4 |
| 7 | 140 | 3.1 | 20.0 | 76.9 |

Appendix

GPC DATA

Complexes used for poly- α -olefins synthesis

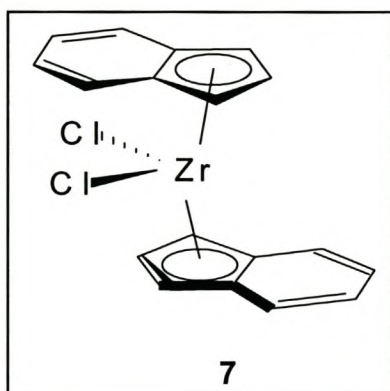
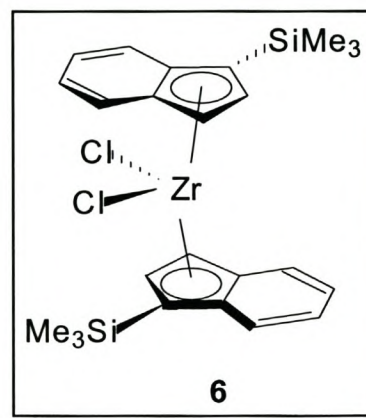
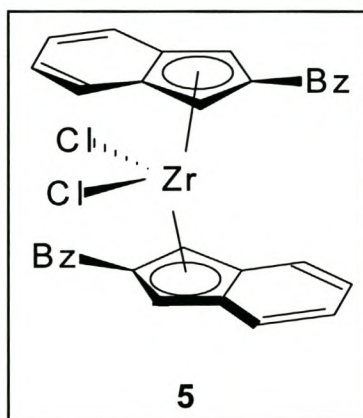
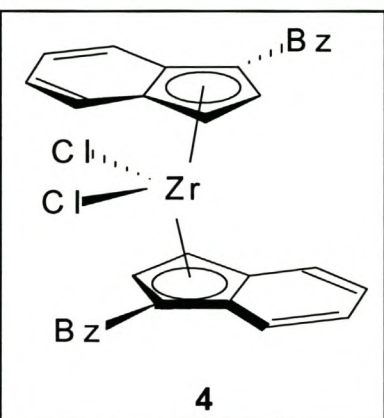
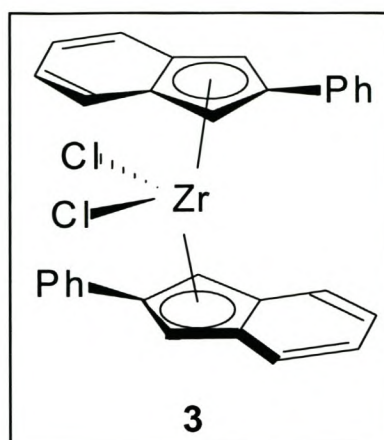
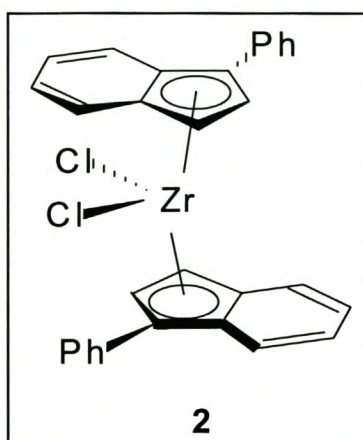
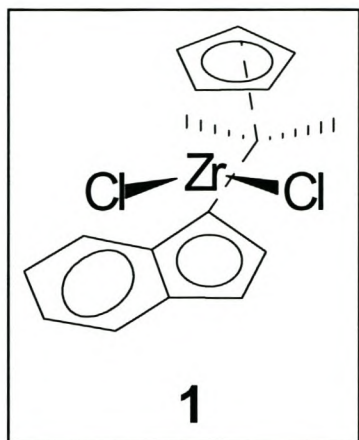


Table B1: Results obtained using complex 1

| Sample No | Monomer | Zr No. | Temp | Mao/Zr | Mon/Zr | Yield(mg) | Conversion (%) | NMR No. | Mn(g/mol) | Mw(g/mol) | Mw/Mn |
|-----------|---------|--------|------|--------|--------|-----------|----------------|---------|-----------|-----------|-------|
| IL1.1 | C5 | 1 | RT | 2500 | 30000 | 199.9 | 14.79 | 009 | 2030 | 4030 | 1.97 |
| IL1.2 | C6 | 1 | RT | 2500 | 30000 | 174.9 | 15.92 | 005 | 2210 | 4280 | 2.01 |
| IL1.3 | C8 | 1 | RT | 2500 | 30000 | 106 | 4.88 | 007 | 2540 | 4700 | 1.84 |
| IL1.4 | C6 | 1 | 0 | 2500 | 30000 | 12.9 | 0.59 | 001 | 770 | 2430 | 3.1 |
| IL1.5 | C6 | 1 | 100 | 2500 | 30000 | 59.3 | 2.73 | 003 | 864 | 2010 | 2.32 |
| IL1.6 | C6 | 1 | 140 | 2500 | 30000 | 28.7 | 1.32 | 004 | 692 | 1040 | 1.5 |
| IL1.7 | C6 | 1 | 50 | 2500 | 30000 | 572.3 | 26.33 | 008 | 1930 | 3430 | 1.77 |
| IL1.8 | C6 | 1 | RT | 10000 | 30000 | 247 | 11.36 | 002 | 2640 | 6010 | 2.27 |
| IL1.9 | C6 | 1 | RT | 500 | 30000 | 17.7 | 0.81 | 006 | 2390 | 7080 | 1.7 |
| IL1.10 | C6 | 1 | RT | 1000 | 30000 | 172.4 | 7.93 | 010 | 3810 | 6490 | 2.71 |
| IL1.11 | C6 | 1 | RT | 2500 | 10000 | 291.5 | 54.22 | 011 | nd | nd | nd |
| IL1.12 | C6 | 1 | RT | 2500 | 5000 | 333.2 | 30.99 | 012 | 230 | 3150 | 1.37 |

Table B2: Results obtained using complex 2

| Sample No | Monomer | Zr No. | Temp | Mao/Zr | Mon/Zr | Yield(mg) | Conversion (%) | NMR No. | Mn(g/mol) | Mw(g/mol) | Mw/Mn |
|-----------|---------|--------|------|--------|--------|-----------|----------------|---------|-----------|-----------|-------|
| IL2.1 | C6 | 2 | RT | 500 | 30000 | 54.3 | 2.50 | 013 | 2270 | 5990 | 2.63 |
| IL2.2 | C6 | 2 | RT | 1000 | 30000 | 110.2 | 5.07 | 014 | 1790 | 4780 | 2.66 |
| IL2.3 | C6 | 2 | RT | 2500 | 30000 | 30.4 | 1.40 | 015 | 1500 | 3880 | 2.5 |
| IL2.4 | C6 | 2 | RT | 10000 | 30000 | 191.5 | 8.81 | 016 | 1270 | 3310 | 2.6 |
| IL2.5 | C6 | 2 | RT | 2500 | 5000 | 12.8 | 4.75 | 017 | 1100 | 2370 | 2.1 |
| IL2.6 | C6 | 2 | RT | 2500 | 10000 | 51.4 | 9.56 | 018 | 1190 | 2490 | 2.09 |
| IL2.7 | C5 | 2 | RT | 2500 | 30000 | nd | nd | nd | nd | nd | nd |
| IL2.8 | C8 | 2 | RT | 2500 | 30000 | 78.6 | 3.62 | 019 | 1890 | 4870 | 2.57 |
| IL2.9 | C10 | 2 | RT | 2500 | 30000 | 36 | 1.40 | 020 | 1580 | 4910 | 3.09 |
| IL2.10 | C6 | 2 | 50 | 2500 | 30000 | 329 | 15.13 | 021 | 610 | 1020 | 1.68 |
| IL2.11 | C6 | 2 | 100 | 2500 | 30000 | 341 | 15.69 | 022 | 350 | 390 | 1.11 |
| IL2.12 | C6 | 2 | 140 | 2500 | 30000 | 62.5 | 2.88 | 023 | 1210 | 5120 | 4.23 |

Table B3: Results obtained using complex 3

| Sample No | Monomer | Zr No. | Temp | Mao/Zr | Mon/Zr | Yield(mg) | Conversion (%) | NMR No. | Mn(g/mol) | Mw(g/mol) | Mw/Mn |
|-----------|---------|--------|------|--------|--------|-----------|----------------|---------|-----------|-----------|-------|
| NL3.1 | C5 | 3 | RT | 10000 | 30000 | 70.2 | 5.19 | 024 | 5970 | 27200 | 4.56 |
| NL3.2 | C8 | 3 | RT | 10000 | 30000 | 44.3 | 2.04 | 025 | 6760 | 30800 | 4.56 |
| NL3.3 | C10 | 3 | RT | 10000 | 30000 | 67.9 | 2.65 | 026 | 5430 | 28700 | 5.28 |
| NL3.4 | C6 | 3 | 50 | 10000 | 30000 | 204.8 | 9.42 | 027 | 830 | 2900 | 3.47 |
| NL3.5 | C6 | 3 | 100 | 10000 | 30000 | 348.9 | 16.05 | 028 | 410 | 1710 | 4.12 |
| NL3.6 | C6 | 3 | 140 | 10000 | 30000 | 28.2 | 1.30 | 029 | 870 | 9430 | 10.79 |
| NL3.7 | C6 | 3 | RT | 500 | 30000 | 19.1 | 0.88 | 030 | 25100 | 6100 | 2.42 |
| NL3.8 | C6 | 3 | RT | 1000 | 30000 | 85 | 3.91 | 031 | 12500 | 59700 | 4.79 |
| NL3.9 | C6 | 3 | RT | 2500 | 30000 | 136.3 | 6.27 | 032 | 7190 | 46300 | 6.44 |
| NL3.10 | C6 | 3 | RT | 10000 | 30000 | 31.6 | 1.45 | 033 | 3740 | 23000 | 6.17 |
| NL3.11 | C6 | 3 | RT | 10000 | 5000 | 51 | 18.92 | 034 | 2700 | 9600 | 3.52 |
| NL3.12 | C6 | 3 | RT | 10000 | 10000 | 42.7 | 7.94 | 035 | 3580 | 15500 | 4.32 |

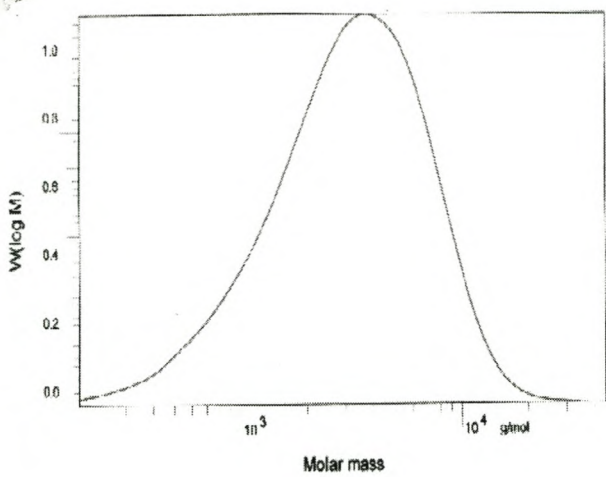
Table B4: Results obtained using complex 4

| Sample No | Monomer | Zr No. | Temp | Mao/Zr | Mon/Zr | Yield(mg) | Conversion (%) | NMR No. | Mn(g/mol) | Mw(g/mol) | Mw/Mn |
|-----------|---------|--------|------|--------|--------|-----------|----------------|---------|-----------|-----------|-------|
| NL4.1 | C5 | 4 | RT | 10000 | 30000 | 20.7 | 1.53 | nd | 890 | 2480 | 2.77 |
| NL4.2 | C8 | 4 | RT | 10000 | 30000 | 17.2 | 0.79 | nd | 900 | 2180 | 2.42 |
| NL4.3 | C10 | 4 | RT | 10000 | 30000 | 20.3 | 0.79 | nd | 840 | 1440 | 1.71 |
| NL4.4 | C6 | 4 | 50 | 10000 | 30000 | 19.9 | 0.92 | nd | 650 | 1080 | 1.66 |
| NL4.5 | C6 | 4 | 100 | 10000 | 30000 | 48.3 | 2.22 | nd | 460 | 660 | 1.43 |
| NL4.6 | C6 | 4 | 140 | 10000 | 30000 | 15.8 | 0.73 | nd | 620 | 2340 | 3.77 |
| NL4.7 | C6 | 4 | RT | 500 | 30000 | 11.5 | 2.22 | nd | 610 | 1170 | 1.91 |
| NL4.8 | C6 | 4 | RT | 1000 | 30000 | 9.2 | 2.22 | nd | 810 | 2870 | 3.54 |
| NL4.9 | C6 | 4 | RT | 2500 | 30000 | 16.1 | 2.22 | nd | 1220 | 3850 | 3.15 |
| NL4.10 | C6 | 4 | RT | 10000 | 30000 | 13.5 | 2.22 | nd | 900 | 1770 | 1.97 |
| NL4.11 | C6 | 4 | RT | 10000 | 5000 | 2.5 | 0.93 | nd | 650 | 940 | 1.45 |
| NL4.12 | C6 | 4 | RT | 10000 | 10000 | 11.4 | 2.12 | nd | 690 | 1130 | 1.63 |

Table B5: Results obtained using complex 7

| Sample No | Monomer | Zr No. | Temp | Mao/Zr | Mon/Zr | Yield(mg) | Conversion (%) | NMR No. | Mn(g/mol) | Mw(g/mol) | Mw/Mn |
|-----------|---------|--------|------|--------|--------|-----------|----------------|---------|-----------|-----------|-------|
| L7.1 | C6 | 7 | RT | 500 | 30000 | 2.6 | 0.12 | nd | nd | nd | nd |
| L7.2 | C6 | 7 | RT | 1000 | 30000 | 6.7 | 0.31 | nd | nd | nd | nd |
| L7.3 | C6 | 7 | RT | 2500 | 30000 | 136.7 | 6.29 | 036 | 3530 | 8780 | 2.48 |
| L7.4 | C6 | 7 | RT | 10000 | 30000 | 570.6 | 26.25 | 037 | 2360 | 6200 | 2.62 |
| L7.5 | C6 | 7 | RT | 10000 | 5000 | 29.5 | 10.94 | 038 | nd | nd | nd |
| L7.6 | C6 | 7 | RT | 10000 | 10000 | 163.7 | 30.45 | 039 | 2340 | 5930 | 2.53 |
| L7.7 | C5 | 7 | RT | 10000 | 30000 | 97.9 | 7.24 | 040 | 2680 | 6670 | 2.48 |
| L7.8 | C8 | 7 | RT | 10000 | 30000 | 276.9 | 12.74 | 041 | 3320 | 8240 | 2.47 |
| L7.9 | C10 | 7 | RT | 10000 | 30000 | 166.5 | 6.49 | 042 | 3240 | 8890 | 2.74 |
| L7.10 | C6 | 7 | 50 | 10000 | 30000 | 950.3 | 43.71 | 043 | 770 | 1380 | 1.79 |
| L7.11 | C6 | 7 | 100 | 10000 | 30000 | 645.3 | 29.68 | 044 | 300 | 380 | 1.27 |
| L7.12 | C6 | 7 | 140 | 10000 | 30000 | 59.5 | 2.74 | 045 | nd | nd | nd |

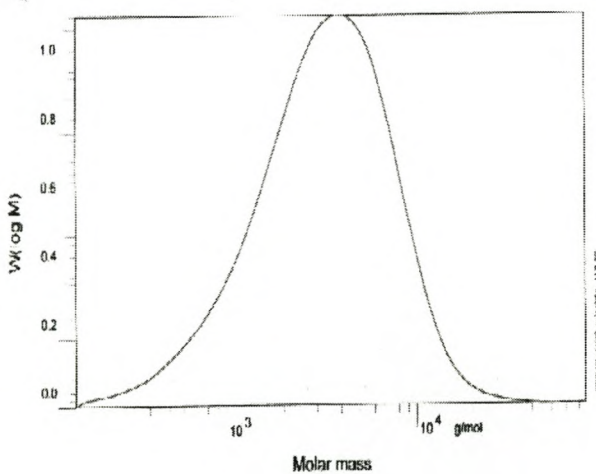
GPC Results for poly α -olefins obtained with complex 1(as examples)



Waters RI 410

| | | |
|---------|----------|-------------------|
| Mn : | 2.0360e3 | g/mol |
| Mw : | 4.0302e3 | g/mol |
| Mz : | 6.5698e3 | g/mol |
| Mv : | 0.000000 | g/mol |
| D : | 1.9795e0 | |
| [n] : | 0.000000 | ml/g |
| Vp : | 2.2659e1 | ml |
| Mp : | 3.5260e3 | g/mol |
| A : | 1.203e-1 | ml ² V |
| < 185 | 0.00 | |
| w% : | 100.00 | |
| > 45146 | 0.00 | |

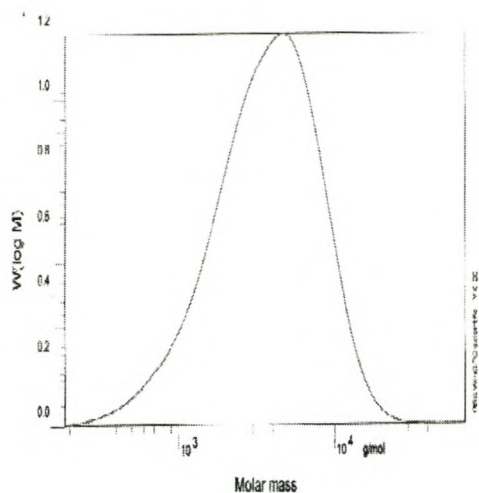
Figure B1 : NL 1.1



Waters RI 410

| | | |
|---------|----------|-------------------|
| Mn : | 2.1213e3 | g/mol |
| Mw : | 4.2802e3 | g/mol |
| Mz : | 7.3745e3 | g/mol |
| Mv : | 0.000000 | g/mol |
| D : | 2.0177e0 | |
| [n] : | 0.000000 | ml/g |
| Vp : | 2.2612e1 | ml |
| Mp : | 3.6504e3 | g/mol |
| A : | 3.569e-1 | ml ² V |
| < 163 | 0.00 | |
| w% : | 100.00 | |
| > 76224 | 0.00 | |

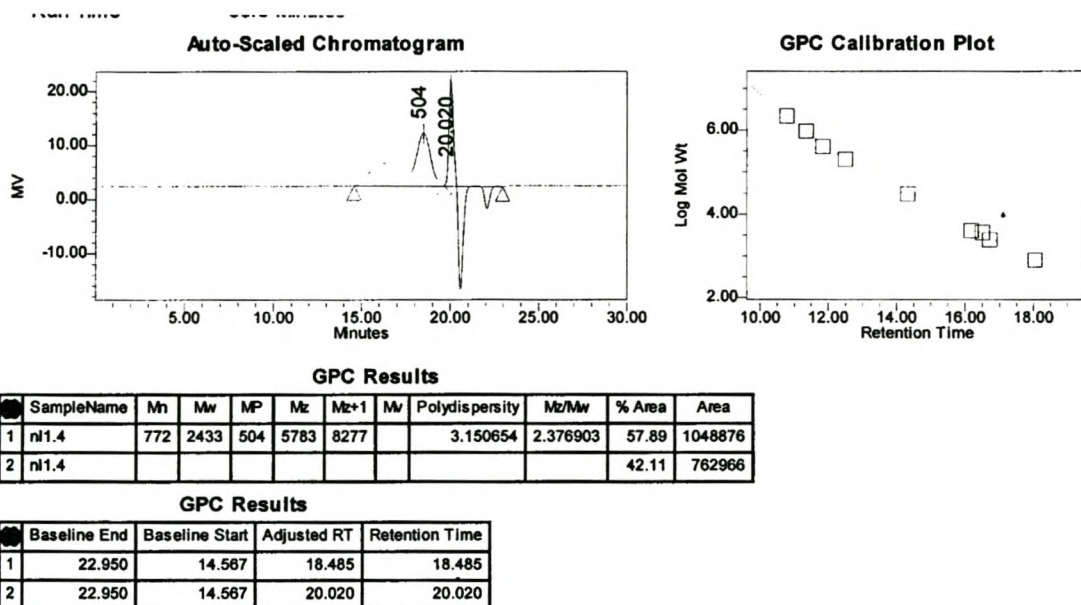
Figure B2 : NL 1.2



Waters RI 410

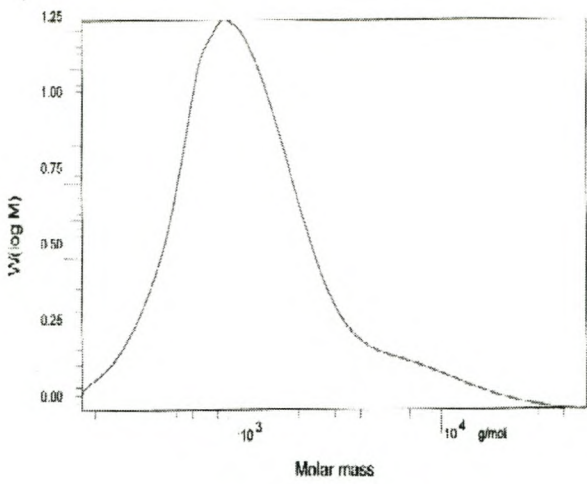
| | | |
|-------------------|----------|-------------------|
| Mn : | 2.5474e3 | g/mol |
| Mw : | 4.7017e3 | g/mol |
| Mz : | 7.5151e3 | g/mol |
| Mv : | 0.000000 | g/mol |
| D : | 1.8457e0 | |
| [η] : | 0.000000 | ml/g |
| Vp : | 2.2319e1 | ml |
| Mp : | 4.5176e3 | g/mol |
| A : | 2.171e-1 | ml ² V |
| < 185 | 0.00 | |
| w% : | 100.00 | |
| > 69926 | 0.00 | |

Figure B3 : NL 1.3



Instrument Method Id 1960

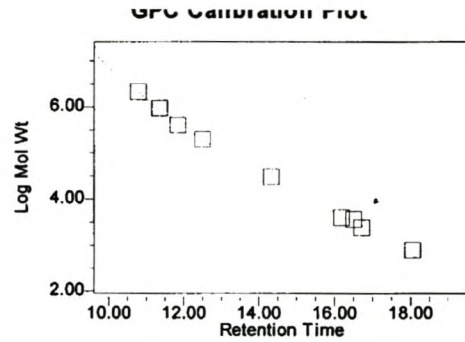
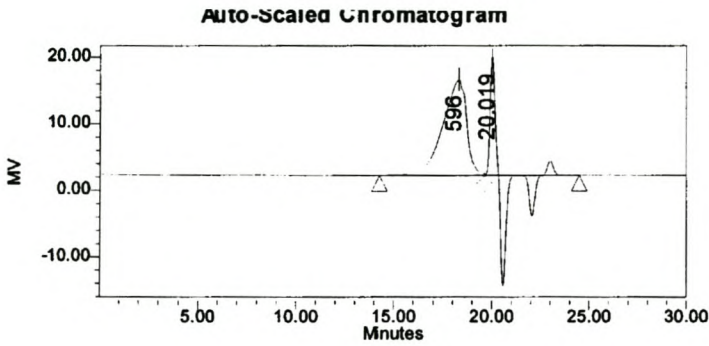
Figure B4 : NL 1.4



Waters RI 410

| | | |
|-------------------|----------|-------------------|
| Mn : | 8.6449e2 | g/mol |
| Mw : | 2.0127e3 | g/mol |
| Mz : | 7.3749e3 | g/mol |
| Mv : | 0.000000 | g/mol |
| D : | 2.3282e0 | |
| [n] : | 0.000000 | ml/g |
| Vp : | 2.4504e1 | ml |
| Mp : | 8.3960e2 | g/mol |
| A : | 1.351e-1 | ml ³ V |
| < 170 | 0.00 | |
| w% : | 100.00 | |
| > 51968 | 0.00 | |

NL 1.5



GPC Results

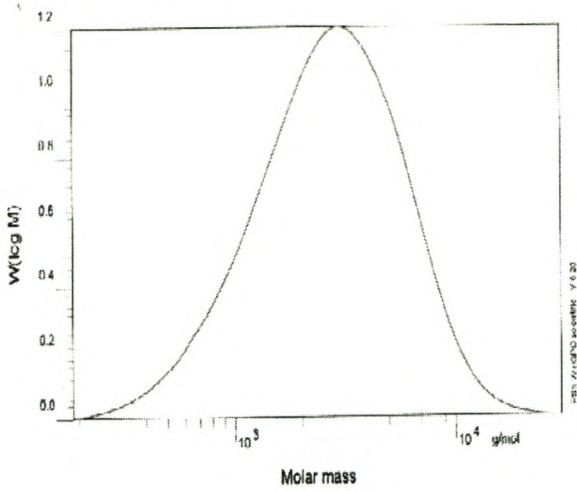
| SampleName | Mn | Mw | MP | Mz | Mz+1 | Mv | Polydispersity | Mz/Mw | % Area | Area |
|------------|-----|------|-----|------|------|----|----------------|----------|--------|---------|
| 1 n1.6 | 692 | 1042 | 596 | 2262 | 6916 | | 1.506063 | 2.169543 | 60.97 | 1217982 |
| 2 n1.6 | | | | | | | | | 39.03 | 779776 |

GPC Results

| Baseline End | Baseline Start | Adjusted RT | Retention Time |
|--------------|----------------|-------------|----------------|
| 1 24.483 | 14.267 | 18.316 | 18.316 |
| 2 24.483 | 14.267 | 20.019 | 20.019 |

Instrument Method Id 1960

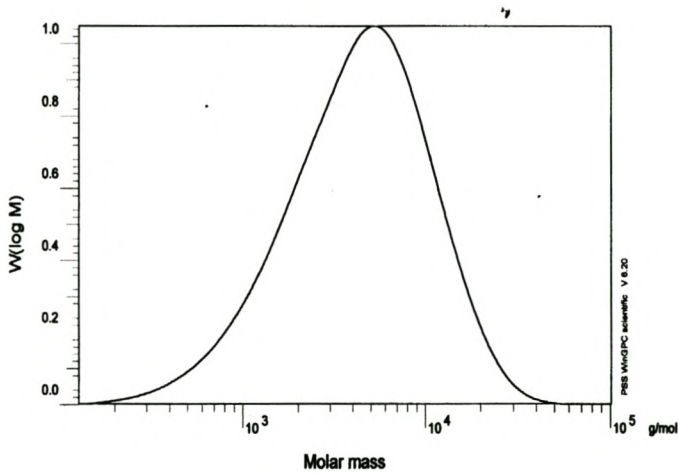
Figure B6 : NL 1.6



Waters RI 410

| | | |
|-------------------|----------|-------------------|
| Mn : | 1.9320e3 | g/mol |
| Mw : | 3.4314e3 | g/mol |
| Mz : | 5.4386e3 | g/mol |
| Mv : | 0.000000 | g/mol |
| D : | 1.7761e0 | |
| [n] : | 0.000000 | ml/g |
| Vp : | 2.2944e1 | ml |
| Mp : | 2.8568e3 | g/mol |
| A : | 1.964e-1 | ml ² V |
| < 185 | 0.00 | |
| w% : | 100.00 | |
| > 29660 | 0.00 | |

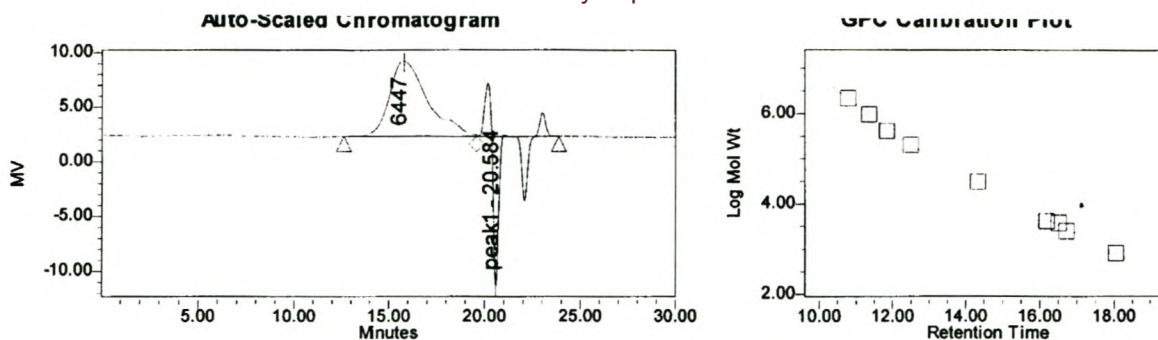
Figure B7 : NL 1.7



Waters RI 410

| | | |
|-------------------|----------|-------------------|
| Mn : | 2.6485e3 | g/mol |
| Mw : | 6.0168e3 | g/mol |
| Mz : | 1.0794e4 | g/mol |
| Mv : | 0.000000 | g/mol |
| D : | 2.2717e0 | |
| [n] : | 0.000000 | ml/g |
| Vp : | 2.2185e1 | ml |
| Mp : | 4.9726e3 | g/mol |
| A : | 3.213e-1 | ml ² V |
| < 126 | 0.00 | |
| w% : | 100.00 | |
| > 10197 | 0.00 | |

Figure B8 : NL 1.8



GPC Results

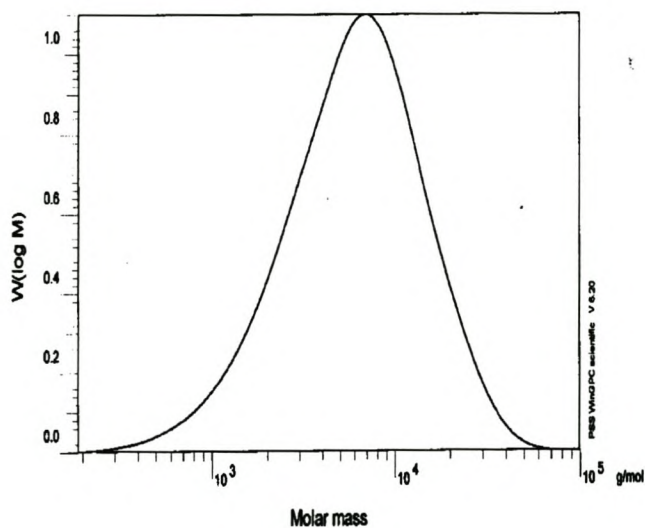
| SampleName | Mn | Mw | MP | Mz | Mz+1 | Mv | Polydispersity | Mz/Mw | % Area | Area |
|------------|------|------|------|-------|-------|----|----------------|----------|--------|--------|
| nl1.9 | 2396 | 6496 | 6447 | 12692 | 25790 | | 2.711490 | 1.953821 | 65.79 | 961479 |
| nl1.9 | 161 | 161 | | 161 | 161 | | 1.000225 | 1.000224 | 34.21 | 499897 |

GPC Results

| Baseline End | Baseline Start | Adjusted RT | Retention Time |
|--------------|----------------|-------------|----------------|
| 1 | 23.850 | 12.600 | 15.783 |
| 2 | 23.850 | 12.600 | 20.584 |

Instrument Method Id 1960

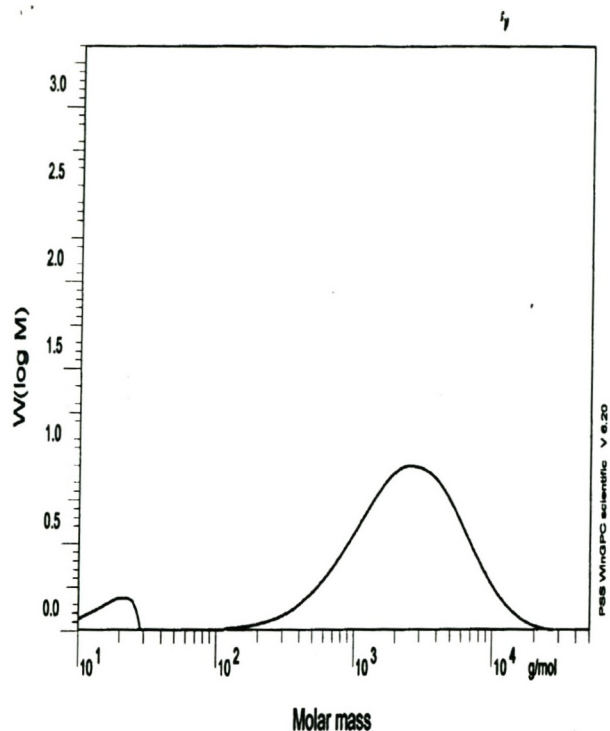
Figure B9 : NL 1.9



Waters RI 410

| | | |
|-------------------|----------|--------------------|
| Mn : | 3.8183e3 | g/mol |
| Mw : | 8.2427e3 | g/mol |
| Mz : | 1.4661e4 | g/mol |
| Mv : | 0.000000 | g/mol |
| D : | 2.1588e0 | |
| [n] : | 0.000000 | ml/g |
| Vp : | 2.1783e1 | ml |
| Mp : | 6.6088e3 | g/mol |
| A : | 4.275e-1 | ml ² /V |
| < 187 | 0.00 | |
| w% : | 100.00 | |
| > 99868 | 0.00 | |

Figure B10 : NL 1.10



Waters RI 410

| | | |
|-------------------|----------|-------------------|
| Mn : | 2.2983e2 | g/mol |
| Mw : | 3.1510e3 | g/mol |
| Mz : | 6.2765e3 | g/mol |
| Mv : | 0.000000 | g/mol |
| D : | 1.3710e1 | |
| [n] : | 0.000000 | ml/g |
| Vp : | 2.3195e1 | ml |
| Mp : | 2.3659e3 | g/mol |
| A : | 3.548e-1 | ml ² V |
| < 10 | 0.00 | |
| w% : | 100.00 | |
| > 50655 | 0.00 | |

Figure B11 : NL 1.2

Appendix C

CRYSTAF CURVES

Propene/4-methyl-1-pentene

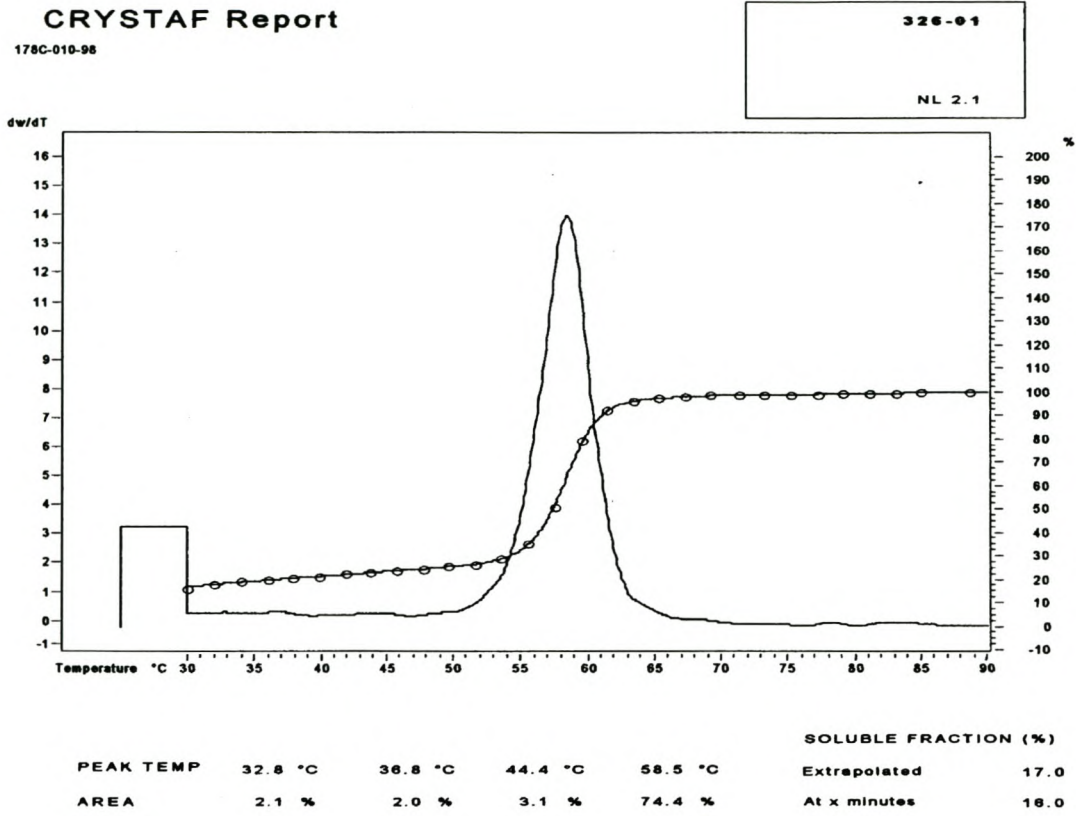


Figure C1: Sample NL 2.1

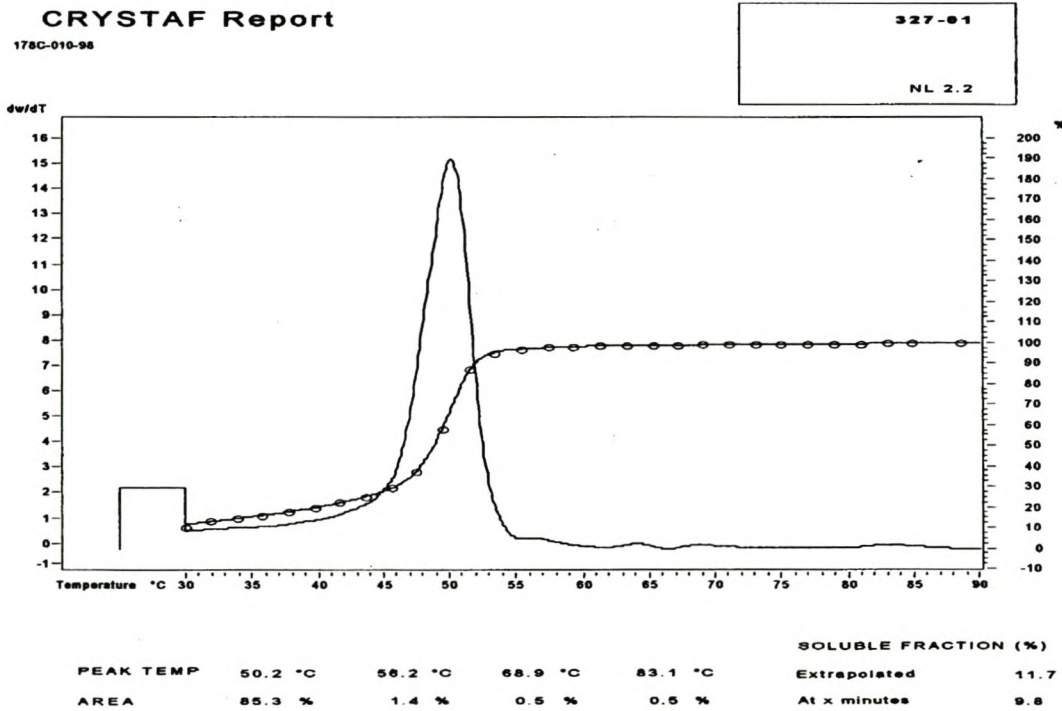


Figure C2: Sample NL 2.2

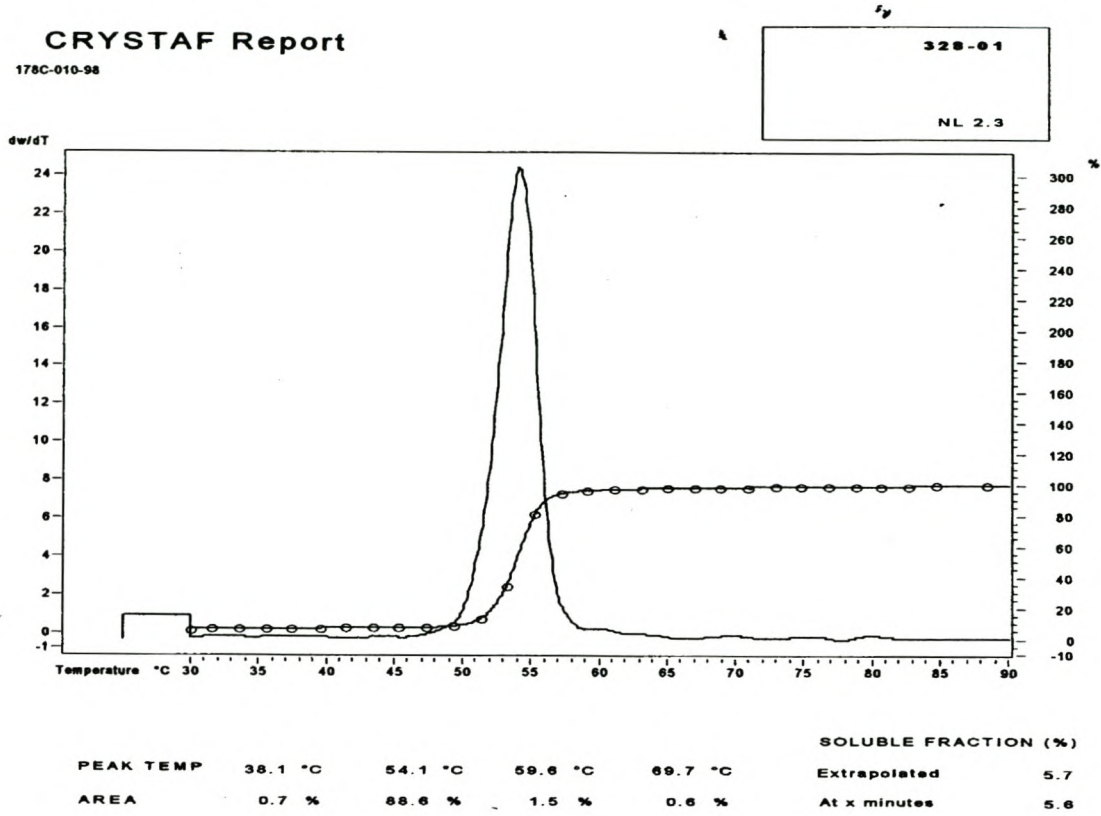


Figure C3: Sample NL 2.3

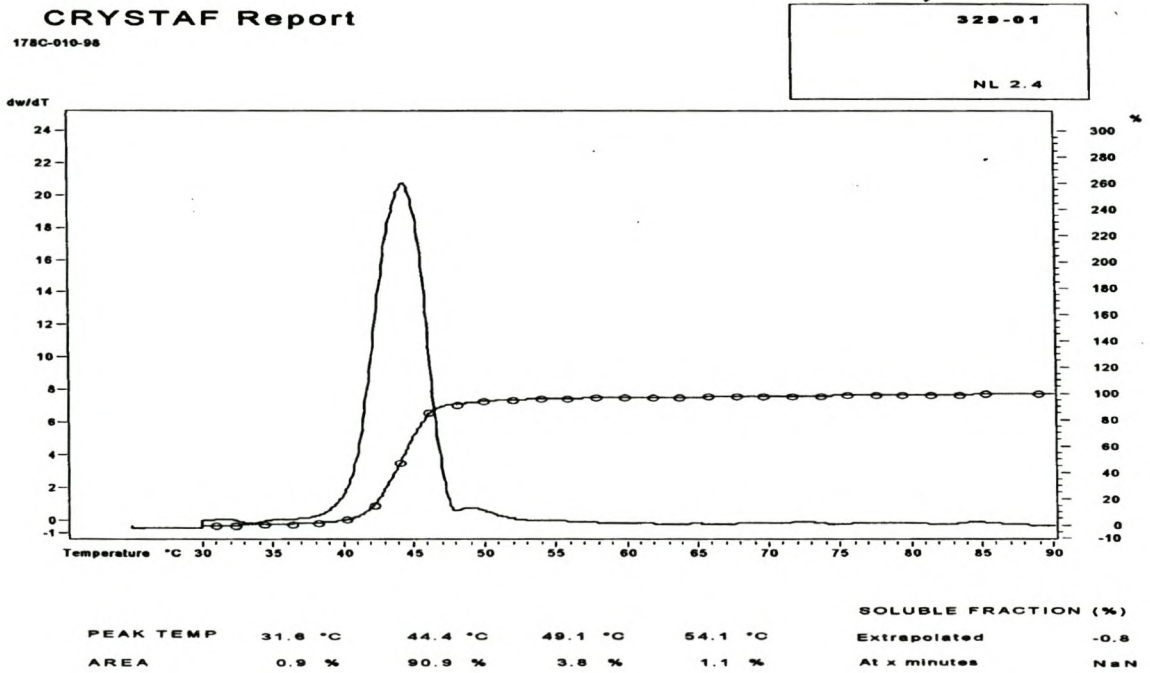


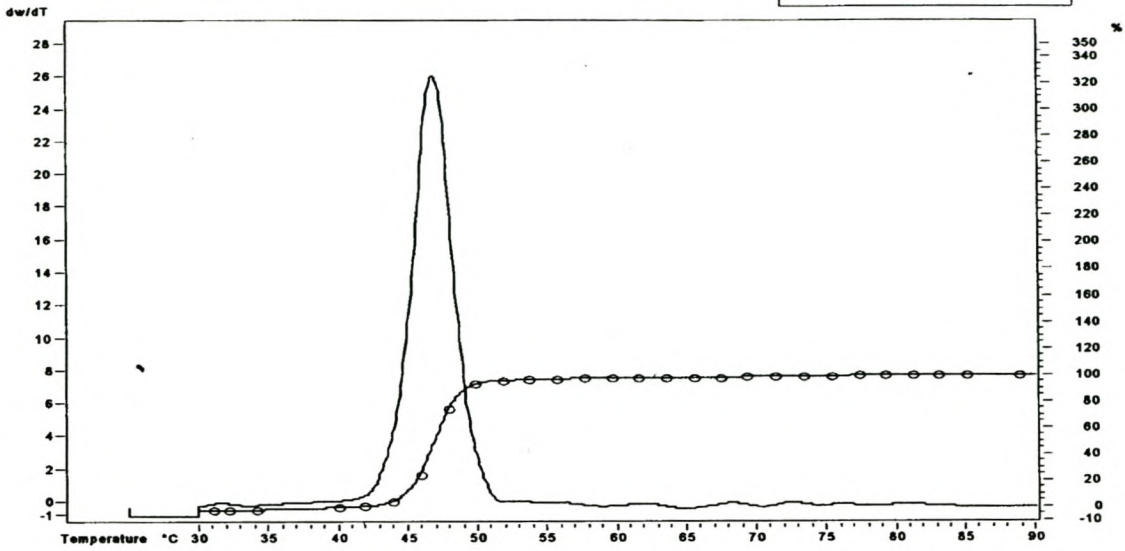
Figure C4: Sample NL 2.4

CRYSTAF Report

178C-010-98

330-01

NL 2.5



| PEAK TEMP | 48.9 °C | 52.8 °C | 72.6 °C | 80.8 °C | SOLUBLE FRACTION (%) |
|-----------|---------|---------|---------|---------|----------------------|
| AREA | 97.3 % | 1.1 % | 0.7 % | 0.7 % | Extrapolated -2.5 |
| | | | | | At x minutes NaN |

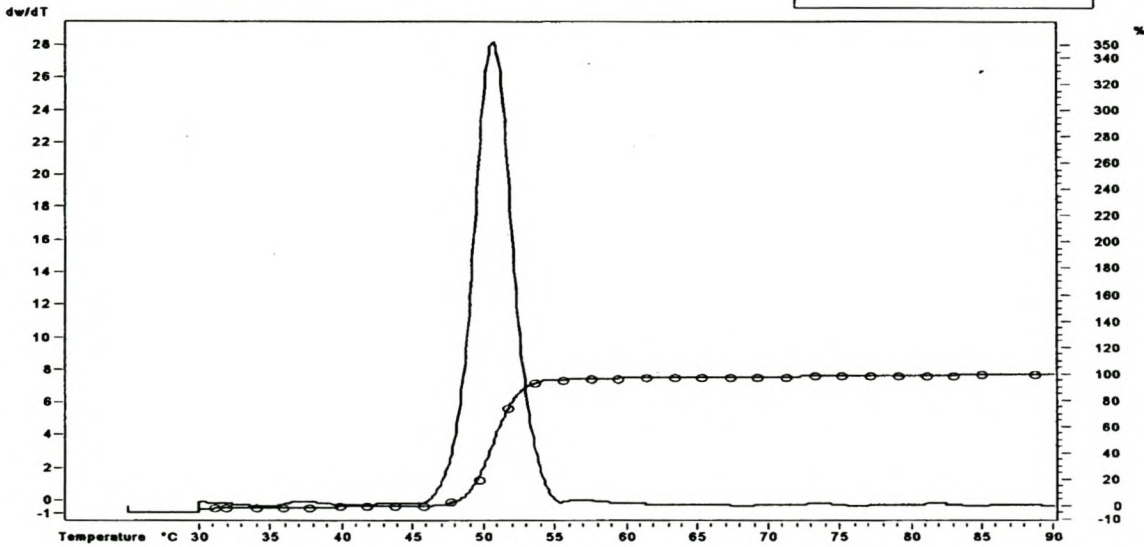
Figure C5: Sample NL 2.5

CRYSTAF Report

178C-010-98

331-01

NL 2.6



| PEAK TEMP | 37.3 °C | 50.7 °C | 58.9 °C | 73.7 °C | SOLUBLE FRACTION (%) |
|-----------|---------|---------|---------|---------|----------------------|
| AREA | 0.9 % | 98.2 % | 1.7 % | 0.8 % | Extrapolated -1.9 |
| | | | | | At x minutes NaN |

Figure C6: Sample NL 2.6

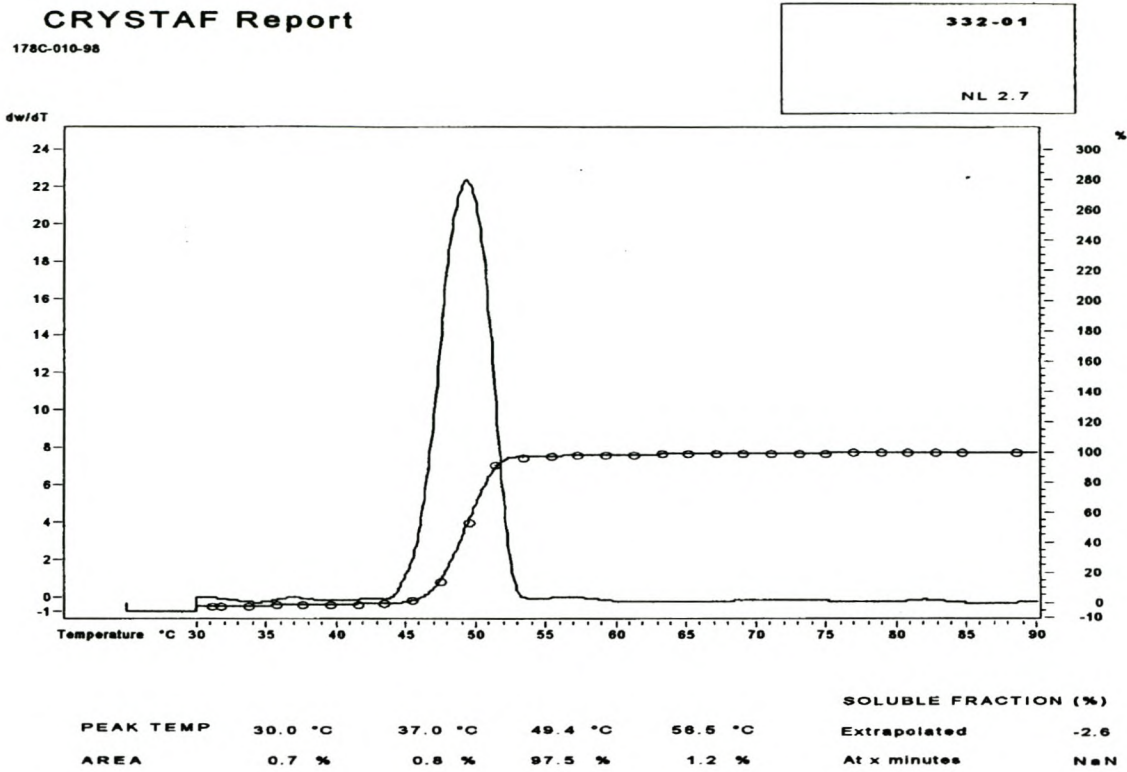


Figure C7: Sample NL 2.7

Propene/1-pentene

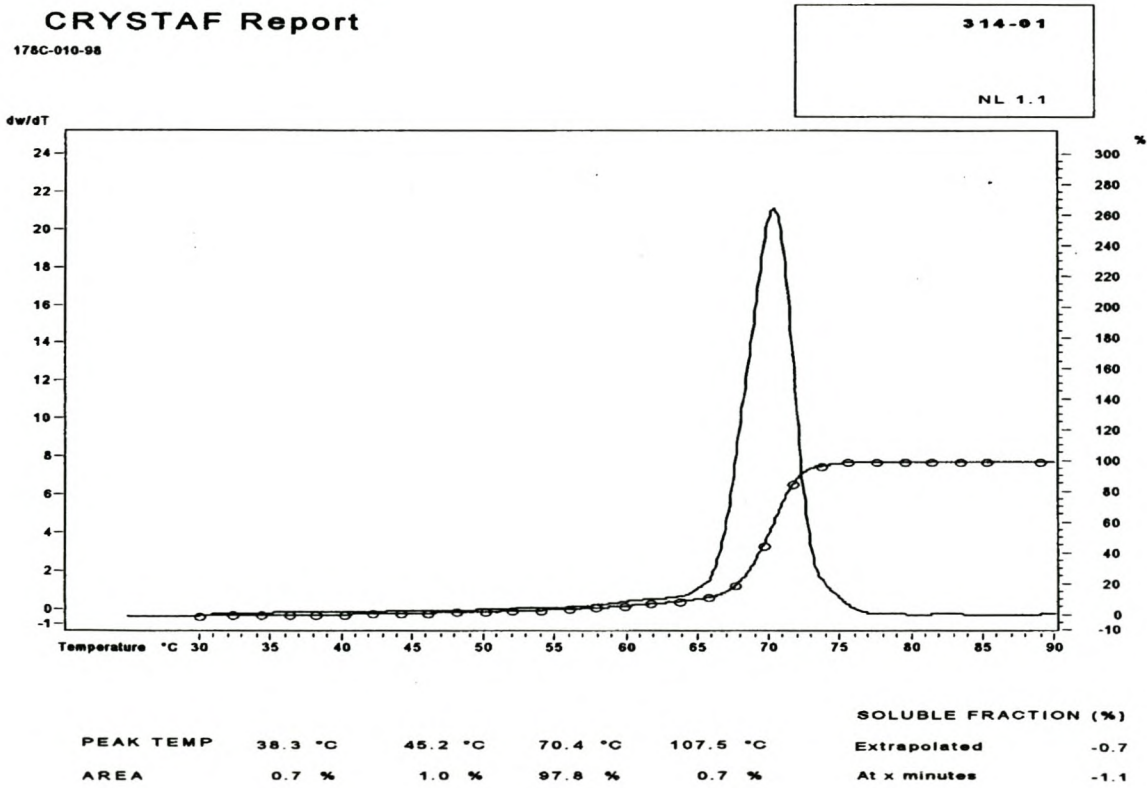


Figure C8: Sample NL 1.1

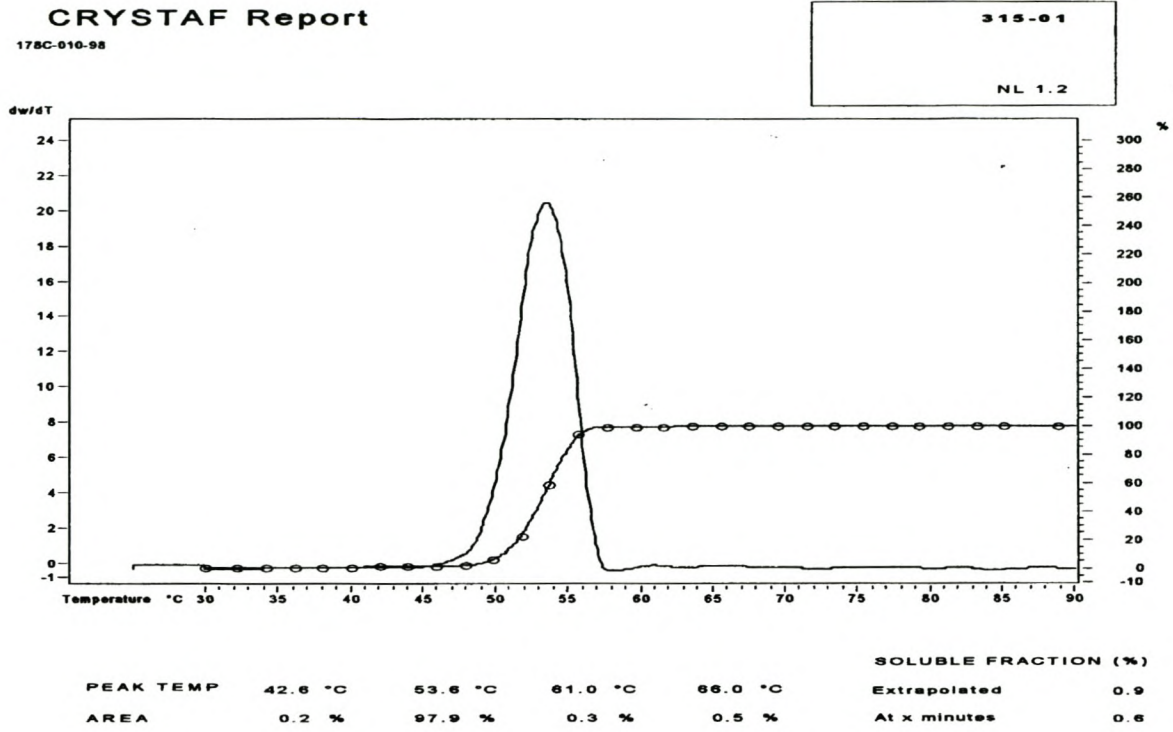


Figure C9: Sample NL 1.2

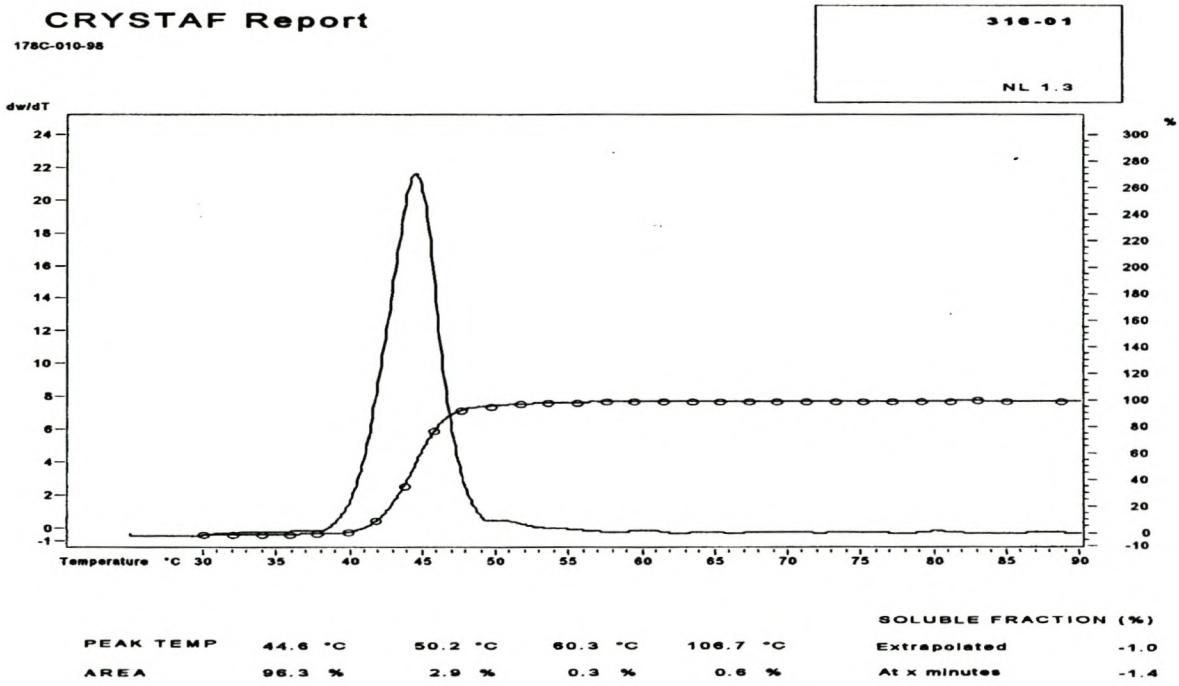


Figure C10: Sample NL 1.3

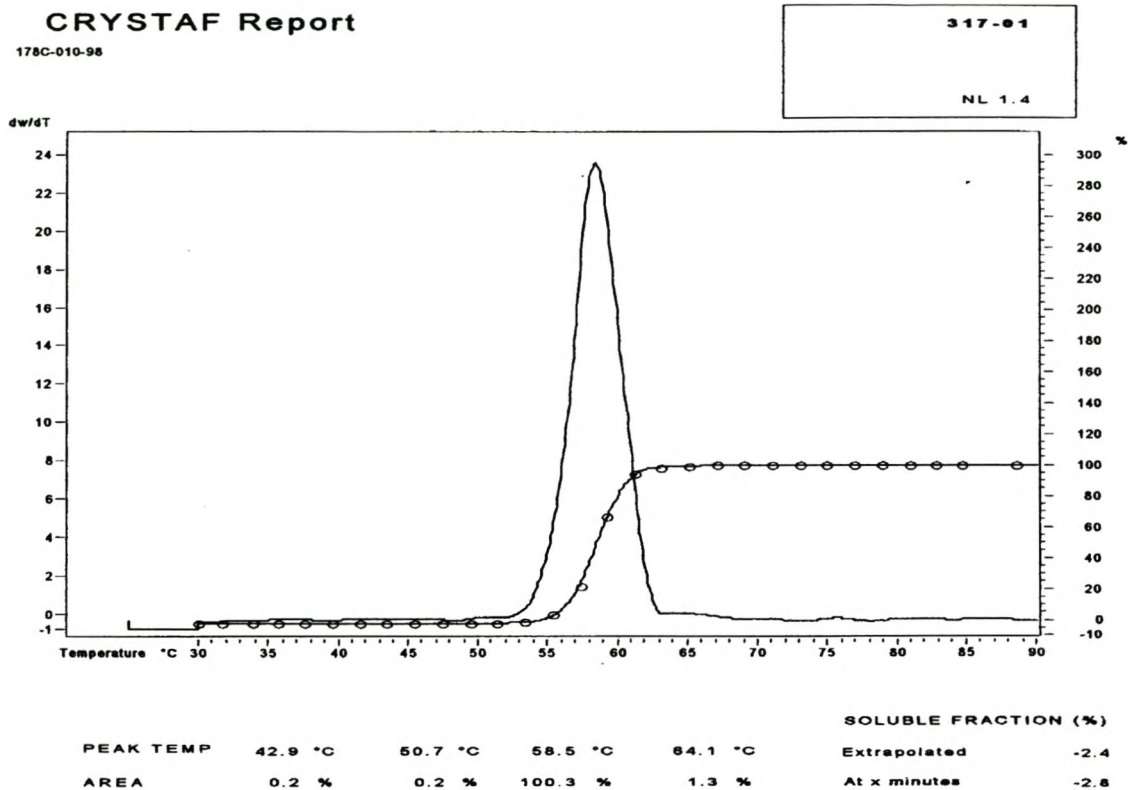


Figure C11: Sample NL 1.4

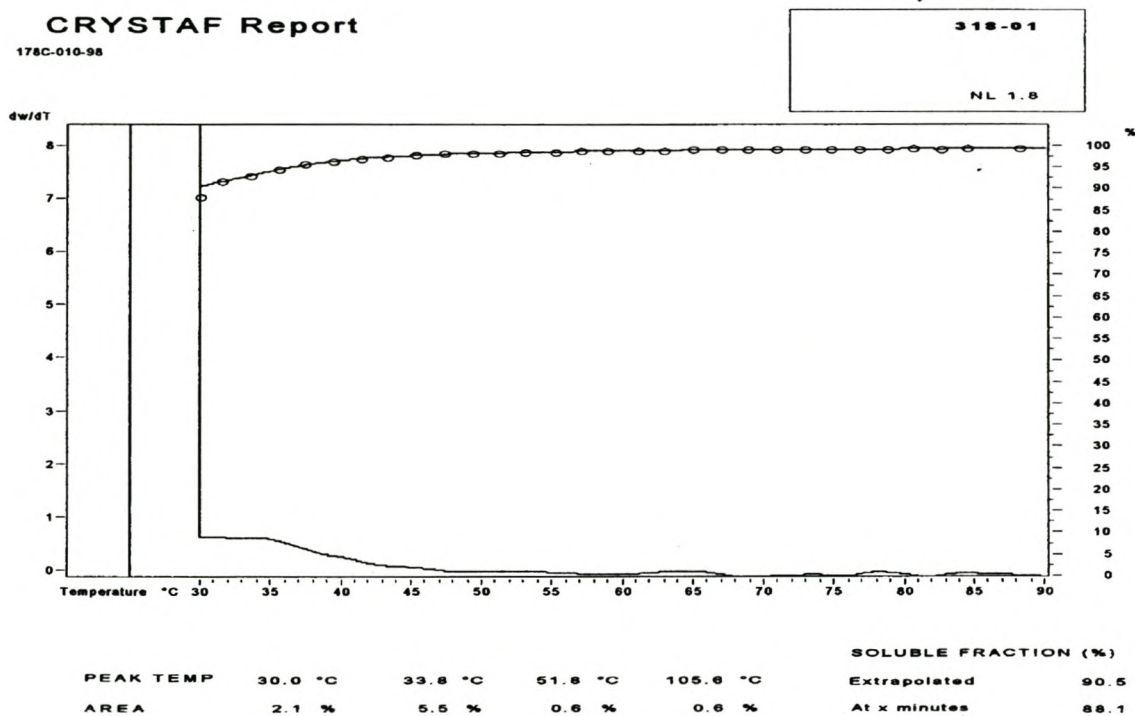


Figure C12: Sample NL 1.8

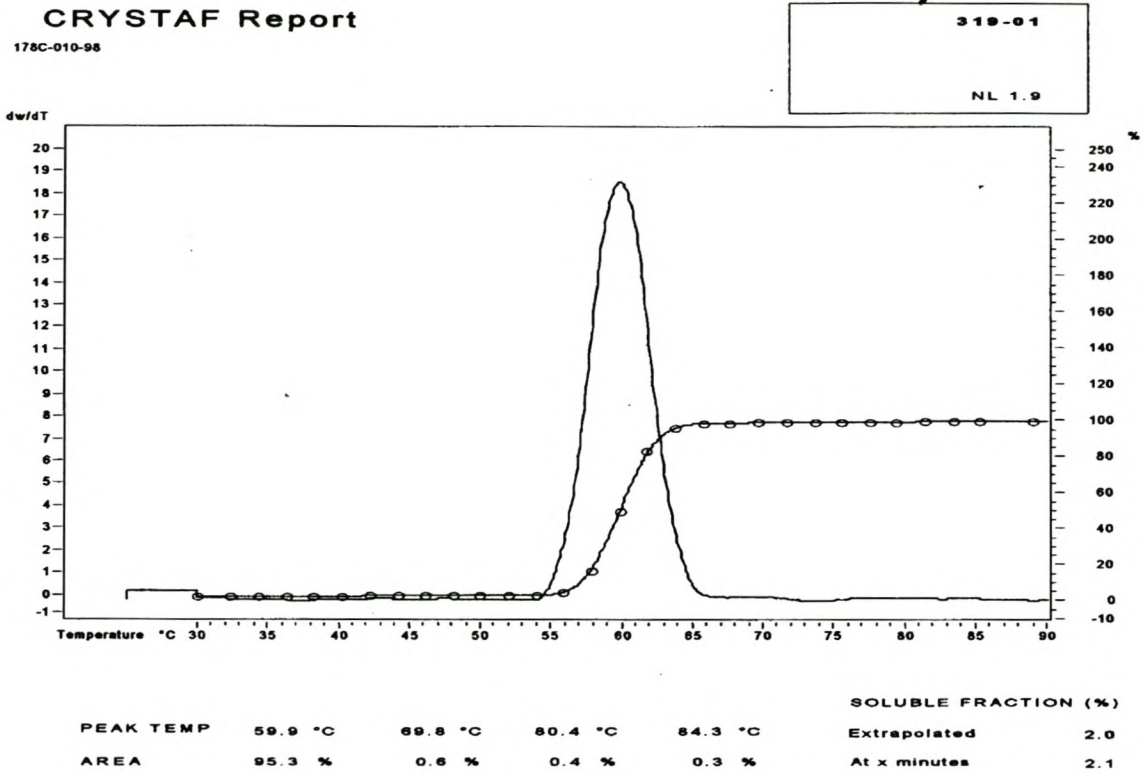


Figure C13: Sample NL 1.9

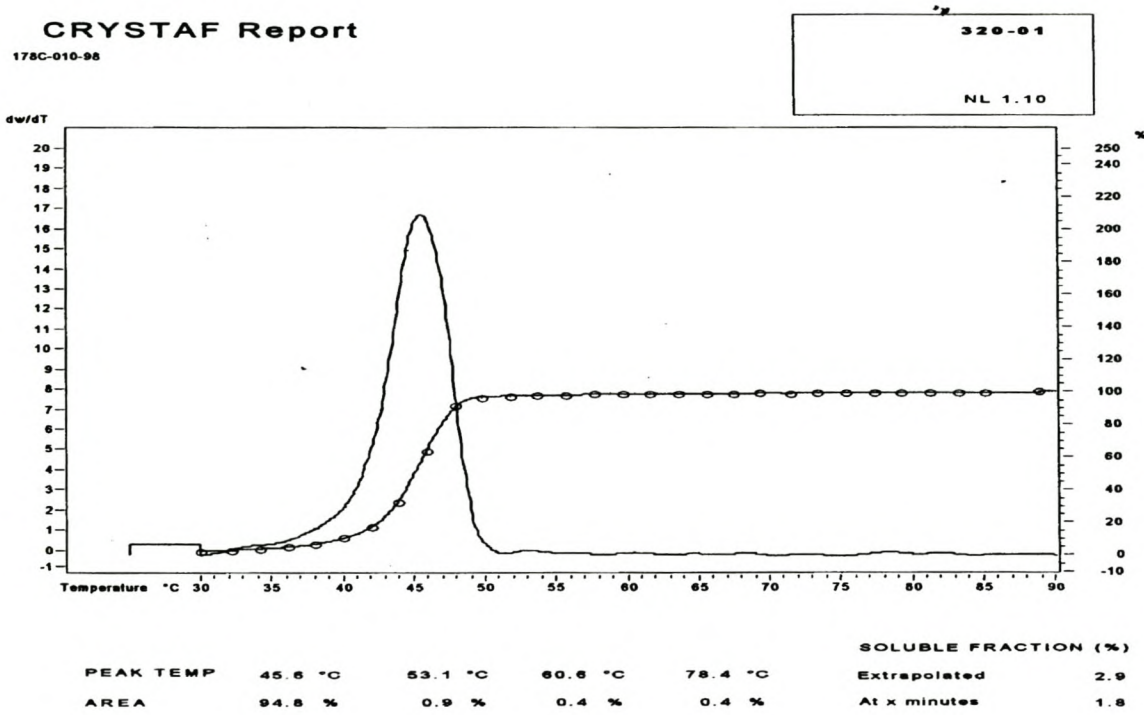


Figure C14: Sample NL 1.10

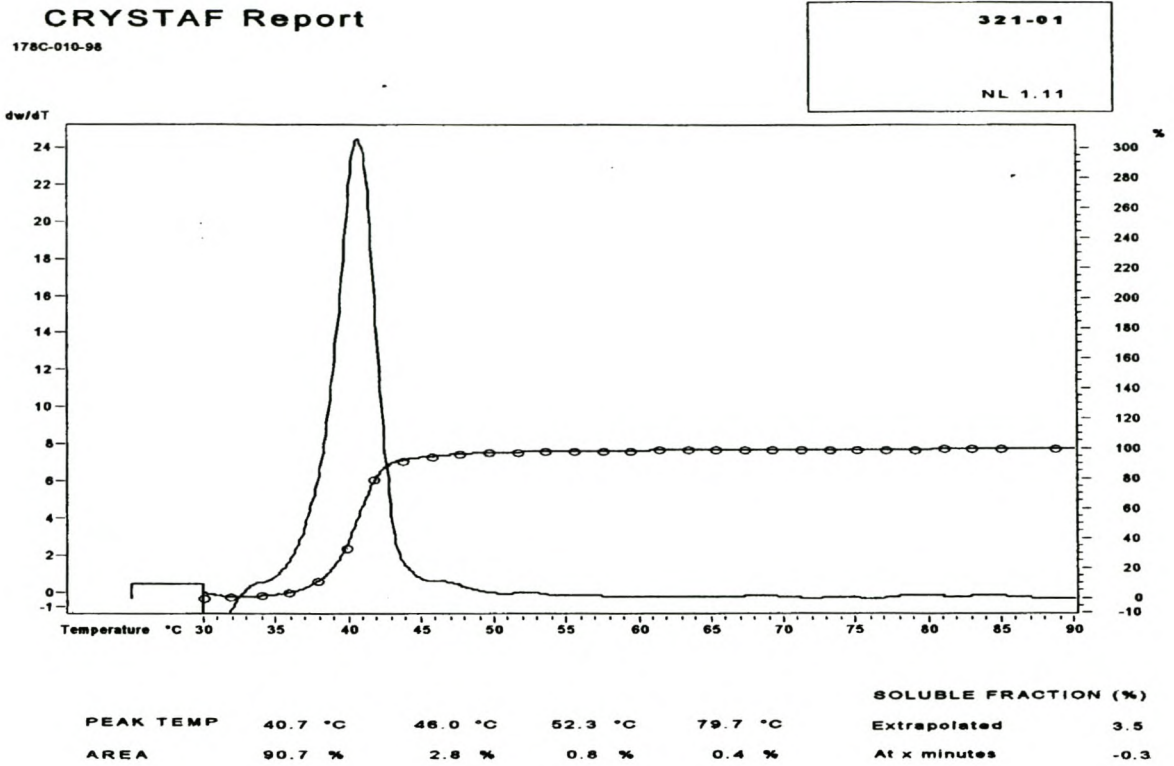


Figure C15: Sample NL 1.11

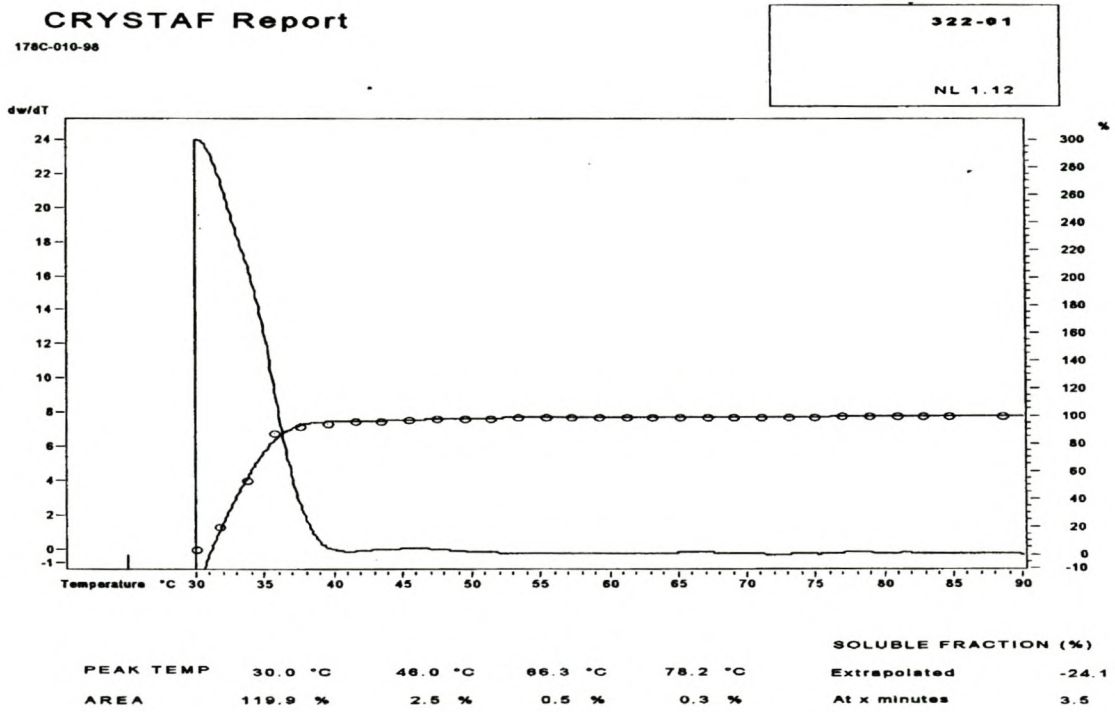


Figure C16: Sample NL 1.2

Appendix D
DSC CURVES

DSC results of propene/4-methyl-1-pentene copolymers (as examples)

Cooling curves

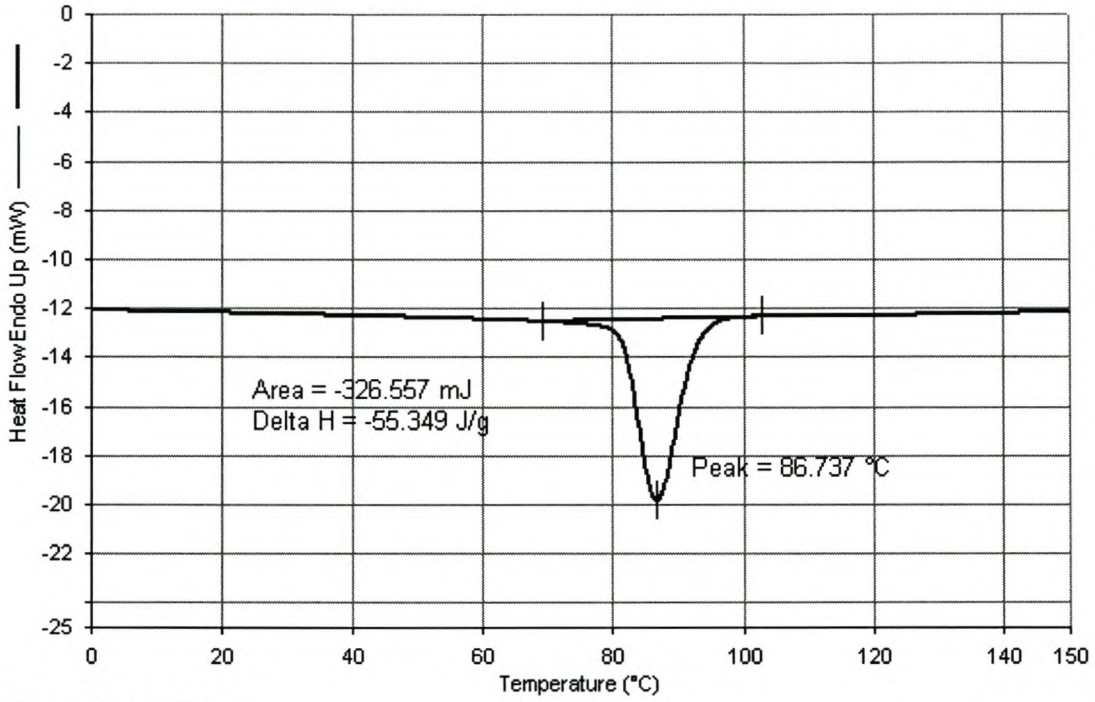


Figure D1. NL 2.1

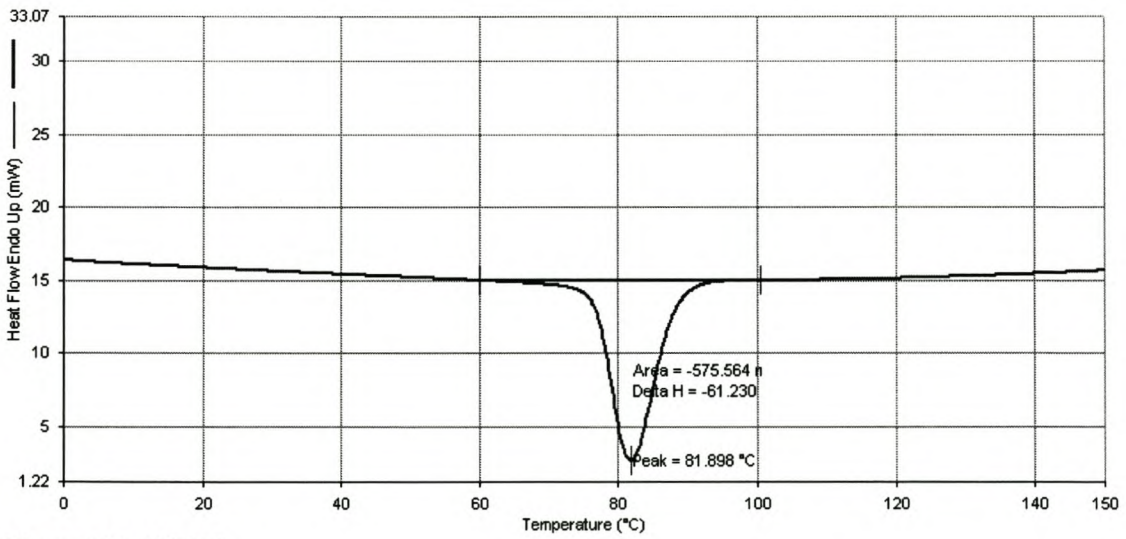


Figure D2 : NL2.2

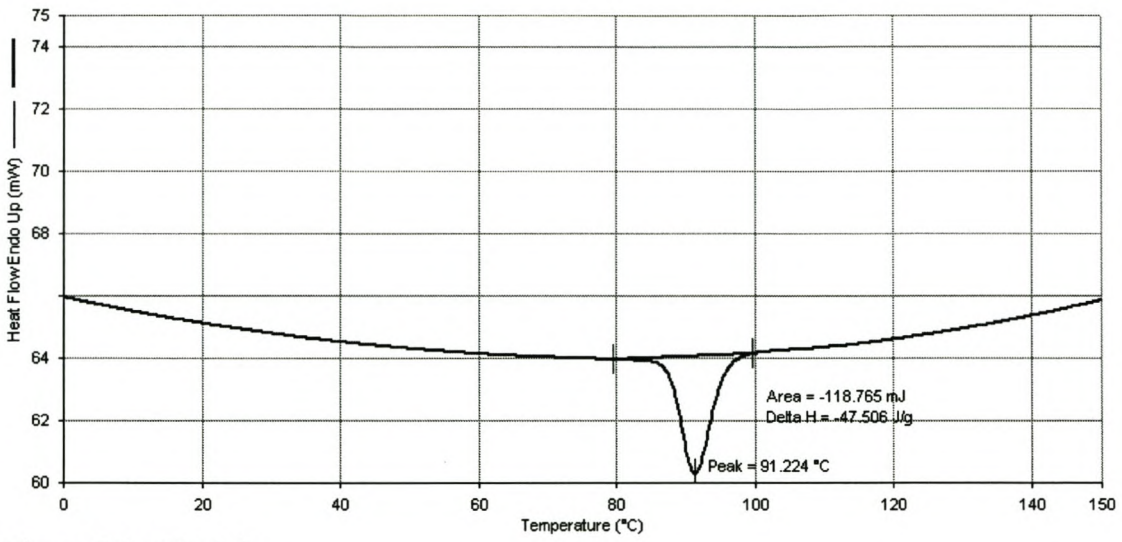


Figure D3 : NL 2.3

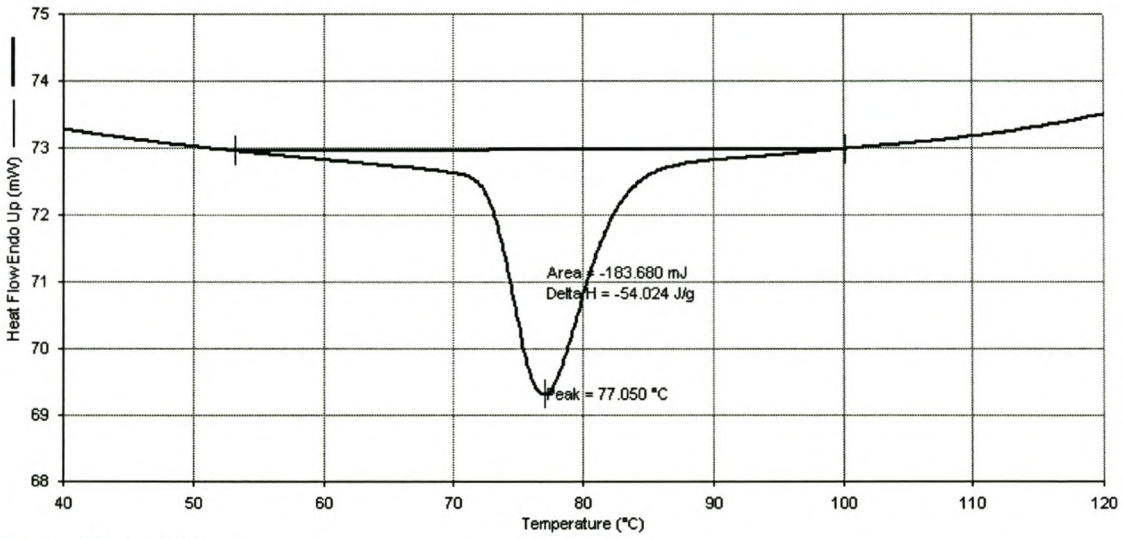


Figure D4 : NL2.4

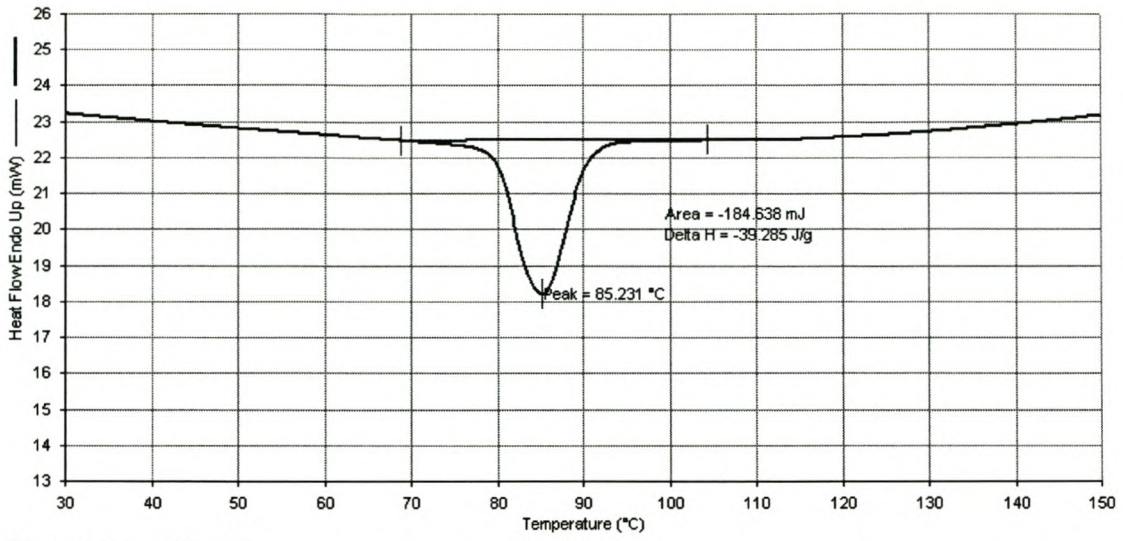


Figure D5 : NL 2.5

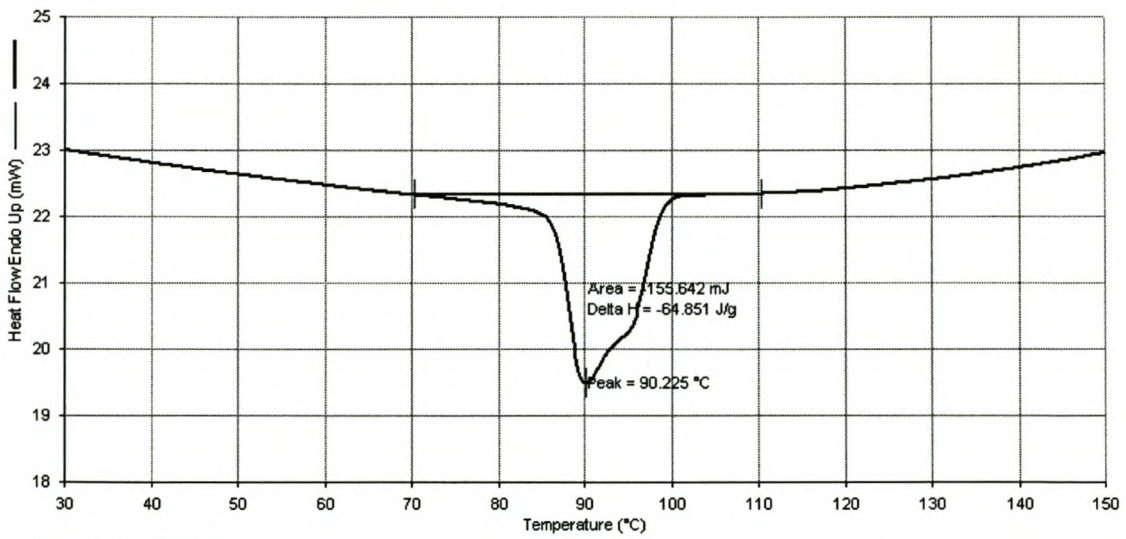


Figure D6 : NL2.6

Heating curves

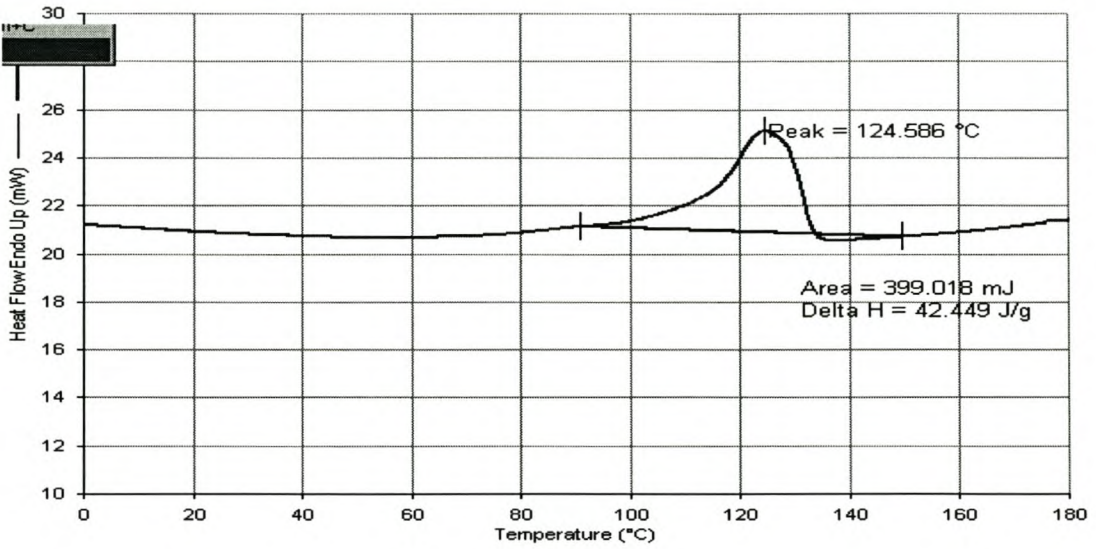


Figure D7 : NL 2.3

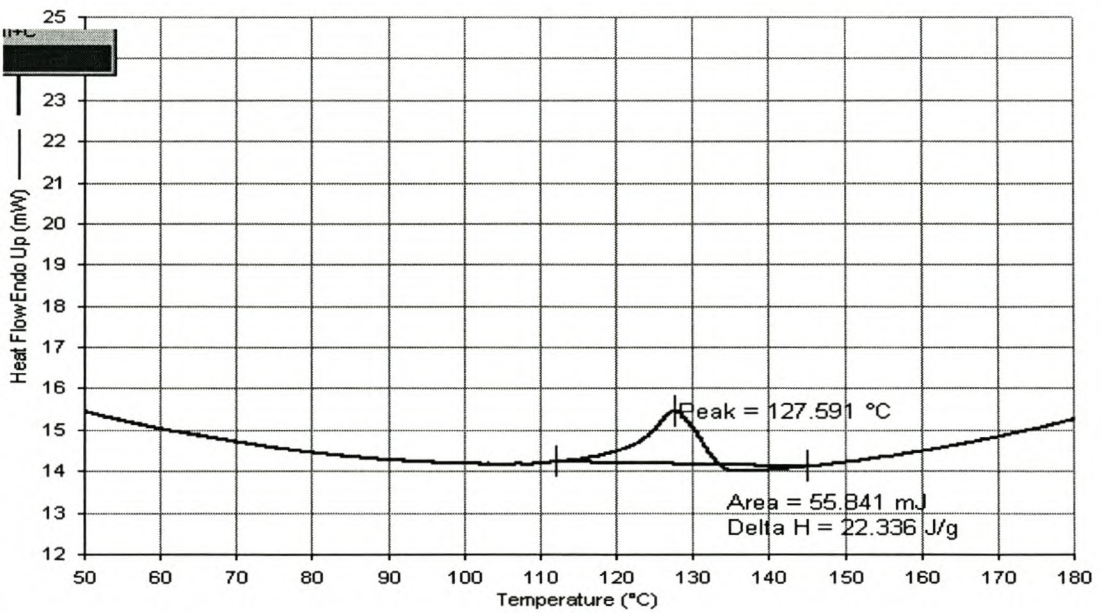


Figure D8 : NL2.3